SEDIMENT DYNAMICS OF THE AMATIKULU ESTUARY, CENTRAL KWAZULU-NATAL COAST, SOUTH AFRICA

Alain Le Vieux

School of Geological Sciences

Faculty of Science and Agriculture

University of KwaZulu-Natal

(Westville Campus)

Submitted in fulfilment of the academic requirements for the degree of Master of Science in the School of Geological Sciences, University of KwaZulu-Natal, Durban

December 2010

As the candidate's supervisor, I agree to the submission of this thesis.

Signed:………………………………Name:…………………………….Date:………………

ABSTRACT

The combined Nyoni River/Amatikulu Estuary is located on the microtidal, wave-dominated central KwaZulu-Natal (KZN) coastline, ~16km north of the Thukela River mouth. The Thukela River provides enough sediment to the coastline to cause net progradation on an otherwise eroding shoreline of KZN. It is within this geomorphological setting that the morpho- and sediment dynamics of the Amatikulu Estuary are addressed. Short-term coastline and estuarine evolution were assessed using polynomially rectified aerial photographs in conjunction with bathymetric and topographic data. This study shows that net seaward growth of the shoreline is a complex process linked to flooding episodes of the Thukela River where sediment is ejected are slowly reworked post-flood onto the beaches. The lag time between these floods and the maximum coastal progradation is ~ 2-6 years. Intervening pre-flood years are characterised by shoreline retreat as the ambient sedimentary supply of the Thukela River is below the threshold required to overcome the amount of sediment lost by wave erosion and transport via the northward longshore drift. Net seaward progradation occurs at 2.9m.year^{-1} over the 48 year period from 1957 to 2005.

In terms of the Amatikulu Estuary, the dominant control on morphology appears to be the strong wave activity and the very high volumes of sediment within the longshore drift, derived from the adjacent Thukela River. The extensive tidal channel of the combined Nyoni River and Amatikulu Estuary is the result of the net northward migration of the Nyoni Estuary until its capture by the Amatikulu Estuary forming a ~14km long, 500m wide spit. Time sequence aerial photography indicates that breaching of the spit occurs during flooding of the Amatikulu River, thereafter the flood inlet is quickly plugged by longshore derived sediments and wave activity and its usual inlet re-opened some 4km northward. Inlet migration does not occur as plugging is particularly rapid due to the high longshore drift component. The lack of inlet migration causes very little barrier modification and the long shore-parallel channel/barrier morphology is entrenched.

The Amatikulu Estuary's coast parallel channel, in light of empirically derived hydrological models, appears to be a relict feature, formed by higher flow velocities than currently experienced. Theoretical bedload sizes, based on the channel architecture, are at odds with

sediments sampled in the channel and suggest that the system behaves in a similar manner to river-dominated microtidal estuaries. Channel form, particularly sinuosity, is controlled by marine overwashing of the extended barrier. These form overwash plains of extensive blanketing marine sediments and comprise the dominant source of marine sediment to the estuary.

Surface sediment distribution is relatively homogenous, the estuary is dominated by fine, well-sorted sands. Isolated patches of mud appear where small scours have been in-filled by organic-rich mud. The coarsest sediment corresponds to the terminal lobes of washover fans, where they abut the main channel and are exposed to current winnowing. Geochemically, these samples show relatively little anthropogenic enrichment to the estuary when compared with other estuaries with urbanised catchments. Typically, the geochemistry of the estuarine sediments does not depart drastically from those values from, the catchment geology, indicating pristine conditions. High Ni, Ca and Sr values indicate marine sediment incursion and conform to the distribution of the coarsest washover sediments.

This study proposes an amendment to the classification of microtidal estuaries for KwaZulu-Natal, whereby a third category of normally open estuary is introduced: the *longshore drift dominated* estuary. These estuaries may exhibit some characteristics of either tide or river dominated estuaries, though they depart form this on the basis of their barrier/tidal channel configurations. This type of estuary is located on areas of prograding coastline, up-drift of large sediment sources where wave activity is sufficient to subdue delta formation. These estuaries are the surface features of sub-aqueous deltas which experience high sediment loads within the longshore drift and result in continuous, shore parallel extensions of the tidal channel and barrier.

PREFACE

This work was carried out in the School of Geological Sciences, University of KwaZulu-Natal, Durban, from March 2007 to December 2010, under the supervision of Dr. Andrew Green and the co-supervision of Dr. Ron Uken.

This study represents original work by the author. Where use has been made of the work of others it is duly acknowledged in the text.

DECLARATION 1

PLAGIARISM

I, Alain Le Vieux, declare that:

1. The research reported in this dissertation, except where otherwise indicated, is my original research.
2. This thesis does not contain other persons' data, pictures, graphs or other information, unless specifically acknowledged as being sourced from other persons.
3. This thesis does not contain other persons' writing, unless specifically acknowledged as being sourced from other researchers. Where other written sources have been quoted, then:
    a. Their words have been re-written but the general information attributed to them has been referenced
    b. Where their exact words have been used, then their writing has been placed in italics and inside quotation marks, and referenced.
4. This thesis does not contain text, graphics or tables copied and pasted from the Internet, unless specifically acknowledged, and the source being detailed in the thesis and in the References sections.

Signed:…………………………….……………… Date:………………………………………..

TABLE OF CONTENTS

LIST OF TABLES

LIST OF FIGURES

ACKNOWLEDGMENTS

Thank you Dr. Andrew Green for putting up your personal research funding for the field work and laboratory analysis of this project. I am extremely grateful to you for offering me this opportunity.

To my family; thank you so much for your unwavering support and all that you have done for me. Thank you! Mom, Dad, Patrique and Amy Horncastle, I love you all so much! You are all amazing.

To my supervisors Dr. Andrew Green and Dr. Ron Uken, thank you for your patience through the never ending barrage of questions and your continual support. Andy you have been and will continue to be first and foremost a friend, your honesty is truly appreciated and your uncanny ability to make any dull situation into an enjoyable one is a rare and truly unique talent. Your hunger for knowledge has made you a true role model. Thank you, I am eternally grateful for all that you have done for me.

I would like to thank Mr. Rio Leuci and Mr. Zane Thackeray from *Environmental Mapping and Surveying* for the loaning of their time and equipment in the field. Without you techno gadget wizardry I would still be lost in the field. Rio for going out of your way to help me when I phoned you for help, you are a life saver. Thank you.

To all my friends that came to help in the field and endured the sweltering heat, driving rain and stinging wind without complaint, thank you! The many nights around the fire with a cold beer or two will never be forgotten. Thank you, Mr. Patrick Gardiner (The fisherman), Mr.Richard Parkinson (from commercial plane captain to inflatable boat captain), Dr. Andrew Green (my unwavering leader), Mr. Rio Leuci and Mr. Zane Thackeray (the techno wizards).

Mr. Mark David (laboratory man), Mr. Paul Young (GIS extraudaire), Dr. Marc Humphries (Dr. Geochemist), Mr. Warwick Hastie and Miss Lauren Hoyer, thank you for your help but above all the tea room chats and friendship.

CHAPTER 1

INTRODUCTION

1.1. BACKGROUND

Microtidal estuaries such as those of KwaZulu-Natal (KZN) (Cooper, 2001) are amongst some of the most impacted and at-risk natural features along our coastlines (Cooper et al., 1994). The tendency for these systems to function as sediment sinks (Roy and Crawford, 1984) naturally raises concerns over their ability to accommodate pollutants generated in urbanised catchment areas. In this light, it is critical to understand the geomorphic properties of such estuaries, in particular their short term evolutionary response to changes in sediment supply and hydrodynamics.

Models of estuarine functioning (e.g. Dyer, 1979; 1986; 1997; Dalrymple et al.,1992) are constantly evolving and are often refined to cater for local conditions. These can be from both regional (e.g. Begg, 1978, 1984; Cooper, 1991a) and site specific perspectives (e.g. Reddering, 1983; Cooper, 1986; Njoya, 2002; Green, 2004; Tinmouth, 2009). This thesis examines the short term evolution of the microtidal Amatikulu/Nyoni Estuary. This estuary is unique in that it is situated on the only portion of the east coast of South Africa where sediment supply is sufficient to cause natural beach progradation (Cooper, 1991b). The response of such an estuary and its accompanying barrier/beach system to high levels of sediment supply is of particular interest when viewed in the context of most microtidal estuarine models for KZN. In general, these document a situation where sediment supply maintains a balance with rising sea-levels (e.g. Cooper, 1993, 1994) creating a monotonous fill with little variation throughout the Holocene (Cooper et al., 2010 in review).

1.2. AIMS AND OBJECTIVES

This thesis aims to provide a model for the sedimentary dynamics of the Amatikulu Estuary. Within this overall aim, several objectives are proposed. These comprise:

1) An assessment of the historical changes to the coastline for the past ~80 years between the Thukela Estuary to 4km north of the Amatikulu Estuary. These are to be reconciled with hydrological data from the Thukela River for the past 54 years.

2) An assessment of the geomorphology of the Amatikulu Estuary from air photo, survey and sedimentological data.
3) An investigation of the heavy metal geochemistry of the estuarine sediments.
4) The establishment of a model for the inlet response to flooding and post flood recovery in the estuary.

These will create a physically based framework which will better inform the management plans for the Amatikulu Estuary and other similar estuaries in KZN.

1.3. THEORETICAL BACKGROUND

1.3.1. Introduction

Coastal areas are amongst the most dynamic sedimentary environments in the world. The morphology of coastal environments is dictated by processes which operate on the micro- to macro scale and are ultimately driven by changes in sea-level and sediment supply. This refers to the amount of sediment and related accommodation space required to form particular sedimentary features in the coastal landscape. Fluctuations in either of these are related to various influences from climatic to anthropogenic in nature (Cowell and Thom, 1994). This aids in establishing and continuously modifying coastal landforms and environments. This dissertation is concerned specifically with the barrier beach and back barrier estuarine environments of the Amatikulu River area. Consequently this section focuses on introducing the various existing evolutionary and morphodynamic classification schemes for beaches, dunes and estuaries and the specific sub-environments therein.

1.3.2. Beaches

Of the World's coastlines, 40% of these are covered by unconsolidated sediments; these areas are known as beaches and consist of many different shapes, sizes and environmental settings (Bird, 2000). Beach sediment originates from many different sources; namely fluvial sources (Tanner, 1987; Blake, 2006), sediment eroded from dunes (Short and Hesp, 1982), cliff and rocky shore erosion (Moore and Griggs, 2002) and aeolian inputs (Allen and Posamentier, 1994). These influence the composition and the nature of the sediments that accumulate on the beach. Ultimately, sediment composition is determined by the geology at the source of the sediments.

Losses of sediments from the beach take place through onshore losses via overwash into lagoons and inlets (Reddering, 1983; Cooper, 1986) and wind transport towards the hinterland or offshore (Lynch et al., 2009). Offshore losses occur via longshore drift (Reddering, 1983) and exchange between the upper shoreface and the outer shelf during storms which drive return offshore flows at the seabed (Green et al., 1995). Often this type of sediment transport is seasonal (Wright and Short, 1984). *In situ* weathering and attrition is a means by which sediment volume is reduced (Bird, 2000). Due to the multitude of sediment sources (from a local to global scale), many different assemblages of sediment characteristics on a single beach may be found. This means that grain size, shape, composition and sorting all vary from place to place and over time; dependant on the local conditions which influence both inputs and losses to sediment.

1.3.2.1. Morphodynamic Definitions

Morphodynamically, beaches may be defined in several ways, the simplest definition related to the sediment budget of a particular beach as defined by net loss or gain of sediment. The outcome of this is two canonical end-members encompassing progradation and erosion. In the former, constantly high levels of sediment are introduced to the beach and upper shoreface environments, causing net seaward growth as the most proximal areas for sediment deposition are choked and then bypassed as the beach progrades (Raymond, 2002). Conversely, where losses in sediment exceed supply, the beaches must retreat in the form of beach erosion.

The transverse profile of a prograding beach has a convex seaward profile or a terrace ending in a seaward slope (Bird, 2000). A morphological indication that a beach is prograding is the presence of successive beach ridges built above the high water mark (Tanner, 1987; McBride et al., 2007). The most likely situations for progradation occur on emergent coastlines where the land mass is undergoing uplift from the postglacial isostatic recovery. The uplift of the land stimulates shoreward drift of nearshore sediments (Bird, 2000). Longshore drift may also cause progradation where the shore parallel current is intercepted by a structure causing the deposition of the transported sediments, the accretion occurring on the up-drift side (Wallace, 1988).

Psuty (1988) provides a further refinement of this basic progradation-retrogradation scheme, whereby specific morphological features are related to both positive (thus prograding) and negative beach budgets (Fig. 1.1). The key to this scheme is the presence or absence of foredunes; these features are considered an active component of the budget itself. All conditions of the beach-dune budget are represented along a continuum with respect to temporal and spatial requirements. The names of each of the quadrants are determined by relative budget proportions of the beach-dune profile.

Simply put, a strongly positive quadrant with both positive foredune and beach budgets results in increasing foredune dimensions. These are limited to some extent by increasing seaward growth and extremely rapid coastal accretion resulting in *dune* ridge fields. Conversely, where sediment is not stored in foredunes, an equivalent *beach* ridge field develops. Under conditions of moderate progradation there is increased time for dune accretion which results in a foredune-ridge topography.

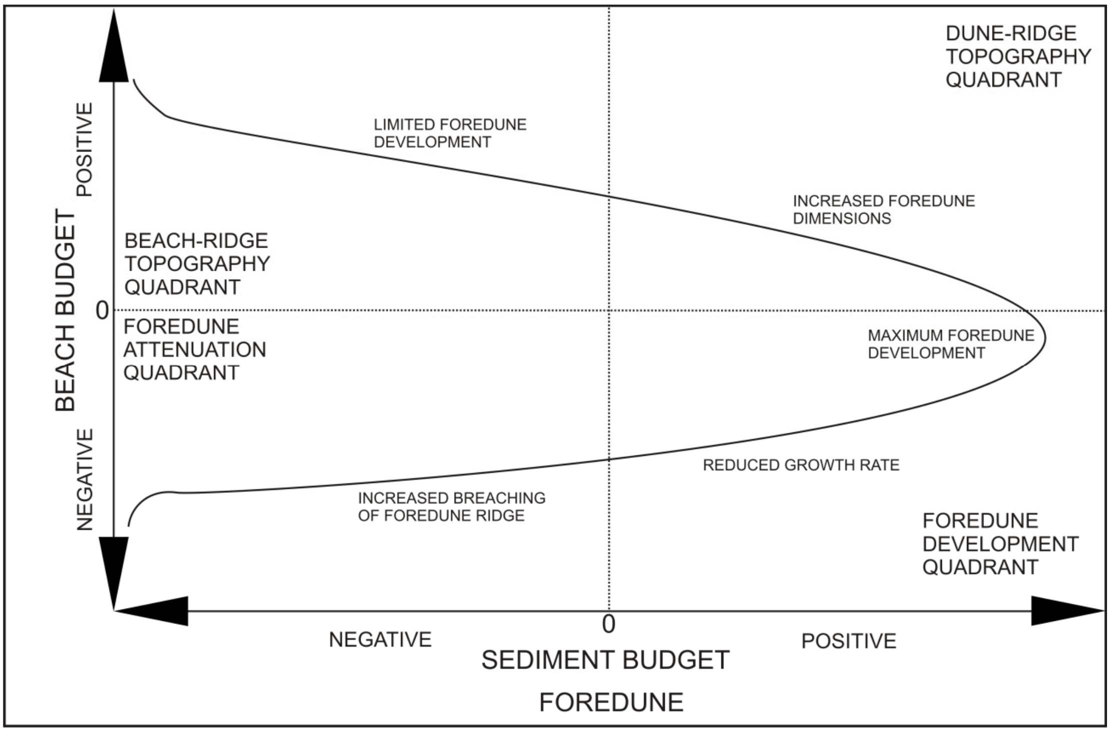

Figure 1.1 Beach and foredune budget modelled together with foredune development (after Psuty, 1988).

Wave energy, particularly in light of the wave-dominated nature of the east coast of South Africa (Smith et al., 2010), should also be included in such a scheme. Clearly large wave events, coupled with high tides can cause protracted coastal erosion (Smith et al., 2010). This is often seasonal, in KZN the maximum period of erosion is during winter when south-to-north longshore drift is enhanced by stronger winter swells (Smith et al., 2010). Morphodynamically, Wright and Short (1984) discuss models of morphological variability within surf zones and beaches, based on the hydrodynamic process that influences the depositional forms of each beach state. Two end members are considered: fully dissipative and fully reflective. A further four intermediate states which possess features common to the two end members exist, but will not be discussed further. The end members of the spectrum of morphodynamic states are provided in Figure 1.2.

The reflective beach state is defined by waves with a strong standing wave motion, surging and collapsing breakers and resonance at sub-harmonic frequencies. This results in turbulence on the beach face in the area of run up in the swash zone which is characterised by rhythmic cusps, as wave height increases so does depth at the beach face. Beach faces are steep and linear consisting of coarser material with limited ability for subaqueous sand storage. Under low energy conditions the beach is characterised by a straight crested berm. These types of beaches are common on the south and north coasts of KZN (e.g. Umhlanga and uMdloti beaches).

The dissipative beach model is defined by spilling waves and waves that dissipate energy by plunging. This results in flat, shallow multi barred surf zones and wide beaches that cause further energy dissipation of wave energy to a point where the waves impacting on the beach face are substantially small. Dissipative beaches have the ability to store large amounts of subaqueous sediment, generally consisting of fine sand and transported in a shore normal direction. The profiles are consistent with profiles of storm or winter profiles in seasonally variable beaches.

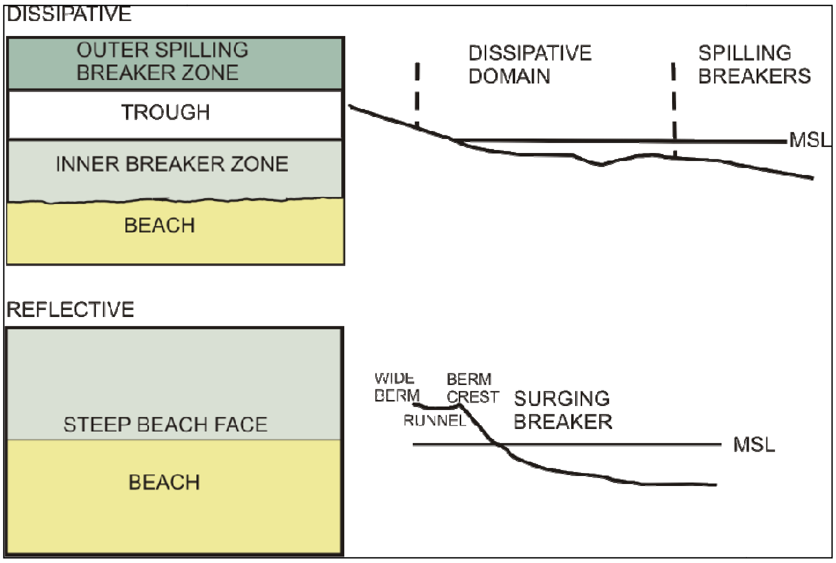

Figure 1.2 The two end members of Short and Wright (1984) beach states. The dissipative beach state is characterised by spilling breakers in the outer breaker zone, the inner dissipative zone is characterised by a long flat concave beach face with low frequency swash bores and fine grained sediments. The beach has no longshore variability (after Short and Wright, 1984). The reflective beach state is characterised by a steep beach face with cusps, a wide high berm, surging breakers, coarse sediments and a linear low gradient nearshore profile (after Short and Wright, 1984). Based on the wave climate of KZN, the Amatikulu coastline should conform to Short and Wright's (1984) dissipative scheme.

1.3.2.1.1. Foredunes

Foredunes defined in the South African context by Olivier and Garland (2003) are ephemeral shore parallel, sand ridges that are typically less than 5m in height, 20m wide and which are built up at the back of a beach seaward of the storm line. Foredunes generally form around accreted beach material which allows the germination and formation of pioneer plant communities (Hesp, 2002; Olivier and Garland, 2003). The rate at which foredune grow is dependent on the rate of accretion (Olivier and Garland, 2003). On a prograding coast it has been suggested that seaward advance of the foredunes is dependent on the rate of the vegetation growth (Bauer and Sherman, 1999). Foredunes are active features that are constantly changing (Olivier and Garland, 2003). Under onshore wind conditions, aeolian transport occurs and the dune receives sediment from the beach where the vegetation stores it and the dune accretes (Bauer and Sherman, 1999; Olivier and Garland, 2003). During stormy weather the foredunes are attacked by storm waves and offshore winds (Psuty, 1990; Bauer and Sherman, 1999). This releases sediments and erodes the dunes supplying sediment to the beach and the nearshore environment (Bauer and Sherman, 1999). Foredune size is related to beach-surf zone type; the larger foredunes occur on the disspasive beaches described by Short and Wright (1984) (Hesp, 2002).

1.3.2.1.2. Beach Ridges

Beach ridges are coast parallel relict morphological features that comprise wave-built berm ridges, transgressive and regressive ridges, cheniers, foredune ridges and laterally accreted ridges created through the lateral movement of the shoreline (McBride et al., 2007). Beach ridges are features located on regressive coastlines, whereas cheniers form under transgressive conditions (Tanner, 1988; 1995; Otvos, 2000; McBride et al., 2007). Otvos (2000) and McBride et al., (2007), similarly recognise the distinction between regressive and transgressive scenarios of beach ridge formation, yet make subtle distinctions. In this light, transgressive ridges migrate in a landward direction and are often modified by wind and waves. The successive establishment of each ridge as the beach progrades seaward creates a ridge plain (Otvos, 2000; McBride et al., 2007). Ridge plains themselves can be divided into different sub-plains distinguished by ridge height or, when viewed in plan view by coastal orientation (Tanner, 1988; 1995; McBride et al., 2007).

1.3.3. Estuaries

1.3.3.1. Definition

The definitions of estuaries are widespread and numerous. In general they are defined as coastal bodies of water that are partially enclosed; where rivers and oceans meet and where the water within the estuaries is a mixture of saline water from the ocean and fresh water from fluvial sources (Dyer, 1979). The definition of Cameron and Pritchard (1963) was for many years the most widely accepted where: “an estuary is a semi in-closed coastal body of water having a free connection with the open sea and within which sea water is measurably diluted with fresh water derived from land drainage. ” In a South African context, Day (1980) considers an estuary as “a coastal body of water in intermittent contact with the open sea and within which sea water is measurably diluted with fresh water from land drainage”. This definition implies that coastal bodies of water may become temporally closed and separated.

In terms of sedimentological studies the most useful definition is that of Dalrymple et al., (1992) which considers an estuary as “the seaward portion of a drowned river valley system which receives sediment from both fluvial and marine sources, and contains facies influenced by tide, wave and fluvial processes. The estuary is considered to extend from the inner limit of tidal facies at its head to the outer limit of coastal facies at its mouth.” This definition implies that estuaries form only under transgressive conditions (Dalrymple et al., 1992). This definition has widely become the sedimentological definition of choice and has been used by many authors (e.g. Ainsworth and Walker, 1994; MacEachern and Pemberton, 1994).

1.3.4. Classification Schemes

1.3.4.1. Salinity Structures

Estuaries may also be classified by the degree of mixing apparent between the salt and freshwater components (Prichard, 1955; Cameron and Pritchard, 1963; Dyer, 1997). These will be summarily ignored here on the basis of the shallowness (see Chapter 5) of the Amatikulu Estuary which would result in the water column being well mixed at all times.

1.3.4.2. Sedimentological and Evolutionary Classification

In the geological context estuaries are ephemeral features which change morphology depending on the prevailing wave, river, tide and sedimentary characteristics at the time (Dalrymple et al., 1992). Estuaries, deltas and strand plain/tidal flats can all morphologically alter into each other (Dalrymple et al., 1992), dependant on the dominance of any one factor as outlined in Dalrymple et al.,'s (1992) scheme of coastal evolution. This classification is based on the physical characteristics of the site (wave, tide and river influences) and the temporal changes that occur at the site with respect to sea level fluctuation and the ensuing progradational or transgressive nature of the coastline (Fig. 1.3). This assumes a tripartite classification whereby rivers, tides and waves are the dominant forces in coastal morphodynamics. This tripartite classification has being used very successfully in many estuarine and incised valley studies (Zaitlin et al., 1994; Kindinger et al., 1994). Estuaries in this classification occupy the intermediary position between all three, as they depend to some degree on all of these processes. Areas with dominant fluvial influence result in deltas, those dominated by waves and tides form strand plains or tidal flats. The fourth dimension of time, relative to sea level fluctuation, shows that estuaries are indubitably linked to transgressive conditions and coastal drowning. Where estuaries exist on a progradational coastline they become in-filled and evolve into deltas, strand plains or tidal flats depending on the dominant coastal process. Dalrymple et al., (1992) consider that if there is sufficient river influence an estuary will evolve into a delta and reach an equilibrium form despite zero fluctuation in sea level.

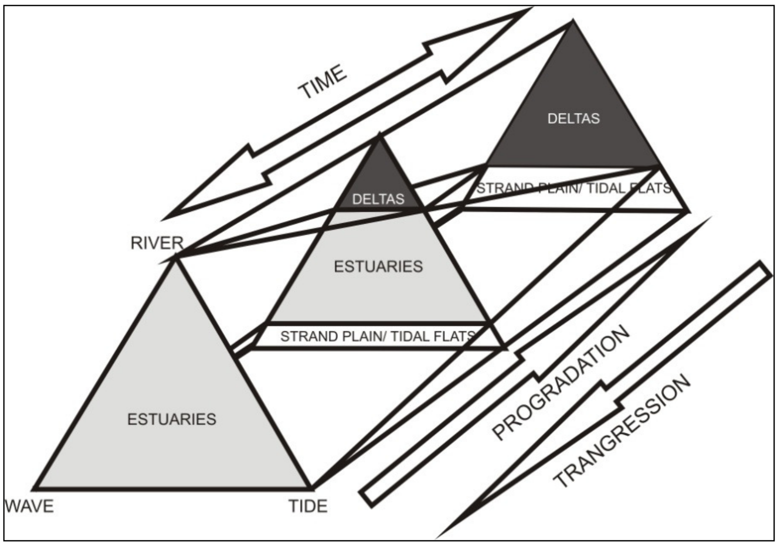

Figure 1.3 Ternary diagrams indicating the evolution of coastal environments with respect to time and the dominant coastal conditions (after Dalrymple et al., 1992).

Zaitlin et al., (1994) further differentiate between estuaries relative to the dominant of wave or tidal energy. In this aspect, river dominance is assumed to form deltaic coastlines and is summarily ignored by this scheme. Here tide and wave dominated estuaries are divided into three zones based on their dominant processes (Fig. 1.4) where the differing energy regimes produce distinguishable sedimentary assemblages.

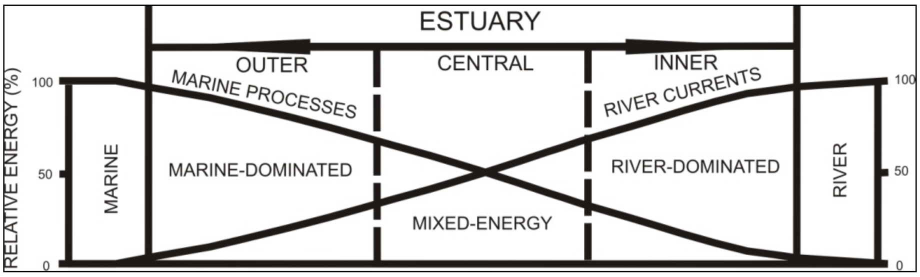

Figure 1.4 Estuary zones and the physical processes operating within the zones (after Dalrymple et al., 1992).

Wave-dominated estuaries (Fig. 1.5) produce a clearly defined tripartite distribution of facies, based on energy within the estuary. A marine sand body accumulates on the barrier adjacent and fronting the estuary mouth transported by longshore drift. The mouth is generally an area of sandy deposition, and can comprise a coarse marine sand plug. Overall this sediment body consists of wash-over deposits and a landward prograding flood-tidal delta where those tidal currents that do exist, shoal during the flood tide advance. There is a low energy central zone where fine grained organic muds accumulate by settling and flocculation, followed by the deposition of a bayhead delta where sand or gravel is deposited at the terminus of the fluvial energy entering the system. Wave-dominated estuaries occur in micro- and meso- tidal conditions (Davies, 1964, Dyer, 1997). These estuaries are most likely to occur where friction exceeds the effects of convergence and the tidal range decreases towards the head of the estuary this is know as ‘hyposynchronous’ (Nichols and Biggs, 1985; Dyer, 1997).

Tide-dominated estuaries (Fig. 1.6) have a limited facies zonation because the tidal energy penetrates deeper into the estuary compared to that of waves. The result is an estuary dominated by mixed tidal and fluvial energy, with no clear energy peaks or troughs. The mouth usually comprises a series of longitudinal bars orientated long axis to the prevailing ebb and flood tide currents. These exist in a zone of higher energy and are consequently coarser when compared to that of the fringing tidal flats which are marked by suspension settling. Tidal channels are often sandy due to the higher current velocities related to channelised tidal flows. Estuaries of this nature tend to be located in areas with macrotidal range (Davies, 1964) and hypersynchronous conditions (Nichols and Biggs, 1985).

The overall tripartite facies model presented here is the result of redefinition of many authors (e.g. Roy, 1994; Nichol, 1991). The limitations of the 'process-dominated' tripartite facies models have been highlighted in rock bound estuaries by Fenster and FitzGerald (1996) and FitzGerald et al., (2000) indicating that the inherent structural framework provides the dominant control over the estuary. The fundamental idea in the tripartite facies model of a wave-dominated estuary is that marine sediments are introduced into the estuary through landward migrating flood tidal deltas and barrier overwashing. In tide-dominated estuaries sediment is introduced from marine origin through bedload transport in the tidal channels. The Kennebec River estuary is a tide-dominated estuary where the net sediment transport is towards the mouth of the estuary and where sediments are simultaneously recirculated in the estuary along the nearshore and on the adjacent barrier. This is in stark contrast to the tripartite facies model.

This is due to a deep rock bound channel which distorts the processes that operate within the estuary, coupled with a lack of accommodation space resulting in the seaward migration of the sediment. This type of structural control on estuarine morphodynamics is not unique and has not gone unnoticed. Burningham (2008) argues that the constraints imposed structurally on a coastal system provide a framework within which different types of systems are able to form, this amounts to an important source of spatial variability in basic and essential geomorphic control.

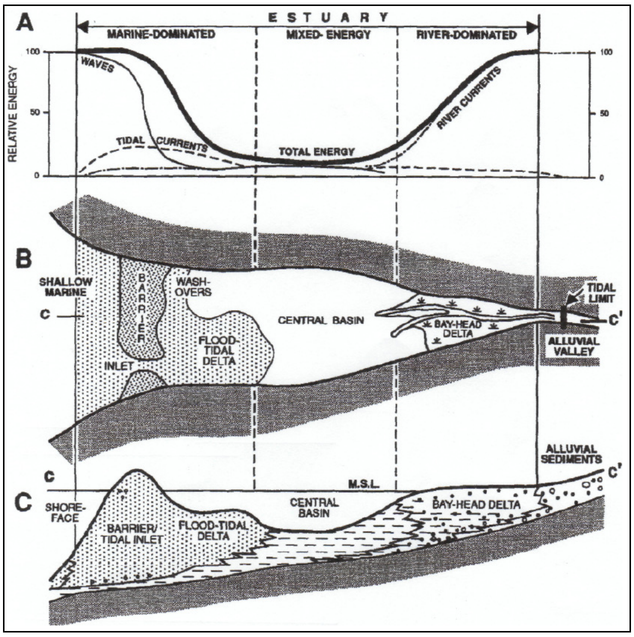

Figure 1.5 Distribution of A) energy types, B) morphological components in plan view, and C) sedimentary facies in longitudinal cross section within an idealised wave-dominated estuary. Note that the shape of the estuary is schematic. The barrier/sand plug is shown here as headland attached, but on low-gradient coasts it may not be connected to the local interfluves and is separated from the mainland by a lagoon. The section in C represents the onset of estuary filling following a period of transgression (from Dalrymple et al., 1992).

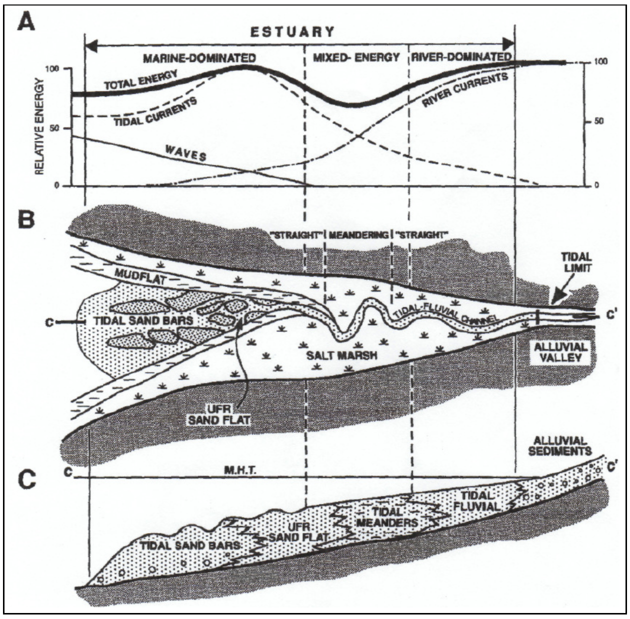

Figure 1.6 Distribution of A) energy types, B) morphological elements in plan view, and C) sedimentary facies in longitudinal section within an idealised tide-dominated estuary. The section in C is taken along the axis of the channel and does not show the marginal mud flats and salt marsh facies. It illustrates the onset of progradation following transgression, the full extent of which is not shown (from Dalrymple et al., 1992).

1.3.4.3. Morphological Classification of South African Microtidal Estuaries

Cooper (2001) provides a classification scheme for the microtidal east coast of South Africa, whereby tidal variance within the tripartite coastal evolution schemes may be ignored and the summary difference in facies accounted for by variation between fluvial discharge and wave energy. Here he recognises that the South African coastline has a unique set of coastal factors. The swell dominated coastline is characterised by a micro-tidal (Davies, 1964) or low mesotidal (Hayes, 1979) range of between 1.8-2.0 m (SAN, 2009) and a common sea-level history. In addition, the rivers which flow through KZN are sediment rich because of the steep hinterland and the catchment geology. What results is a series of what Cooper (1991a) terms "river mouth" configurations each with a distinctive morphology and facies zonation.

This classification scheme at the highest level is based on the open/closed nature of the estuary mouth. Those open to the ocean 70% of the time are considered open estuaries, those closed 70% are considered temporarily closed. Using this scheme, Cooper (1991a) defines the Amatikulu Estuary as open. Closed estuaries will not be discussed further and the reader is referred to Cooper (2001) for an in depth consideration of these features. Open estuaries are further subdivided into *barred open estuaries* and *non-barred estuaries*. Non-barred estuaries have little relevance to this study and will not be discussed further.

Barred open estuaries have supratidal barriers. Rivers that flow into these systems vary tremendously in size and discharge capacities. The smaller rivers have small tidal prisms and the open mouth is maintained by the river's discharge. These are often located in the lee of a headland. Typical examples include the Mvoti Estuary (Cooper, 1994) uMgeni (Cooper, 1991a; Cooper, 1993; Tinmouth, 2009) and the Keurbooms Estuary in the Western Cape (Reddering, 1983). Flood tidal deltas are seldom formed in these systems and marine sediment is usually transferred by over-washing and barrier seepage. Barred estuaries are further divided into two types of estuaries; *tide-dominated* estuaries and *river-dominated* estuaries.

Tide-dominated estuaries are estuaries which, despite a small coastal tidal range, are still able to maintain an open inlet and tidal prism. The facies in a tide-dominated estuary are most similar to those of the wave dominated estuary of Dalrymple et al., (1992), where a set of well defined prograding flood-tidal deltas occur and ebb-tidal deltas are absent due to high wave energy. If there is sufficient sediment supply a delta may be present. The dominance of flood-tide deltas in such estuaries show their tendency to act as sinks for marine sediment. Where these estuaries form coast parallel water bodies, the inlets can migrate. The upstream side of the flood-tidal delta is deep and suspended sediment settling of fine grain sediment is dominant. Further upstream extensive bayhead deltas form which are dominated by the deposition of fluvial sediment. These estuaries evolve by gradual infilling of the estuary due to bayhead delta extension; coupled with sediment supplied from the coast and from bank erosion. Floods provide an important function by scouring out the estuary and slowing down the infilling process. Tide-dominated estuaries occupy the coastal environment where fluvial sediment supply is low and where low gradients do not impede the tidal prism in the estuary. The inlet may close due to large coastal storms but will open during high discharge periods (floods) or through human interference.

River dominated estuaries lack the ability to maintain an inlet due to an insufficient tidal prism. This may be due to infilling of a previously tide-dominated estuary or a pre-existing morphological constraint on the tidal prism. There is a marked difference in the morphology between river-dominated and tide-dominated estuaries. The flood delta is very small or mainly absent and the ebb-tidal delta is absent or ephemeral due to the high wave energy. Often times, the elevated bed levels of the estuary mouth aid in reducing the flood tide-delta. The inlet in these systems is maintained by the discharge alone. These systems have thought to be degraded by some authors (Begg, 1978) but Cooper (2001) indicates that these systems have functioned in such a manner since the Holocene. Floods again play an important role in increasing the depth of the channel and removing sediment (Cooper, 2002). River-dominated estuaries are generally located on the KZN coastline because of the steep hinterland and, subtropical climate with high rainfall. The ensuing high sediment supply promotes the rapid infilling of the incised river valley.

A final concern is that dissipative barrier states, when coupled with an estuarine systems, are prone to extensive overwashing due to their subdued relief and gentle slopes. In this light they can often reflect wave-dominated features (c.f. Zaitlin et al., 1994) such as extensive overwash and mouth plug complexes. In this case, the estuary is less also likely to be perched.

CHAPTER 2

REGIONAL SETTING

2.1. STUDY AREA

The study area is located along the central KZN coastline (Fig. 2.1). The southern extent of the study area starts from the northern bank of the Thukela River to 7km past the Amatikulu Estuary. The area north of the Thukela River has been identified as one of the few areas where coastal progradation is occurring in South Africa (Bird, 1985; Cooper, 1991b; Olivier and Garland, 2003). Cooper (1991b) notes that the accretion rates of this section of coastline are in the order of 5 m a year. Cooper (1991b) further notes that episodic events, such as floods and storm, have caused small but noticeable shoreline retreats. These are likely to play a major role in the migration of the coastline. Olivier and Garland (2003) noted that during their three year study period of the dune development of the beach area north of the Thukela River, a drought had reduced the sediment supply to the area resulting in the steeping of the foreshore and narrowing of the beaches. This indicates how rapidly the area will adjust to current climatic conditions in order to maintain equilibrium. In terms of the sediment supplied to the coastline, here it is dominated by the Amatikulu and Thukela Rivers (Cooper, 1991b).

2.2. CLIMATE AND COASTAL HYDRODYNAMICS

The coastal climate along the KZN coast line is subtropical with a mean annual rainfall of between 900mm-1000mm and mean monthly temperatures of ~25°C in winter and ~30°C in the summer months. Between 60 to 80% of this rainfall occurs during summer (Tyson, 1987). Summer rainfall is a result of orographic forcing rainfall and cyclonic conditions whereas winter rainfall is a result of coastal low pressure systems moving in an easterly direction (Tyson and Preston-Whyte, 2004). Flood patterns are thus highly seasonal for the rivers of KZN (Cooper, 1990). Wind data from Cape St Lucia, ~ 120km north of the study area, show that the winds predominate from the SW, with subordinate peaks from the NNE (Cooper, 1991b).

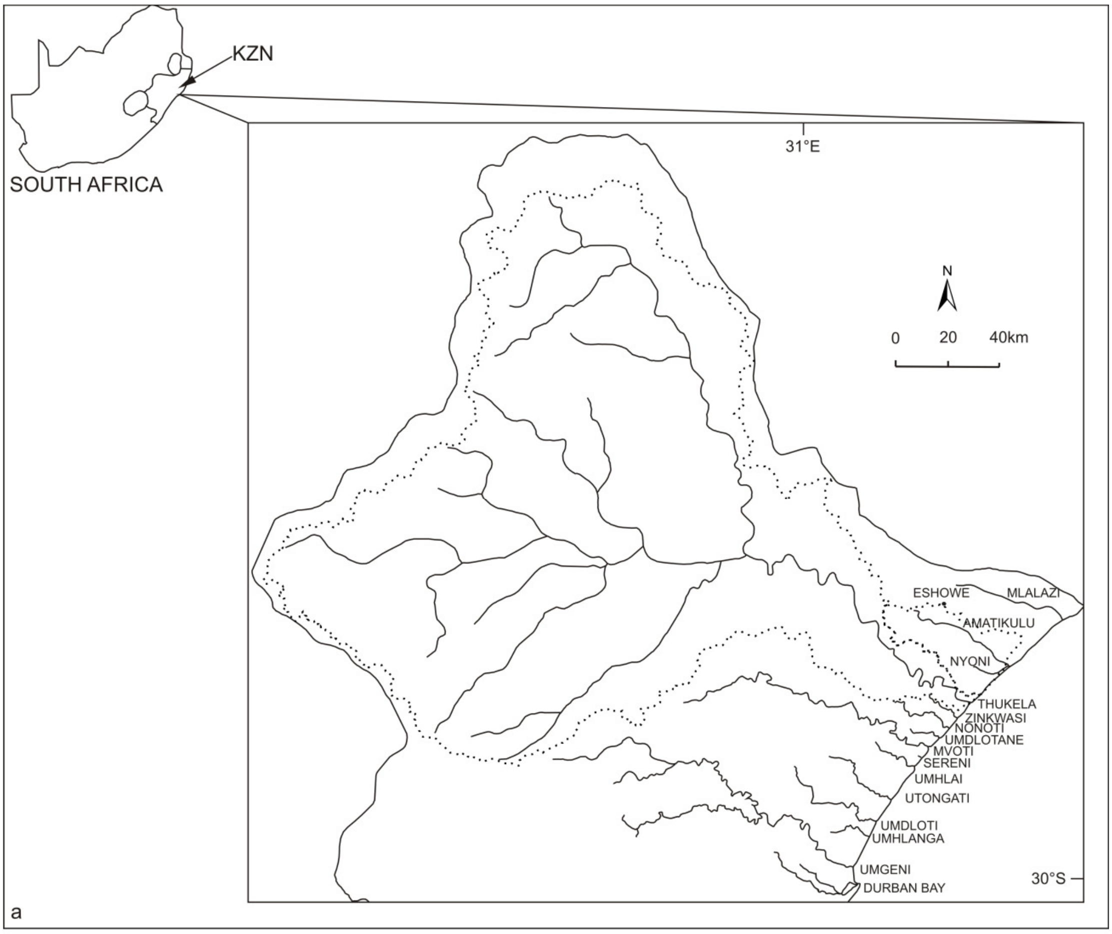

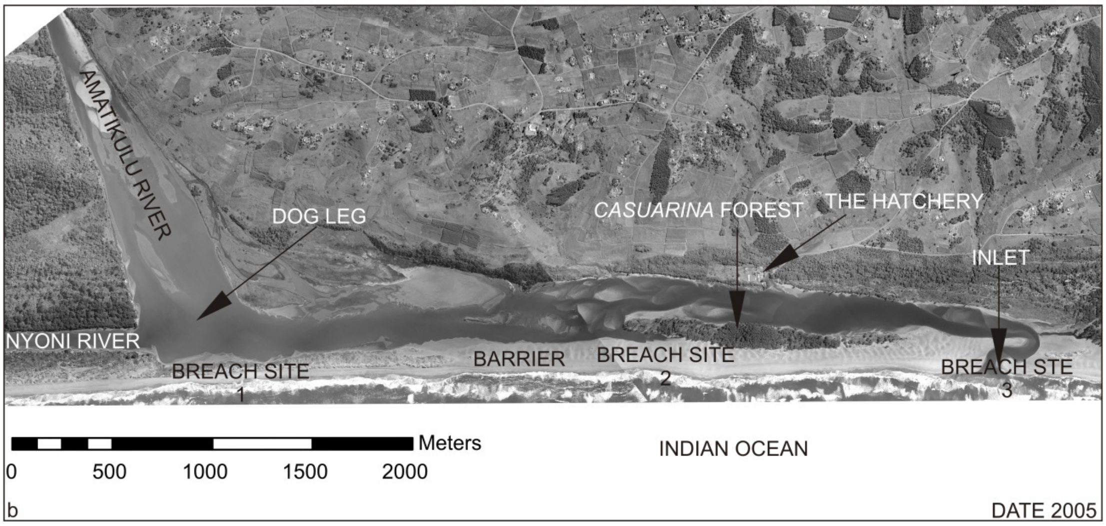

Figure 2.1 a) The Amatikulu River in relation to the other rivers north of Durban. The catchments of the Amatikulu and Thukela Rivers are indicated by a dashed line. b) The Amatikulu Estuary showing the named features used in Chapters 3-8.

The wave climate of the KZN coastline is generally classed as having a bi-modal distribution between the southwest and northeast direction (Roussouw, 1989). The dominant wave approach is from the SE all year round with a smaller subordinate ENE component. Occasional deep ocean swell from the S and the SW are rarer (Cooper, 1991b) (Fig. 2.2.).

Swells during storm activity can achieve a height of 14m (Smith et al., 2010). The coastline orientation from the Thukela to Amatikulu Rivers is striking at 042° (Cooper, 1991b). The dominant SE wave approach thus results in a northerly longshore drift direction (Fig. 2.2.). Longshore drift is enhanced during the winter swell regime (Smith et al., 2010) with a calculated annual erosion volume of 500 000m^3 at Richards Bay (Schoonees, 2000). In addition, the coastal orientation plays a major roll in aeolian sediment transport. Where the dominant wind blows onshore and sediments are transported landward, these are deposited in the fringing dune corridor which aids in the further construction of the dunes (Olivier and Garland, 2003).

2.3. COASTLINE GEOMORPHOLOGY

The rivers of the KZN coastline drain a steep hinterland with an average gradient greater than 1:100 (Cooper, 1990). The rivers provide large amounts of sediment to the coastline due to their catchments draining well developed soils that were formed by deep tropical weathering during the Pleistocene (Cooper, 1990). Cooper (1990) regards the Thukela and Amatikulu Rivers' catchments as large as they both cover an area of greater than 500km^2. Each catchment has an area of 29100km^2 and 995km^2 respectively. The Amatikulu River has a mean annual run off of 201.07$m^3 \times 10^6$ with a gradient of 1:126 (Cooper, 1990).

The coastal geomorphology of the shoreline comprises a linear, sediment-rich coastline with a beach that is approximately 80m wide (Cooper, 1991b). The beach is backed by coast parallel beach ridges that are of an average height of 5m (Cooper, 1991b). The beach ridges north of Amatikulu Estuary are separated by a low lying area roughly 200m wide (Cooper, 1991b). This

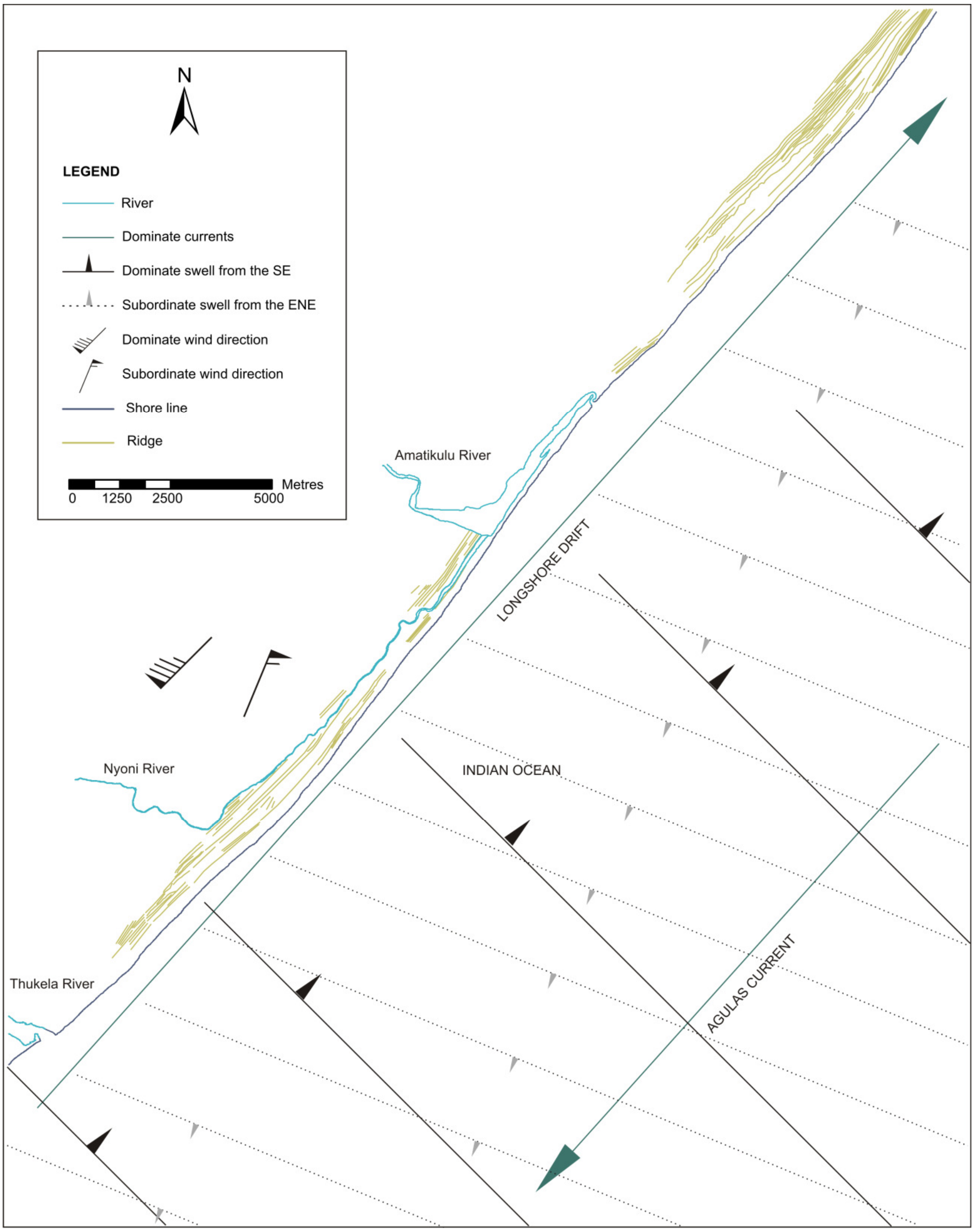

Figure 2.2 The Amatikulu coastline indicated the major processes that influence the morphology of the area.

low lying area is presumed by Cooper (1991b) to be a palaeo-extension of the Amatikulu Estuary ~5000 years ago during a minor sea level high at + 2m MSL (Fig. 2.3) (Cooper, 1991b; Ramsay, 1995). The presumed presence of the palaeo-estuary infers that the beach ridges are of different ages resulting from two discrete minor regressions (Cooper, 1991b).

Both the Thukela and Amatikulu Rivers play a major role in the progradational nature of this area by providing sufficient sediment to the coastal area thereby aiding in the creation of new landforms (Cooper, 1991b). The Thukela River since the latest Holocene sea level fall (Fig. 2.4) has obtained a new base level, allowing the direct transport of sediment through the Thukela Estuary. This sediment has been reworked by the wave action and transported in a northerly direction by the prevailing longshore drift direction (Cooper, 1991b). These sediments, along with the wave action, have constructed the many beach ridges in the area. The Amatikulu River in contrast to the Thukela River is a shallow, bedload dominated river, perennially open to the ocean (Cooper, 1991b).

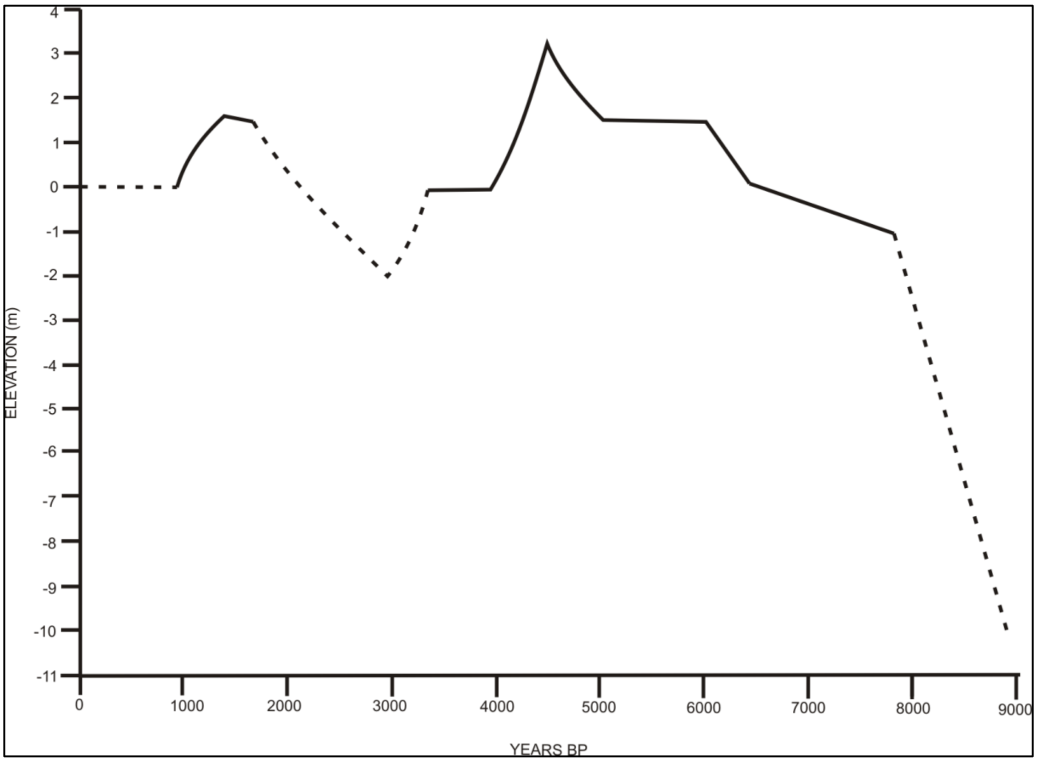

Figure 2.3 Holocene sea-level fluctuations of South Africa by Ramsay (1995) based on beachrock and shell dating techniques (from Ramsay, 1995).

2.4. SEA-LEVEL

The most influential events in terms of sea-level fluctuations for the study area correspond to the Last Glacial Maximum (LGM) (18 000 BP, Oxygen Isotope Stage 2) and the subsequent Flandrian transgression which resulted in the formation of the present coastal barrier (Ramsay and Cooper, 2002) (Fig. 2.4). Sea-levels of the LGM were between -130m and -125m below present sea level (Green and Uken, 2005) and began to rise rapidly from 18 000 BP (Ramsay and Cooper, 2002). A mid-Holocene high stand is evident, occurring ~ 4500BP at an elevation of 3.5m (Ramsay, 1995) (Fig. 2.4). A small regression occurred between 3880 to 3360 years ago, lowering sea-levels to -2 m MSL followed by a small rise at 1610 BP to +1.5m MSL. This level was maintained until 900 BP where it subsequently lowered to modern day MSL (Ramsay, 1995).

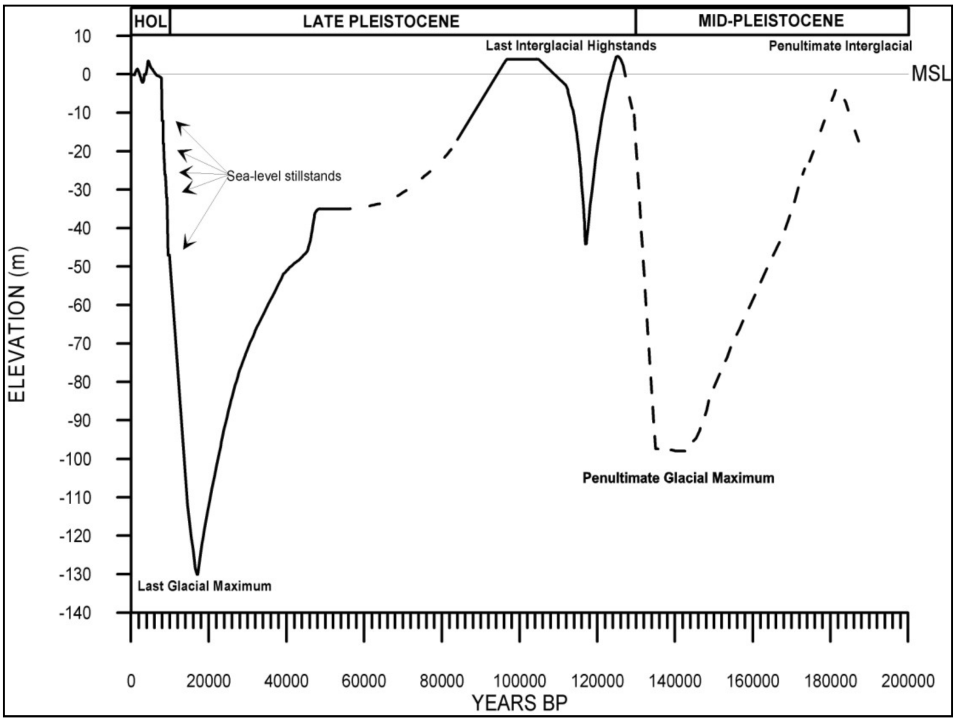

Figure 2.4 Mid-Pleistocene to Holocene Sea-level curve for the East coast of South Africa (from Ramsay and Cooper, 2002).

2.5. CATCHMENT GEOLOGY AND SOIL CHARACTERISTICS

The catchment of the Amatikulu River consists of Proterozoic basement granites, Natal Group and the lower units of the Karoo Supergroup, namely the rock units of the Dwyka and Ecca Groups (Begg, 1978; Cooper, 1991b) (Fig. 2.5). The estuary itself is underlain by deposits of Cretaceous age (Begg, 1978). Table 3.1 summarises the geology of the hinterland, detailing the different lithologies and soil weathering products. The lithologies that the Amatikulu River flows over provide mainly clay and sand sediment sized fractions to the Amatikulu River mouth and estuary (Fig 2.5) (Cooper, 1991a).

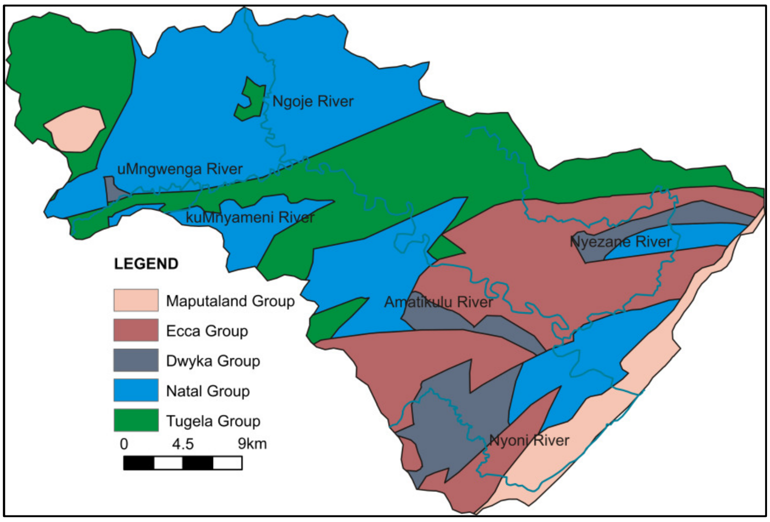

Figure 2.5 The geology (excluding Karoo Supergroup dykes) of catchment of the Amatikulu River and the tributaries that flow into the Amatikulu River (Catchment and river shape file courtesy of DWAF, geology of KZN shape file courtesy of Council for GeoScience.

Table 2.1 Regional geology of the Amatikulu River Catchment.

Age	Supergroup	Group	Formation	Member	Lithology	Additional comments	Reference
Holocene		Maputaland Group	Sibayi Formation		Cenozoic Coastal deposits	Parabolic dunes forming composite coastal barrier dune cordon	(Roberts et al., 2006)
Early Pliocene		Maputaland Group	Umkwelane Formation		Cenozoic Coastal deposits. Berea-type red sand with high clay content.	Karst-weathered aeolianite that is decalcified and rubified to form the Berea red sand with a high clay content a result of weathering of feldspar and mafic minerals.	(Roberts et al., 2006)
Permian	Karoo Supergroup	Ecca Group	Volksrust Formation Vryheid Formation Pietermaritzburg Formation		Mudstone to sandstones in an upward coarsening sequence.	Consists of 16 formations divided into geographical regions. NE region consists of: • Volksrust Formation. Deposited in a range of environments from shallow coastal to open shelf sequences. • Vryheid Formation. Upward coarsening sequence deposited in a deltaic environment • Pietermaritzburg Formation. Upward coarsening sequence consisting of mudstone to sand stone. The Ecca Group weathers to form a soil that consists up to 80% clay.	(Johnson et al., 2006) (Cooper, 1991a)
Late Carboniferous to Early Permian	Karoo Supergroup	Dwyka Group	Mbizane Formation		Diamictite	Deposited in a marine environment by ice sheets/glaciers. Tillite weathers to form fine sand loam that comprises of: 50% fine sand 25% medium to coarse sand 25% silts and clays.	(Johnson et al., 2006) (Cooper, 1991a)
4900Ma		Natal Group	Durban Formation	Eshowe Member	Medium-coarse arkosic sandstone and shale	Sediment derived from the Pan-African orogenic belt. Sediments deposited in debris flows and in a range of fluvial activities. Weather to produce loamy sands of 5-15% clay. The sand fraction is mainly quartzose and the feldspars weather to kaolinite.	(Marshall, 2006) (Cooper, 1991a)
~1000Ma to ~1200Ma	Namaqua-Natal Metamorphic Province (Tugela Terrane)	Tugela Group			Gneiss	Tugela gneisses intruded by grantoid body which weathers to form soil containing 30% clay. Amphibolites weather to produce a sandy loam comprising 60% sand of the medium to coarse sediment fractions.	(Cornell et al., 2006) (Cooper, 1991a)

2.6. PREVIOUS STUDIES OF THE GEOMORPHOLOGY OF THE AMATIKULU ESTUARY

The Amatikulu Estuary (Fig. 2.1a) is located at 29° 04'S; 31° 38'E, 105km north of Durban and 56km south of Richards Bay. Many values have been given for the size of the catchment area of the Amatikulu River. These range from 583km^2 (van Bladeren and Burger, 1989), 850-900km^2 (Begg, 1978) and 814km^2 (Cooper, 1991a). The river length is estimated to be between 84 to 108km long (Begg, 1978), with Cooper (1991a) defining it as 96km long from the source (762m above sea level) to the estuary mouth and Department of Water Affairs and Forestry defining the length as 58.70km. The Amatikulu Estuary is fed by the Amatikulu River and its five tributaries the Nyoni, kuMnameni, uMngwenya, Ngoje and the Nyezane Rivers (Fig. 2.5). Together these rivers have a combined length of 173.39km. Begg (1978) considers the mean annual run-off of the Amatikulu River to be from 132×10^6m^3 to 186×10^6m^3 whereas Cooper (1991a) quotes a value of 201.07 million cubic metres. The estimated flow rates range from 0.7m^3/sec to 4.2m^3/sec (Begg, 1978). During the 1987 cut off-low floods, the Amatikulu River recorded flood peaks of 3170m^3/s (van Bladeren and Burger, 1989). Overall, the average sediment yield of the Amatikulu River is ~224440 tonnes per year (Cooper, 1991a). In terms of the estuary itself, Begg (1978) defines its aerial coverage at 122ha (Begg, 1978). According to him, the bathymetry ranges from the deepest point at 7m at the dog leg bend of the river (Fig. 2.1b) to 1.5m near the contemporary mouth of the estuary (Begg, 1978).

The land use of the combined catchments of the Amatikulu and Nyoni Rivers consists of 60% agricultural comprising of sugar cane cultivation, subsistence farming and a small fraction of commercial forestry (Harrison et al., 2001). Natural grassland, bushland and forest comprise 33% of the catchment. Six percent is degraded bushland and less than 1% is urbanised (Harrison et al., 2001). This corresponds to Eshowe (Fig. 2.1a) and consists of residential, commercial and industrial components (Harrison et al., 2001).

2.6.1. Inlet and Sandbar Characteristics

The inlet mouth of the estuary has shifted many times in the past, frequently migrating from the most northerly extent of the estuary to the south at the dog leg (Fig. 2.1a, Begg, 1978). Begg (1978) documents the inlet in this southern-most position during March of 1976, when floods broke through the adjacent barrier. Begg (1978) further noted the migration of the inlet to its most northerly position in 1978. This dissertation deals with the inlet mouth dynamics of the estuary in more detail in Chapters 4 and 5. The inlet according to Begg (1978) is rarely closed.

The Nyoni River, which drains into the Amatikulu River, had a separate inlet until the floods of 1971. Thereafter the Nyoni River has flowed into the Amatikulu River sharing a common mouth (Begg, 1978; Day, 1981). Of particular importance is the subsequent contribution of the Nyoni River's $21.6 \times 10^6 m^3$ runoff flow to the Amatikulu system, undoubtedly assuring the near permanence of an open inlet.

The fringing barrier system is one of the most laterally extensive sediment bodies on the KZN coastline. When the inlet is in its northerly position, the sandbar can obtain a length of 4.8km in length. The sediment of the sandbar is supplied from the Thukela River in the south and transported, deposited and maintained by waves from the southeast (Begg, 1978; Cooper, 1991b). The length of the barrier is controlled by the position of the inlet on the barrier (Cooper, 1991b).

CHAPTER 3

METHODOLOGY

3.1. INTRODUCTION

This chapter outlines the methods used in this study. The photogrammetric techniques; bathymetric and topographic profiling; sediment sample collection, and the ensuing analyses methodologies are discussed in the following chapter.

3.2. AERIAL PHOTOGRAPHIC EVALUATION

Aerial photography spanning the years 1953, 1972, 1973, 1983, 1989, 1992 and 2005 were obtained for measurement purposes. Contact prints of A1 size were scanned at 400 DPI using an A0 scanner and then polynomially rectified using *Golden Software Didger 3* to an accuracy of 10 metres RMS. All images were projected to the WGS 84, UTM projection zone 36S. These were mosaiced in ArcGIS 9.2. Measurement of shoreline changes were made from the same transects as Cooper (1991a) and the shoreline defined by the high tide line as observed from photography (Moore and Griggs, 2002; Hanslow, 2007). All data were normalised to a common data set (1983), so that shoreline changes were comparable between this study and Cooper (1991a) (Fig. 3.1). Subsequent positions of the shoreline, beach ridges, embryo dunes, estuary extents, major bedforms, sand bars and tidal channels were digitised as ESRI shape files and later imported into *ArcGIS 9.2* where morphological changes could be accurately measured and compared. The shoreline changes were compared to the mean surface water discharge (m^3/s) values for the neighbouring Thukela River (DWAF, 2009) in order to assess coastal advance or retreat as related to flooding of the Thukela River. The surface discharge was measured at site V2H002 on the Thukela River at Mandini (Fig. 3.1).

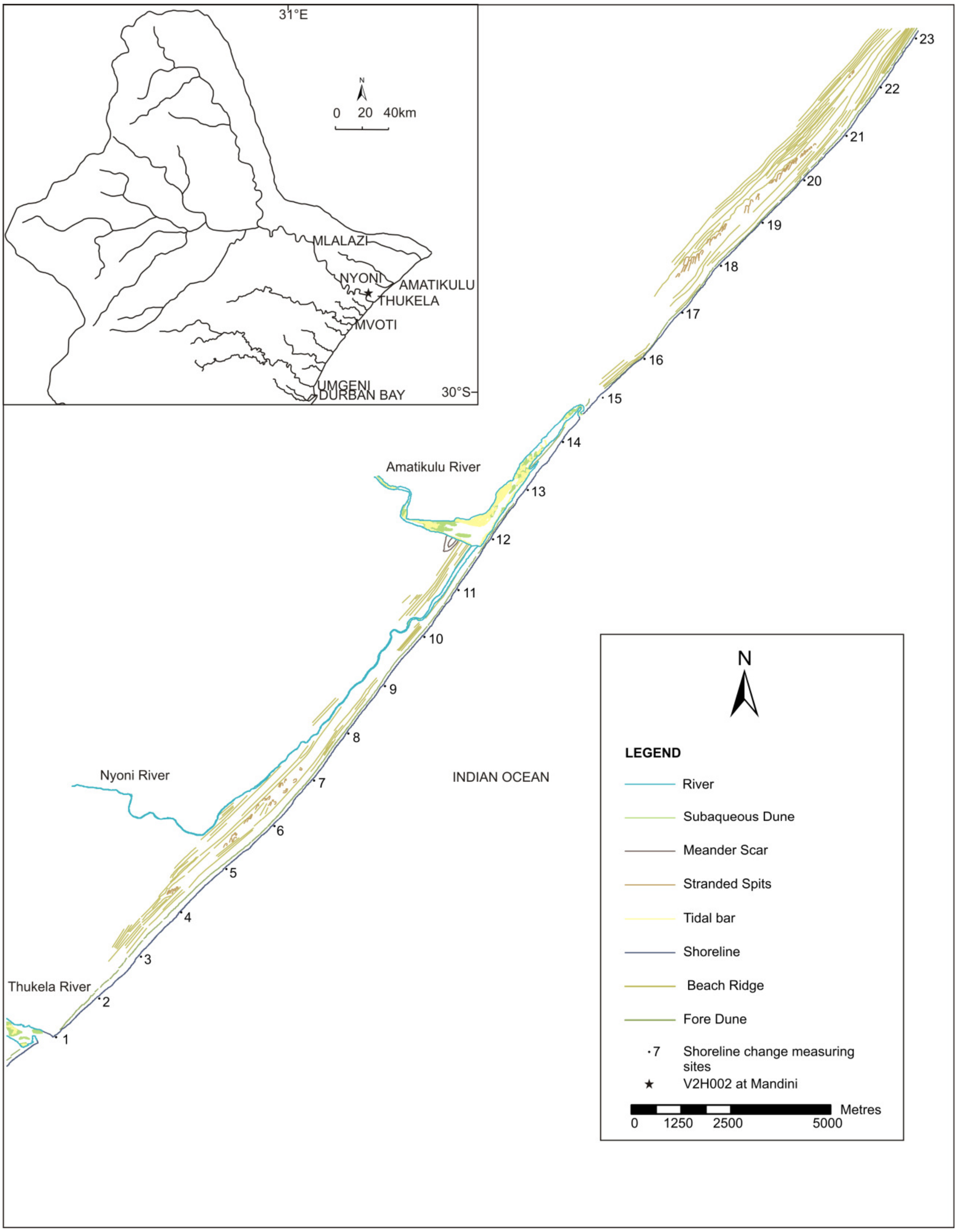

Figure 3.1 Shoreline change sample sites as per Cooper (1991b) and this study, represented on a basic geomorphological map of the Amatikulu Coastline to site 23 south of the Mlalazi River.

3.3. BATHYMETRIC AND TOPOGRAPHIC METHODOLOGY

The bathymetric and topographic data were collected over the period 25th-29th of May 2009 using echo sounding and survey technologies. The known base location for the survey was tied to the Betwa trig beacon, located at 6783357.20 N; 366409.24 E (UTM Zone 36S) with an orthometric height of 121.4m. The base for the survey was set up on the western shoreline of the Amatikulu Estuary to minimise transmission distance and maximise accuracy (Fig. 3.2a and b).

3.3.1. Data collection

3.3.1.1. Topography

Topography was assessed using a *Leica GS 20* GPS capable of resolving X, Y, Z data to an accuracy of under 2cm in all fields. The *Leica GS 20* base station was coupled to a roving unit which established uncorrected X, Y and Z data in the field area. This was initialised for 12 minutes. Thereafter the roving unit was set in both kinematic mode and stream mode in order to collect continuous data. Transects of the barrier and dunes were undertaken for 38 minutes along a profile with a spacing of 50m. Topographic features such as dunes were further traversed along the strike of the crest and on the seaward and landward side of the feature. Once the 38 minutes were completed, the kinematic mode was exited and the data were saved. The rover base was relocated and re-initialised for 12 minutes before repeating the entire process. All the *Leica GS 20* data were post processed using the following procedure. Data from the rover base and rover hand unit were extracted to *Leica Geo Office* where the base coordinate data were added to correct GPS drift of the rover hand unit and the rover base. This established the X, Y and uncorrected Z values of each logged point. The antennae height of the roving hand unit was then corrected to establish an accurate height value.

3.3.1.2. Bathymetry

A *Novatel RTK* GPS linked bathymetric survey was undertaken, with positioning and tides corrected to the pre-mentioned Betwa trig beacon (6783357.20 N; 366409.24 E). The GPS base (Fig. 3.2a) was set alongside the study area, at a known point of X, Y and Z co-ordinates. The roving unit was connected to a computer running *Hypack Survey Software* in order to log the X, Y navigational data on an inflatable boat (Fig. 3.3a). Bathymetry was acquired using a

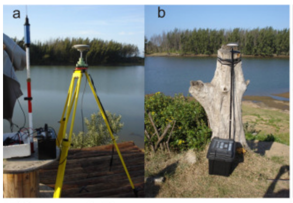

Figure 3.2

Figure 3.3

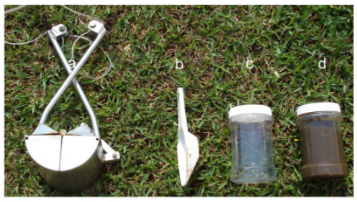

Figure 3.4

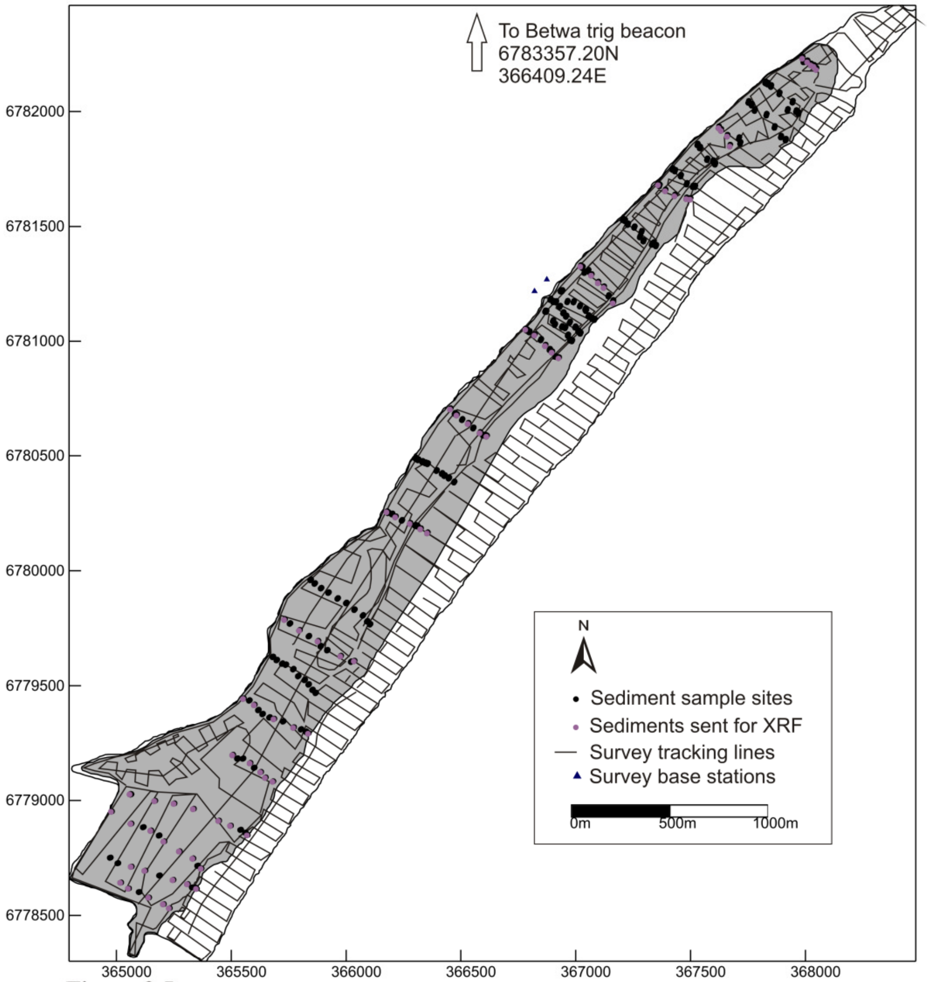

Figure 3.5

Figure 3.2 a) Real Time Kinematic base station. The RTK base station consists of a Novatal RTK GPS, survey tripod, Pacific Crest radius antenna (5 volts, range 6-10 km), and Pacific Crest Positioning Data Link low power base and battery pack. b) Leica GS 20 post processing kinematic GPS base station consisting of ranging rod, Pacific Crest radius antenna, base GPS and battery pack (All courtesy of Environmental Mapping & Surveying).

Figure 3.3 a) Inflatable duck, the echosounding equipment, computer with *Hypack Survey Software* linked to the Novavel RTK GPS. b)The *CEESTAK* survey grade echo sounder transducer, mounted on a small inflatable boat. The transducer operates on a 200 kHz-30kHz frequency resulting in a 0.01% depth accuracy (All courtesy of Environmental Mapping & Surveying).

Figure 3.4 Sediment Sampling tools. a) Modified van Veen sediment grab (Courtesy of Dr Brent Newman from the CSIR). b) 50ml spoon (Courtesy of Dr Brent Newman from the CSIR). c) Empty 230ml sample bottle. d) Full sediment bottle containing sediment sample with sample number located on lid.

Figure 3.5 Sample sites of the Amatikulu Estuary. The coverage of the bathymetric survey of the Amatikulu Estuary is highlighted by the grey area. The topographic survey lines on the barrier correspond to the unshaded portion. The base station sites for the surveys are indicated. The 219 sediments sample sites are indicated by black points and samples sent for XRF analysis are indicated by purple points.

CEESTAK survey grade echo sounder (200kHz-30kHz. 0.01% depth accuracy) (Fig. 3.3b). All data collected were corrected in real time to the base station's transmitted X, Y and Z co-ordinates, thus reducing all soundings to MSL via the RTK feed.

3.4. SEDIMENTOLOGICAL METHODOLOGY

3.4.1. Surface Sediment Sampling

Sediment sampling was conducted over the 28th and 29th of September 2009 throughout the Amatikulu Estuary (Fig. 3.5). Sediments were collected using a Van Veen grab (Fig. 3.4) along predetermined transects. Each sample was then transferred into a sample jar, sealed, labelled and transported back to the laboratory for analysis. Co-ordinates were fixed for each sample using a *Garmin Etrax* 12 channel GPS capable of a 5 metre position accuracy. A total of 219 samples of approximately 500g each were collected from a variety of sedimentary environments to ensure reproducibility.

3.4.2. Sediment Analysis

Sediment was analysed for grain size distribution, carbonate content, organic carbon content and chemical constituents (Fig. 3.6). Each sample (500g) was oven dried at 70°C, mixed and split into two sub samples of ~40g. The first sample was used for grain size analysis; the second sample was ground into a fine powder for carbonate and organic carbon content analysis. Selected remaining subsamples from the grain size analysis were reserved for XRF analysis (for a complete summary of the analysis procedure see Figure 3.6)

3.4.2.1. Grain Size Analysis

Grain size characteristics were analysed using the *Malvern Mastersizer 2000* laser based analyser. Three thirty second sample periods were recorded and averaged to reduce the risk of rogue grain skewing of the results. All values were calculated using a volume percentage. The results were used to calculate the median (Md), mean (M), sorting (σ) and the skewness (Sk) characteristic of each sample, based on the graphical equations of Folk and Ward (1957). The equations are calculated in phi (Φ) using the 5th, 16th, 50th, 84th, 95th percentiles. The sediment statistical parametres are presented as contoured maps of the Amatikulu Estuary.

3.4.2.2. Calcium Carbonate

Calcium carbonate content was measured using the gaseometric technique outlined by Schink et al., (1978). This technique has been proven in its effectiveness by many authors in estuarine and coastal research (Dyer, 1986; Cooper, 1991a; Olivier, 1998; Olivier and Garland, 1998; Wright, 2002; Tinmouth, 2009). With respect to expense and accuracy, when analysing large numbers of samples, the gaseometric method is the simplest and best (Seisser and Rodgers, 1971). Calcium carbonate is predominantly derived from marine shell fragments, the calcium carbonate content can therefore be used to indicate the extent of marine influence into the estuarine system (Dyer, 1986).

3.4.2.3. Organic Testing

Organic content was calculated using the organic material digestion technique set out by Walkley and Black (1934) and Walkley (1947). This method was adopted for ease in conducting the testing on multiple samples and the yielding of consistent results. The method results in complete organic digestion without removing bound water from the clay minerals which can cause elevated organic content results, considered a problem with weight loss by ignition methods (Meade et al., 1975; Cooper 1991a). The digestion method can further allow for direct comparison of organic content of other estuaries in which this method was employed, such as the uMgeni Estuary (Cooper, 1986, Tinmouth, 2009).

3.4.2.4. Geochemistry

XRF analyses were conducted within accordance to International certified standards of calibration (Table 3.1) on 73 selected samples (Fig. 3.5) in order to asses the major and minor elemental composition of sediments of the Amatikulu Estuary (Appendix B). These elements provide reliable indicators of anthropogenic pollution, when compared to natural levels (Binning and Baird, 2001). A similar methodology of bulk sample analysis was used by Leuci (1998) and Tinmouth (2009) for the analysis of Durban Harbour and the uMgeni Estuary respectively.

For the XRF analyses, a Phillips PW 105 and Phillips X' unique II X-Ray photo meter were employed. The samples were prepared by drying of ~100g of sediment at 100°C for 12 hours. The dry samples were milled with a pestle and mortar to a fine powder. The sample was split into ~10g for the XRF testing. Approximately 1g of sample underwent organic matter testing using the loss of ignition method where the sample was heated at 550°C to calculate the organic matter of the sample. The XRF analyses were conducted via two methods. The trace elements were tested by pressing a powdered disk of the sample. The results for the trace element method were represented in parts per million. The major and minor constitutes were made into a glass bead, where the powdered sample is fused with lithium metaborate or tetraborate. These results are presented as a weight percentage.

Normalisation of data were conducted in order to make the data regionally applicable and directly comparable to other estuarine analysis. Normalisation to a reference element removes the effect of grain size on the concentration on particular elements (Schropp et al., 1990; Chapman and Wang, 2001). The calculated conservative reference element for this study is Aluminium. The calculation for normalisation was conducted in the following manner:

- Major and minor elements:
  1. Major and minor elements converted into molecular weight by removing oxygen.
  2. Major and minor elements converted into a ratio with Al therefore normalising the element.
- Trace elements:
  1. Al converted from parts per hundred to parts per million by multiplying by 10000.
  2. Trace elements are converted into ratio with Al (trace element $_{ppm}$ /Al $_{ppm}$) therefore normalising the trace elements to the conservative element Al.

Table 3.1 International certified standards used in the XRF analysis

	Major and Minor elements			Trace elements	
	Detection Limits (%)	Analytical Accuracy (%)		Detection Limits (ppm)	Analytical Accuracy (%)
SiO2	0.004	0.2	Nb	0.1	3
Al2O3	0.005	0.5	Y	0.3	3
Fe2O3	0.001	0.5	Rb	0.4	2
MnO	0.001	0.5	Zr	0.3	3
MgO	0.011	0.3	Sr	0.2	3
CaO	0.0003	0.2	U	0.1	20
Na2O	0.018	2	Th	0.5	20
K2O	0.0003	0.2	Zn	0.3	10
TiO2	0.0004	0.2	Cu	0.2	10
P2O5	0.001	0.2	Ni	0.1	5
			Cr	0.6	5
			V	0.5	10
			La	1.5	15
			Pb	1	10
			Ga	0.2	10
			Co	1	10
			Ce	0.13	5
			Nd	0.3	5
			AS	0.001	10
			Cd	1	20
			Sn	1	10
			S	0.001	10

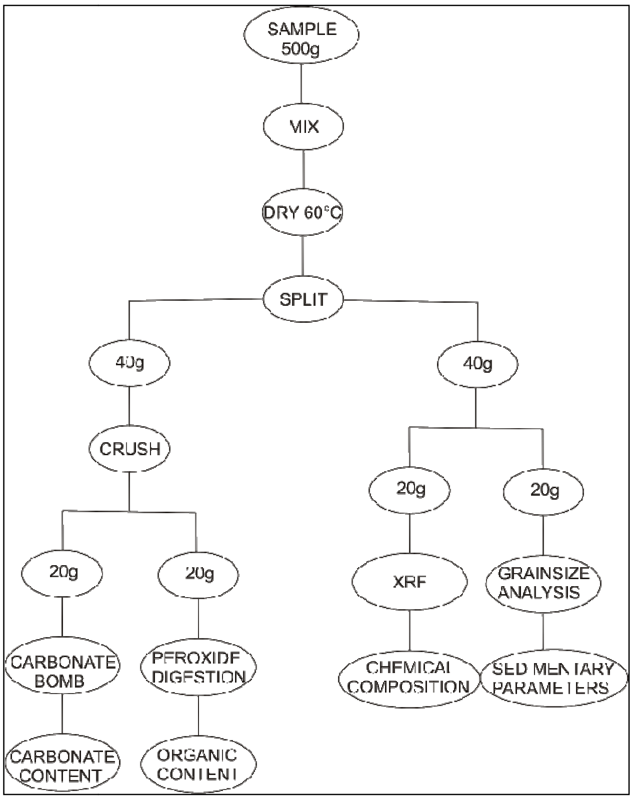

Figure 3.6 Flow chart of the laboratory analyses of sediment samples.

3.5. DATA REDUCTION

3.5.1. Survey Data

Topographic maps were created using the *Surfer 9* software package. Data were gridded using the Kriging method with a line spacing of 5m and a search ellipsoid of 100m, divided into 8 search sectors. The data were then spline smoothed using the insert nodes method where 4 nodes were introduced between columns and 4 nodes between rows. Spurious data were edited out using the grid node editing function. The data were then cropped to the limits of the Amatikulu Estuary and barrier using an ESRI shape file.

3.5.2. Sedimentological and Geochemical Data

Sedimentological and geochemical data maps were created using the *Surfer 9* software package using the Kriging method with a line spacing of 100m and a search ellipsoid of 400m, divided into 8 sectors. The data were then spline smoothed using the insert nodes method where 6 nodes were introduced between columns and 6 nodes between rows. The data were then blanked using an ESRI shape file created for the outline of the Amatikulu Estuary.

CHAPTER 4

HISTORICAL EVALUATION

4.1. INTRODUCTION

Aerial photography has been used successfully in estuaries and along coastlines in several studies of short to medium term change of coastal landforms (e.g. Smith and Zarillo, 1989; Cooper, 1991a; Moore and Griggs, 2002; Wright, 2002; Green et al., 2006; Hanslow, 2007). Related to this study was the analysis, by Cooper (1991b), of several sets of aerial photography covering the Thukela-Amatikulu coastline. These spanned the years 1937, 1978 and 1983 (Fig. 5.1). Additional sites in the northern portions of the study area included photography from the years 1957 and 1960. A specific number of sites were chosen where coastal advance or retreat could be measured from, based on the line of high water (or wet sediment) as a benchmark (Moore and Griggs, 2002; Hanslow, 2007). In all, Cooper (1991a) examined 23 sites starting in the south of the area at the Thukela River mouth (site 1), spaced 1500m apart and extending in a northerly direction. These sites were used to observe shoreline changes, the value for the change was later calculated as the net rate of change over the entire photographed time. The aim of this chapter is to supplement the study of Cooper (1991b) with additional aerial photography in an attempt to not only refine figures of coastal advance or retreat, but to extend this assessment to later years. In addition, this chapter aims to provide a morphodynamic assessment of the Amatikulu Estuary from this aerial photography.

4.2. RESULTS

4.2.1. Shoreline Changes

Figures 4.2-4.6 depict shoreline change between the Thukela River mouth and the northernmost extent of the study area, separated into the measurement sites as described by Cooper (1991b). The southernmost sites all indicate 1) two sharp and well-defined post-catastrophic flood peaks in shoreline growth from 1973 to 1978, and 1983 to 1989; and 2) a dramatic period of shoreline erosion subsequent to the maximum peak in shoreline advance. Sites 1-6 experience a mean shoreline advance of 55m/yr between 1983 and 1989, with peak progradation at site 1 of 680m. Likewise, sites 7-12 experience similar mean shoreline advances of 31m/site/yr for this period. Shoreline erosion from 1989-1992 was comparatively rapid following this period of growth, sites 1-12 all experiencing at least 50m of erosion. Site 1 experienced a maximum erosional shoreline adjustment of 418m. Between 1973 and 1978, an overall period of progradation was experienced (mean = 25m/site/yr). Sites 9, 11 and 12 are anomalous, experiencing minor erosion of 1m (within the RMS error), 17m and 18m respectively.

The northern sites 13 to 23 show a significantly smaller peak in coastal retreat between 1983 and 1989, with a mean of -2m/site/yr. In addition, minor changes in shoreline position from 1972 to 1978 are evident, though site 19 and 20 experienced erosion of ~ 190 m in 1972. Complete photographic coverage in the north over the years 1957 to 1972 reveals that the sites 16-21 experienced a gradual shoreline progradation (mean = 26m/site/yr) from 1957 to 1972. This was followed by a rapid phase of coastline retreat corresponding to ~136m/site for the northern sites (13-20).

Since 1990, an overall slight net seaward growth of the shoreline has occurred throughout both the southern and northern sites. Marked departures of this trend are evident in site 1, where the shoreline has receded from the survey baseline by 200m.

A clear pattern emerges from data showing mean overall coastline change over time for the entire area. Progradation is marked by relatively slower rates when compared to erosion which usually follows a protracted period of coastline advance. Maximum values of coastline progradation correspond to peaks in 1972 and 1989, with less intense progradation occurring in 1978. Values of 140m, 45m and 150m occurred respectively. Peaks in coastal erosion of 40m, 30m and 42m corresponded to the years 1973, 1983 and 1992. Time elapsed between maximum discharge or catastrophic flooding events and maximum coastline advance is calculated as 2.6 years from the 1987 floods to the 1989 peak; 4 years between a recorded 4090 m^3/s discharge and the small peak in 1978; and 6 years between Cyclone Claude and the 1972 peak (Fig. 5.1). Erosion in most cases occurred after or during periods below a threshold of $300m^3/s$. Overall the net coastline advance is calculated at 2.9m/yr. This was assessed by the sum of the total change in coastline position between sequential photo sets, divided by the time elapsed and the number of sites.

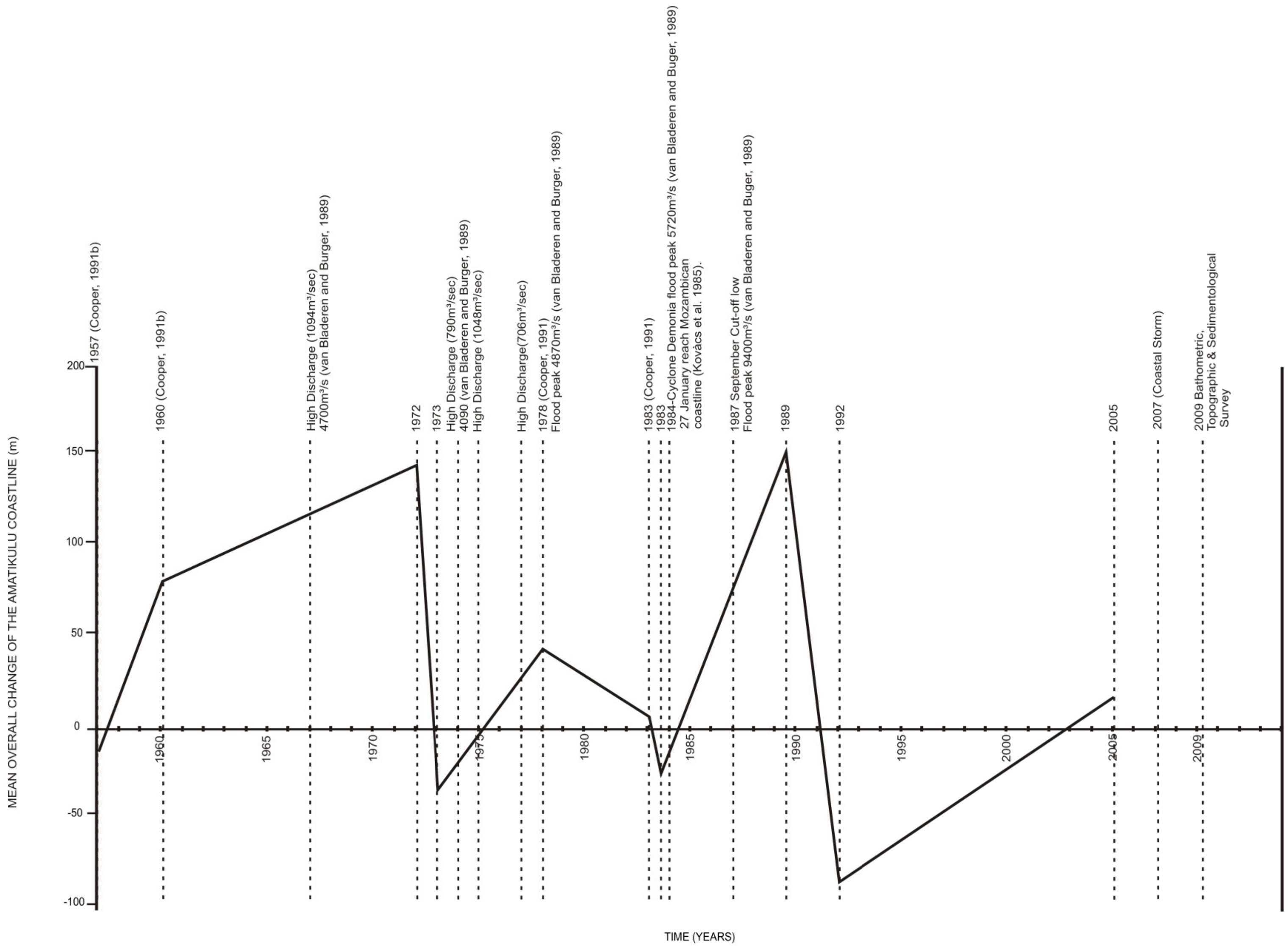

Figure 4.1 Mean change(m) of the Amatikulu Coastline with all the recorded catastrophic events with the corresponding catastrophic events with the peak recorded discharge for the Thukela River and the years where Cooper's (1991b) data was supplemented in to the calculated data.

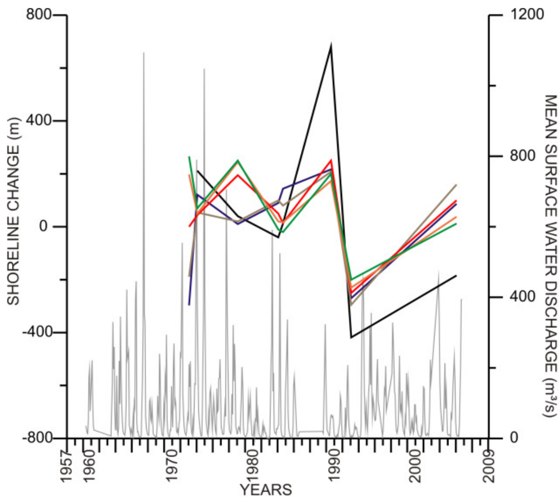

Figure 4.2 Shoreline measurement sites 1 to 6.

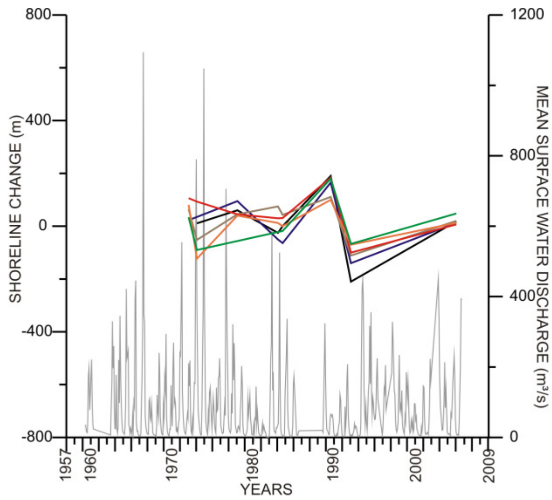

Figure 4.3 Shoreline measurement sites 7 to 12.

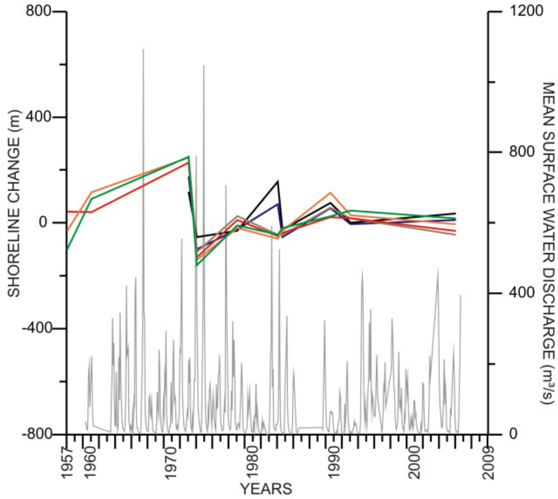

Figure 4.4 Shoreline measurement sites 13 to 18.

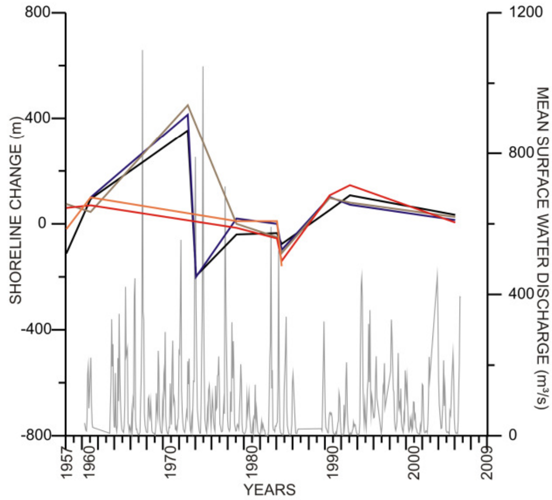

Figure 4.5 Shoreline measurement sites 19 to 23.

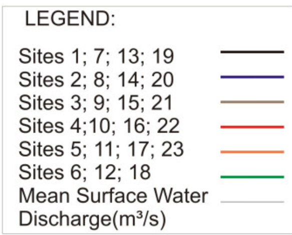

Figures 4.2-4.5 Show shoreline change sites of the coastline from the northern bank of the Thukela River spaced at 1.5km apart plotted against the Mean Surface Water Discharge (m^3/s).

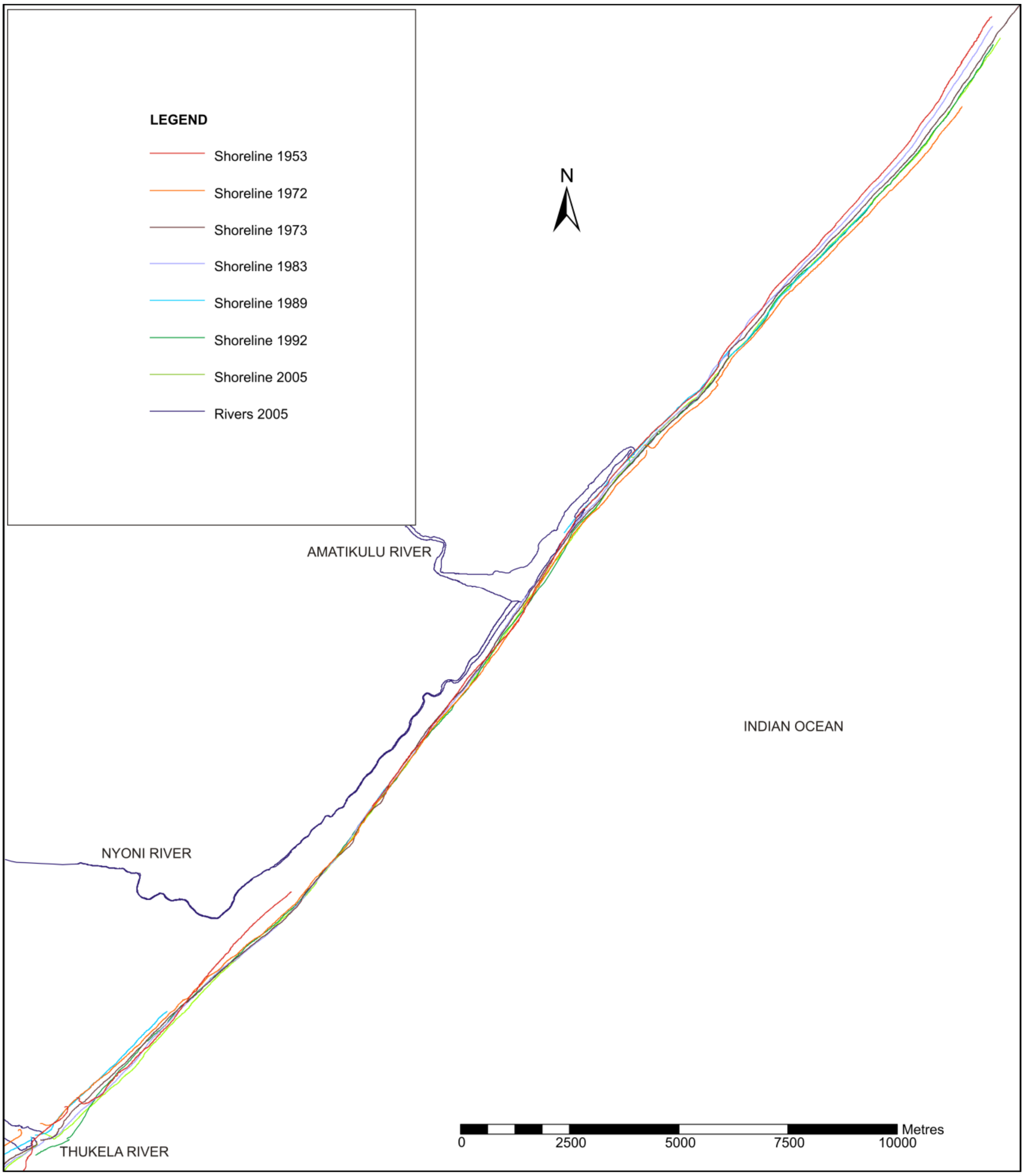

Figure 4.6 Changes along the Amatikulu coastline from 1953 to 2005.

4.2.2. Changes in the Amatikulu Estuary and Barrier

The earliest sets of aerial photography (1937) (Fig. 4.7) are problematic in that they lack the fiducial points necessary for rectification purposes. In this case, only a descriptive view of the morphology may be put forward. This photographic set shows a well defined main channel that flows shore parallel. Within the main tidal basin, the channel appears to be significantly wider than in later years. There appear to be few distinguishable features in these reaches of the estuary, though in the upper reaches three large bank attached supratidal bars occur, drained by an anastomosing network of smaller tidal channels. The tidal inlet is located midway between the Nyoni River confluence and the northernmost extent of the Amatikulu Estuary. This is characterised by recurved spits on both sides of the inlet and what appears to be a very crude ebb-tidal delta, likely an ephemeral mouth bar as described by Cooper (1990). The Nyoni River at this point is almost completely plugged by sediment. The barrier fringing the entire estuary comprises well developed foredunes which terminate on the southern side of the inlet mouth.

Several changes in estuarine morphology are apparent from the 1953 photo set, namely the narrowing of the tidal channel. This now contains at least eleven large (548m in length) and several smaller washover fans, the largest of which appear to have plugged the old 1937 inlet (Fig. 4.8). In addition, the more sinuous northern reaches of the estuary are completely inundated by sediment with several small parabolic dunes developing on the landward side of the channel terminus. The upper reaches of the Amatikulu Estuary are defined now by a single large supratidal bar (147 190m^2) dividing the main channel into two separate smaller channels. One of the older bank attached bars has become welded to the northern bank of the Amatikulu Estuary and is covered by extensive vegetation (most likely salt marsh). Foredunes on the barrier have been blanketed by overwash sediments which have widened the barrier considerably. Overwashing into the Nyoni River is also evident, maintaining the separation between the Nyoni and Amatikulu Rivers.

The most striking changes to the 1972 Amatikulu Estuary are the development of an inlet (77m wide) in the northernmost portion of the estuary and the now unimpeded confluence of the Nyoni and Amatikulu Rivers (Fig. 4.9). Within the inlet, the southern bank has a recurved morphology, whereas the outer bank is eroding. In the western portions of the estuary, the supratidal areas have consolidated and now maintain bank attached bars. Overall downstream migration of this package of sediment is ~140m. This has resulted in the Amatikulu Estuary being confined to a single channel which bends at ~ 90° into the main tidal basin. The total extent of the upstream supratidal bar complex is now 345 040m^2.

In addition to the inlet and backbarrier changes, the barrier has also changed significantly. Vegetation, which once separated the Nyoni River from the Amatikulu River, has been removed. Seaward and just north of this area, embryonic dune vegetation now covers an area of 7970m^2. Where the overwash fans were situated in the mid portions of the barrier, these have now been vegetated by *Casuarina* plantation. On the western shore of the estuary, the emerging parabolic dune field has been vegetated, presumably by artificial means.

Within a year the estuary inlet migrated to a more northerly position by 398m (Fig. 4.10). An extensive sediment plume has been ejected from the Amatikulu Estuary extending ~7km out to sea. Submerged and emergent bars are present in the upstream of the inlet and represent reworked flood-tide deltaic material. Further downstream extension of the supratidal complex is apparent, constricting the main tidal channel to a narrow point of 47m wide near the confluence of the Nyoni River. The vegetated areas of 1972 have matured and thickened in all three areas.

In 1983 the estuary closed with the plugging of the northern inlet (Fig. 4.11). A single main channel is visible throughout the estuary with subaqueous very large dune crests visible from the photographs (wavelength = 300m). A small splay has developed on the northern bank of the supratidal area, though the main channel is still confined to its 1973 position. By this point, the Nyoni River has been permanently captured by the Amatikulu Estuary. The barrier still only has three isolated areas of vegetation. Isolated overwash fans are present north of the established *Casuarina* Forest. A relict overwash fan is apparent in the mid portions of the barrier parallel tidal channel. It is around this that the channel meanders. The barrier itself has begun to develop an extensive, shore perpendicular embryonic dune field.

The 1989 images show that the Amatikulu Estuary inlet is closed. There is evidence of a recent breach closure in the south of the barrier (Fig. 4.12) where the previous southern inlet had reached a width of 1113m removing the fringing barrier vegetation (Fig. 4.13). Large overwash fans are present inland of both the southern and northern closed inlets, in addition to the central regions south of the *Casuarina* forest. The supratidal bank attached bars have been substantially reduced in size and are reduced to three small islands that have a combined area of 107 519m^2. The main subtidal channel is no longer confined to the southern bank by these bars. With respect to the barrier, it is now covered from the Nyoni/Amatikulu River confluence in the south, to the now well established *Casuarina* forest in the north, by embryonic dunes.

Again the images for the 1992 Amatikulu Estuary depict a closed system (Fig. 4.14). Large overwash fan have buried the barrier vegetation south of the *Casuarina* forest. Some intertidal bars are apparent in the mid-sections of the tidal basin, however the estuarine morphology has changed little since 1989.

By 2005 the inlet has once more opened in its northern position, possessing a meandering inlet 67m wide (Fig. 4.15). Extensive supratidal bars are present at the head of the estuary covering an area of 161 206m^2. The supratidal bank attached bars have once again grown and have now attained an aerial extent of 107 417m^2. Their position is essentially the same as that of the 1992 data set, indicating that this portion of the estuary is an effective sediment trap. The sediment trapping capabilities of these areas is further confirmed by the enrichment of these areas above natural levels in Cu, Sn and Zn (See Chapter 7 Fig. 7.7) and concentrating Cd (See Chapter 7 Fig. 7.5). Small transverse braided bars are exposed in the middle reaches of the tidal basin. Most strikingly, the tidal channel is attempting to establish a new course around the well developed *Casuarina* forest on the seaward side.

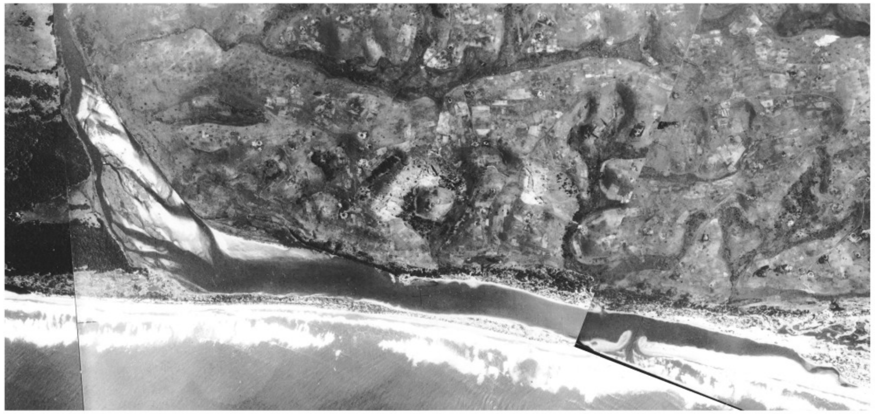

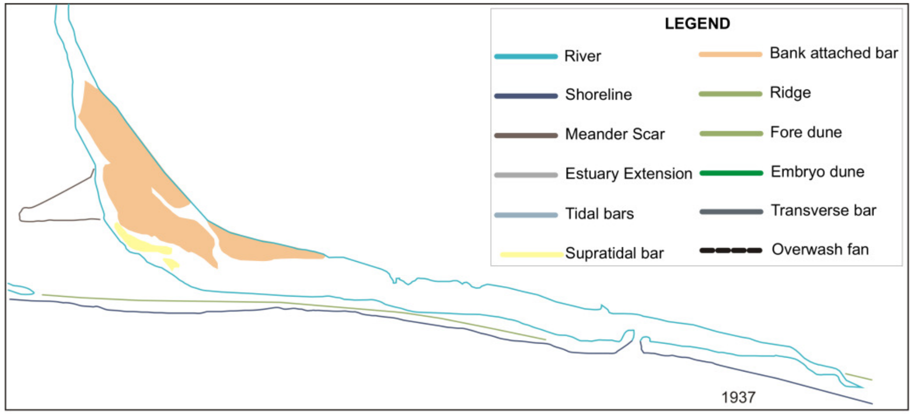

Figure 4.7 Unorthorectiable but indicates the Amatikulu and Nyoni Estuaries individual inlets and the Amatikulu breaching through the central area of the barrier.

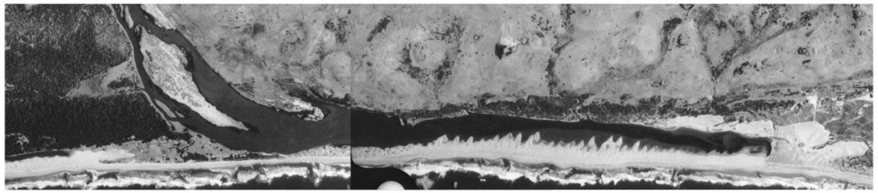

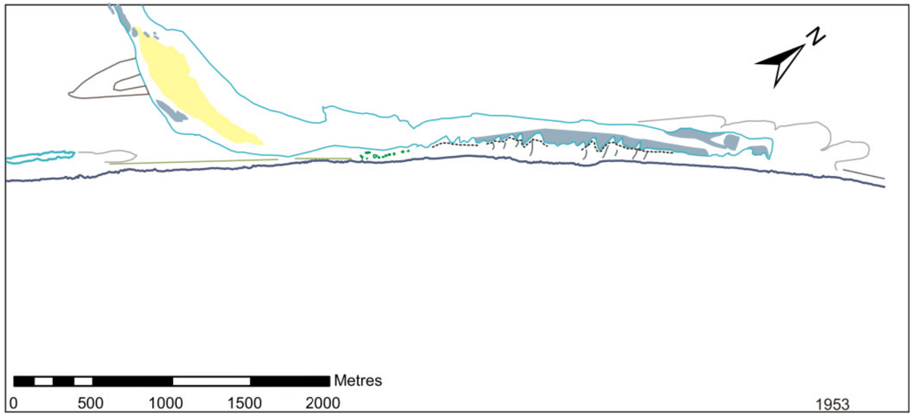

Figure 4.8 The Nyoni Estuary extensions approaching the Amatikulu Estuary. The Amatikulu Estuary extending into the north east. Large overwash fans are visible on the Amatikulu barrier.

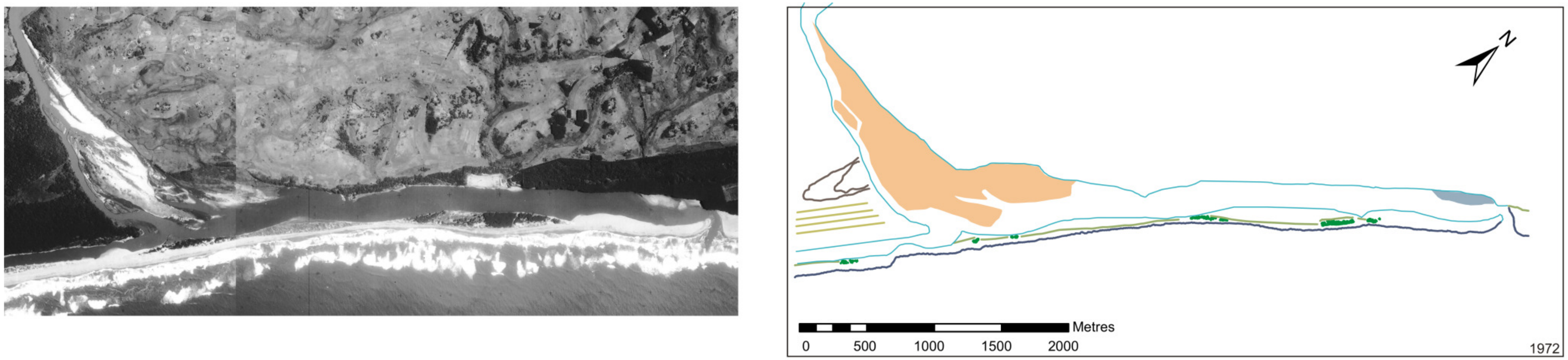

Figure 4.9 The capture of the Nyoni Estuary by the Amatikulu Estuary in 1972.

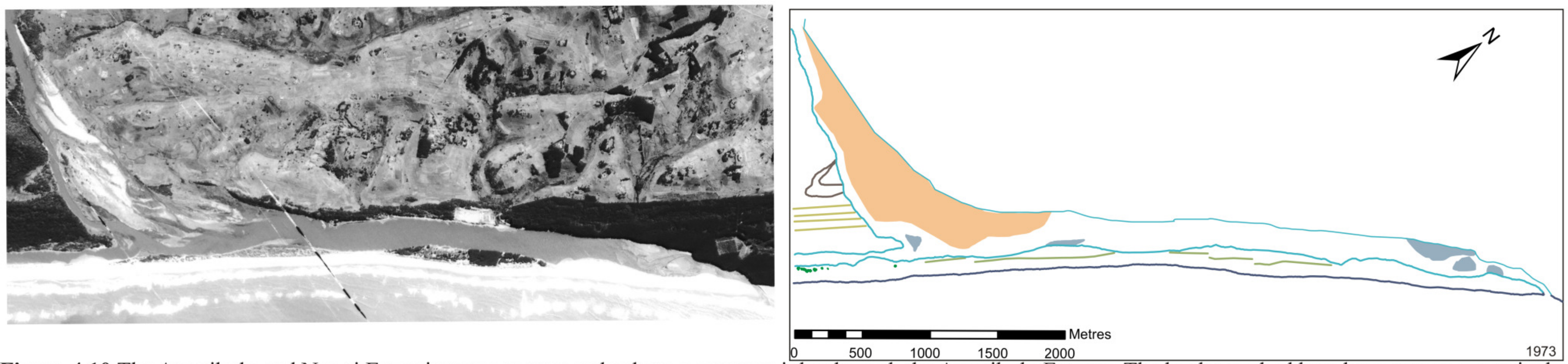

Figure 4.10 The Amatikulu and Nyoni Estuaries now permanently share a common inlet through the Amatikulu Estuary. The bank attached bars have grown extensively confining the Amatikulu River to the south bank.

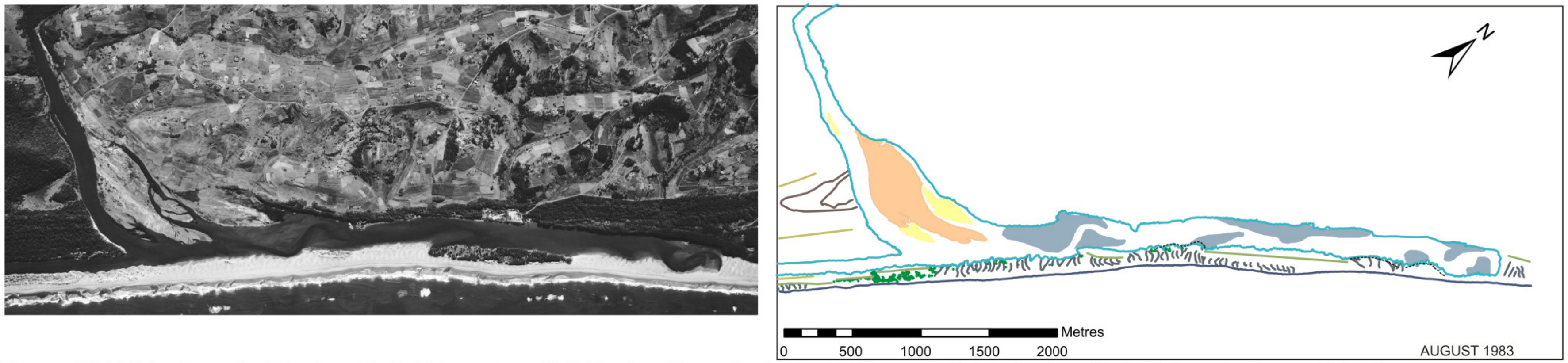

Figure 4.11 Main channel of the Amatikulu Estuary is well defined and large bank attached bars confining the Amatikulu Estuary to the south bank.

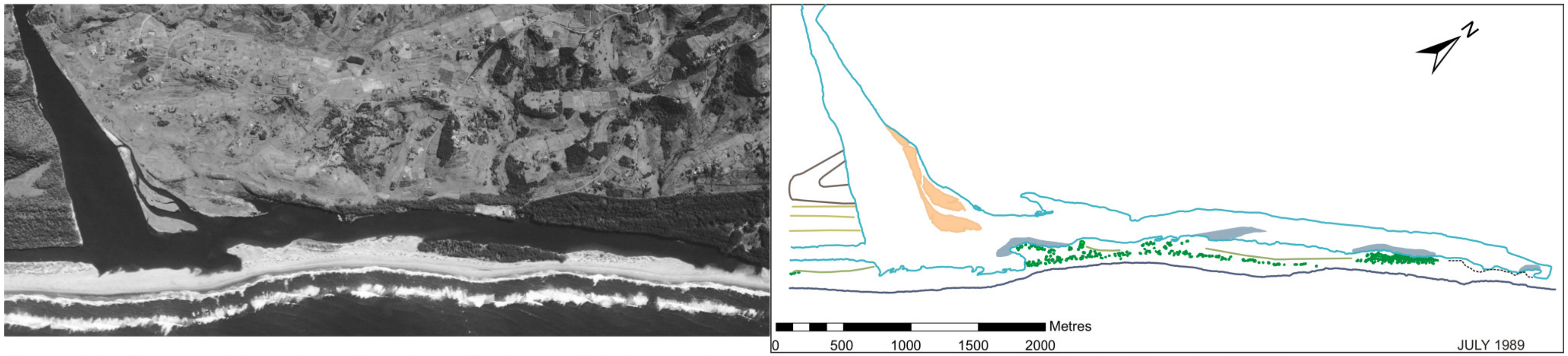

Figure 4.12 The loss of channel morphologies in the Amatikulu Estuary and post flood recovery (see figure 4.13 for flood breach of 1987)

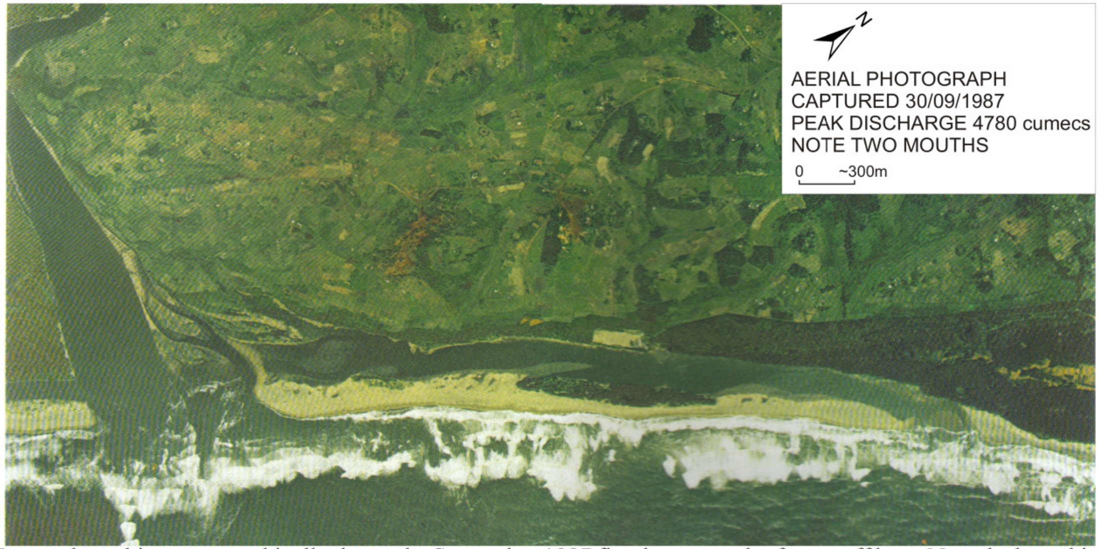

Figure 4.13 The Amatikulu Estuary breaching catastrophically due to the September 1987 floods as a result of a cut-off low. Note the breaching of the barrier at the dog leg bend and the maintenance of two mouths. The flood breach is approximately 900m wide (Figure adapted from Perry (1989)).

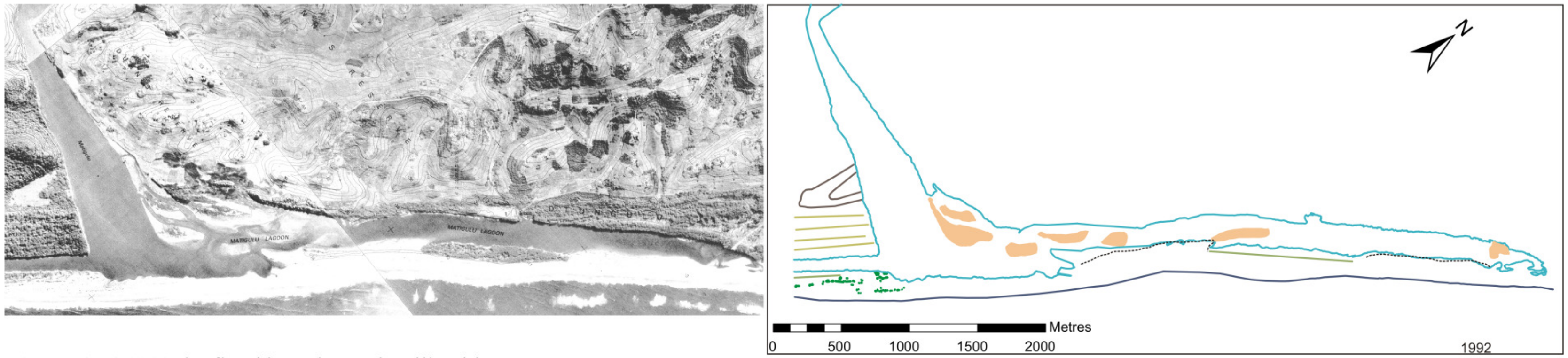

Figure 4.14 1992 the flood breach scar is still evident.

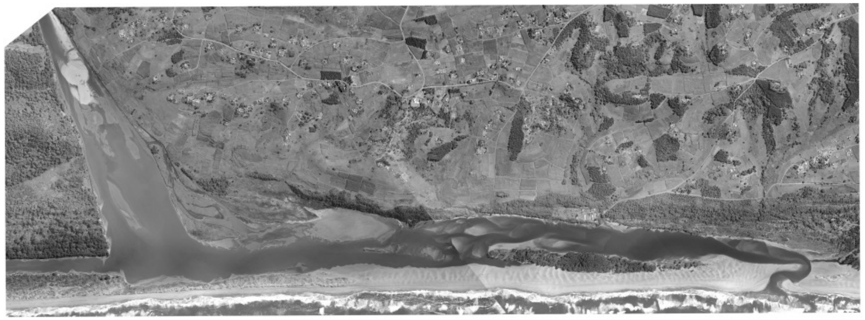

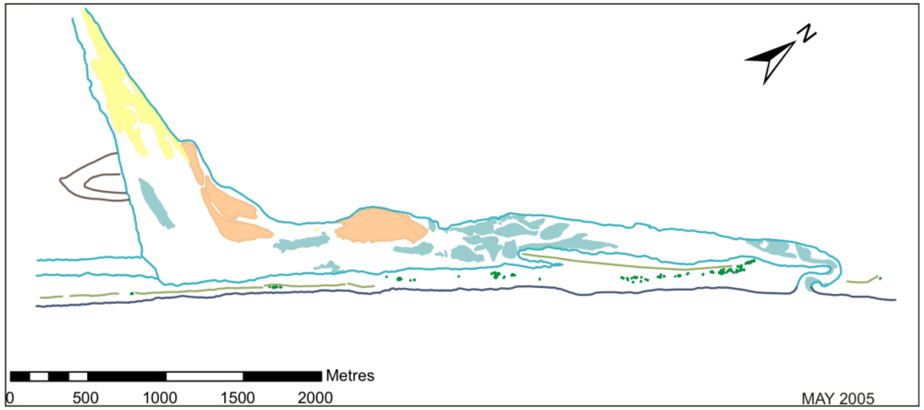

Figure 4.15 2005 the regrowth of the channel morphologies is evident.

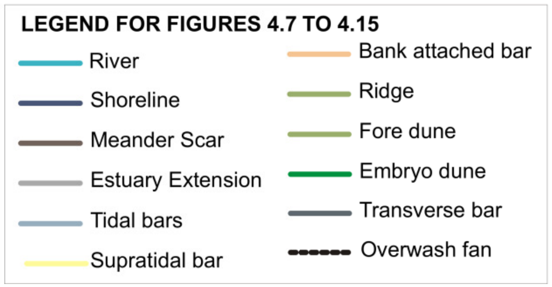

4.3. DISCUSSION

4.3.1. Coastline Morphology

These data sets do have drawbacks related to the irregularity between measurement intervals. Time intervals are irregular, in some instances data is separated by a single year (1972 and 1973) whereas other intervals can be as large as 19 years (1953 to 1972). It can thus be difficult to account for changes that occur due to catastrophic events such as flooding on a sub-decadal scale, or abnormally high wave conditions which occurs seasonally. Other authors have noted similar difficulties (e.g. Barnard and Warrick, 2010). Nevertheless, this does provide an initial data set with which longer term changes to the coast may be analysed. At these temporal scales, these data will overlap with at least one in twenty year flooding periodicities, thus these data do provide a means to assess change on the time scales applicable to long term coastal management. A similar case is made by Hanslow (2007), who calculated the recession of the MacMasters Beach in South Eastern Australia using these techniques.

Site 1 (Fig 5.2) is extremely dynamic, with periods of marked accretion followed by periods of erosion. The highest accretion is recorded here (from 1972-1973) with a net accretion of 212m. Such large accretion events at river mouths are not rare and are recorded regularly. A similar example is provided by the San Lorenzo River mouth delta that progrades at approximately 200m in a single year (Hicks and Inman, 1987). This rapid accretion at site 1 is due to the deliverance of the river load preferentially to the most proximal site as it is being reworked by longshore drift and the local gyre currents. Here sediment is transported in a northerly direction on the shelf (Flemming, 1980; Bosman et al., 2007) where it is intercepted by the change in coastline orientation. Rather than a case of shelf over spilling arising e.g. Boyd et al., (2008), these sediments are reworked by the high wave activity onto the beaches (Austin and Masselink, 2006; Brooke et al., 2008). According to Bosman et al., (2007), wave activity is sufficient to rework sediment at depths of 30 m or less, in addition to the dominant fine grained sediment ejected as turbidity plumes which ultimately remain in suspension for long periods of time. Once incorporated into the longshore drift, this sediment adds to the current beach ridge plain and may take many years to be redistributed along the coastline (Cooper, 2002; Bosman et al., 2007; Brooke et al., 2008).

A similar pattern of sediment cycling was observed by Bremner et al., (1990) in the Orange River where fine suspended sediments were reworked to form a flood deposited pro-delta. This type of fine sediment accumulation contributes to the sub aerial growth of post-flood barrier complexes (e.g. Cooper, 2001). From a morphological perspective, the Orange River looks strikingly similar to the Thukela River, mirroring the up-drift appearance of beach ridges and coastal progradation (Fig. 4.16). In the Thukela River's case, the sediments deposited at a depth of 30 to 60m show fining upward sequences capped with fluvially derived muds up to 1.5m thick, strong evidence for flooding followed by fair-weather settling lag sedimentation (Bosman et al., 2007).

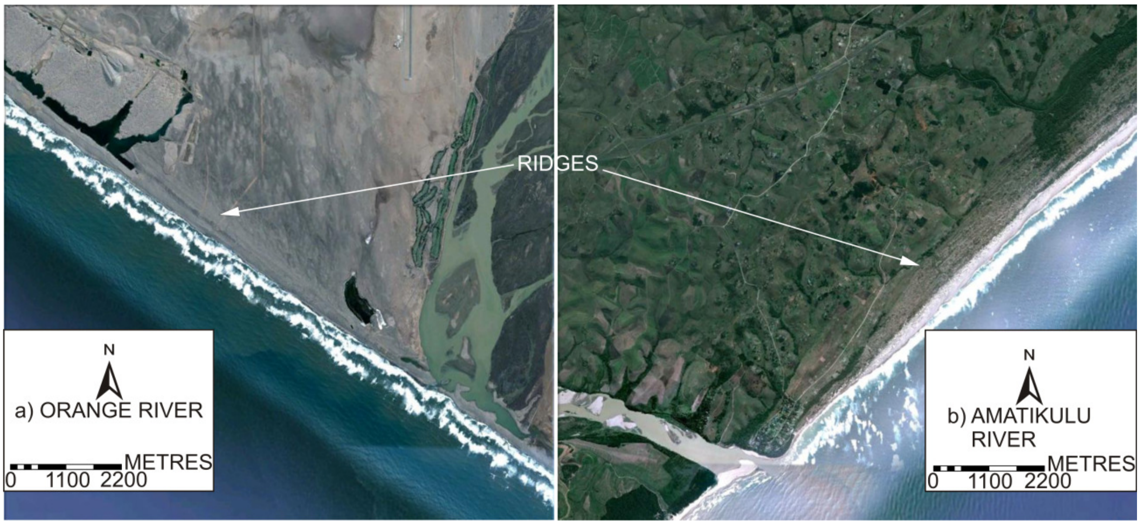

Figure 4.16 Comparison of the a) Orange River coastline (adapted from Google Earth imagery 17/10/2010) and b) Amatikulu River coastline have similar morphological features (adapted from Google Earth imagery 17/10/2010). Beaches ridges on the up-drift side of the sediment source and coastal progradation.

In terms of sediment load, the Thukela River provides the area with $6.79\times10^6 m^3/yr$ of sediment, compared to the 0.85 to $1.0\times10^6 m^3/yr$ of sediment contributed by longshore drift (Bosman et al., 2007). During the cut-off low of September 1987 it was calculated that 79.21×10^6 m^3 of sediment was supplied by channel erosion from the catchment and summarily ejected out of the Thukela River (van Bardeen and Burger, 1989). During Cyclone Domoina suspended sediment load of the Thukela River increased by 3200% (van Bladeren and Burger, 1989). Clearly, this increase in sediment load by an order (or more) of magnitude resulted in a pronounced phase of growth of this portion of coastline (Fig. 5.1). It appears from the data collected in this study that, on average, a lag time of 2-6 years is experienced from flooding to peak growth in beaches.

On a comparative basis, the Amatikulu River is of little consequence to the overall supply of sediment to the beaches, contributing 2.55% of the Thukela Rivers load (Dunkley et al., 1998). Similar sized rivers in KwaZulu-Natal (e.g. the uMgeni River) are themselves located on receding coastlines and it appears unlikely that the Amatikulu River alone can supply enough sediment to stabilize, let alone cause active progradation of the coastline. It thus appears that the Thukela River is singularly responsible for the coastal progradation of this area.

Overall, every site experienced a stage of erosion during the study period. Five of the sites (sites 12, 14, 15, 16, 17) showed net erosion in three or more of the photographed intervals. The overall rates of change for the years 1983 to 1989 showed a net accretion rate of 25.47m/yr followed by a net retreat rate of -28.08m/yr in 1989 to 1992. The rapid accretion rate between 1983 and 1989 is the result of Cyclone Domoina (seen as the discharge peak in 1984) and the 1987 floods. The subsequent aerial photographs from 1989 to 1992 showed net erosion of -28.08m/yr. This short erosion period is the coastline attempting to regain equilibrium (e.g. Wright and Short, 1984) with the large amounts of sediment that were deposited during Cyclone Domoina (Kovàcs et al., 1985). After each flooding phase and attendant beach progradation, a period of coastline re-adjustment follows where the coastline recedes. This is reflected in the 1992 data set by a rapid phase of erosion. It is most likely this happened in order to maintain equilibrium between the dominant wave energy which would ordinarily erode beaches and the introduction of “excess” flood-derived sediment. Erosion in this case manifests as the establishment of an equilibrium profile (e.g.Türker and Kabdaşli, 2006; Meilianda et al., 2010) based on the ordinary background sedimentation of the Thukela River. It is possible this sediment was removed completely from the system, and deposited off-shelf by counter Agulhas Current flows as shown by Flemming (1980) and Green (2009).

Cooper (2002) considers that any shoreline may vary between episodes of erosion, accretion and stability, all of which are dependent upon the time since the last major flood. These include such disparate sized systems as the Thukela River (Cooper, 1990) and the uMgeni Estuary (Cooper, 1994). Similar such cyclic relationships were noted by Barusseau et al., (1998) and Brooke et al., (2008). Barusseau et al., (1998) describes the Langue de Barbarie coastline in Senegal where fluvial flooding results in the direct growth of the beach where longshore drift later removes this sediment and deposits it further down the beach lengthening the Langue de Barbarie spit. Brooke et al., (2008) noted that sediment ejected by the Fitzroy River in Australia by medium to high magnitude floods is reworked, deposited and stored as the Keppel Bay beach-ridge formation. According to Cooper (1990; 2002) the post flood recovery of a system like this will follow the reworking of the ejected sediment in a landward direction to reform the barrier and also in an alongshore manner by wave activity. The sediment discharged may aid in rapid coastal progradation on the up-drift side (northern bank) for some time after the event (Cooper, 2002). The accretion is thought by Olivier (1998) to occur more rapidly after a flood event. This indicates that the surplus sediment is redistributed rapidly and reworked back on to the beach to aid in the beach ridge formation along this section of coastline. Data presented here confirm this. The coastline obliquity and oblique swell approach establishes a very strong longshore drift component which results in mass progradation immediately down drift of the Thukela River mouth tailing off northwards, a scenario reflected in the progressively reducing accumulation rates in the northern sites.

By 2005 almost all of the sites have maintained their 1992 position by prograding in small amounts. A general trend across all sites is the net erosion coinciding with discharge values less than $400m^3/s$. Alternately, the coastline may maintain its position. The erosion or maintenance of position must again be based on the equilibrium at the time between the wave energy and the low discharge, ambient sediment supply. This equilibrium is a delicate balance that is easily disrupted by man. In the case of the Senegal River Estuary, when a dam was built, it resulted in the Senegal River Estuary flowing coast parallel for over 2.8km in 1990. This dam effectively reduced the relative effect of fluvial inputs and caused the role of longshore drift derived sediments to become more prominent. In this respect shore parallel spit extension became the dominant process and deltaic growth slowly subsided. The end result is a strikingly similar morphology to the Amatikulu Estuary's barrier and back barrier configuration.

In summation, the Amatikulu coastline would ordinarily experience coastal erosion, as the rate of sediment supplied to the coastline by longshore drift is usually less than the rate of erosion by wave activity. This is indicated by the small episodes of coastal readjustment and erosion. Post flood, the sediment supplied to the coastline by the Thukela River greatly exceeds that experienced normally. This is indicated by the long duration taken to reach maximum progradation. The overall net result is that sediment supplied is greater than that lost by erosion, resulting in a net progradational coastline. This has important managerial implications in that the damming of this Thukela River would reduce the detritus provided to the updrift areas and consequently result in coastal erosion in those areas.

4.3.2. Estuarine Morphology

According to Begg (1978), the Amatikulu Estuary breaches during flooding conditions where the river enters the estuary closest to the barrier. This form of breaching in estuaries with extensive coast parallel extension is well documented in the Keurbooms (Reddering, 1983) and the Gamtoos Rivers (Reddering and Scarr, 1990). These systems are classed as tide-dominated estuaries according to Cooper (2002). This is the only similarity between the Amatikulu River estuary and these two systems. The Amatikulu Estuary corresponds to Cooper's (2001; 2002) river-dominated estuarine model. The continual seaward growth of large, supratidal bank attached-bars (by 140m from 1953 to1972) further indicates the river's dominance in the inner regions of the Amatikulu Estuary. Cyclone Demonia in 1984 caused the uMgeni and Mvoti Estuaries to erode their entire fringing barriers coupled with significant volumes of channel sediments (Cooper, 1990; 1993; 1994). In comparison, the Amatikulu Estuary's barrier was breached at a single point, though all the supratidal bars and bank attached bars were eroded (Fig. 4.12). The only reasons that the barrier was not eroded more extensively relate to the presence of more substantial anchoring vegetation and a greater barrier length as compared to the uMgeni and Mvoti River mouth situations. The subsequent re-establishment of the supratidal bars and associated channel infilling occurred rapidly (by 1992-Fig. 4.14). This is a typical response, as documented by Cooper (2001; 2002), to post-flood recovery of a river-dominated estuary. The limited response of the banks to this catastrophic flooding is due to the cohesive nature of the bank sediments in river-dominated estuarine sediments. Cooper (1994) made the same observations of the banks at the Mvoti Estuary after Cyclone Demonia.

Inlet migration is a common response of estuaries to changing dynamics and generally occurs in the longshore drift direction e.g. Keurbooms Estuary (Reddering, 1983), Gamtoos Estuary (Reddering and Scarr, 1990), and the Ancã and Fuzeta Inlets (Vila-Concejo et al., 2004). Migration of inlets creates problems in inhabited areas and generally need to be stabilised by hard engineering (uMgeni, Durban Harbour) or dredging (Ancã Inlet and Fuzeta Inlet) (Vila-Concejo et al., 2004). This is done to ensure that the inlet successfully captures the tidal prism and no longer migrates (Vila-Concejo et al., 2004). In general when a new breach occurs, a slow inlet migration begins making the return to the original inlet position e.g. Senegal River

Estuary (Barusseau et al., 1998), Keurbooms Estuary (Reddering, 1983) and the Mvoti Estuary (Cooper, 1993; 1994; 2002). The Amatikulu Estuary responds differently. Once a new breach occurs, the breach is rapidly plugged and reopening occurs in the original position to the north. This is due to four factors as described by Hughes and Brundrit (1995): the high levels of sediment in the nearshore available to close the new breach; the strong northerly longshore drift created by the Agulhas counter currents (Bosman et al., 2007); the high wave energy of KZN; and finally the ability of the adjacent river to sufficiently supply adequate sediment than can be reworked by waves. Estuaries in other areas do not respond in this way as they do not have these factors acting simultaneously. This results in a gradual migration of the mouth. These factors do not only influence the morphology on the Amatikulu Estuary but also other estuaries situated on the same coastline namely the Nyoni (14km shore parallel channel) and the Mlalazi Estuaries. These two estuaries have similar beach ridges and long shore-parallel tidal channels due to the sediment rich longshore drift (Fig. 4.17).

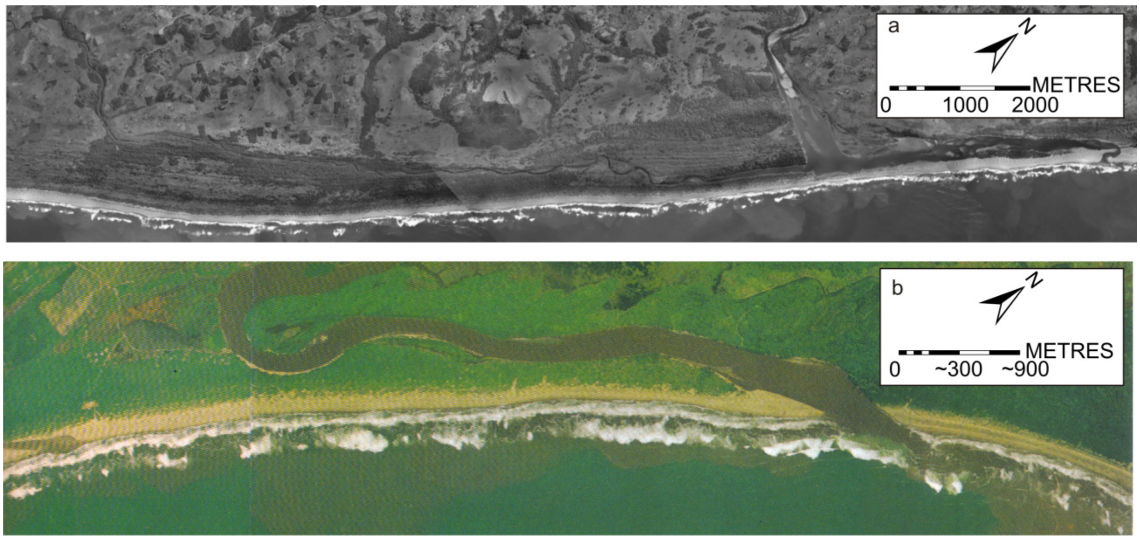

Figure 4.17.a) The Nyoni and Amatikulu Rivers (2005) .b) Mlalazi River (30/09/1987 with a peak discharge of 1600 cumecs (adapted from Perry, 1989) note the morphological similarities such as coastal extension of the estuaries and beach ridges indicating the sediment laden longshore drift that is influencing the morphology of the coastline north of the Thukela River.

CHAPTER 5

DIGITAL ELEVATION AND MORPHOLOGY

5.1. INTRODUCTION

This chapter is concerned with the interpretation of elevation data collected throughout the Amatikulu Estuary's tidal basin and fringing barrier. Basic measurements of channel dimensions and architecture are discussed in light of empirical equations of other authors and a synopsis of the estuary's shaping processes is advanced.

Theoretical sediment size classes for bedload (Table 5.1) are calculated according to the calculations and methodology of Nordfjord et al., (2005). These equations were empirically derived hydraulic equations that were applied to the palaeo-channel geometry of buried estuaries. From the observed channel architecture in Table 5.1 that following equations were used in the following order:

1) The palaeo-discharge for tidal system based on the power law.

   $Q=A^{\alpha}$ — Q= water discharge (m^3/s)

   A=channel cross-sectional area (m^2)

   $^{\alpha}$=0.96 (exponent value based on world wide studies)

2) Mean flow velocity.

   $Q=Av$ — v=mean velocity (m/s)

3) Estimation of boundary shear stress (τ) based on the quadratic stress law.

   $\tau=C_d\rho_f v^2$ — C_d=Drag coefficient (0.0025 based on the assumption of velocity 100cm above channel bottom

   ρ_f=Fluid density ($1g/cm^3$)

4) Modified shield equation (Miller et al., 1977).

   $v_{100}=122.6(D)^{0.29}$ — v_{100}=mean velocity (m/s) assumed 100cm above channel bottom

   D=diameter of sediments grains(cm)

   122.6 and $^{0.29}$ are calculated through linear regression for sediment grains less than 0.2cm in diameter by Miller et al., (1977) The boundary shear stress (for which equations are widely debated e.g. Camenen and Larson, 2005) is the dominant driving mechanism for both bed load transport of sediments and suspended sediment transport (Barnes et al., 2009). The Modified Shield equation of Miller et al., (1977) assumes that the sediment grains are comprised of the same density as quartz, and the water velocity is at is strongest 100cm above the channel bed. A calculation of the theoretical sediment size transported as bedload was calculated using the Modified Shield equation.

5.2. RESULTS

5.2.1. Estuarine and Back Barrier Morphology

The backbarrier tidal basin of the Amatikulu Estuary is dominated by a narrow, barrier-parallel tidal channel (Fig. 5.1a and b). The channel is characterised by very large dunes (amplitude = 0.5m; wave length=200m; Table 5.1) in its mid-sections, and by a prominent flood tide delta in the inlet (Fig. 5.1b). Where the flood tide delta extends into the estuary, the tidal channel reaches its maximum depth of -2.2m MSL on the northern edge of the flood tide delta. Typically the channel bifurcates around the emergent body of the delta. The channel morphology is less well defined in the areas fringed by tidal flats where it is wider (475m) and less incised (Figs. 5.1 and 5.2). Here it attains a minimum depth of +1m MSL, the thalweg 1.9m below the exposed tidal flat sediments. Dramatic shallowing, particularly at low tide, also occurs along the crests of the very large dunes. Overall, incision increases towards the inlet, as does sinuosity. Sinuosity along the entire length of the tidal channel is calculated as 1.1. The Amatikulu Estuary channel architecture (Table 5.1) at bank full stage (Fig. 5.2) has a width depth ratio mean >100 and a width >160m and an average depth of 1.2m Table 5.2 presents a summary of the morphological measurements of the tidal channel.

The crests of the very large subaqueous dunes define three distinct zones within the tidal channel (Fig. 5.3). These comprise an inner zone where dunes are orientated with their lee slopes towards the inlet; a middle zone where crests are flattened; and an outer zone where bedforms (including the flood tide delta) are orientated with the flood tide direction. Superimposed on these very large dunes are subordinate large dunes (amplitude=0.15; wave length=40m), orientated with the ebb tide direction (Fig. 5.2). At the inlet, the flood tide delta occurs as an elongated feature (Fig. 5.1b) emergent throughout the tidal cycle (+0.43m MSL).

It is 86m wide and 302m long with a maximum ramp slope of 9.56° (Table 5.2). Table 5.1 presents the predicted hydraulic conditions for the Amatikulu Estuary tidal channel.

5.2.2. Barrier Morphology

Topographically the barrier/beach is very wide and has a very low gradient (Fig. 5.4). The barrier reaches a maximum height and width of 7.5m in the *Casuarina* forest 341m in transects 12 and 17 respectively (Fig. 5.4.b and c; Table 5.2). The average height of the barrier is +3.5m MSL. Where localised steepening occurs (Fig. 5.5), this takes the form of the termini of several large washover fans (Fig. 5.1.b). These occur at the dog leg bend and just south of the *Casuarina* forest (Fig. 5.1a and 5.5), usually where the slope gradient of the barrier is less than the average of 2.19°. The overwash deposits comprise an aerial extent of ~ 118009m^2. The slope of the termini is ~5° for all overwash fans (Fig. 5.5). Where the barrier gradient exceeds 2.5°, overwashing is not present. In most instances, these areas correspond to better developed dune fields on the barrier, anchored by sparse vegetation. Where the overwash deposits enter the estuary these areas correspond to the shallowest portions of the tidal channel (Fig. 5.1a and b).

The barrier contains few beach ridges along the barrier in front of the estuary. Beach ridge density is at a maximum on the southern edges of breach site 1 and adjacent to the *Casuarina* forests (Fig. 5.6). Where the barrier has undergone a catastrophic event or been recently disturbed, all the vegetation has been removed and there is no evidence of any dune form (Fig. 5.1a and 5.1b). From a historical perspective, the dunes in front of breach site 1 were not visible prior to 1983 when they were removed by a breaching event (Fig. 5.6a and b). Thereafter the dunes have been re-established. On this basis, conservatively assuming a scour to 0m MSL, the dunes have attained an elevation of 7.5m in 26 years. Dune growth occurs roughly at a vertical rate of 0.29m per year (Fig. 5.6c).

5.2.3. Breach Points

Three breach sites are identified from low points on the digital elevation model and confirmed from time sequence aerial photography (Fig. 5.1a and b; Fig. 5.7; Chapter 4 Fig. 4.7, 4.8, 4.13 and 4.14). Breach site 1 occurs at the confluence of the Nyoni and Amatikulu Rivers (Fig. 5.1b;

Fig. 5.7). Breach site 1 has a maximum altitude of +3.5m MSL, ascertains a maximum width of 250m and corresponds to the narrowest portion (250m wide) of the barrier. It is fringed by a deep channel (Fig. 5.1). A conservative calculation on the volume of sediment required to fill the breach from +0m MSL benchmark is ~84000m^3.

Breach site 2 is located behind the *Casuarina* trees (Fig. 5.1b; Fig. 5.7). The scar of a previous breach is still evident from the elevation data (Fig. 5.1a and b; Fig. 5.7). The breach site behind the *Casuarina* trees reaches a width of 70m and a depth of 2m (Fig. 5.7). The contemporary inlet, breach site 3 (Fig. 5.1b; Fig. 5.7) is located in the North East corner of the Amatikulu Estuary. Here the normal inlet mouth channel reaches a maximum depth of -0.5m MSL with a maximum width of 100m. In comparison, the central tidal channel is confined to a single channel 50m wide and a depth of -1.6m MSL. Overall, the contemporary inlet is deeper, and more v-shaped than the other recognised breach sites (Fig. 5.7).

Table 5.1 Tidal **c**hannel morphometrics showing predicted hydraulic conditions, bedload transport capabilities and theoretical bedform response to *predicted* shear flow velocity and grain size of bedload. Bold denotes cross sections intersecting very large dunes.* denotes derivation from Nordfjord et al., (2005), $^{\Delta}$ denotes derivation from the equations of Miller et al., (1977), † denotes derivation from Ashley (1990). Cross sections shown in figure 5.3.

Cross section	Bankfill stage width (m)	Cross sectional area (m^2)	Mean depth (m)*	Mean observed depth (m)	Max. depth (m)	Width/depth ratio	Theoretical shear stress (dyn/mm^2 where 1dyn/mm^2= 0.1Pa)	Theoretical tidal discharge (m^3/s)*	Theoretical mean velocity (m/s)*	Theoretical bedload fraction$^{\Delta}$	Theoretical bedform†	Actual observed bedforms
1	268.25	383.24	1.43	1.20	2.08	129.17	0.001553327	302.08	0.79	-1.12Φ (2.18mm)	Dunes	Very large dune (wavelength = ~200m)
2	330.50	536.57	1.62	1.22	1.76	188.14	0.001512063	417.29	0.78	-1.06Φ (2.08mm)	Dunes	Very large dune (wavelength = ~200m)
3	332.75	389.22	0.83	1.02	2.24	148.77	0.001551401	306.61	0.79	-1.12Φ (2.18mm)	Dunes	Very large dune (wavelength = ~200m)
4	331.67	277.25	0.84	0.56	1.83	181.57	0.001594079	221.39	0.79	-1.19Φ (2.28mm)	Dunes	Very large dune (wavelength = ~200m)
5	200.90	211.08	1.05	0.56	2.06	97.68	0.001629235	170.40	0.81	-1.24Φ (2.37mm)	Dunes	Very large dune (wavelength = ~200m)
6	265.42	255.79	0.96	0.97	1.96	135.17	0.001604645	204.52	0.80	-1.21Φ (2.31mm)	Dunes	Very large dune (wavelength = ~200m)
7	199.83	234.75	1.17	1.18	2.08	96.23	0.001615444	188.70	0.80	-1.22Φ (2.33mm)	Dunes	Very large dune (wavelength = ~200m)

8	263.75	322.36	1.22	1.23	2.67	98.78	0.001574972	255.86	0.79	-1.16Φ (2.23mm)	Dunes	Very large dune (wavelength = ~200m)
9	268.33	368.38	1.37	1.51	2.26	118.73	0.001558248	290.83	0.79	-1.13Φ (2.19mm)	Dunes	Very large dune (wavelength = ~200m)
10	262.58	344.66	1.31	1.7	2.26	116.19	0.001566567	272.83	0.79	-1.15Φ (2.14mm)	Dunes	Very large dune (wavelength = ~200m)
11	161.50	284.19	1.76	1.7	2.83	57.07	0.001590932	226.70	0.80	-1.18Φ (2.27mm)	Dunes	Very large dune (wavelength = ~200m)
12	264.83	274.14	1.04	1.04	2.83	93.58	0.001595522	219.00	0.80	-1.19Φ (2.28mm)	Dunes	Very large dune (wavelength = ~200m)
13	251.67	225.10	0.89	0.89	2.81	89.56	0.001620879	181.25	0.81	-1.23Φ (2.34mm)	Dunes	Very large dune (wavelength = ~200m)

Table 5.2 Morphological measurements of the Amatikulu Estuary and Barrier

Location	Feature measured	Lowest elevation MSL	Highest elevation MSL	Width (m)	Length (m)	Area (m^2)	Average slope (°)
Backbarrier	Subtidal channel	-2.2m	+1 to -0.2m	475m (max) 74m (min)	5189 (thalweg)	519981	1.1
	Flood tidal delta	n/a	+0.43m	87m (max)	302 m	10948	2; 9.56 at maximum
	Tidal flats	n/a	+0.45m	168.15m	n/a	87267	0.46
	Washover fans	n/a		180	484	118009	0.68; 5 at termini
Barrier	Barrier/beach		+7.5m	341m (max) 84m (min)	5230.69	855456	2.19
	Contemporary inlet	-0.37m	n/a	50 m	n/a	n/a	4.14
Alternative inlets	Breach site 1	1.27m	+6.40m (adjacent banks)	250m	n/a	37928	4.77
	Breach site 2	1.70m	+2.91m	70m	n/a	76479	1.45

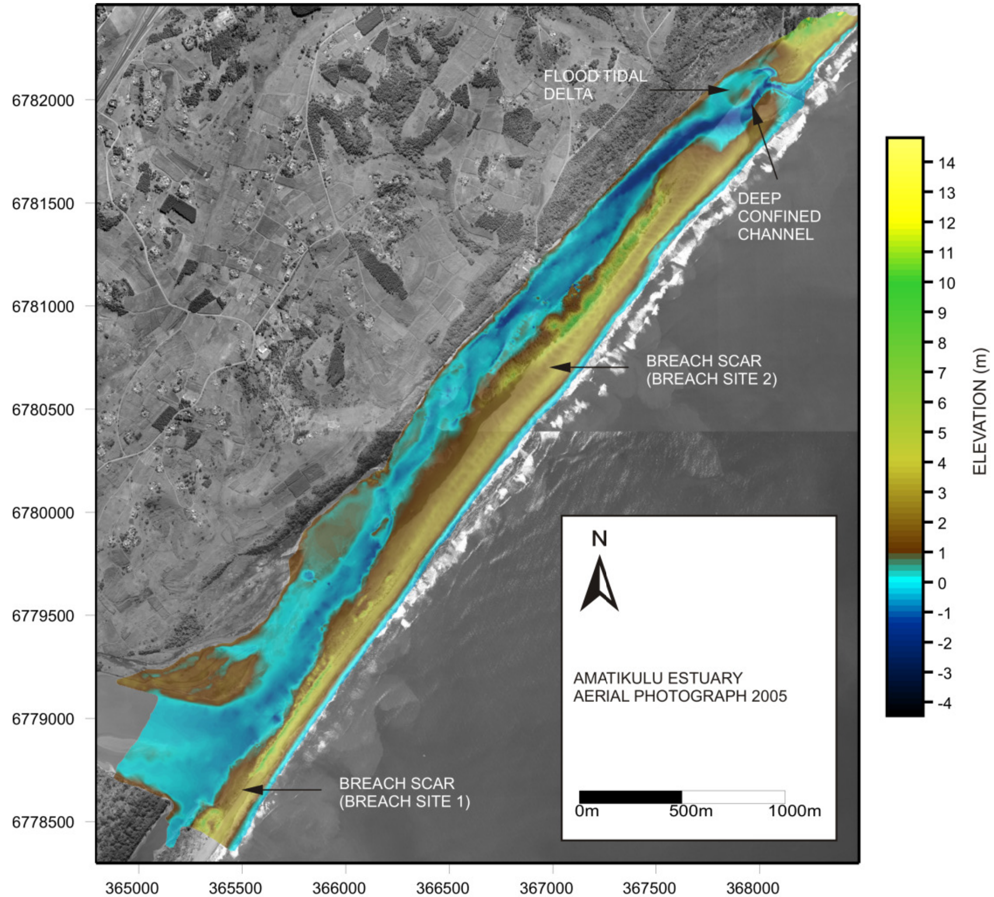

Figure 5.1.a) Digital terrain model of the Amatikulu Estuary and fringing barrier. The main channel runs parallel to the barrier. Large subaqueous sand dunes in the middle sector of the estuary can be identified.

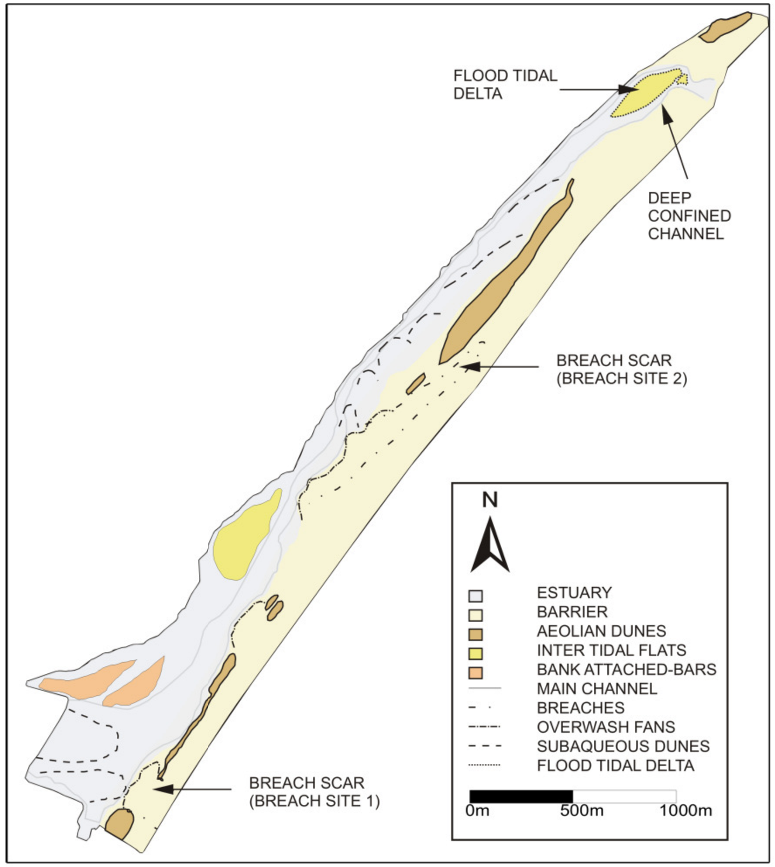

Figure 5.1.b) An interpreted morphological map of the Amatikulu Estuary and Barrier. The major morphological units as discussed in this chapter are depicted.

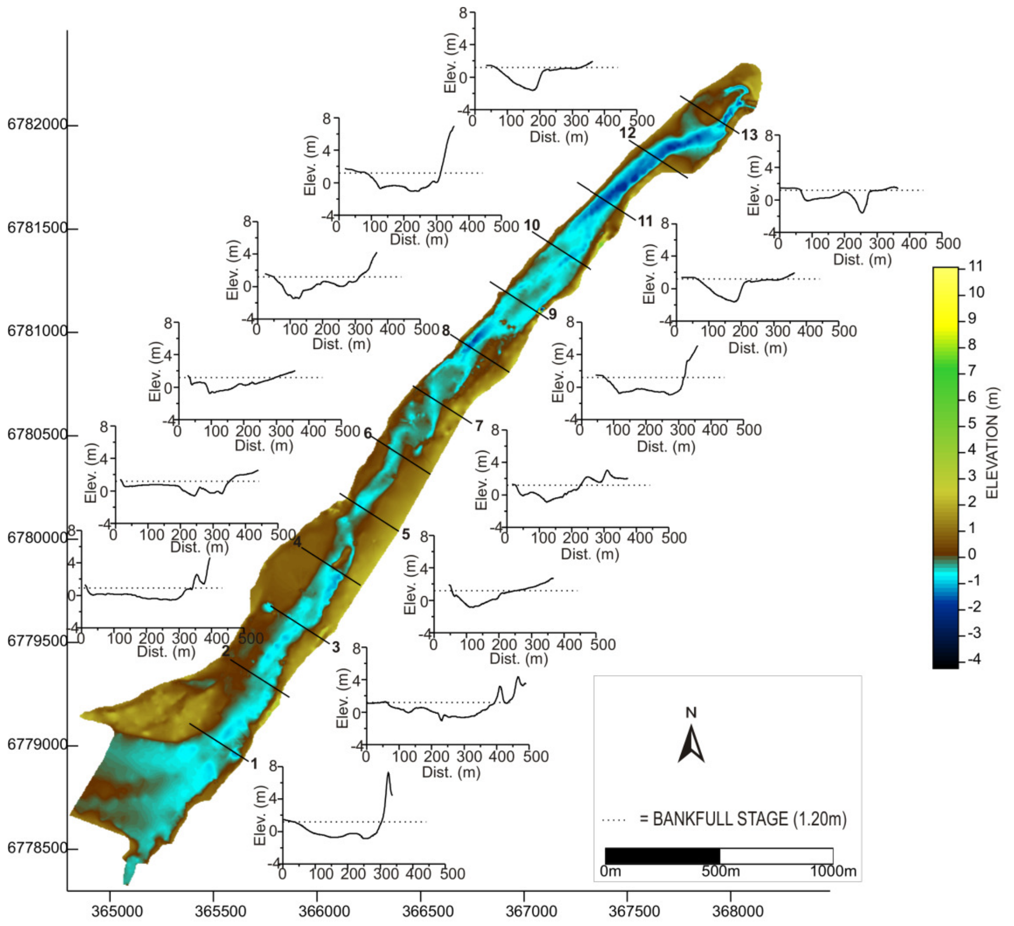

Figure 5.3 The main channel of the Amatikulu Estuary with the localities of the 13 cross profiles and accompanying sections. The bankfull stage is located 1.2m above mean sea level (MSL), as depicted by the dotted lines.

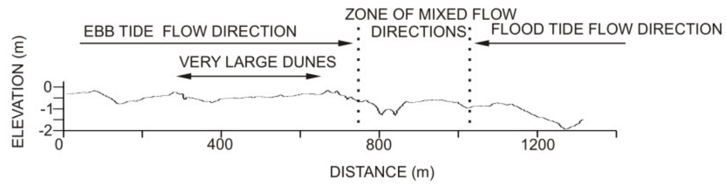

Figure 5.2 Along channel profile of the Amtikulu Estuary showing subaqueous dune morphologies (A=0.5m; λ= 200m). The crest of the morphologies indicate two flow directions, an ebb dominated upper sector and a flood dominated lower portion.

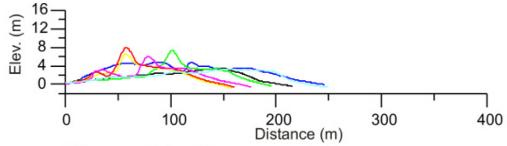

Figure 5.4.a Transects 1-7.

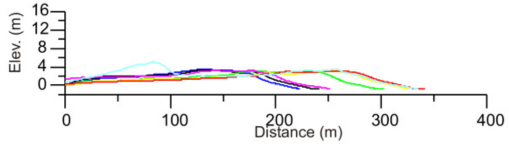

Figure 5.4.b Transects 8-14.

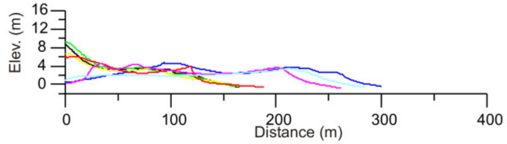

Figure 5.4.c Transects 15-21.

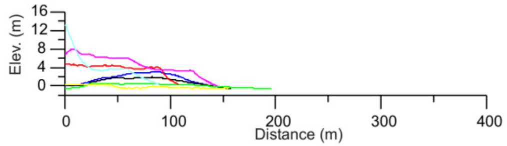

Figure 5.4.d Transects 22-28. Transects 25 to 28 are north of the contemporary inlet.

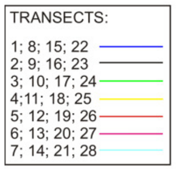

Figures 5.4 Transects of the Amatikulu barrier. Transect localities indicated on Figure 5.5

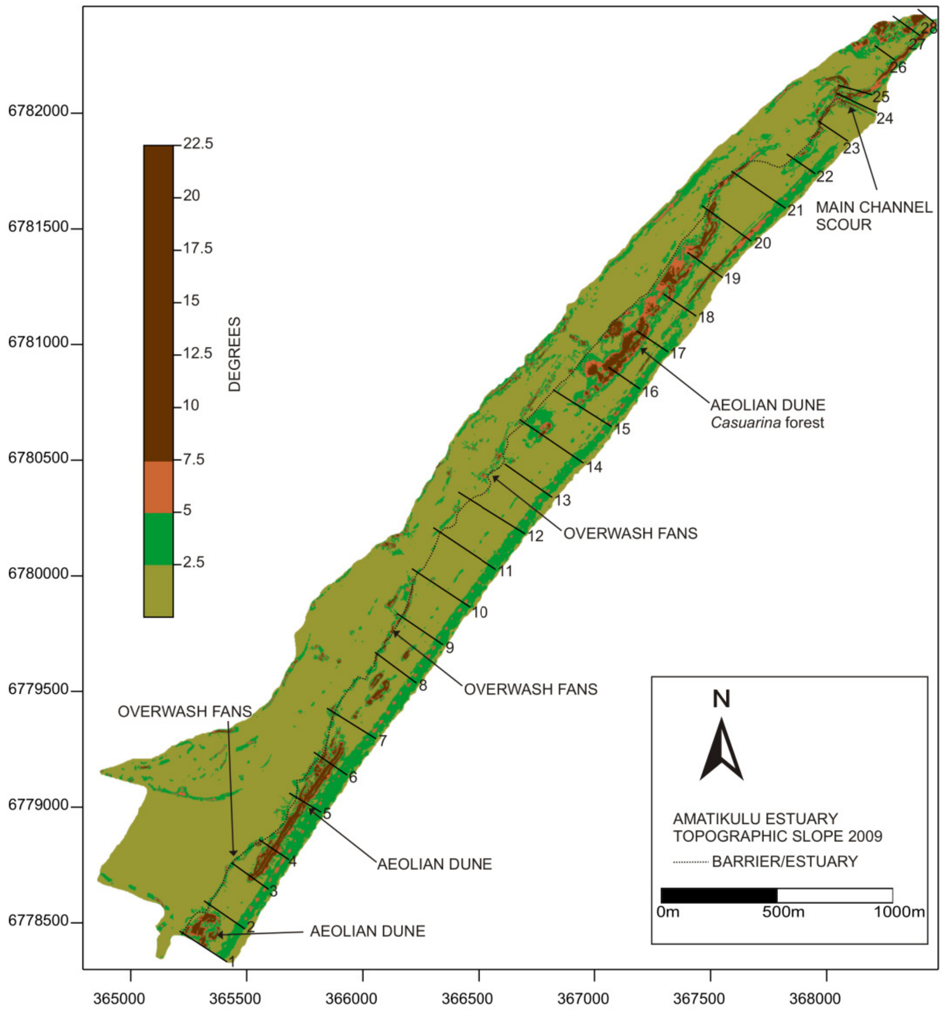

Figure 5.5 Topographic slope map of the Amatikulu Estuary and barrier. The uniformity of the slope of the estuary and barrier is disrupted by dunes and the terminal lobes of overwash fans. Transects from Figure 5.4 are labelled.

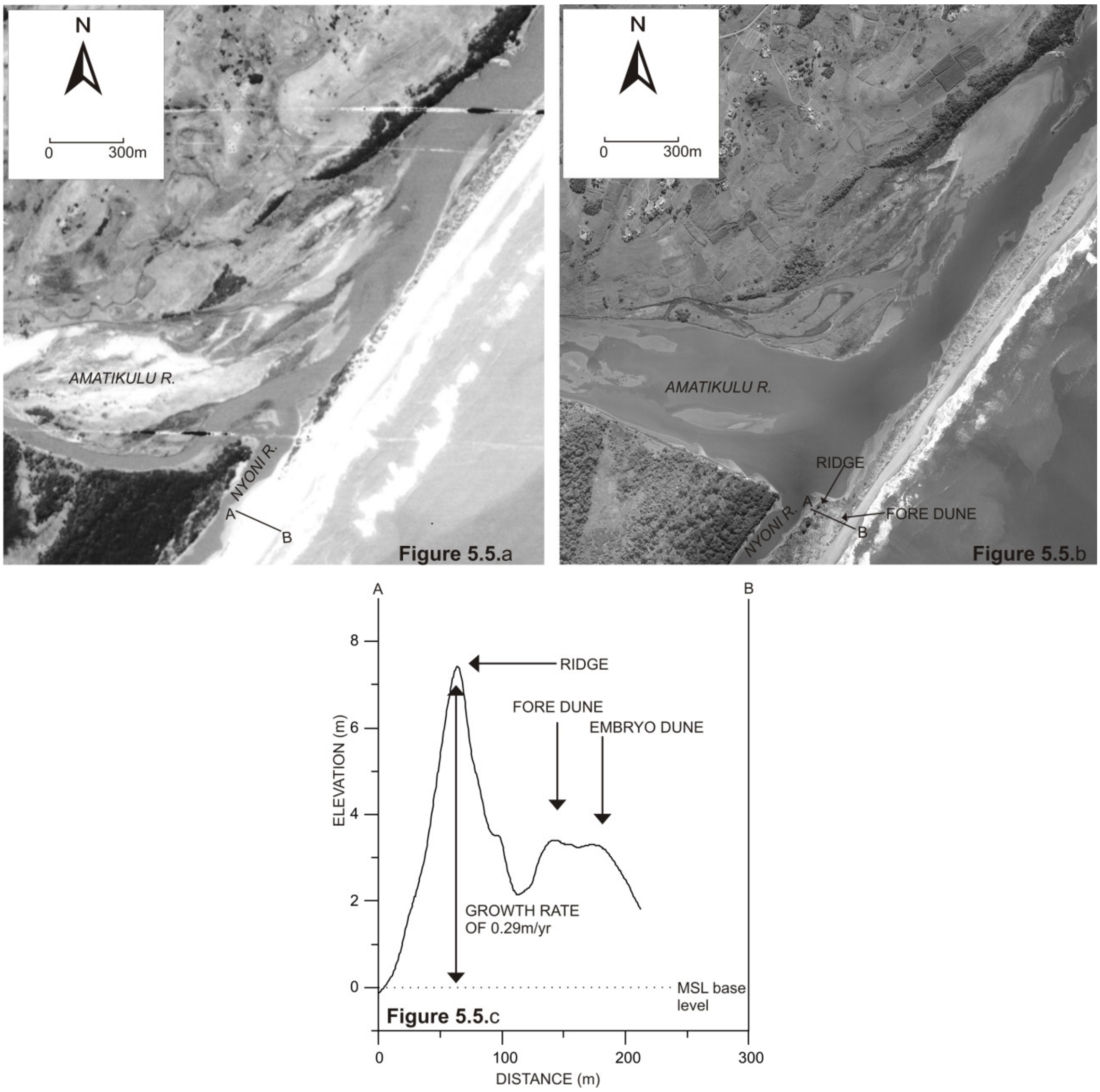

Figure 5.6 Three stages of dune evolution are clearly present showing the evolution from an inactive ridge to an active fore dune and newly formed embryo dune. These aeolian features have only been visible since 1983. The area of profile is indicated with the relevant morphologies. a) Aerial photograph of the Amatikulu barrier in 1973, pre ridge and fore dune development. b) Aerial photograph of the Amatikulu barrier in 2005, the most recent imagery available post ridge and fore dune development. c) Cross profile of the ridge fore dune complex from the 2009 *RTK* GPS survey with calculated growth rate.

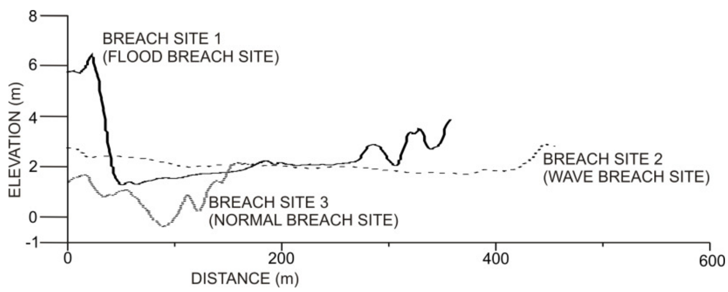

Figure 5.7 The three breach sites of the Amatikulu Estuary. The breach sites are named from south to north as; breach site 1 (the extreme flood breach site), breach site 2 (the extreme wave breach site south of the *Casuarina* forest) and breach site 3 (the normal breach site located in the north eastern corner of the estuary).

5.3. DISCUSSION

5.3.1. Estuarine and Back Barrier Morphology

The channel morphology, width-depth ratios and sinuosity conform to the model of a braided stream with longitudinal and transverse bars, set in a very wide channel with eroding banks (e.g. Rosgen, 1994). In this scheme, the channel is undergoing active lateral adjustment concomitant with high volumes of upstream (fluvial) sediment supply (Rosgen, 1994). This is at odds with the Amatikulu Estuary as 1) the catchment is small and relatively undegraded producing small amounts of fluvial detritus and 2) the dominant source of sediment appears to be introduced from the marine realm via overwashing (Chapter 7; Fig. 7.4.b and e; Fig. 7.5.k and p). The source of sediment may differ from Rosgen (1994), but the morphological description is still valid.

According to the classification scheme of Leeder (1999), the degree of anastomosing is between 35-65% which should theoretically reflect split channels and sinuous anabranches, features not notable in the tidal channel. It seems unlikely that fluvial controls are affecting both erosion and deposition and the resultant architecture of the estuarine tidal channel. Rather, it appears that the impingement of overwash into the tidal channel, in addition to flow constriction around the flood tide delta, is responsible for the "braided" appearances of the channel form. In this case, allochthonous marine sediment bodies appear to control the channel morphology, rather than sediment transported as bedload by the Amatikulu/Nyoni Rivers.

The theoretical mean current velocity calculated from the channel architecture is ~0.8m/s with a mean bedload sediment size of -1.17Φ (2.31mm) (Table 5.1). On the basis of the Modified Shield equation, the Amatikulu Estuary is able to transport sediments of between -1.05Φ (2.07mm) to -1.24Φ (2.36mm), essentially very coarse sand to gravel, as bedload. The presumed theoretical sediment classes that Rosgen (1994) considered able to form this channel morphology are diverse and range from cobbles to clay size fractions (Rosgen, 1994). The actual observed sediment within the Amatikulu Estuary is typically fine sand (2.08Φ or 0.24mm) (see Chapter 6). The discrepancy between the observed sand sized moving as bedload and those calculated on the basis of empirical equations can be ascribed to two factors. Firstly the fact that significantly finer material is present suggests that the channels are relict features, formed by floodwaters of higher velocities (and greater attendant bedload sizes) than present day. In this case, tidal channels are very slowly being modified by ordinary tidal processes.

Secondly, the estuary was sampled during a low-flow dry season which may be at odds with the bankfull stage calculations at a higher elevation. As the sampling survey was limited to the tidal channel, it seems likely that the bankfull stages here relies more on tidal elevations than catchment waters particularly in these lowermost reaches. In this case the former argument is preferred to the latter

Bedforms are a function of the forces exerted on the channel by the river flow and the flood tidal influence (Prent and Hickin, 2001). The formation and migration of the bedform is the instantaneous response to bedload transport which is a response to flow (Buijsman and Ridderinkhof, 2008). With the Amatikulu Estuary's predetermined theoretical mean velocity and sediment class, the calculated bedforms according to Ashley (1990) (Table 5.1; Fig. 5.8) are dunes. This corresponds to the observed dunes with a wave length of ~200m.

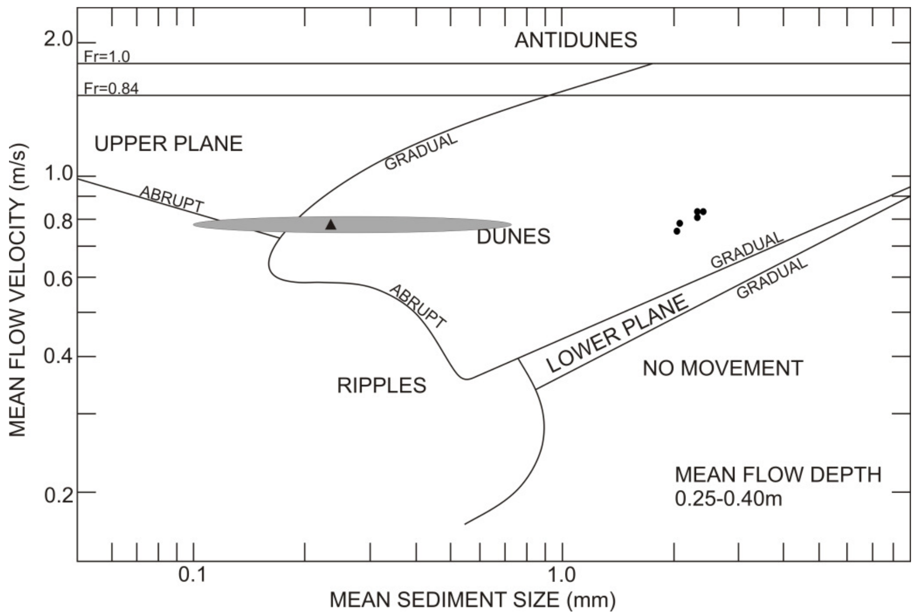

Figure 5.8 Theoretical bed forms of the Amatikulu Estuary calculated using mean sediment size and mean flow velocity, Fr = mean velocity Froude number (Figure adapted from Ashley, 1990). Black spots actually represent the theoretical grains size of bedload fraction. The position of these indicates the bedload form Table 5.1, the grey shaded area indicated the field of the actual observed mean sediment sizes for the Amatikulu Estuary, and the triangle indicates the overall mean sediment size for the Amatikulu Estuary (0.24mm; 2.08Φ).

In examining the bedform orientations, the upper portion of the tidal channel appears to be ebb-dominated, before mixing of the various currents occurs, flattening the bedform crests. Thereafter, these become flood-tide dominated, particularly in the inlet mouth. The subaqueous dunes have a very large wave length but a small height, this was attributed to the increasing energy of the water flow eroding the dune crests but simultaneously increasing the wave length resulting in the 'flattening' of the dunes (Prent and Hickin, 2001).

The agreement between the predicted bedforms and observed bedforms suggests that despite the channel being perhaps a relict feature, the flow velocities has been sufficient to maintain dunes even under the tidal processes occurring today. Unfortunately it is not possible to calculate dune size from Ashley's (1990) scheme. It seems likely that the dunes, as plotted, are in their earliest (gradual) phase of development and are probably much smaller than the very large dunes (wavelength = 200m) observed from the bathymetry. It this is the case, then the discrepancy in size would be accounted for by the idea of a channel (and attendant large bedforms) formed under higher velocities, whose architecture is mismatched with contemporary hydrodynamic processes. A study by Whitmeyer and FitzGerald's (2008) near Long Island shows a similar case where dunes are inactive until they are mobilised by extreme flow events, the waning flow being insufficient to modify or maintain the dunes. A further reason for the mismatching of the grain sizes is due to the limitations of the Modified Shield equation which assumes sediments are composed of only quartz grains and are perfectly symmetrical, an unlikely real-world scenario. Sediments of the Amatikulu Estuary are discussed in Chapter 6.

The ebb orientation of the dunes points to the Amatikulu Estuary functioning as a conduit for sediments rather than the long term sediment sink as proposed by Dalrymple et al., (1992) in the wave-dominated model or by Roy (1994) for microtidal estuaries. If anything, the Amatikulu Estuary acts as a temporary sediment sink controlled by flooding (see Chapter 4) where 'stored' sediments are expelled as sediment plumes (as evidenced in Figure 4.10).

5.3.2. Barrier Morphology

The wave dominated barrier would have formed during the post glacial marine transgression such as other barrier systems worldwide (e.g. Burrill Lake barrier, Australia) (Sloss et al., 2006). The sediment that was deposited on the continental shelf would migrate landward and fill the estuarine system (Dalrymple et al., 1992; Roy, 1994; Zaitlin et al., 1994). During the subsequent highstand, the rate of sediment supply exceeded the marine advance resulting in the barrier formation prograding (Dalrymple et al., 1992; Zaitlin et al., 1994).

The Amatikulu barrier profiles from the estuary to the beach (Fig 5.4 and 5.5) show that the Amatikulu shoreline exists as an intermediate beach state where the profile varies along the length of the beach, showing elements of both the reflective and dissipative models described by Wright and Short (1984). The Amatikulu barrier resembles the intermediate beach state of Wright and Short (1984), where a dissipative beach profile occurs aver a long shore perpendicular distance, yet is locally steepened seaward from the berm Wright and Short (1984) ascribe this to localised rips forming and entraining sediments away in this area. This is typical of accretionary areas, such as the Amatikulu coastline. The profiles for this study are horizontally extensive in comparison to Wright and Short's (1984) profiles, and show that the beach morphology is more that of a dissipative beach state. Dissipative assemblages are sinks for sediments, which go hand in hand with the progradational nature of the Amatikulu coastline which receives large quantities of sediment from the Thukela River in the south.

The overwash fans of the Amatikulu barrier cover large low lying areas that are free of vegetation that hinder the advance of the overwash. These overwash morphologies can be described as overwash plains that blanket the barrier according to Matias et al., (2010), as opposed to overwash lobes that cut channels into dune fields (Matias et al., 2010). These are characteristically absent from the Amatikulu coastline. Similar examples include overwash fans of the Santa Rosa Island in northwest Florida (Houser et al., 2008) and the Ria Formosa islands of southern Portugal (Matias et al., 2008). Both show thick blanketing sediments which flatten topography along barrier strike and impinge into the barrier channel.

Large overwash plains are present on the Amatikulu barrier and impact the Amatikulu Estuary. Overwash plains of similar size (100-300m) to the Amatikulu barrier were documented in estuaries along the KZN coastline by Smith et al., (2010). These features were a result of a storm in March 2007 that produced a shallow water wave height of 8.5m and a period of 16 seconds (Smith et al., 2007; Smith et al., 2010). The timing of the storm and the Amatikulu barrier morphology conform to what is described by Matias et al., (2010) as the most important mechanisms for barrier overwashing; an anomalous wave height and a relatively subdued barrier topography. The storm occurred over an unusually high equinox spring tide where extremely high waves encountered a low berm and were able to penetrate into the estuary unhindered. These overwash deposits have been preserved in the back barrier environment and will be visible for many years as emergent sediment bodies (see Chapter 4).

5.3.3. Breach Points

Three inlet points are clearly identified for the Amatikulu Estuary (Fig. 5.9). A model is proposed for the breach response of the estuary on this basis (Fig. 5.10).

Breach site 1:

Under high magnitude fluvial floods, the river's excess energy straightens its course, eroding the barrier directly at the dog leg bend and creating a new temporary inlet (Breach site 1) (Fig. 5.1b). It must be stressed that only floods of very high magnitudes will create morphological changes to river–dominated estuaries (Cooper, 2002). In this light, the Amatikulu Estuary is not the only estuary to undergo channel straightening under high magnitude floods, the Mvoti Estuary during the 1987 floods completely removed the barrier when straightening its course (Cooper, 1993). Floods of this magnitude result in channel scouring and removal of any channel sediments. These sediments, along with some barrier sediments are later deposited as an ephemeral mouth bar (Cooper, 1990; 1994; 2002).

The post flood recovery begins with the waning flood flow and the deposition of the ephemeral ebb-delta. The ebb-delta comprises of sediments from the Amatikulu River catchment, barrier and from sediments derived by longshore drift. This accumulation of sediments is reworked towards the barrier by the prevailing waves which are refracted inwards to the area because of the deposition of the ephemeral ebb-delta (Cooper, 1990). The ebb-delta is reworked by the wave front and the delta becomes emergent (Cooper, 1990). The sediments from the ephemeral mouth deposits provide sufficient sediment to facilitate mouth closure via the wave induced longshore drift (Cooper, 1990), as well as to supplement the barriers progradation (Cooper, 1990, 1991b, 2002; Olivier, 1998) (Fig. 5.10).

Breach site 2:

The second type of breaching occurs as a result of wave induced plugging of the contemporary inlet, resulting in a temporary breach south of the *Casuarina* forest (Fig.5.1b and Fig.5.7). An additional outcome of the aforementioned March 2007 storm was the blocking of the contemporary inlet. This resulted in water levels rising by over 3m and the flooding of local infrastructure (Myburg, 2009 pers comms). The mouth was breached illegally by the local community using a tractor to prevent further flooding (Myburg, 2009 pers comms). During this period a proto-breach attempted to form on the estuary side of the *Casuarina* forest. A breach was formed but did not attain any size as the estuary was artificially breached in its most northern inlet position before a substantial inlet could form (Myburg, 2009 pers comms). The temporary inlet is evident in Figures 5.1a and b. This site may be controlled by wave refraction patterns, whereby sediment preferentially plugs the northern inlet as waves are refracted around the ephemeral subaqueous delta formed at breach site 1. In this case

Breach site 3:

The final and most common inlet position of the Amatikulu Estuary is located at the northern most extent of Amatikulu Estuary (Fig. 5.7). This breach occurs when the Amatikulu River has sufficient energy to maintain an inlet over the wave activity and the large amount of sediment being deposited in the mouth by longshore drift. The high longshore sediment influx is the main contributing factor to all mouth closures of the Amatikulu Estuary.

The Amatikulu Estuary temporary inlets do not slowly migrate to the usual northern position. The Amatikulu Estuary responds to temporary breaching by instantaneous closure of the temporary inlets and near instantaneous re-opening of the normal inlet in the northern section of the estuary. This response is because of the high amount of sediment supplied by longshore drift along this coastline. This is much greater than other estuaries in KZN where inlet migration is more gradual. These ephemeral inlets are out of equilibrium and get plugged very quickly by the prevailing longshore drift conditions. The mouth reverts back to the preferred mouth position which is in equilibrium with the prevailing estuarine and nearshore conditions. The maintenance of the open inlet is dependent on the ebb flow provided by the Amatikulu River and Nyoni River. This form of inlet maintenance does not conform to Cooper's (2001) river-dominated estuarine classification scheme. Inlet migration instead is limited. A result the inlet rapidly returns to the original inlet position at breach site 3. This suggests that a new morphodynamic classification is needed for microtidal estuaries with exposure to such high degrees of littoral sediment influx. In the Amatikulu system's example, the inlet itself is still maintained by river discharge. However the positioning of the inlet and its resultant dynamics are instead broadly dominated by the longshore drift components here.

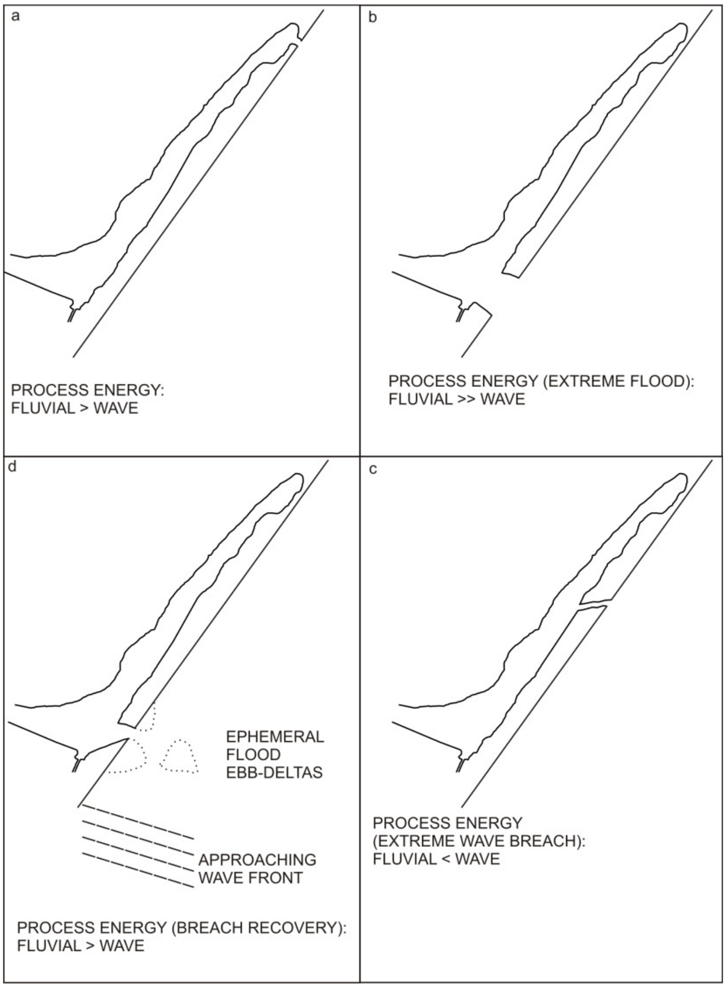

Figure 5.9 Breach sites of the Amatikulu Estuary. a) The normal breach position of the Amatikulu Estuary under stable conditions (breach site 3). b) High magnitude flood of the Amatikulu Estuary resulting in barrier erosion (breach site 1). c) Flood recovery with the ephemeral flood ebb-deltas being reworked by the local wave climate to become augmented with the barrier and close the ephemeral flood breach. d) The extreme wave breach and wave plugging of the normal inlet closer due to coastal storms and associated high wave activity (breach site 2).

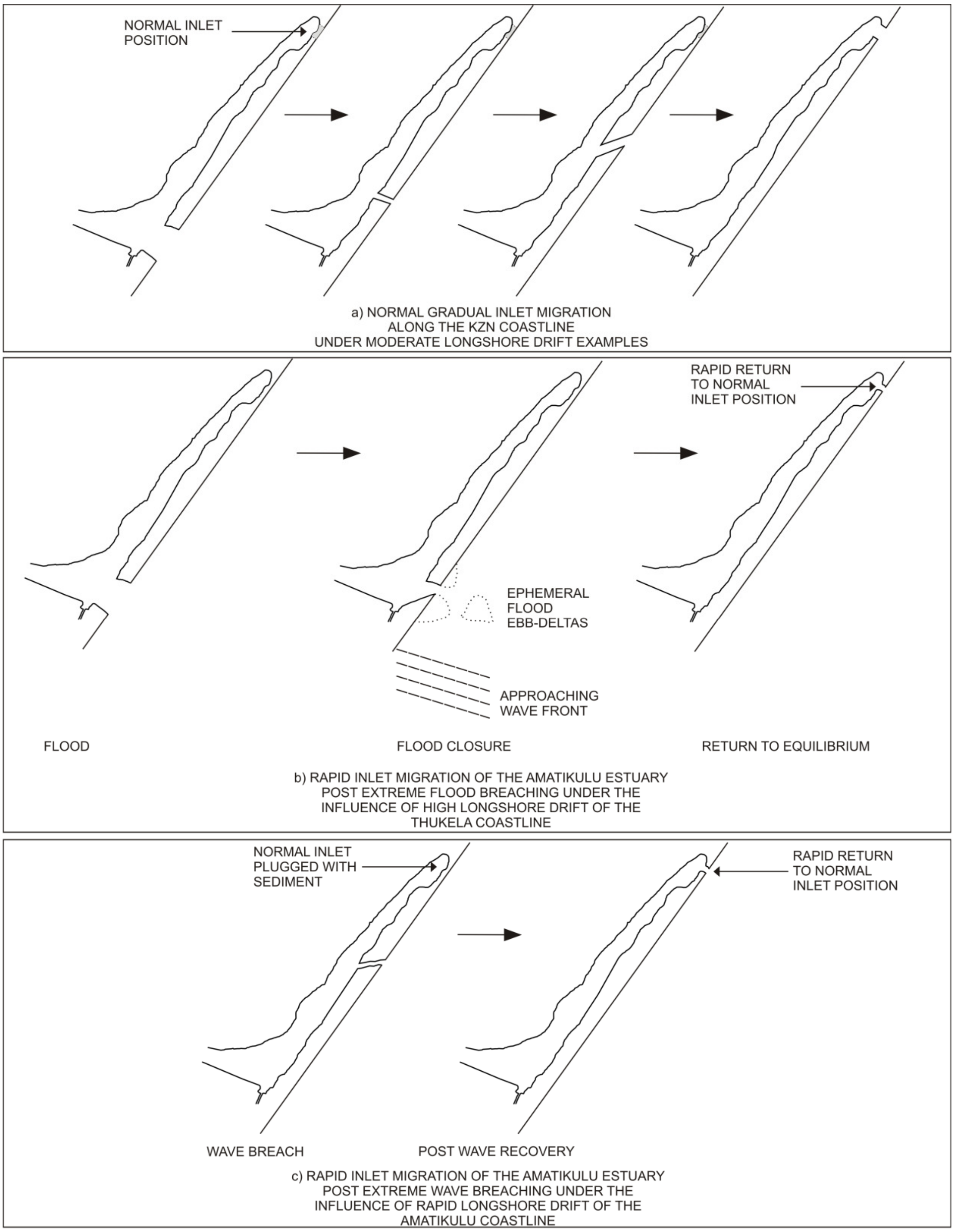

Figure 5.10 A model for the inlet dynamics of the Amatikulu Estuary. The rapid inlet migration is the result of high volumes of sediment incorporated in the longshore drift. This causes the inlet 'jumping' as opposed to the gradual inlet migration usually encountered. a) Flood breach inlet that is showing gradual migration along the barrier in a northerly direction under the influence of typical longshore drift rates and sediment loads. This is a typical response to barrier breaching along the KZN coastline. b) The inlet response to flood breaching along the sediment laden longshore drift dominated Amatikulu coastline. The inlet does not migrate along the barrier back to the equilibrium breach position. The inlet, on closure of the flood breach by reworking of ephemeral flood deposited ebb-deltas on the barrier coupled with sediments introduced by longshore drift, almost immediately re-opens in its northerly position. c) The Amatikulu Estuary's extreme wave breach site (breach site 2) in the middle of the barrier. The ephemeral inlet undergoes closure in the same manner as the flood breach and the inlet rapidly reopens in the equilibrium position to the north.

CHAPTER 6

SEDIMENTS

6.1. INTRODUCTION

The results of the analysis of the Amatikulu sediments provide insight into the sources of sediment and transport mechanisms acting within the estuary especially when compared with other estuarine studies locally and globally. The surface sediments characteristics investigated were; particle size analysis, calcium carbonate content and organic content.

6.2. RESULTS

6.2.1. Sand and Mud Distribution

The mean sediment size for the Amatikulu Estuary is 2.08Φ (0.24mm) which equates to the fine sand grain size in the Udden-Wentworth scale (Wentworth, 1922) (Fig. 6.1). The coarsest sediments (0.99Φ (0.50mm) to 0.68Φ (0.62mm)) are located in the inlet of the estuary, these sediments are classed as coarse sand.

The mud fraction (Fig. 6.2) (<4Φ; 0.063mm) is constrained to one main area of 320904m^2 located where the Amatikulu Estuary makes the characteristic dog leg bend in the south western corner of the map (Fig. 6.2). Here sediments contain more than 75% mud by weight percent. There is a smaller tongue extending in a north easterly direction from the main body of mud. The mud continues south into the Nyoni River. The last grouping of mud is a small area located near the Amatikulu Inlet in the north eastern corner of the Amatikulu Estuary. Both these areas rest in deep scour channels with a depth greater than 1.5m, corresponding to sours in the main channel and an abandoned inlet channel (Chapter 5). Figure 63 indicates the grain morphology of the Amatikulu Estuary sediments. This shows a high degree of sphericity with sub-angular grains.

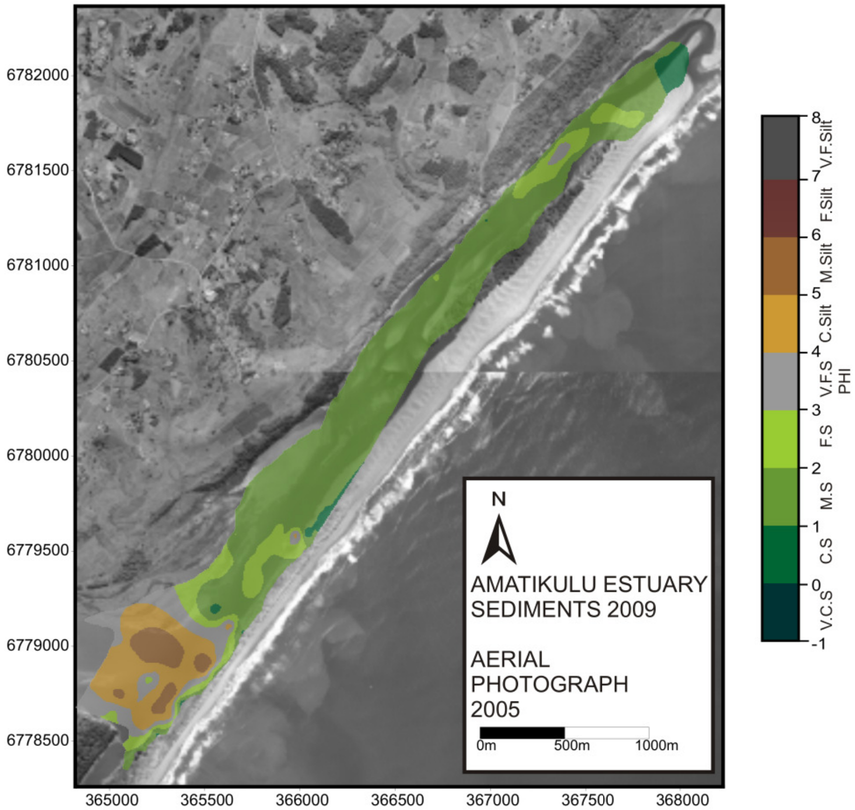

Figure 6.1 Mean sediment size distribution for the Amatikulu Estuary. Silt size fractions are accumulating at the dog leg bend of the Amatikulu Estuary. Coarse and very coarse sand are located along the barrier and in the inlet adjacent to the flood tide delta. Fine sands are predominantly transported along the main channels of the estuary.

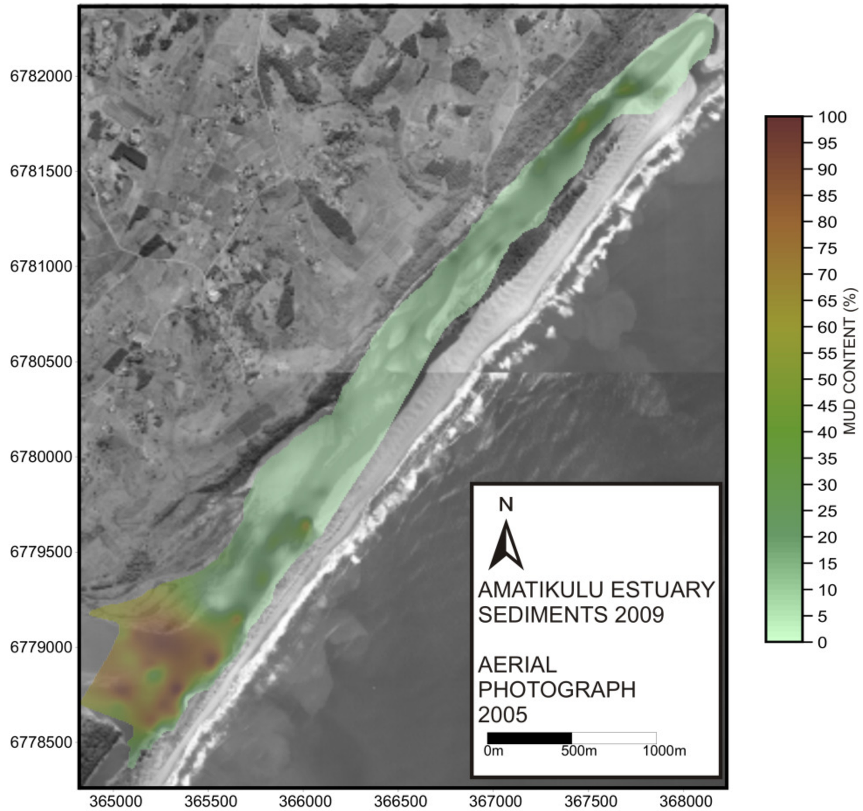

Figure 6.2 Mud distribution within the Amatikulu Estuary. The highest concentrations of mud are located at the dog leg bend. Mud concentrations increase in the main channels of the Amatikulu Estuary. This is visible as an extension of the main body of mud towards the inlet.

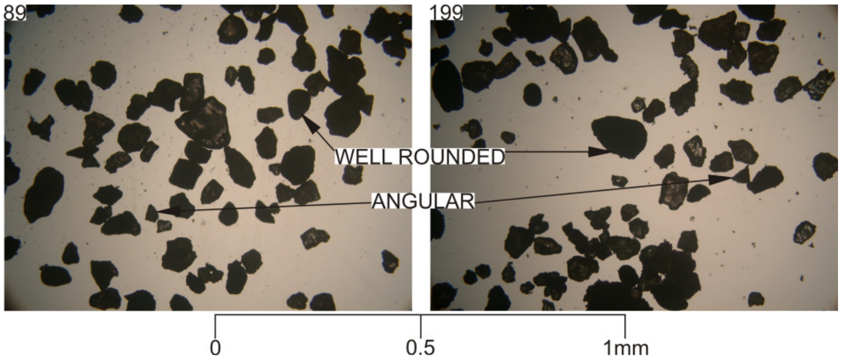

Figure 6.3 Very well sorted sediments of the Amatikulu Estuary. Sample 89 is located near the inlet whereas sample 199 is from the middle of the estuary where large overwash fans are present. Sample 89 shows rounded grains, with high sphericity. Sample 199 indicates rounded, sub-angular grains.

6.2.2. Sorting

Sorting is an indication of the spread of the grain sizes and can be used to interpret the efficiency of the transportation of sediments, the consistency of the currents and the maturity of sediments (Tucker, 1991). The more constant the sediments transportation methods the more well sorted the sediments (Tucker, 1991). The Amatikulu Estuary is entirely very well sorted (Fig. 6.4) with a narrow sediment size range.

6.2.3. Skewness

Skewness is the statistical measure of symmetry in the distribution of sediment size. The skewness of the Amatikulu Estuary (Fig. 6.5) ranges from finely skewed to coarsely skewed. These sediments are located in the inlet mouth and against the barrier and suggest that the coarse sediments are introduced into the estuary by barrier overwashing and through the inlet as a flood tide delta (see Chapter 5 and section 6.2.1).

Sediments that are symmetrically skewed are all located on the fringes of the finely and coarsely skewed sediments. This indicates that the sediments are mixed and reworked by tidal currents in these areas, resulting in the symmetry of grain size distribution. Coarsely skewed sediments are distributed in isolated pockets in the estuary and generally on the barrier side of the estuary, indicating aeolian winnowing of fine sands on the barrier.

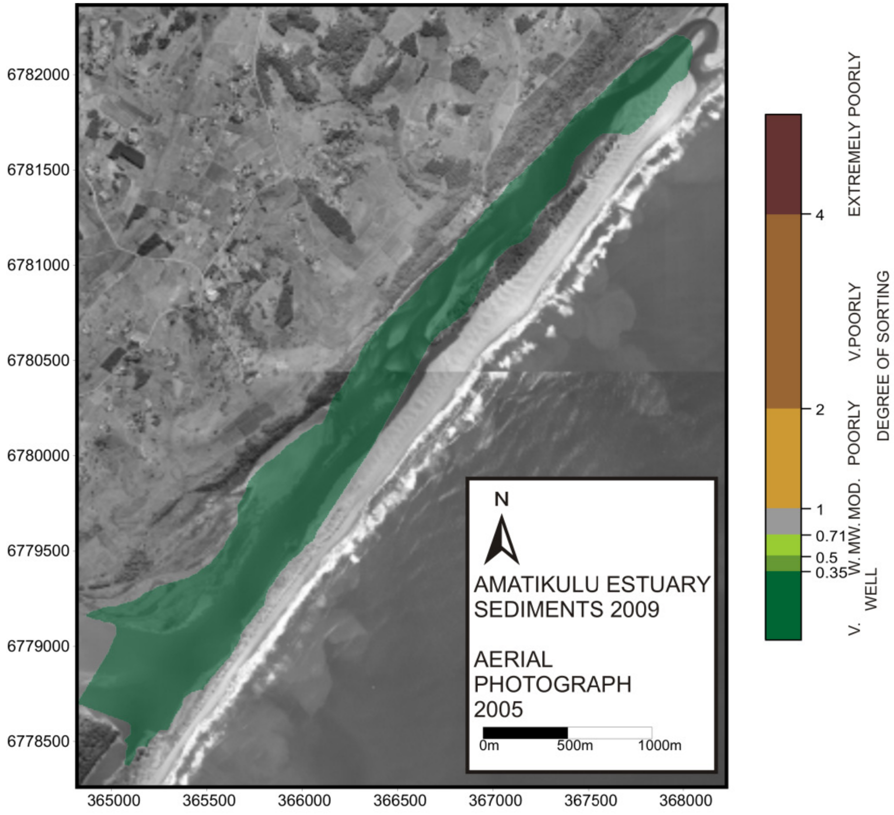

Figure 6.4 Sediment sorting within the Amatikulu Estuary. Note the homogeneity of the sorting values, the majority are classed as very well sorted.

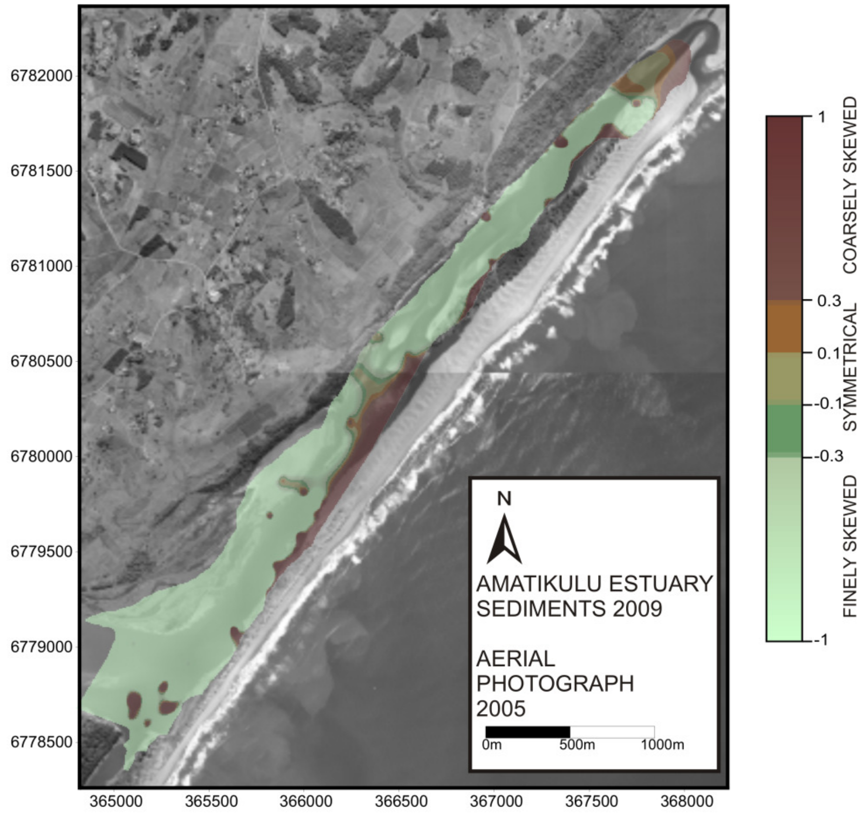

Figure 6.5 Degree of skewness of sediment samples in the Amatikulu Estuary. The Amatikulu Estuary is finely skewed on the landward side of the estuary and coarsely skewed on the barrier side.

The inlet in the north east of the Amatikulu Estuary is coarsely skewed indicating that coarser marine sediments deposited in the mouth contain large amounts of fine sediments carried in suspension to the inlet by the ebb tide and fluvial processes. A small portion of fine sediments are deposited with the coarse sediments, on the landward side of the flood deltas, in the slack waters provided by the large flood-tidal delta.

6.2.4. Calcium Carbonate Content

Calcium carbonate is derived from shells in the marine environment and provides an indication of the extent of marine influence into the estuary (Fig. 6.6) (Leeder, 1999). The mean calcium carbonate of the Amatikulu Estuary is typically 0.83% with very few values greater than 2%. The areas with the highest values are located near the inlet in the north eastern section of the estuary. These isolated pockets are considered remnants of flood-tidal deltas. The highest concentrations of calcium carbonate are located against the estuary side of the barrier. A tongue of calcium carbonate extends in a north easterly direction from the higher concentrations on the barrier. This accumulation of carbonate is assumed to have formed as overwash sediments from the coastal storm of March 2007. Carbonate dilution of the overwash results from sediments being reworked by tidal currents in the Amatikulu Estuary. This carbonate plume is linked to the main channel (See Chapter 5) of the Amatikulu Estuary that flows against and erodes the barrier in this section of the estuary, dispersing the carbonate.

6.2.5. Organic Content

The organic content is the measure of organic matter (i.e. plant material) in the sediments. This plays an important role in the adsorption of pollutants (Turner et al., 2004) (Fig. 6.7). High organic content is constricted to one main area, at the confluence of the Amatikulu and the Nyoni River’s. Sediments in this area contain organic content up to 10% whereas areas of lowest content are found against the barrier. There are small areas of higher organic content located within the main channel of the Amatikulu Estuary where it meanders through very shallow bars within the central areas of the surveyed area (see Chapter 5).

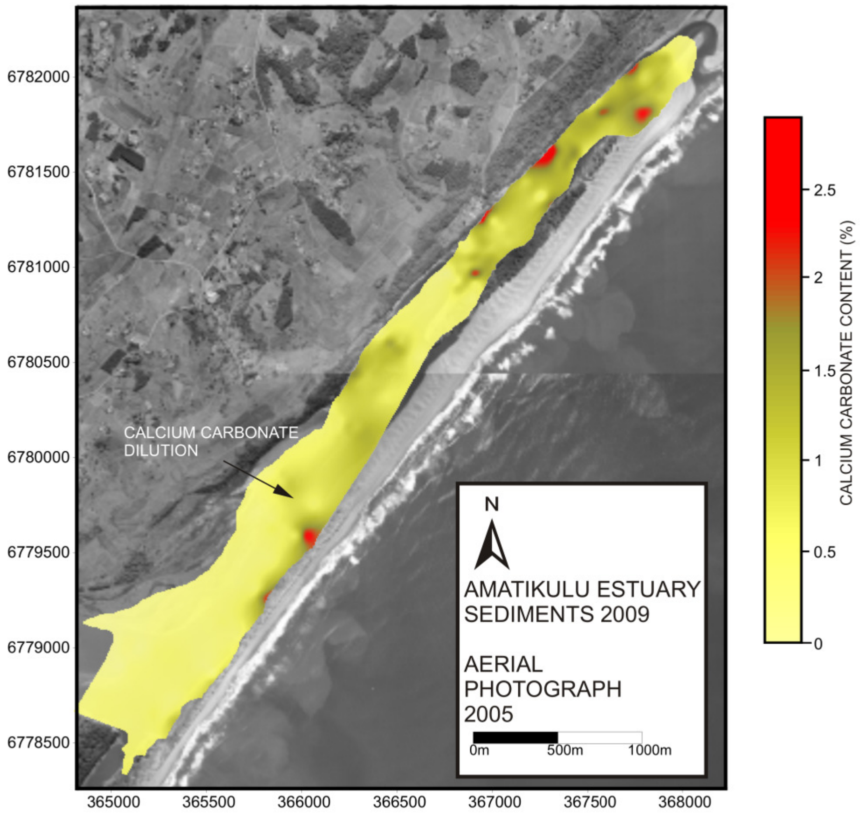

Figure 6.6 Carbonate content of the Amatikulu Estuary. Sediment of the Amatikulu Estuary generally comprise less than 2% carbonate. Areas of higher content are located against the barrier and near the inlet.

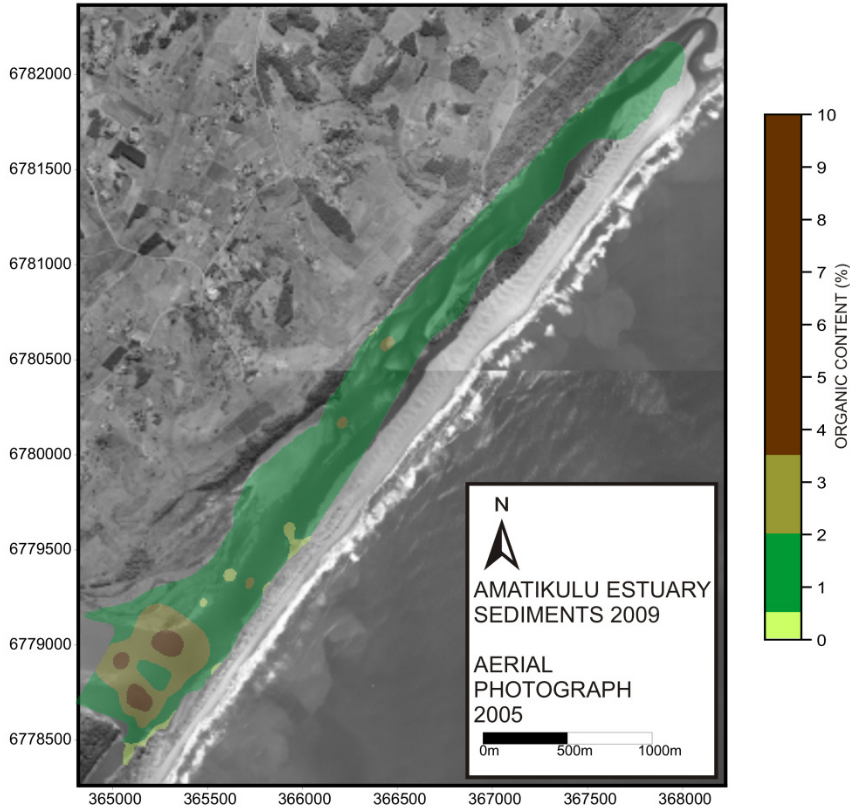

Figure 6.7 Organic content within sediment of the Amatikulu Estuary. Areas of high organic content are located at the dog leg bend and in isolated patches in the main channels in the estuary. In general the, estuarine sediment contains under 2% organic matter.

6.3. DISCUSSION

6.3.1. Sand and Mud Distribution

The sedimentological characteristics of the Amatikulu Estuary closely approximate the wave-dominated facies described by Dalrymple et al., (1992). Sandy deposits occur throughout the length of the estuary, forming the large subaqueous dunes (Chapter 5) and flood tidal delta. The sedimentological facies arrangement described also conforms to that of a delta top estuary (Cooper, 1991a) similar to the uMgeni Estuary, which he later classified as a river-dominated estuary (Cooper, 2001). This is where catchment derived sediments extend to the barrier. Fine sediment in the deeper channels of the Amatikulu Estuary is a key characteristic of Cooper's (1991a) delta top classification where under low flow periods suspension settling of mud is favoured by flocculation and agglomeration in the channels. It is unlikely that mud is introduced from the marine environment or the Thukela River, Olivier and Garland (1998) found that beach and dune sediments of the Thukela dune field south of Amatikulu Estuary contained low concentrations of mud. This was attributed to the Thukela River transporting the majority of the mud offshore and depositing it on the inner shelf (Mkhize, 2010; Bosman et al., 2007). It is most likely that mud is introduced from catchment derived material in the form of clay mineral floccules or by fine organic material. During accelerated flow this mud is then transported and ejected out the inlet in the form of a turbid plume (captured in aerial photograph in 1973 Chapter 4, Fig. 4.9).

6.3.2. Sorting

The Amatikulu Estuary shows very well sorted sediments (Fig. 63 and 6.4) unlike the uMgeni Estuary which contains poorly to very poorly sorted sediments (Tinmouth, 2009). Well sorted sediments in the uMgeni Estuary are located only in the tidal inlet and the flood-tidal delta. The very well sorted characteristics of the Amatikulu Estuary are attributed to the continual reworking by flood and ebb currents. The well sorted sediments also indicate that the sediments are influenced by a constant energy supply and a homogeneous source (Larson et al., 1997). Wright (2002) found the sediment on the margins of Lake Nhlange and Amanzinyama to be very well sorted and attributed this to wind-induced waves removing finer sediment and the reworking of well sorted Pleistocene dune cordons. The uniform nature of the sorting characteristics conforms to the sedimentation characteristics of river-dominated estuaries. Cooper (1993) states that river-dominated estuaries are essentially river channels that are dominated by fluvial input and the energy levels show very little downstream variation. The constant energy levels combined with a single sediment source will create a uniform, very well sorted sediment population.

6.3.3. Skewness

The coarsely skewed sediments of the Amatikulu Estuary are a result of coarse sediments being introduced into the estuary from tides and overwashing. Similar results were discovered by Tinmouth (2005, 2009) in the uMgeni Estuary. Cooper (1986) showed that overwashing is a major source of sediment for altering the function of the uMgeni Estuary, where the entire Beachwood mangrove channel was filled with sediments introduced from overwashing events.

6.3.4. Calcium Carbonate Content

The Amatikulu Estuary is characterised by generally low calcium carbonate content (<2%) when compared to the Sundays River (35%) for example (Illenberger, 1993; 1996). This may be more typical of KZN estuaries as the uMgeni Estuary is also low in terms of calcium carbonate (<2%). Areas of increased carbonate content correspond to areas that are coarsely skewed with the coarser sediments having higher carbonate content. These areas (Fig. 6.5) are located at the mouth of the inlet, in particular the flood tidal deltas and on the estuary side of the barrier. The samples that showed a low carbonate content correspond to samples that are finely skewed. Areas with high carbonate content and coarse particles represent overwash fans that introduce coarser marine sediments containing marine shells into the estuary. This is analogous to the overwash fans documented at Beachwood near the uMgeni Estuary (Cooper, 1986). In the case of the Amatikulu Estuary the overwashing extended the barrier into the main channel and introduced coarse marine derived sand with elevated carbonate content into the estuary. These sediments are constantly reworked by tidal current flow and transported towards the inlet of the estuary (Cooper, 1991a). Due to the coarse nature of the sediment, transport takes place as bed load transport only under much higher flow conditions. Cooper (1991a) highlights the importance of overwashing in the functioning of the estuaries, by introducing sediments and water of marine origin into the estuary which is vital for the functioning of these unique ecosystems.

Olivier and Garland (1998) found the carbonate content of the Thukela dune field to be very low. Tinmouth (2005, 2009) found that uMgeni Estuary had a carbonate content of below 2%, whereas Leuci (1998) found that samples in the uMgeni Estuary contain no more than 5% $CaCo_3$. Both values are considered very similar to that of the Amatikulu Estuary. Tinmouth (2005, 2009) concluded that carbonate was introduced into the uMgeni Estuary through barrier overwashing and introduced through the flood tidal current. In the Kosi Bay system calcium carbonate levels did not reach above 9% (Wright, 2002). Wright (2002) concluded that low carbonate contents are typical of northern KZN marine-sediment. Olivier and Garland (1998) attributed the low values of the Thukela dune field to a strong fluvial influence, low biological activity in the area and a catchment that lacks carbonate rich rocks. Carbonate content is thus directly linked to marine incursions into the estuary by overwashing and flood tide delta formation with carbonate exclusively introduced through barrier overwashing, transporting shells and shell fragments into the estuary.

6.3.5. Organic Content

Organic content is mainly isolated to a single area (Fig. 6.7). The percentage mud fraction plotted against the organic percentage gives only a small positive relationship of R^2=0.36 (Fig. 6.8). This suggests that the organic content is not entirely dependant on the accumulation of organic rich mud floccules in the Amatikulu Estuary. The organic material does not have the same distribution pattern throughout the Amatikulu Estuary as the mud distribution, hence the low relationship strength. The greatest degree of similarity between the two is at the confluence of the Amatikulu and the Nyoni Rivers. The fine material at the confluence thus appears to be an organic mud. The Beachwood mangroves of uMgeni Estuary in the Leuci (1998) study showed that organic matter is generally less than 10%. This is similar to the amount of organic matter in the sediments of the Amatikulu Estuary.

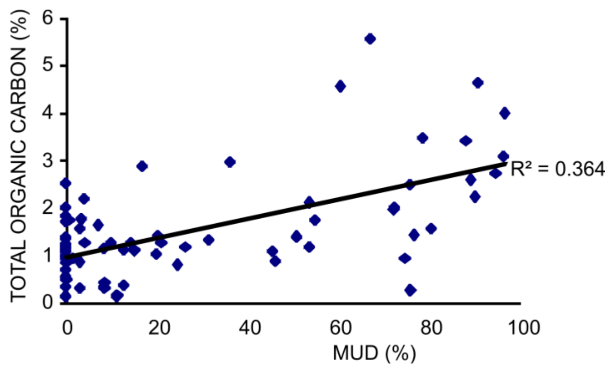

Figure 6.8 Total organic carbon calculated plotted against total mud content indicates a weak positive relationship of R^2=0.36.

CHAPTER 7

GEOCHEMISTRY

7.1. INTRODUCTION

Estuaries form an important geochemical link between the land, sea and atmosphere in the geochemical cycle, where material from land drainage, the marine environment and the atmosphere are remobilised by estuarine processes (Chester, 2003). An understanding of the chemical properties of estuaries provides a base level for which any impact of further utilization in the areas surrounding an estuary can be monitored. Increasing human activity has resulted in the increase in accumulation of metals in estuaries (Thomson et al., 1975). In many cases the accumulation of pollutions is far from the point of injection into the environment (Thomson et al., 1975). Trace elements do not stay in the sedimentary environment indefinitely and can become remobilised through a change in environmental characteristics. Heavy metals may become remobilised and ingested by organisms thus, entering the food chain (Cross et al., 1975). The chemical analysis of sediments provides a temporal and spatial indication of the state of the chemistry within the estuary (Schropp et al., 1990). It also allows for comparisons to be made between different estuarine systems. This chapter focuses on the chemistry of the Amatikulu Estuary and compares it to similar studies undertaken in the uMgeni Estuary.

7.2. RESULTS

7.2.1. Normalisation

A plot of Al against the mud fraction of sediment (Fig. 7.1) shows a significant positive relationship (R^2= 0.85). The positive relationship that Al has with the mean sediment size makes it suitable for use as the normalising element, Al was thus used to normalise the elemental concentrations. This has been used as a standard by many authors in coastal marine sediments (e.g. Windom et al., 1989, Schropp et al., 1990; Laighati et al., 2003; López-González et al., 2006; Shi et al., 2010). This is because Al is not present in most anthropogenic inputs (Schropp et al., 1990; Summers et al., 1996; Laighati et al., 2003; Bourennane et al., 2010). Al is the second most abundant metal in the earths crust (Schropp et al., 1990) and an important element in the aluminosilicate lattice (Laighati et al., 2003; Shi et al., 2010).

Geochemical normalisation was conducted in order to compensate for the natural variability of metal elements caused by grain size and mineralogy as the majority of elements and their concentrations are linked to sediment size (Shi et al., 2010). If this is not done, the results may reflect grain size rather than contamination (Chapman and Wang, 2001). It is important that the results are not site specific but allow comparison of data from different areas (e.g. analysis of specific grain size, normalisation by an index of geoaccumlation) (Schropp et al., 1990). Normalisation to a reference element e.g. mathematical normalisation (Chapman and Wang, 2001) allows the comparison of sediment geochemistry on a regional scale (Schropp et al., 1990). Normalisation to a reference element only requires the collection of metal concentration data of the sediments (Schropp et al., 1990). This method assumes a linear relationship between the normalising element and the trace metals. The normalising element must be an important constituent of the fine grained sediment fraction (Loring and Rantala, 1992).

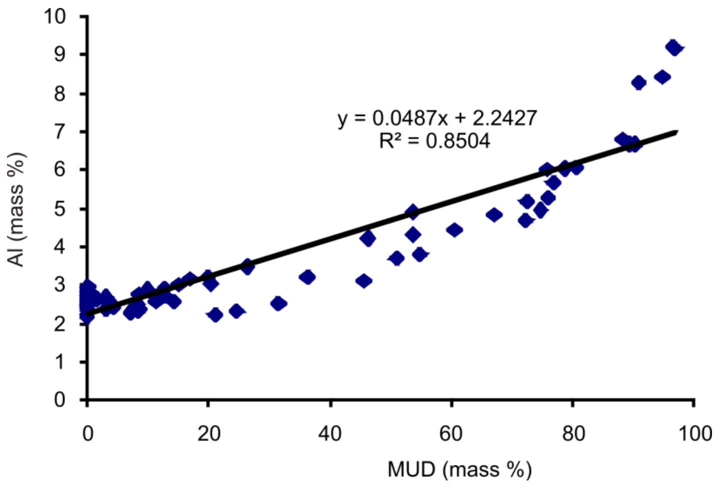

Figure 7.1 Al (wt. %) plotted against Mud (wt. %), indicating a significant relationship with Al and the fine sediments of the Amatikulu Estuary.

7.2.2. Sediment Chemistry

Major and minor element constitutes of the Amatikulu Estuary, as a weight percentage, indicate that the major constituent of the sediments are Si, Al, and Fe with 38.47%, 3.60% and 3.06% respectively (Table 7.1). Trace element concentrations (Table 7.1) in the Amatikulu Estuary were found to increase with the organic content (see Chapter 6 for mud distribution) located at the confluence of the Amatikulu and Nyoni Rivers. This relationship has been noted by many authors (e.g. Binning and Baird, 2001; Liaghati et al., 2003). Elements with a negative relationship between themselves and organic carbon content are also common e.g. Nb, Y and Rb) (Table 7.1). The strongest of these relationships with organic carbon is Sr with an R^2 value of -0.3 (Table 7.1).

7.2.3. SiO_2/Al_2O_3 Ratios

The ratio between SiO_2 and Al_2O_3 gives an indication of the maturity of the sediments as chemically immature sediment tends to be enriched in Al_2O_3 due to an abundance of Al-rich phyllosilicates (Weltje and von Eynatten, 2004; López-González et al., 2006). As the sediment matures, the Al_2O_3 is removed, elevating SiO_2. The Amatikulu SiO_2/Al_2O_3 values range from 3.74 to 22.26 (Appendix B). López-González et al., (2006) consider a value of less than 9 immature and greater than 9 mature. Sediment maturity increases from the confluence of the Amatikulu and Nyoni River towards the mouth, with the only immature sediments situated at the dog leg bend (Fig. 7.2). Regression analysis shows a direct negative relationship with SiO_2/Al_2O_3 (bulk values) ratio with the mean sediment size (in phi units) for the sediment samples with a R^2 value of -0.84 (Fig. 7.3).

7.2.4. Element Spatial Distribution and Provenance

Weltje and von Eynatten (2004) state that there is no prescribed method for provenance analysis and each study needs to be tailor-made for the area. They do also point out that for a good study, an inventory of the petrofacies and the spatial-temporal distribution is required. This study provides the first spatial distribution analysis of sediment geochemistry for the area. The majority of the trace elements come from the catchments and are transported to the Amatikulu Estuary by the Amatikulu River and Nyoni River, although some elements are marine in origin.

The following distinct spatial concentrations of the elements are identified in the Amatikulu Estuary:

1) Concentrations that are at the minimum at the confluence of the Amatikulu and Nyoni Rivers but are evenly distributed throughout the rest of Amatikulu Estuary (Fe, K, Mn, Na, Si, As, Co, Ga) (Fig. 7.4 c, d, f, g, h and Fig. 7.5 a, d, g)
2) Concentrations that are at the maximum at the confluence of the Amatikulu and Nyoni Rivers but are evenly distributed throughout the rest of Amatikulu Estuary (Cu, La) (Fig. 7.5 f, h)

Table 7.1 Major, minor and trace elements normalises to Aluminium to eliminate the effects of grain size. (-) or (+) indicates the nature of the relationship between element and Organic carbon in regression analysis. ✦Denotes normalised to Al, value in Al ratio.

Major and minor elements (wt. %)

	$Al^σ$	$Si^σ$	$Fe^σ$	$Mn^σ$	$Mg^σ$	$Ca^σ$	$Na^σ$	$K^σ$	$Ti^σ$
Mean $(Bulk)^σ$	3.60	38.47	3.06	0.05	0.68	1.34	0.89	1.15	0.37
Min (Bulk)	2.20	30.17	1.15	0.2	0.14	0.31	0.52	1.07	0.19
Max (Bulk)	9.21	42.36	6.63	0.10	1.01	0.83	1.82	1.83	0.61
Mean✦	36530.15	128587.2	9259.74	167.7551	2214.366	4658.899	2612.652	3516.375	1134.751
Min ✦	21282.4	32775.5	5046.09	69.4126	658.674	701.899	1672.49	1975.07	242.702
Max✦	92064.7	196184	31995.9	508.909	5507.31	12238.3	4012.92	4872.08	6086.85
R^2 Al	**1**	0.75	0.1	0.2	0.25	0.39	0.2	0.64	0.05
R^2 Organic carbon	(-) 0.4	(-) 0.27	(-) 0.05	(-) 0.08	(-) 0.14	(-) 0.2	(-) 0.06	(-) 0.22	(-) 0.02

Trace elements (ppm)

	Nb*	Y*	Rb*	Zr*	Sr*	U*	Th*	Zn*	Cu*	Ni*	Cr*	V*	La*	Pb*	Ga*	Co*	Ce*	Nd*	As*	Cd*	Sn*	S*
Mean $(Bulk)^σ$	7.63	18.07	47.14	297.60	128.35	1.73	7.93	25.15	9.53	11.54	72.78	83.90	9.27	11.29	10.67	13.62	42.53	17.01	10.78	12.48	121.44	1549.26
Min (Bulk)	5.20	12.10	38.90	210.90	66.80	1.50	5.60	0.10	0.00	1.90	1.40	23.00	0.00	12.00	10.00	5.00	23.00	0.00	8.00	3.00	262.00	363.00
Max (Bulk)	12.70	34.50	96.50	232.60	114.30	3.10	16.90	78.60	47.10	23.20	80.90	120.80	14.80	14.00	14.00	24.00	86.00	39.00	21.00	10.00	29.00	2221.00
Mean✦	0.000225	0.000530382	0.001352542	0.009694	0.004208	ER	0.000238	0.000639	0.000196	0.000346	0.002181	0.00255	0.000199	0.000333	0.000329	0.000408	0.001174	0.000455	0.000315	0.00041	0.004147	0.041035
Min ✦	0.0001	0.0003	0.0010	0.0024	0.0011	0.0000	0.0000	0.0000	0.0000	0.0001	0.0001	0.0008	0.0000	0.0000	0.0002	0.0001	0.0000	0.0000	0.0002	0.0000	0.0000	0.0032
Max✦	0.0011	0.0017	0.0018	0.0583	0.0069	0.0002	0.0012	0.0018	0.0006	0.0007	0.0151	0.0116	0.0018	0.0007	0.0005	0.0010	0.0050	0.0020	0.0005	0.0012	0.0119	0.1742
R^2 Al	0.04	0.07	0.25	0.07	0.64	0.05	0.03	0.16	0.69	0.15	0.02	0.08	0.1	0.06	0.67	0.18	0	0.01	0.24	0.19	0.28	0.02
R^2 Organic carbon	(-) 0.01	(-) 0.04	(-) 0.07	(-) 0.04	(-) 0.3	(-) 0.01	(-) 0.02	(+) 0.05	(+) 0.27	(-) 0.09	(-) 0.03	(-) 0.04	(+) 0.07	(-) 0.02	(-) 0.3	(-) 0.13	ER	0	(-) 0.08	(-) 0.07	(-) 0.1	(+) 0.03

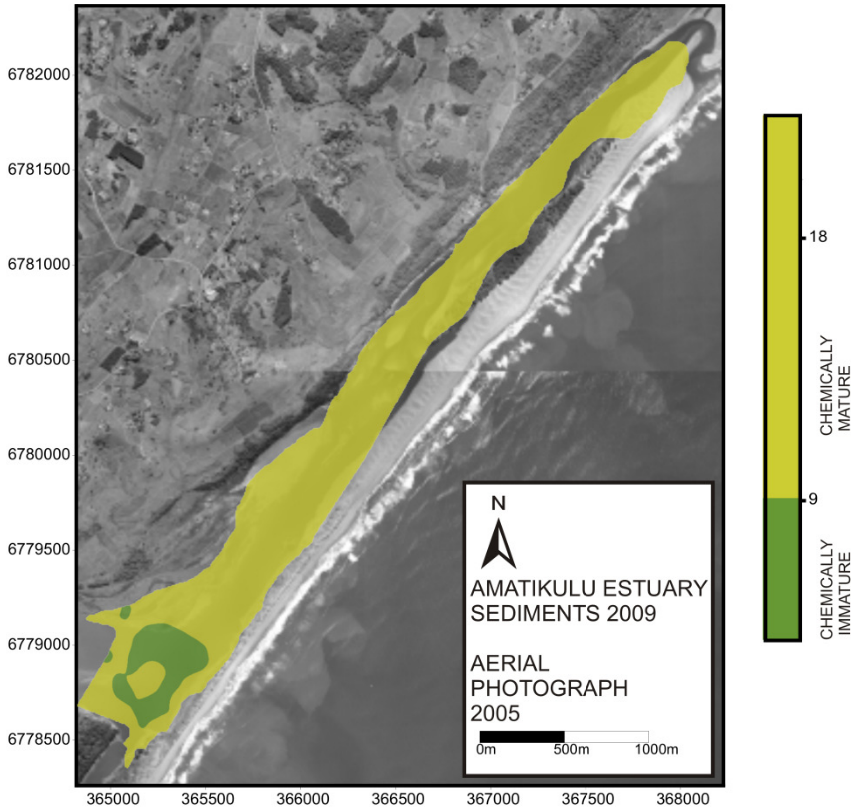

Figure 7.2 Chemical maturity of the Amatikulu Estuary sediments based on the bulk values ratio of SiO_2/Al_2O_3. This shows chemically immature sediments are located at the 90° bend of the Amatikulu Estuary.

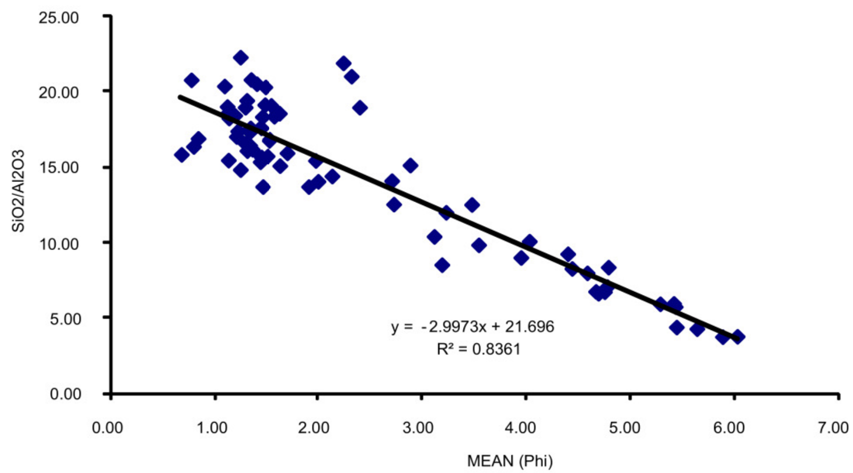

Figure 7.3 Chemical maturity of the Amatikulu Estuary sediments based on the bulk value ratio of SiO_2/Al_2O_3 plotted against mean sediment size. This indicates a significant negative relationship between the two (R^2= 0.84).

3) Concentrations that are highest at the *Casuarina* forest (Ce, Cr, Nb, Nd, Th, U, V, Y, Zr) (Fig. 7.5 c, e, i, j, q, r, s, t, v).
4) Concentrations that are highest on the landward side of the Amatikulu Estuary (Cd, S, Sn) (Fig 7.5 b, n, o).
5) Concentrations uniformly distributed throughout the Amatikulu Estuary (Rb, Zn) (Fig. 7.5 m, u).
6) Concentrations that are highest at the barrier and decrease out from the barrier (Ca, Mg, Ni, Sr) (Fig 7.4 b, e and Fig 7.5 k, p).
7) Patchy distribution throughout the estuary (Pb) (Fig 7.5 l).

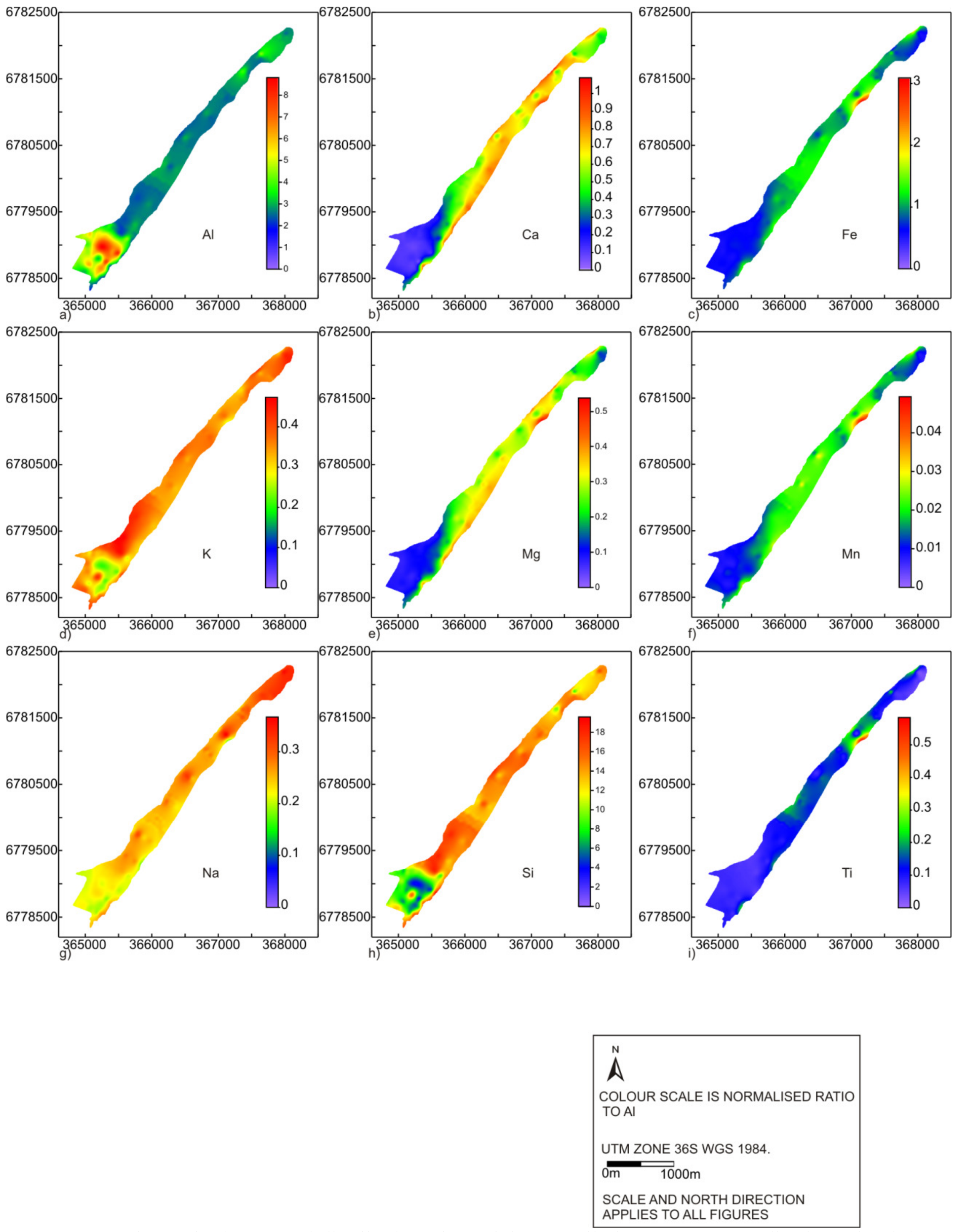

Figure 7.4 Major and minor metal distribution plots of the Amatikulu Estuary normalised to Aluminium. Ca, Fe, Mg and Mn all follow similar distribution plots, where abundance decreases as distance increases from the barrier. Na increases with decreasing distance from the inlet. Ti distribution is isolated to the Casuarina Forest. The highest concentration of K is located on the landward margins of the Amatikulu Estuary. Al and Si is are in contrast and are conversely distributed.

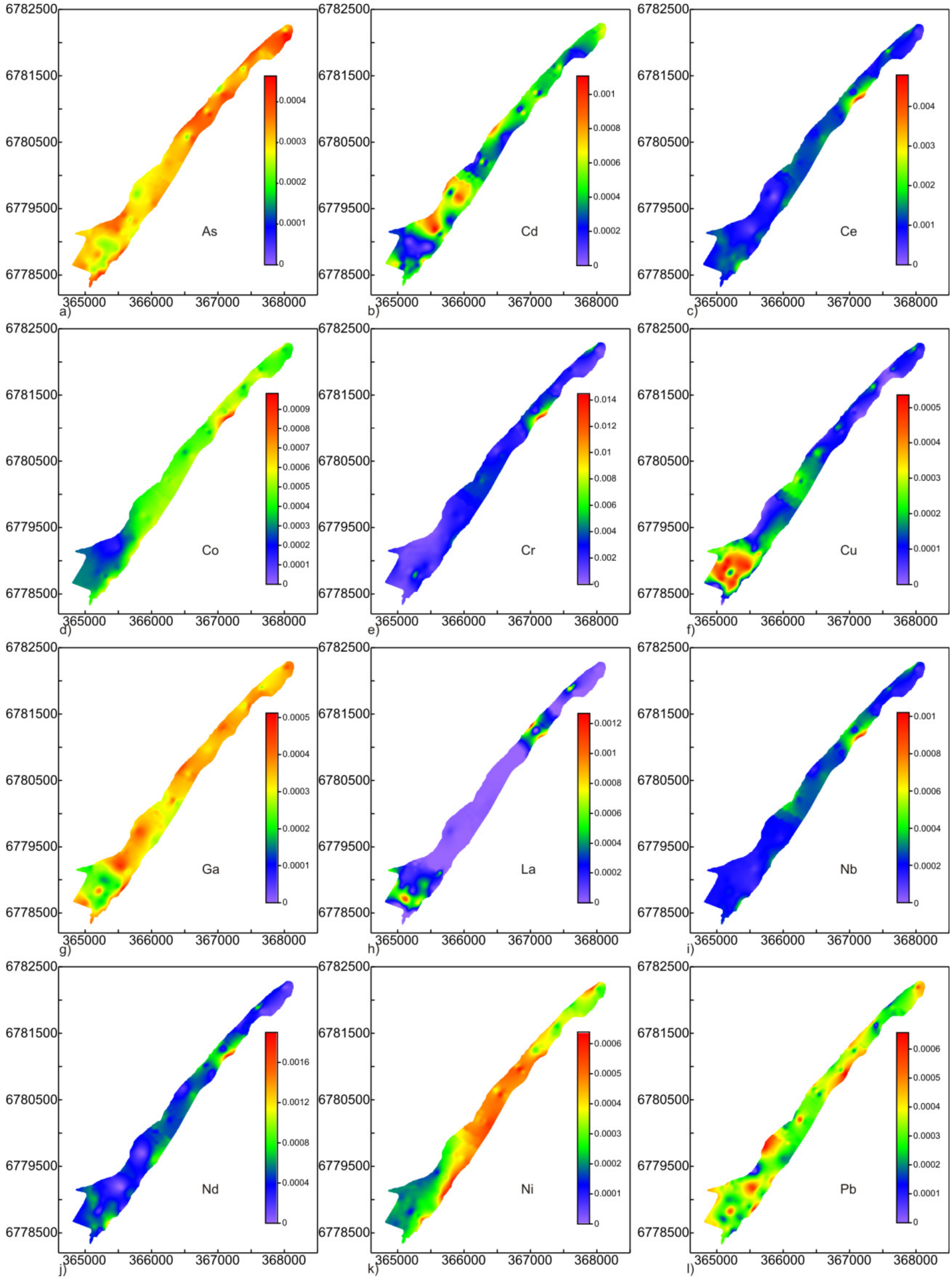

Figure 7.5 Continued over leaf.

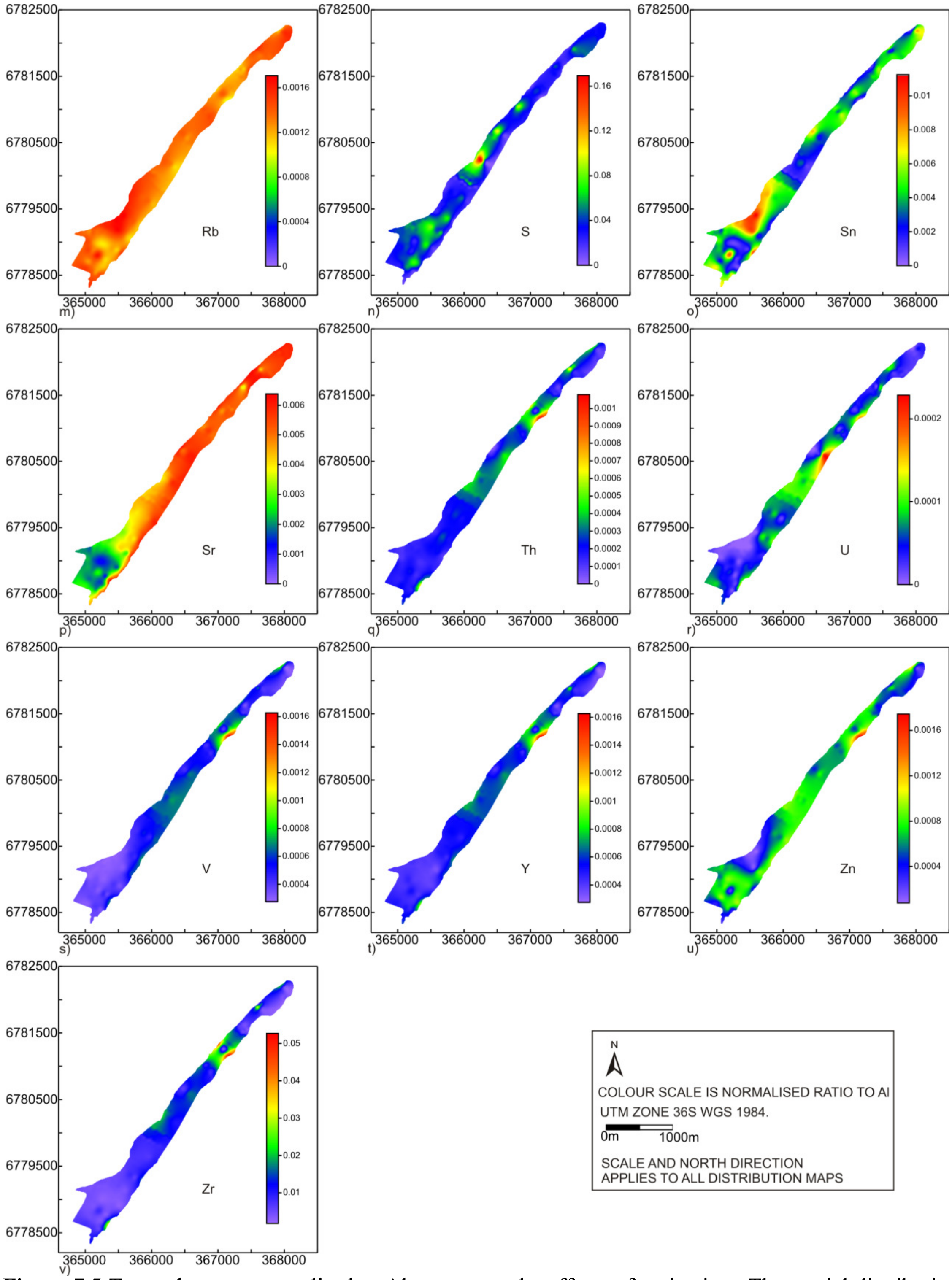

Figure 7.5 Trace elements normalised to Al to remove the effects of grain size. The spatial distribution of the elements can be divided into seven distinct distribution patterns;1) Concentration at a minimum at the confluence of the Amatikulu and Nyoni Rivers but evenly distributed though out the rest of the Amatikulu Estuary (As, Co and Ga). 2) Concentration at a maximum at the confluence of the Amatikulu and Nyoni Rivers but evenly distributed throughout the rest of the Amatikulu Estuary (Cu and La). 3) Concentration highest at the *Casuarina* forest (Ce, Cr, Nb, Nd, Th, U, V, Y and Zr). 4) Concentration highest on the landward side of the Amatikulu Estuary (Cd, S and Sn). 5) Uniformly distributed concentrations throughout the Amatikulu Estuary (Rb, Zn). 6) Concentration highest at the barrier and decreasing out from the barrier (Ni and Sr). 7) Patchy distribution throughout the Amatikulu Estuary (Pb).

7.3. DISCUSSION

7.3.1. Sediment Chemistry

In the Amatikulu system the relationship between mean sediment size and Al_2O_3 is very strong with an R^2 value of 0.87; whereas the mean sediment size plotted against Fe_2O_3 displays a weak relationship with an R^2 value of 0.25. The relationship between Al_2O_3 and Fe_2O_3 is also weak, with R^2= 0.27. Fe is most likely present in an oxide or hydroxide form. Fe is typically mobile in the reduced (anoxic) state, but precipitates in sediments under aerobic conditions.

Sediments are influenced heavily by the provenance and weathering processes that leave their impact on the chemistry of the sediments (Rollinson, 1993). To understand and quantitatively assess the abundance of the elements found in the Amatikulu Estuary, comparisons with the catchment geology is vitally important as this aids in understanding the background chemical values found in the Amatikulu Estuary. When the trace metal concentrations of the Amatikulu Estuary are compared to the various rock types located in the catchment (Table 7.2), the Amatikulu Estuary's values are always lower, except for Sn which is many times higher. In comparison to the uMgeni Estuary, Sn is also considerably higher, suggesting the possibility of either a Sn-rich source rock or some anthropogenic enrichment (Table 7.2).

Once Tinmouth's, (2009) data for the uMgeni were normalised to Al, direct comparisons between the uMgeni and Amatikulu Estuaries could be made as the two systems drain similar catchment geologies. The levels of trace elements in the uMgeni Estuary are many times greater than the concentrations found in the Amatikulu Estuary (Table 7.3). Of the potential polluting elements highlighted by Leuci (1998) and Tinmouth (2009), the uMgeni Estuary has concentrations many times greater than the Amatikulu Estuary. For example, Ni and Zn concentrations are both ~6 times higher in the uMgeni Estuary. The ternary plots of Figure 7.6 indicate that the Amatikulu trace plots plot in a similar manner to the uMgeni Estuary's pre-anthropogenic trace values, further indicating the pristine nature of the Amatikulu Estuary. Ternary plots of various heavy metals within sediments of Amatikulu Estuary, allows for further discrimination on the basis of sub-environment or facies (Fig. 7.6). These have been recognised as having unique chemical finger prints, and comprise the overwash, channel, mud and land derived samples. The values of the uMgeni Estuary are typical of a non-pristine system and plot in a vastly different manner to both the Amatikulu and pre-anthropogenic uMgeni Estuary.

Table 7.2 Trace metal concentrations of the Amatikulu Estuary with catchment geology trace metal values and Clarke value, world shale average, world soil average and the crustal average (All values are in parts per million) (table adapted from Leuci, 1998).

	As	Cd	Co	Cr	Cu	Ni	Pb	Sn	V	Zn
Amatikulu Surface Sediments (Bulk)	10.78	12.48	13.62	72.78	9.53	11.54	11.29	121.44	83.9	297.6
ERL-ERM (Long et al., 1995)	8.2-70	1.2-9.6	*	81-370	34-270	20.9-51.6	46.7-218	*	*	150-410
uMgeni surface sediments (Tinmouth, 2009)	21	*	33	97	27	123	53	21	60	233
Pre-Anthropogenic Beachwood sediments (Normalised to Fe) (Leuci, 1998)	18	*	41	116	34.5	41.5	33.4	10.5	186	109
Pre-Anthropogenic Beachwood sediments 95% confidence(Leuci, 1998)	10-26	*	28 -54	72-160	25-44	33-50	22-47	3-19	145-224	93-125
South African Coastal sediments	*	*	*	2.6-388.8	0.5-74.0	0.09-51.0	0.4-117.0	*	*	0.09-51.0
Granites of uMgeni (ave) (Kerr and Milne, 1994)	*	*	*	*	*	*	34	*	*	93
Dwyka tillite (Leuci, 1998)	*	*	*	144	19	48	*	*	104	72
Pietermaritzburg Shale (Marsh and Eales, 1984)	25	*	25	49	37	25	26	*	127	127
Clarke Value	2	*	18	83	47	58	16	*	90	83
World Average Shale	*	*	*	*	45	68	20	*	*	90
World Average Soil	*	*	*	*	20	40	10	*	*	50
Crustal Average	*	*	*	100	55	75	12.5	*	*	70

Table 7.3 The trace element content of the Amatikulu Estuary in direct comparison with the uMgeni Estuary.

Trace Element	Zn	Cu	Ni	Cr	V	Pb	Co	As	Sn
$Trace_{(uMgeni)}/Trace_{(Amatikulu)}$	6.07	2.26	5.80	0.86	0.45	3.03	2.02	1.25	0.11

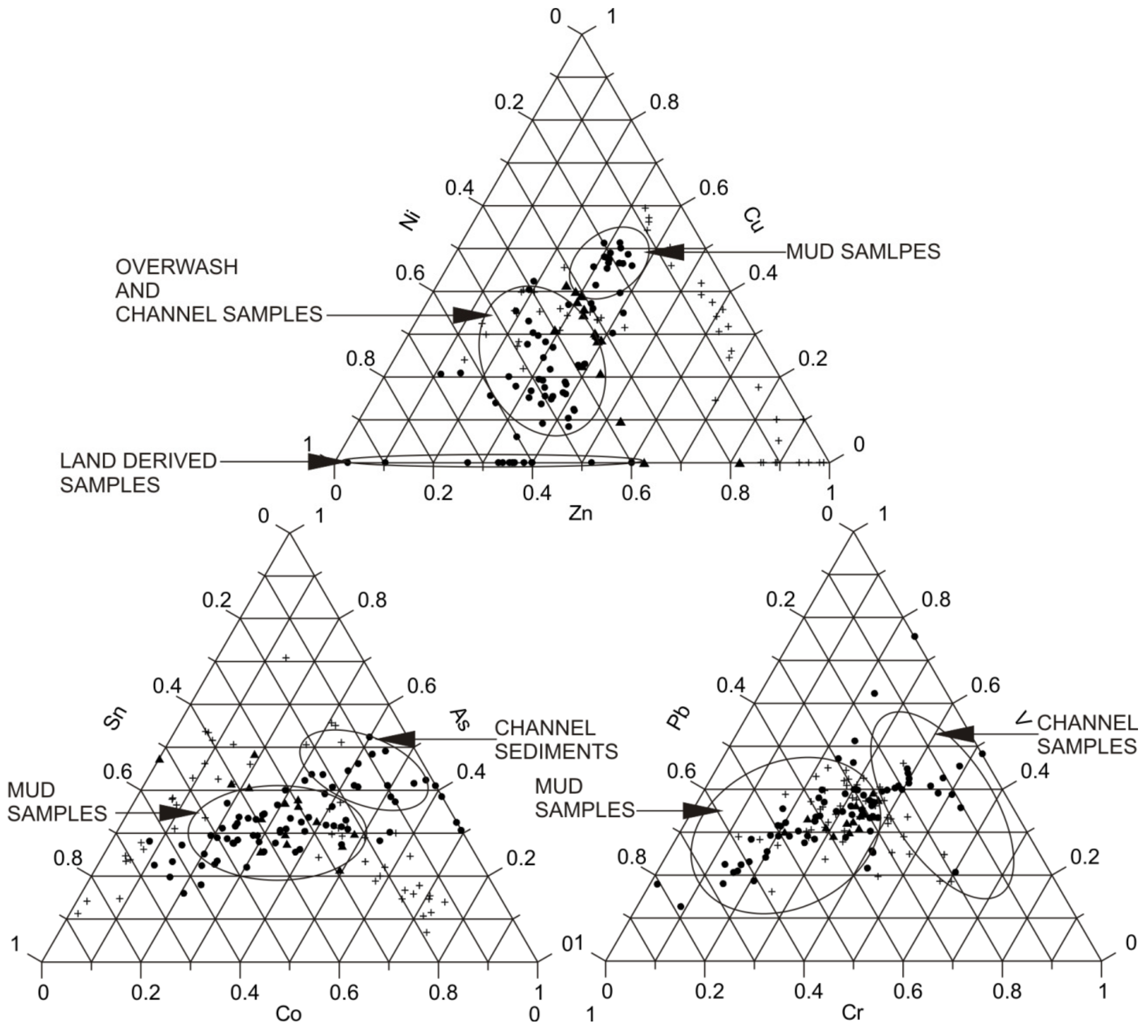

Figure 7.6 Ternary plots of heavy metal from the Amatikulu Estuary (•), uMgeni Estuary in 1998 (▲) uMgeni Estuary in 2008 (+). The ternary plots indicate that the Amatikulu Estuary has a similar chemical signature of the pre-anthropogenic uMgeni Estuary of Leuci (1998). Within the Amatikulu Estuary ternary plots chemical signatures of the mud samples, channel samples and the land derived samples sub-environments can be recognised.

7.3.2. Enrichment and Contamination

Sediments are excellent indicators of contaminants as these are integrated into sediments which are in constant flux with the water column (Binning and Baird, 2001). It is estimated that 90% of contaminants transported to estuaries and coastal areas are deposited there (Binning and Baird, 2001). Chemicals are introduced mainly through runoff into rivers which then flow into estuaries (Chapman and Wang, 2001; Harrison et al., 2001). Estuaries serve as sediment and nutrient sinks (Harrison et al., 2001; Kennedy, 1984) and provide a record of pollution levels. No base line for pre-anthropogenic levels has been established, making it difficult to evaluate contamination in the Amatikulu system. For pre-anthropogenic element levels, strategically placed cores will have to be undertaken together with XRF analysis, similar to the study of the uMgeni Estuary done by Leuci (1998). Coring was not conducted as this fell outside the scope of this study, though it is recommended for follow up studies.

Both Leuci (1998) and Tinmouth (2009) used pre-anthropogenic levels to compare present day contamination levels. These two studies provide a proxy for a preliminary desktop contamination study of the Amatikulu Estuary as the two estuaries have similar catchment geology. Using other estuaries as a proxy for contamination studies is useful where there is a lack of baseline data. Examples of studies of this nature are Callow (1994) where chemical analysis done in St. Lucia Estuary, a presumed pristine estuary, was used as base line data for the chemical analysis of Durban harbour sediments.

Using pre-anthropogenic data from the uMgeni Estuary (Leuci, 1998), enrichment values were constructed for the Amatikulu system. The levels of contamination using the enrichment equations varied. Shi et al., (2010) considers values >2 as being enriched and contaminated, whereas Tinmouth (2009) and Bourennane et al., (2010) used values greater than 1.5 as indicative of enriched and contaminated. The parameters of Tinmouth (2009) and Bourennane et al., (2010) are used here. Three levels of contamination are recognised; 0-0.5 no contamination, 0.5-1.5 negligible contamination, >1.5 indicates that large proportions of the trace metal are not derived from a natural source. Only the mean metal values presented by Leuci (1998) are used for enrichment calculations.

The enrichment factor was calculated by dividing the metal content by the Al content of each sample of the Amatikulu Estuary, this was than divided by the mean metal content of the uMgeni Estuary, divided by the mean Al content of the uMgeni Estuary:

Enrichment = $(ME/Al)_{Amatikulu} / (ME_{mean}/Al)_{uMgeni}$ (following Liaghati et al., 2003; Fang et al., 2006; Bourennane et al., 2010; Shi et al., 2010)

The distribution plots of enrichment factors (Fig 7.7) indicate 5 distinct patterns:

1) Enriched throughout the estuary (Co, Pb and Sn) (Fig. 7.7 b, f and g).
2) Barrier enrichment (Ni, V and Zn) (Fig. 7.7,e, i and h).
3) Amatikulu River enrichment (Cu) (Fig. 7.7 d).
4) Enrichment at the *Casuarina* forest (As) (Fig. 7.7 a).
5) Scattered enrichment (Cr) (Fig. 7.7 c).

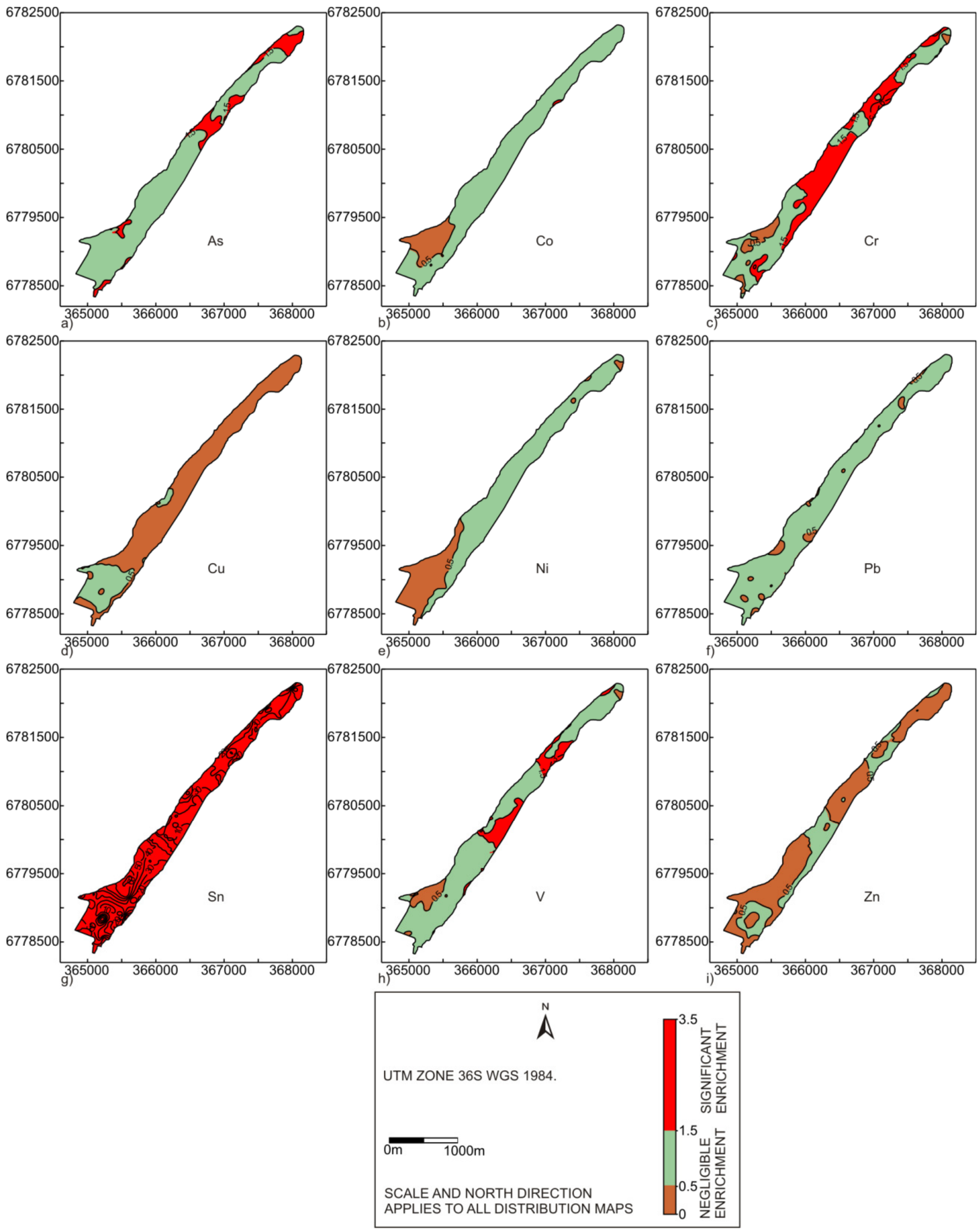

Figure 7.7 Enrichment plots of the Amatikulu Estuary using the uMgeni Estuary's (Leuci, 1998) mean pre-anthropogenic values as a proxy for the Amatikulu Estuary. Significant enrichment is only present for As, Cr, Sn and V. Tin indicating that the entire estuary has under gone significant enrichment where as As, Cr and V all have isolated pockets of enrichment in the central areas of the Amatikulu Estuary towards the Casuarina forest and inlet. Five distinct distribution patterns for the sources of enrichment are distinguishable: Co, Pb and Sn show enrichment through out the estuary. Nickel, Zn and V are enriched from the barrier. Cu shows enrichment from Amatikulu River. Arsenic shows enrichment at the Casuarina forest. Scattered enrichment indicated by Cr.

Enrichment based on the mean pre-anthropogenic metal values form the uMgeni Estuary indicates that As, Cr, Sn and V have areas of significant enrichment. Along the Amatikulu River the main source of anthropogenic influence will be from pesticides and fertilisers used in the sugar cane fields along the banks of the Amatikulu River and influxes from the sea through the inlet and barrier overwashing. This is what is expected when the catchment is less than 1% urbanised (the town of Eshowe), 33% is considered natural and 60% is agricultural with the majority comprising of sugar cane farming and small percentage subsistence farming (Harrison et al., 2001). Chemicals are routinely sprayed on the crops and these accumulate in the soil which is transported to the Amatikulu Estuary via the Amatikulu River. The anthropogenic contamination is considered to be from *pesticides* and *inorganic wastes* which may contain the elements Cd, Pb, As, Ni, Cu, Zn and Mn (Brady, 1974). Inorganic waste bio-accumulates in the food chain and the adsorption of contamination is directly linked to the organic matter content of the sediments (Brady, 1974). Finding a direct source for any pollution in the estuary is difficult due to the influence of overwashing, which introduces sediment from the Thukela River, and the additional input from the Nyoni River. Munksgaard et al., (2003) found that the longshore sediment transport on the eastern Gulf of Carpentaria results in a large sediment supply and masks the ability to distinguishing different populations within the sediments and therefore their provenance in the area. Liaghati et al (2003) feel that elevated values within estuaries may be purely natural and found that Cr tends to be elevated due to the immobility of the metal.

In comparison to Long et al.,'s (1995) international sediment contamination study, the only element that can be considered to be an environmental health risk is Zn which exceeds Long et al.,'s (1995) Ecological Response Medium (ERM) level. As and Cd both exceed the ERL (Ecological Response Low) indicating that there may be a slight contamination. Leuci's (1998) pre-anthropogenic As, Cr, Cu and Ni values for the uMgeni all exceed the ERL values. Due to the pre-anthropogenic sediments exceeding the ERL it suggests that a source rock to the uMgeni and Amatikulu Estuaries contains higher trace metals than what is described by Long et al., (1995). This highlights the importance of individual site specific studies and evaluation of site specific pre-anthropogenic studies.

7.3.3. SiO_2/Al_2O_3 Ratio

The SiO_2/Al_2O_3 ratio (Fig. 7.2) is linked to the sediment maturity in the Amatikulu Estuary as is grain size to the textural maturity. The relationships between these and their ranges (from 3.74 to 22.26) match the Odiel Estuary in South Spain. In the Odiel Estuary texturally immature sediments were associated with the muds (López-González et al., 2006) as is also found in the Amatikulu Estuary (See Fig. 6.2 for mud content). The greater textural maturity throughout the rest of the Amatikulu Estuary implies these sediments have undergone considerable reworking. Generally the sediments in the Amatikulu Estuary are texturally mature (Chapter 6) and increase in chemical maturity as the proximity to the inlet decreases.

7.3.4. Spatial Distribution and Provenance

The distribution of elements (Figs. 7.4 and 7.5) in sediments is important to understand in environmental studies, as sediments reflect the current state of the estuary and provide insight into the transportation and fate of contaminants within the estuary (Lam et al., 1997).

1) Fe, K, Mn, Na, Si, As, Co, Ga concentrations are at the minimum at the confluence of the Amatikulu and Nyoni Rivers but evenly distributed throughout the rest of Amatikulu Estuary (Fig. 7.4 c, d, f, g, h and Fig. 7.5 a, d, g). Na, K and Mn are found in saline water (Sun and Dickinson, 1995) and the distribution indicates the extent of saline water in the Amatikulu Estuary. The minimum concentrations at the confluence are due to increased fresh water entering the system through the two river systems. The increase in Si concentration is due to the progressive chemical maturation of sediments through reworking and the removal of Fe.

2) Cu and La concentrations are at their maximum at the confluence of the Amatikulu and Nyoni Rivers but evenly distributed throughout the rest of Amatikulu Estuary (Fig. 7.5 f, h). Cations adsorb to the surface of clay minerals a relationship noted by many authors (Rae and Aston, 1982), Cu and La would readily adsorb with the clay particles from solution hence increasing the concentrations in this area (Shi et al., 2010).

3) Ca, Mg, Ni, Sr Concentrations are highest at the barrier and decrease out from the barrier landwards (Fig 7.4 b, e and Fig 7.5 k, p). These elements that are not of fluvial

origin having clearly accumulated along the barrier and the inlet of the Amatikulu Estuary, indicating a marine origin. Sr is a major component of sea water and can be present in quantities as high as 8ppm (Turekian, 1964). Sr, as with many other major, minor and trace elements that are concentrated marine sediment, is removed from the surrounding sea water and incorporated into the shell lattice during shell formation of calcareous organisms such as foraminifera, molluscs and coral-oolite-algae (Turekian, 1964; Cravo et al., 2002). Clays however, in the deep sea are not good removers of Sr and this relationship is expected to continue onto the continental margins (Turekian, 1964). This explains why Sr is not concentrating in the muds in comparison with many of the other elements. Sr is however introduced via carbonate shells indicating the extent of marine intrusion into the Amatikulu Estuary (Chapter 6, Fig.6.6), hence the identical spatial distribution of Ca (in $CaCO_3$) and Sr. Similarly Mg and the trace element Ni have exactly the same spatial distribution patterns. This is due to the incorporation of Mg and Ni from the surrounding water into the shell during formation (Cravo et al., 2002; Kondo et al., 2005). This distribution indicates that marine intrusion occurs over the barrier through a process of overwashing and the tidal influx of the flood tide through the inlet. Sr levels at the uMgeni mouth (Tinmouth, 2009) are the same indicating that the Sr was introduced in a similar manner. With a range of 66.8-114.3ppm and a mean value of 128.35ppm the values are substantially lower than the Upper Continental Crust (UCC) value of 350ppm (Taylor and McLennan, 1995). Sr levels in cores collected on the lower continental slope between northern Taiwan and the southern Okinawa Trough also showed Sr level significantly below the UCC (Bentahila et al., 2008). The Sr, Ca and calcium carbonate spatial distribution patterns provide unequivocal evidence for the extent of marine incursion of sediment into the Amatikulu Estuary (Chapter 6).

4) Pb has a patchy distribution throughout the estuary (Fig 7.5 l). The amount of Pb found in the estuary is lower than the UCC values of roughly 20ppm (Taylor and McLennan, 1995). The Amatikulu Estuary has a maximum Pb concentration of 14ppm (bulk values); this indicates that there is no Pb contamination within the Amatikulu Estuary.

CHAPTER 8

CONCLUSIONS

The portion of coastline stretching from the Thukela River northwards to the Amatikulu Estuary is unique in terms of the coupling between the large sediment load supplied by the Thukela River and the response of the coastline to this. The following conclusions can be made regarding the coastal geomorphology and more specifically the geomorphology and sediment dynamics of the Amatikulu Estuary.

1) The geomorphological setting of the study area is dominantly progradational in nature. Coastline progradation is most pronounced after flooding episodes of the Thukela River, where the coastal growth is on average of 25m/yr for the period of 1973 to 1978 and an average of 29m/yr during 1983 to 1989. A pronounced lag between the flood and the period of maximum progradation is experienced, indicating that sediments are retained for a 2 to 6 year period of time as shallow, ephemeral offshore-bars. These are later reworked by the energetic wave regime of the area onto the most proximal northern Thukela beaches. Growth is linked to a very high longshore (and most likely beach) drift in this area, as evidenced by progressive tailing off of beach growth rates from south to north in the study area. Superimposed on the net progradation of the area are periods of minor erosion where the coastline readjusts due to disequilibrium between the high wave energy of the coastline and lack of sediment available during these periods. The overall progradation rate has been calculated at 2.9m/yr over a 52 year period. In light of this, the landforms occurring on this coast, including the Amatikulu Estuary, appear to represent the exposed upper surface of the submerged Thukela Delta (cf Bosman et al., 2007). The sediments dealt with in this thesis are reworked portions of this delta, which due to high wave energy exists in a submerged sense. From a managerial perspective, the damming of the Thukela River would result in reduced sedimentary inputs to the study area and produce an erosional situation.

2) The Amatikulu Estuary, and several other estuaries north of the study area, possess extensive shore parallel tidal channels and long (~ 7 km) barrier complexes. This study considers these to form due to the extremely high amounts of sediment carried in the longshore drift. Where other

microtidal estuaries simply involve an inlet which slowly migrates up-drift along the barrier after flood-induced breaching, the flood-inlet of the Amatikulu Estuary appears to almost instantaneously close due to the high rate of sediment delivery to the coastline and re-open in its normal position after flooding. In this light the barrier is maintained with only two main openings to the ocean, and is effectively stretched in this lengthy extension by south to north forcing of the longshore drift. The capture of the Nyoni River to the south by the Amatikulu Estuary is a result of this, extending its course by an additional 14 km.

Major storms and associated storm waves effectively plug the contemporary inlet and cause a minor inlet to begin forming south of the *Casuarina* forest. This is short lived. Either the estuary is artificially breached, as in 2007, or it re-establishes the inlet in its northern position once the estuary hydraulic head is elevated by ordinary catchment inputs (like other river dominated estuaries). Of great importance is the role that overwash sediment plays during inlet plugging. This appears to be the dominant sediment source at present, and one of the controls on channel morphology. Overall, the estuary appears to conform to Dalrymple et al.,'s (1992) model of a wave dominated estuary. In this light, it departs from the model of a river-dominated microtidal estuary of Cooper (2001).

3) Sedimentological data show that the estuary comprises well sorted fine sand, with isolated coarser sand bodies. These represent the terminus of the overwash fans and the steepest portions of the estuary. Overwash fans typically conform to the overwash plain morphology of Matias et al., (2010) and comprise extensive sheet-like bodies of sediment which form the "point bar" sediment in the channel meanders. Mud is isolated and confined to small bathymetric scours which were filled by fine material such as in other river dominated type settings. This fine material at the confluence of the Amatikulu Estuary and Nyoni River is essentially organic mud. Sorting values reflect the homogeneity of the sediment inputs and the extent of reworking in the area.

4) The tidal channel morphology of the Amatikulu Estuary suggests that the channel is a relict feature which formed during elevated flow velocities, like other river dominated estuaries, yet is now out of equilibrium with the tidal processes operating in the tidal basin. This is reflected by the predicted sediment sizes being far greater than those sampled, based on empirical

hydrological equations. The very large dunes may also be a relict set of features which are only active during elevated (though probably not catastrophic flooding) water velocities. On the whole, the channel morphology appears to be controlled to a greater extent by marine overwash inputs than by fluvial sediments, a product of the lengthy barrier increasing the likelihood of overwash plain morphologies developing.

5) Geochemical analyses of the surface sediments of the Amatikulu Estuary indicate no anthropogenic enrichment of the Amatikulu Estuary when compared to that provided from the catchment geology. In a comparison between this estuary and the river-dominated uMgeni Estuary, the Amatikulu Estuary is considered pristine. In addition, based on the chemical signature of these sediments, various facies may be delineated, especially those of marine origin. Sr, Ca, Mg and Ni indicate the extent of marine incursion into the Amatikulu Estuary and correlate well with traditional grain size techniques. These confirm that the sand bodies controlling channel form are marine in origin.

In almost all aspects, the Amatikulu Estuary appears to be dominantly controlled by longshore drift, rather than the river and tidal components recognised by Cooper (2001) as the two canons of open-estuaries. Despite some similarities, it is clear that the form of the estuary departs dramatically from that of a river-dominated scheme. Other such estuaries include the Mlalazi and the Mtunzini Estuaries which share similar components to the Amatikulu system and are located in a similar geomorphological setting. In this light, this thesis proposes a new class of microtidal estuary: the *longshore drift* dominated estuary. It is recommended that the above mentioned estuaries, as well as estuaries which exist on similar prograding, microtidal wave-dominated coastlines be further studied to better constrain the models proposed here for the morphodynamic functioning of such longshore drift dominated systems.

REFERENCES

Allen, G.P., Posamentier, H.W., 1994. Transgressive facies and sequence architecture in mixed tide- and wave-dominated incised valleys: Example from the Gironde Estuary, France. In: Dalrymple, R.W., Boyd, R., Zaitlin, B.A. (Eds.), Incised valley systems: Origin and sedimentary sequences, Special Publication, Society of Economic Paleontological and Mineralogists, 51, 225-240.

Ainsworth, B.R., Walker, R.G., 1994. Control of Estuarine Valley-fill deposition by fluctuations of relative sea level, Cretaceous Bearpaw-Horseshoe Canyon Transition, Drumheller, Alberta, Canada. In: Dalrymple, R.W., Boyd, R., Zaitlin, B.A. (Eds.), Incised valley systems: Origin and sedimentary sequences, Special Publication, Society of Economic Paleontological and Mineralogists, 51, 159-174.

Ashley, G.M., 1990. Classification of large-scale subaqueous bedforms: A new look at an old problem. Journal of Sedimentary Petrology. 60, 1, 160-172.

Austin, M.J., Masselink, G., 2006. Observations of morphological change and sediment transport on a steep gravel beach. Marine Geology. 229, 59-77.

Barnard, P.L., Warrick, J.A., 2010. Dramatic beach and nearshore morphological changes due to extreme flooding at a wave-dominated river mouth. Marine Geology. 271, 131-148.

Barnes, M.P., O'Donoghue, T., Alsina, J.M., Baldock, T.E., 2009. Direct bed shear stress measurements in bore-driven swash. Coastal Engineering. 56, 853-867.

Barusseau, J.P., Bâ, M., Descamps, C., Doip, E.S., Diouf, B., Kane, A., Luc Saos, J., Soumarė, A., 1998. Morphological and sedimentolgical changes in the Senegal River estuary after the construction of Diama dam. Journal of African Earth Science. 26, 317-326.

Bauer, B. O., Sherman, D. J., 1999. Coastal dune dynamics: Problems and prospects. In: Goudie, A.S., Livingstone, I., Stokes S., (Eds): Aeolian Environments, Sediments and Land Forms. John Wiley and Sons, England. 71-127.

Begg, G., 1978. The Estuaries of Natal. Natal Town and Regional Planning Report. Blackhouse, Pietermarizburg. 657pp.

Begg, G., 1984. The estuaries of Natal. Part 2. Natal Town and Regional Planning Report. 55, 631pp.

Bentahila, Y., Othman, D.B., Luck, J.M.., 2008. Strontium, lead and zinc isotopes in marine cores as tracers of sedimentary provenance: a case study around Taiwan orogen. Chemical Geology. 248, 62-82.

Binning, K., Baird, D., 2001. Survey of heavy metals in the sediments of the Swarkop river, Estuary, Port Elizabeth South Africa. Water SA. 27, 461-466.

Bird, E., 1985. Coastline Changes: A Global Review. John Wiley and Sons Ltd, New York. 219pp.

Bird, E., 2000. Coastal Geomorphology: An Introduction. John Wiley and Sons Ltd, England. 322pp.

Blake, D., 2006. Beach Dynamics along the Durban Bight Coastline, KwaZulu-Natal. Unpublished Honours dissertation, University of KwaZulu-Natal. 96pp.

Brady, N.C., 1974. The Nature and Properties of Soils. Macmillan Publishing, New York. 639pp.

Bosman, C., Uken, R., Leuci, R., Smith, A.M., Sinclair, D., 2007. Shelf sediments off the Thukela River mouth: complex interactions between fluvial and oceanographic processes. South African Journal of Science. 103, 490-492.

Bourennane, H., Douay, F., Streckeman, T., Villanneau, E., Ciesielski, H., King, D., Baize, D., 2010. Mapping of anthropogenic trace elements inputs in agricultural topsoil from Northern France using enrichment factors. Geoderma. 157, 165-174.

Boyd, R., Ruming, K., Goodwin, I., Sandstrom, M., Schröder-Adams, C., 2008. Highstand transport of coastal sand to the deep ocean: A case study from Fraser Island, southeast Australia. Geology. 36, 15-18.

Bremner, J.M., Rogers, J., Willis, J.P., 1990. Sedimentological aspects of the 1988 Orange River floods. Transactions of the Royal Society of South Africa. 47, 247-294.

Brooke, B., Ryan, D., Pietsch, T., Olley, J., Douglas, G., Packett, R., Radke, L., Flood, P., 2008. Influence of climate fluctuations and changes in catchment land use on Late Holocene and modern beach-ridge sedimentation on a tropical macrotidal coast: Keppel Bay, Queensland, Australia. Marine Geology. 251, 195-208.

Burningham, H., 2008. Contrasting geomorphic response to structural control: The Loughros estuaries, northwest Ireland. Geomorphology. 97, 300-320.

Buijsman, M.C., Ridderinkhof, H., 2008. Long-term evolution of sand waves in the Marsdiep inlet. II: Relation to hydrodynamics. Continental Shelf Research. 28, 1202-1215.

Callow, S., 1994. Aspects of Heavy Metal Concentration in Natal Estuaries Sediments. Unpublished MSc dissertation, University of Natal, 130pp.

Cameron, W.M., Pritchard, D.W., 1963. Estuaries. In, Hill, M.N.,(Ed): The Sea. Wiley-Interscience, New York. 306-324pp.

Camenen, B., Larson, M., 2005. A general formula for non-cohesive bed sediments transport. Estuarine, Coastal and Shelf Science. 63, 249-260.

Chapman, P.M., Wang, F., 2001. Assessing sediment contamination in estuaries. Environmental Toxicology and Chemistry. 20, 1, 3-22.

Chester, R., 2003. Marine Geochemistry. Blackwell Publishing, United Kingdom. 506pp.

Cooper, J.A.G., 1986. Subaerial Washover Fans In The Beachwood Mangrove Area, Durban. Unpublished Report, University of Natal. 23pp.

Cooper, J.A.G., 1990. Ephemeral stream-mouth bars at flood-breached river mouths on a wave-dominated coast: Comparison with edd-tidal deltas at barrier inlets. Marine Geology. 95, 57-70.

Cooper, J.A.G., 1991a. Sedimentary Models and Geomorphological Classification of River-Mouths on a Subtropical, Wave-dominated Coast, Natal, South Africa. Unpublished PhD Thesis, University of Natal. 401pp.

Cooper, J.A.G., 1991b. Shoreline changes on the Natal Coast Tugela River Mouth to Cape St Lucia. The Natal Town and Regional Planning Commission, Pietermaritzburg, South Africa. 57pp.

Cooper, J.A.G., 1993. Sedimentation in a river-dominated estuary. Sedimentology. 40, 979-1017.

Cooper, J.A.G., 1994. Sedimentation in the river-dominated Mvoti estuary, South Africa. Geomorphology. 9, 4, 271–300.

Cooper, J.A.G., Ramm, A.E.L., Harrison, T.D., 1994. The Estuarine health Index: A New Approach to Scientific Information Transfer. Ocean and Coastal Management. 25, 103-141.

Cooper, J.A.G., 2001. Geomorphological variability among microtidal estuaries from the wave-dominated South African coast. Geomorphology. 40, 99-122.

Cooper, J.A.G., 2002. The role of extreme floods in estuary-coastal behaviour: contrasts between river- and tide-dominated estuaries. Sedimentary Geology. 150, 123-137.

Cooper, J.A.G., Green, A.N., Wright, C.I., 2010. Evolution of an incised valley coastal plain estuary under low sediment supply. Sedimentology. In press.

Cornell, D.H., Thomas, R.J., Moen, H.F.G., Reid, D.L., Moore, J.M., Gibson, R.L., 2006. The Namaqua-Natal Province. In: Johnson, M.R., Anhaeusser, C.R., Thomas, R.J. (Eds.), The Geology of South Africa, Johannesburg/Council for Geoscience, Pretoria. 325-380.

Cowell, P.J., Thom, B.G., 1994. Morphodynamics of coastal evolution. In: Carter, R.W.G., Woodroffe, C.D. (Eds.), Coastal evolution: Late Quaternary shoreline morphodynamics, Cambridge University Press, United Kingdom. 33-86.

Cravo, A., Foster ,P., Bebianno, M.J., 2002. Minor and trace elements in the shell of *Patella aspera* (Röding 1798). Environmental International. 28, 295-302.

Cross, F.A., Willis, J.N., Hardy, L.H., Jones, N.J., Lewis, J.A., 1975. Role of juvenile fish in cycling of Mn, Fe, Cu, Zn in a coastal plain estuary. In: Cronin, L.E., (Ed): Estuarine Research 1. Chemistry, Biology and the Estuarine System. Academic Press, New York. 45-65.

Dalrymple, R.W., Zaitlin, R.A., Boyd, R., 1992. A conceptual model of estuarine sedimentation. Journal of Sedimentary Petrology. 62, 1130-1146.

Davies, J.L., 1964. A morphological approach to world shorelines. Zeitschrift für Geomorphologie. 8, 127-142.

Day, J.H., 1980. What is an estuary? South African Journal of Science, 76, 198pp.

Day, J.H., 1981. Estuarine Ecology with Particular Reference to South Africa. Cape Town: Balkema. 411.

Dunkley, E., Schoonees, J.S., Theron, A.K., 1998. Thukela water project effects of a reduction in the Thukela River sediment Yield on the adjacent coastline. CSIR Report ENV/S-C 98029 Draft report. CSIR, Pretoria, South Africa.

Dyer, K.R., 1979. Estuaries and estuarine sedimentation, In Dyer, K.R. (Ed.), Estuarine hydrography and sedimentation. Cambridge University Press, Great Britain. 1-19.

Dyer, K.R, 1986. Coastal and Estuarine Sediment Dynamics. John Wiley and Sons, England. 342pp.

Dyer, K.R., 1997. Estuaries. A Physical Introduction. John Wiley and Sons, England. 195pp.

Fang, G.C., Wu, Y.S., Chang, S.Y., Huang, S.H., Rau, J.Y., 2006. Size distributions of ambient are particles and enrichment factor analysis of metallic elements at Taichung Harbor near the Taiwan Strait. Atmospheric Research. 81, 320-333.

Fenster, M.S., FitzGerald, D.M., 1996. Morphodynamics, stratigraphy, and sediment transport patterns of the Kennebec River estuary, ME, USA. Sedimentary Geology. 107, 99-120.

FitzGerald, D.M., Buynevich, I.V., Fenster, M.S., McKinlay, P.A., 2000. Sand dynamics at the mouth of a rock-bound, tide-dominated estuary. Sedimentary Geology. 131, 25-49.

Flemming, B.W., 1980. Sand transport and bedformpatterns on the continental shelf between Durban and Port Elizabeth (southeast African continental margin). Marine Geology. 26, 179–205.

Folk, R.L., Ward, W.C., 1957. Brozos River bar: A study in the significance of grain size parameters. Journal of Sedimentary Petrology. 27, 3-26.

Folk, R.L., 1974. Petrology of Sedimentary Rocks. Hemphill Publishing Company, Texas. 194pp.

Green, A.N., 2004. The Fish Traps and Sedimentary Dynamics of the Kosi Bay Estuary, Northern KwaZulu-Natal, South Africa. Unpublished MSc dissertation, University of KwaZulu-Natal. 151pp.

Green, A.N., 2009. The Marine Geology of the Northern KwaZulu-Natal Continental Shelf, South Africa. Unpublished Phd dissertation, University of KwaZulu-Natal. 195pp.

Green, A.N., Uken, R., 2005. First observations of sea level indicators related to glacial maxima at Sodwana Bay, Northern KwaZulu-Natal. South African Journal of Science. 101, 236-238.

Green, A.N., Garland, G.G., Uken, U., 2006. Geomorphological and managerial implications of fish trapping in the Kosi Bay Estuary, KwaZulu-Natal, South Africa. African Journal of Marine Science. 28, 617-624.

Green, M.O., Vincent, C.E., McCave, I.N., Dickson, R.R., Reeso, J.M., Pearsono, N.D., 1995. Storm sediment transport: observations from the British North Sea shelf. Continental Shelf Research. 15, 8, 889-912.

Hanslow, D.J., 2007. Beach Erosion Trend Measurement: A Comparison of Trend Indicators, Journal of Coastal Research, SI 50, 588-593.

Harrison, T.D., Hohls, D.R., Meara, T.P., Webster, M.S., 2001. South African Estuaries: Catchment Land-Cover; National Summary Report. Division of Water, Environment and Forestry Technology, Environmentek CSIR. 1-11.

Hayes, M.O., 1979. Barrier island morphology as a function of a tidal and wave regime. In: Leatherman, S.P., (Ed)., Barrier Islands. Academic Press, New York. 1-27.

Hesp, P., 2002. Foredunes and blowouts: initiation, geomorphology and dynamics. Geomorphology. 48, 245-268.

Hicks, D.M., Inman, D.L., 1987. Sand dispersion from an ephemeral delta on the Central California coast. Marine Geology. 77, 305-318.

Houser, C., Hapke, C., Hamilton., 2008. Controls on coastal dune morphology, shoreline erosion and barrier response to extreme storms. Geomorphology. 100, 223-240.

Hughes, P., Brundrit, G.B., 1995. Sea Level rise and coastal planning: a call for stricter controls in river mouths. Journal of Coastal Research. 11, 887-898.

Illenberger, W.K., 1993. Variations in the sediment dynamics in Algoa Bay during the Holocene. South African Journal of Science. 89, 187-195.

Illenberger, W.K., 1996. The geomorphological evolution of the Wilderness dune cordons, South Africa. Quaternary International. 33, 11–20.

Johnson, M.R., van Vuuren, C.J., Visser, J.N.J., Cole, D.I., de V. Wicken, H., Christie, A.D.M., Roberts, D.L., Brandl, G., 2006. Sedimentary Rock of the Karoo Supergroup. In: Johnson, M.R., Anhaeusser, C.R., Thomas, R.J., (Eds.), The Geology of South Africa, Johannesburg/Council for Geoscience, Pretoria. 461-500.

Kerr, A., Milne, G.C., 1994. The Mgeni granite: an example of the megacrystic mantled-feldspar granite-charnockite intrusives in southeastern Africa. Mineralogy and Petrology. 50, 139-155.

Kennedy, V.S., 1984. The Estuary as a Filter. Academic Press, New York. 511pp.

Kindinger, J.L., Balson, P.S., Flocks, J.G., 1994. Stratigraphy of the the Mississippi-Alabama shelf and the Mobile river incised-valley system. In: Dalrymple, R.W., Boyd, R., Zaitlin, B.A. (Eds.), Incised valley systems: Origin and sedimentary sequences, Special Publication, Society of Economic Paleontological and Mineralogists, 51. 83-96.

Kondo, H., Toyofuku, T., Ikeya, N., 2005. Mg/Ca ratios in the shell cultured specimens and natural populations of the marine ostracode *Xestoleberis hanaii* (Crustacea). Palaeogeography, Palaeoclimatology, Palaeoecology. 225, 3-13.

Kovàcs, Z.P., Du Plessis, D.B., Brancher, P.R., Dunn, P., Mallory, G.C.L., 1985. Documentation of the 1984 Domoina Floods. Department of Water Affairs, Technical Report 122. 43pp.

Lam, M.H., Tjia, A.Y., Chan, C., Chan, W., Lee, W., 1997. Speciation Study of chromium, copper and nickel in coastal estuarine sediments polluted by domestic and industrial effluents. Marine Pollution Bulletin. 34, 11, 949-959.

Larson, R., Morang, A., Gorman, L., 1997. Monitoring the coastal environment; Part II; Sediment sampling and geotechnical methods. Journal of Coastal Research. 13, 2, 308-330.

Leeder, M., 1999. Sedimentology and Sedimentary Basins, From Turbulence to Tectonics. Blackwell Science Ltd, London. 592pp.

Leuci, R., 1998. An Assessment of Trace Metal Contamination in Sediment of Durban Harbour and Beachwood Mangroves. Unpublished Honours dissertation, University of Natal. 79pp.

Liaghati, T., Preda, M., Cox, M., 2003. Heavy metal distribution and controlling factors within coastal plain sediments, Bells Creek catchment, southeast Queensland, Australia. Environmental International. 29, 935-948.

Long, E.R., MacDonald, D.D., Smith, S.L., Calder, F.D., 1995. Incidence of Adverse Biological Effects within Ranges of Chemical Concentrations in Marine and Estuarine Sediment. Environmental Management. 19, 81-97.

López-González, N., Borrego, J., Ruiz, F., Carro, B., Lozano-Soria, O., Abad, M., 2006. Geochemical variation in estuarine sediment: provenance and environmental changes (southern Spain). Estuarine. Coastal and Shelf Science. 67, 313-320.

Loring , D.H., Rantala, R.T.T., 1992. Manual for the geochemical analyses of marine sediments and suspended particulate matter. Earth-Science Reviews. 32, 235-283.

Lynch, K., Jackson, D.W.T., Cooper, J.A.G., 2009. Foredune accretion under offshore winds. Geomorphology. 105, 139-146.

MacEachern, J.A., Pembeton, S.G., 1994. Ichnological Aspects of Incised Valley-Fill Systems from the Viking Formation of the Western Canada Sedimentary Basin, Alberta, Canada. In: Dalrymple, R.W., Boyd, R., Zaitlin, B.A. (Eds.), Incised valley systems: Origin and sedimentary sequences, Special Publication, Society of Economic Paleontological and Mineralogists. 51. 129-158.

Marsh, J.S., Eales, H.V., 1984. The chemistry and petrogenesis of igneous rocks of the Karoo central area, South Africa. Special Publication Geological Society of South Africa. 13, 27-67.

Marshall, C.G.A., 2006. The Natal Group. In: Johnson, M.R., Anhaeusser, C.R. and Thomas, R.J. (Eds.), The Geology of South Africa, Johannesburg/Council for Geoscience, Pretoria. 433-442.

Matias, A., Ferreira, Ó., Vila-Concejo, A., Garcia, T., Dias, J.A., 2008. Classification of washover dynamics in barrier islands. Geomorphology. 97, 655-674.

Matias, A., Ferreira, Ó., Vila-Concejo, A., Morris, B., Dias, J.A., 2010. Short-term morphodynamics of non-storm overwash. Marine Geology. 274, 69-84.

McBride, R.A., Taylor, M.J., Byrnes, M.R., 2007. Coastal morphodynamics and Chenier-Plan evolution in southwestern Louisiana, USA: A geomorphic model. Geomorphology. 88, 367-422.

Meade, R.H., Sachs, P.L., Manheim, F.T., Hathaway, J.C., Spencer, D.W., 1975. Sources of suspended matter in waters of the Middle Atlantic Bight. Journal of Sedimentary Petrology. 45, 171-188.

Meilianda, E., Dohmen-Janssen, C.M., Maathuis, B.H.P., Hulscher, S.J.M.H., Mulder, J.P.M., 2010. Short-term morphological responses and developments of Banda Aceh coast, Sumatra Island, Indonesia after the tsunami on 26 December 2004. Marine Geology. 275, 96-109.

Miller, M.C., McCave, I.N., Komar, P.D., 1977. Threshold of sediment motion under unidirectional currents. Sedimentology. 24, 507-527.

Mkhize, N., 2010. Sediment and Heavy Minerals Distribution on the KwaZulu-Natal Bight. Unpublished Honours dissertation, University of KwaZulu-Natal. 67pp

Moore, L.J., Griggs G.B., 2002. Long-term cliff retreat and erosion hotspots along the central shores of the Monterey Bay National Marine Sanctuary. Marine Geology. 181, 265-283.

Munksgaard, N.C., Lim, K., Parry, D.L., 2003. Rare earth elements as provenance indicators in North Australian estuarine and coastal marine sediments. Estuarine, Coastal and Shelf Science. 57, 399-409.

Myburg, L., 2009. Personal communications. Amatikulu, South Africa, 26/05/2009.

Nichol, S.L., 1991. Zonation and sedimentology of estuarine facies in an incised valley, wave-dominated, microtiadal setting. In: Smith, D.G., Reinson, G.E., Zaitlin, B.A., Rahmani, R.A., (Eds), Clastic tidal sedimentology. Canadian Society of Petroleum Geologists Memoir. 16, 41-58.

Nichols, M.M., Biggs, R.B., 1985. Estuaries. In: Davis, R.A.,(Ed), Coastal Sedimentary Environments. Springer-Verlag, New York, 77-186.

Njoya, S.N., 2002. Post-dam Sediment Dynamics Below the Inanda Dam at the Mgeni Estuary, KwaZulu Natal, South Africa. Unpublished MSc dissertation, University of Natal. 94pp.

Nordfjord, S., Goff, J.A., Austin Jr, J.A., Sommerfild C.K., 2005. Seismic geomorphology of buried channel systems on the New Jersey outer shelf: assessing past environmental conditions. Marine Geology. 214, 339-364.

Otvos, E.G., 2000. Beach ridges – definitions and significance. Geomorphology. 32, 83-108.

Olivier, M.J., 1998. Foredune formation at Tugela River mouth. Unpublished MSc dissertation, University of Natal, Durban. 156pp.

Olivier, M.J., Garland, G.G., 2003. Short-term monitoring of foredune formation on the east coast of South Africa. Earth Surface Processes and landforms. 28, 1143-1155.

Perry, J.E., 1989. The impacts of the September 1987 floods on the estuaries of Natal/KwaZulu; a hydro-perspective. CSIR Research Report, Stellenbosch. 29pp.

Prent, M.T.H., Hickin, E.J., 2001. Annual regime and bedforms, roughness and flow resistance, Lillooet River, British Columbia, BC. Geomorphology. 41, 369-390.

Psuty, N.P., 1988. Sediment budget and dune/beach interactions. Journal of Coastal Research. Special Issue, 3, 1-4.

Pusty, N.P., 1990. Foredune mobility and stability, Fire Island, New York. In: Nordstrom, K.F., Psuty, N., Carter, B (Eds) Coastal Dunes: Forms and Processes. Wiley: Chichester. 159-176.

Rae, J.E., Aston, S.R., 1982. The role of suspended solids in the estuarine geochemistry of mercury. Water Resources. 16, 649-654.

Ramsay, P.J., 1995. 9000 Years of sea level change along the South African Coastline. Quaternary International. 31, 71-75.

Ramsay, P.J., Cooper, J.A.G., 2002. Late Quaternary Sea-Level Change in South Africa. Quaternary Research. 57, 82-90.

Raymond, L.A., 2002. Petrology, The Study of Igneous, Sedimentary and Metamorphic Rocks, McGraw-Hill, San Francisco. 720pp.

Reddering, J.V.S., 1983. An inlet sequence produced by migration of a small microtidal inlet against longshore drift: the Keurbooms Inlet, South Africa. Sedimentology. 30, 201-218.

Reddering, J.S.V., Scarr, N.G., 1990. Sediment dispersal in the Gamtoos Estuary. Institute for Coastal Research, University of Port Elizabeth, Report 24. 37pp.

Roberts, D.L., Botha, G.A., Maud, R.R., Pether, J., 2006. Coastal Cenozoic Deposits. In: Johnson, M.R., Anhaeusser, C.R. and Thomas, R.J. (Eds.), The Geology of South Africa, Johannesburg/Council for Geoscience, Pretoria. 605-628.

Rollinson, H., 1993. Using Geochemical Data: Evaluation, Presentation, Interpretation. Longman, Wiley, New York. 352pp.

Rosgen, D.L., 1994. A classification of natural river. Catena. 22, 169-199.

Roussouw, J., 1989. Design Waves for the South African. Unpublished PhD dissertation, University of Stellenbosch, South Africa. 169pp.

Roy, P.S., Carwford, E.A., 1984. Heavy metals in a contaminated Australian estuary-dispersion and accumulation trend. Estuarine, Coastal and Shelf Science. 13, 341-358.

Roy, P.S., 1994. Holocene estuary evolution-Stratigraphic studies from Southeastern Australia. In: Dalrymple, R.W., Boyd, R., Zaitlin, B.A. (Eds.), Incised valley systems: Origin and sedimentary sequences, Special Publication, Society of Economic Paleontological and Mineralogists. 51. 241-264.

SAN (South African Navy)., 2009. Tide Tables. South African Navy, Simonstown.

Schoonees, J.S., 2000. Annual variation in the net long-shore sediment transport rate. Coastal Engineering. 40, 141-160.

Schropp, S.J., Lewis, F.G., Windom, H.L., Ryan, J.D., Calder, F.D., Burney, L.C., 1990. Interpretation of Metal Concentrations in Estuarine Sediments of Florida Using Aluminum as a Reference Element. Coastal and Estuarine Research Federation. 13, 227-253.

Seisser, W.G., Rogers, J., 1971. An investigation of the suitability of four methods used in routine carbonate analysis of marine sediments. Deep Sea Research. 18, 135-139.

Shi, Q., Leipe, T., Rueckert, P., Di, Z., Harff, J., 2010. Geochemical sources, deposition and enrichment of heavy metals in short sediment cores from the Pearl River Estuary, Southern China. Journal of Marine Systems. 82, 28-42.

Short, A.D., Hesp, P.A., 1982. Wave, beach and dune interactions in southeastern Australia. Marine Geology. 48, 259-284.

Sloss, R., Jones, B.G., McClennen, C.E., de Carli, J., Price, D.M., 2006. The geomorphic evolution of a wave-dominated barrier estuary: Burrill Lake, New South Wales, Australia. Sedimentary Geology. 187, 229-249.

Smith, G.l., Zarillo, G.A., 1989. Calculating long-term shoreline recession rates using aerial photography and beach profiling techniques. Journal of Coastal Research. 6, 111-120.

Smith, A.M., Guastella, L.A., Bundy, S.C., Mather, A.A., 2007. Combined Marine Storm and Saros Spring-high Tide Erosion Event, March 19-20, 2007: A Preliminary Assessment. South African Journal of Science.103, 274-276

Smith, A.M., Mather, A.A., Bundy, S.C., Cooper, J.A.G., Guastella, L.A., Ramsay, P.J., Theron, A., 2010. Contrasting styles of swell-driven coastal erosion: examples from KwaZulu-Natal, South Africa. Geological Magazine, Cambridge University Press. 1-14.

Summers, J., Wade, T., Engle, D., Malaeb, Z., 1996. Normalization of metal concentrations in estuarine sediments from the Gulf of Mexico. Estuaries. 19, 581-594.

Sun, D., Dickinson, G.R., 1995. Salinity effect on tree growth, root distribution and transpiration of Casuarina cunninghamiana and Eucalyptus camaldulensis planted on a saline site in tropical north Australia. Forest Ecology and Management. 77, 127-138.

Taylor, S.R., and McLennan, S.M., 1995. The geochemical evaluation of the continental crust. Reviews of Geophysics. 33, 241-265.

Tanner, W.F., 1987. The beach: where is the "river of sand"? Journal of Coastal Research. 3, 377-386.

Tanner, W.F., 1988. Beach Ridge Data and Sea Level History from the Americas. Journal of Coastal Research. 4, 81-91.

Tanner, W.F., 1995. Origin of beach ridges and swales. Marine Geology. 129, 149-161.

Thomson, J., Turekain, K.K., McCaffrey, J.M., 1975. The accumulation of metals in and released from sediments of Long Island Sound. In: Cronin, L.E., (Ed): Estuarine Research 1. Chemistry, Biology and the Estuarine System. Academic Press, New York. 28-44.

Tinmouth, N., 2005. A sedimentary study of the Mgeni Estuary. Unpublished Honours dissertation, University of KwaZulu-Natal. 120pp.

Tinmouth, N., 2009. The Mgeni Estuary Pre- and Post Inanda Dam Estuarine Dynamics. Unpublished MSc dissertation, University of KwaZulu-Natal. 170pp.

Tucker, M.E., 1991. Sedimentary Petrology. Blackwell Scientific Publications, Oxford, (Second Edition). 259pp.

Türker, U., Kabdaşli, M.S., 2006. The effects of sediment characteristics and wave height on shape-parameter for representing equilibrium beach profiles. Ocean Engineering. 33, 281-291.

Turekian, K.K., 1964. The marine geochemistry of strontium. Geochimica et Cosmochimica Acta. 28, 1479-1496.

Tyson, P.D., 1987. Climatic Change and Variability in Southern Africa. Oxford University Press, Cape Town. 232pp.

Tyson, P.D., Preston-Whyte, R.A., 2004. The Weather and Climate of Southern Africa. Oxford University Press, Cape Town (Second Edition). 369pp.

van Bladeren, D., Burger, C.E.,1989. Documentation of the September 1987 Natal floods. Department of Water Affairs, Technical Report. 166pp.

Vila-Concejo, A., Ferreira, Ó., Matias, A., Morris, B., Dias, J.A., 2004. Lessons from inlet relocation: Examples from Southern Portugal. Coastal Engineering, 51, 967–990.

Wallace, R.S., 1988. Quantification of net shore-drift in Puget Sound and the Strait of Juan de Fuca, Washington. Journal of Coastal Research. 4, 3, 395-403.

Walkley, A., 1947. A critical examination of a rapid method for determining organic carbon m soils: Effect of variations in digestion conditions and of inorganic soil constituents. Soil Science. 63, 251-263.

Walkley, A., Black, L.A., 1934. An examination of the Degtjareff method for determining organic carbon in soils: Effect of variations in digestion conditions and of inorganic soil constituents. Soil Science. 37, 29-38.

Weltje, G.J., von Eynatten, H., 2004. Quantitative provenance analysis of sediments: review and outlook. Sedimentary Geology. 171, 1-11.

Wentworth, C. K., 1922. A Scale of Grade and Class Terms for Clastic Sediments. Journal of Geology. 30, 5, 377-392.

Whitmeyer, S.J., FitzGerald, D.M., 2008. Episodic dynamics of a sand wave field. Marine Geology. 252, 24-37.

Windom, H. L., Schropp , S. J., Calder, F. D., Ryan, J. D., Smith, R.G., Burney JR., L. C., Lewis, F. G., Rawlinson, C. H., 1989. Natural trace metal concentrations in estuarine and coastal marine sediments of the southeastern United States. En~pironmental Science and Technology. 23, 314-320.

Wright, L.D., Short, A.D., 1984. Morphodynamic Variability of Surf Zones and Beaches: A Synthesis. Marine Geology. 56, 93-118.

Wright, C.I., 2002. Aspects of the Cenozoic Evolution of the Northern KwaZulu-Natal Coastal plain, South Africa Council for Geoscience Bulletin, 132. 120pp.

Zaitlin, B. A., Dalrymple, R. W., Boyd, R., 1994. The stratigraphic organization of incised-valley systems associated with relative sea-level changes In: Dalrymple, R.W., Boyd, R., Zaitlin, B.A. (Eds.), Incised valley systems: Origin and sedimentary sequences, Special Publication, Society of Economic Paleontological and Mineralogists. 51. 45-60.

APPENDIX A

SEDIMENT CHARACTERISTICS

Sample no.	x_projection	y_projection	5% (mm)	16% (mm)	50% (mm)	84% (mm)	95% (mm)	5% (ϕ)	16% (ϕ)	50% (ϕ)	84% (ϕ)	95% (ϕ)	Mean size (ϕ)	Sorting	Skewness	Calcium carbonate content (mass %)	Organic carbonate content (mass %)
1	6781122.21	366851.41	0.0142	0.1613	0.3295	0.5224	0.6768	6.14	2.63	1.60	0.94	0.56	1.72	-1.27	-10.05	1.31	
2	6781121.00	366855.68	0.0133	0.2725	0.4262	0.6093	0.7553	6.24	1.88	1.23	0.71	0.40	1.27	-1.17	-12.26	0.46	
3	6781080.19	366885.06	0.0209	0.2976	0.4469	0.6333	0.7812	5.58	1.75	1.16	0.66	0.36	1.19	-1.06	-9.47	1.34	
4	6781064.69	366893.10	0.2204	0.2784	0.3887	0.5382	0.6540	2.18	1.84	1.36	0.89	0.61	1.37	-0.48	-0.06	0.52	
6	6781054.83	366924.10	0.0474	0.3222	0.4567	0.6264	0.7635	4.40	1.63	1.13	0.67	0.39	1.15	-0.85	-5.09	0.80	
7	6781050.73	366937.71	0.0128	0.2592	0.4047	0.5774	0.7109	6.28	1.95	1.31	0.79	0.49	1.35	-1.17	-12.14	1.32	
8	6781018.35	366949.56	0.0119	0.1952	0.3041	0.4306	0.5281	6.40	2.36	1.72	1.22	0.92	1.76	-1.11	-10.71	0.94	
9	6780997.32	366959.72	0.0089	0.1583	0.2695	0.3854	0.4748	6.80	2.66	1.89	1.38	1.07	1.98	-1.19	-11.89	2.31	
10	6780994.30	366967.27	0.2056	0.2474	0.3369	0.4583	0.5508	2.28	2.02	1.57	1.13	0.86	1.57	-0.44	0.00	0.66	
11	6781027.00	367003.76	0.2093	0.2475	0.3265	0.4309	0.5098	2.26	2.01	1.61	1.21	0.97	1.61	-0.39	0.00	0.97	
12	6781036.36	366994.74	0.0046	0.0215	0.2278	0.4157	0.5519	7.77	5.54	2.13	1.27	0.86	2.98	-2.12	-20.50	1.70	
13	6781053.37	366981.25	0.0100	0.2156	0.3652	0.5221	0.6427	6.65	2.21	1.45	0.94	0.64	1.53	-1.23	-13.31	1.53	
14	6781074.24	366957.93	0.0123	0.2346	0.3672	0.5211	0.6407	6.35	2.09	1.45	0.94	0.64	1.49	-1.15	-11.78	1.39	
15	6781100.35	366941.79	0.0456	0.2968	0.4184	0.5729	0.6918	4.45	1.75	1.26	0.80	0.53	1.27	-0.83	-4.87	1.50	
16	6781114.87	366929.68	0.0456	0.3047	0.4310	0.5896	0.7138	4.45	1.71	1.21	0.76	0.49	1.23	-0.84	-5.01	1.19	
17	6781142.60	366914.75	0.0170	0.2626	0.3979	0.5617	0.6890	5.88	1.93	1.33	0.83	0.54	1.36	-1.08	-10.08	0.75	
18	6781162.65	366897.88	0.0070	0.0658	0.4574	0.6684	0.8297	7.15	3.93	1.13	0.58	0.27	1.88	-1.88	-21.52	0.57	
19	6781163.32	366886.82	0.0141	0.2363	0.3669	0.5286	0.6561	6.15	2.08	1.45	0.92	0.61	1.48	-1.13	-10.76	0.46	
20	6781173.52	366873.48	0.0149	0.2451	0.3763	0.5377	0.6660	6.07	2.03	1.41	0.90	0.59	1.44	-1.11	-10.57	0.11	
21	6781209.75	366918.92	0.0189	0.2930	0.4414	0.6297	0.7810	5.73	1.77	1.18	0.67	0.36	1.21	-1.09	-10.03	0.27	
22	6781210.23	366924.50	0.0158	0.2708	0.4115	0.5824	0.7154	5.98	1.88	1.28	0.78	0.48	1.32	-1.11	-10.79	0.45	
23	6781163.71	366947.23	0.0172	0.2847	0.4098	0.5604	0.6716	5.86	1.81	1.29	0.84	0.57	1.31	-1.05	-10.24	0.81	
24	6781162.65	366974.58	0.2200	0.2686	0.3613	0.4837	0.5774	2.18	1.90	1.47	1.05	0.79	1.47	-0.42	-0.03	0.67	
25	6781145.20	367002.03	0.0380	0.2698	0.3806	0.5167	0.6230	4.72	1.89	1.39	0.95	0.68	1.41	-0.85	-5.30	1.44	
26	6781131.29	367025.33	0.0250	0.2714	0.3896	0.5308	0.6414	5.32	1.88	1.36	0.91	0.64	1.39	-0.95	-7.62	0.79	
27	6781125.32	367027.79	0.0248	0.2575	0.3671	0.5001	0.6012	5.33	1.96	1.45	1.00	0.73	1.47	-0.94	-7.33	0.87	
28	6781101.70	367039.17	0.1680	0.2273	0.3362	0.4884	0.6087	2.57	2.14	1.57	1.03	0.72	1.58	-0.56	-0.15	0.92	
29	6781090.27	367054.87	0.1646	0.2067	0.3043	0.4454	0.5540	2.60	2.27	1.72	1.17	0.85	1.72	-0.54	-0.02	1.30	
30	6781086.26	367064.66	0.2012	0.2475	0.3516	0.5002	0.6168	2.31	2.01	1.51	1.00	0.70	1.51	-0.50	0.01	1.00	
31	6781159.22	367145.45	0.1974	0.2374	0.3234	0.4406	0.5307	2.34	2.07	1.63	1.18	0.91	1.63	-0.44	0.00	1.16	1.72
32	6781167.19	367145.36	0.0153	0.1879	0.3028	0.4481	0.5606	6.03	2.41	1.72	1.16	0.84	1.76	-1.10	-8.96	1.00	
33	6781188.39	367125.58	0.0115	0.2278	0.3716	0.5297	0.6522	6.44	2.13	1.43	0.92	0.62	1.49	-1.19	-12.37	0.79	
34	6781226.09	367105.35	0.1921	0.2575	0.3452	0.4540	0.5407	2.38	1.96	1.53	1.14	0.89	1.54	-0.43	-0.16	0.71	1.29
35	6781246.56	367080.46	0.0105	0.2209	0.3648	0.5218	0.6436	6.58	2.18	1.46	0.94	0.64	1.52	-1.21	-12.92	0.91	1.13
36	6781279.04	367051.32	0.0109	0.2823	0.4484	0.6421	0.7946	6.51	1.82	1.16	0.64	0.33	1.21	-1.23	-14.09	0.46	0.14
37	6781297.81	367037.38	0.2581	0.3274	0.4733	0.6833	0.8521	1.95	1.61	1.08	0.55	0.23	1.08	-0.53	-0.02	0.87	
38	6781290.11	367021.47	0.0163	0.2388	0.3798	0.5624	0.7043	5.94	2.07	1.40	0.83	0.51	1.43	-1.13	-10.00	0.43	
39	6781311.75	367012.57	0.3098	0.3829	0.5521	0.8081	1.0299	1.69	1.38	0.86	0.31	-0.04	0.85	-0.53	0.07	0.96	
40	6781317.53	367004.17	0.2333	0.2999	0.4560	0.6987	0.9008	2.10	1.74	1.13	0.52	0.15	1.13	-0.60	0.02	1.92	1.76
41	6781519.05	367187.69	0.2141	0.2618	0.3694	0.5236	0.6450	2.22	1.93	1.44	0.93	0.63	1.43	-0.49	0.02	2.80	
42	6781514.94	367196.10	0.0097	0.0642	0.3259	0.5137	0.6597	6.68	3.96	1.62	0.96	0.60	2.18	-1.67	-14.83	1.44	
43	6781498.15	367209.53	0.0047	0.0221	0.2761	0.5100	0.6836	7.73	5.50	1.86	0.97	0.55	2.78	-2.22	-22.64	0.82	
44	6781485.58	367237.74	0.0057	0.0259	0.2674	0.4801	0.6346	7.44	5.27	1.90	1.06	0.66	2.74	-2.08	-19.88	0.75	
45	6781466.25	367268.61	0.0125	0.1653	0.3226	0.4969	0.6294	6.32	2.60	1.63	1.01	0.67	1.75	-1.25	-10.81	1.06	
46	6781444.36	367261.64	0.0147	0.2016	0.3549	0.5351	0.6772	6.09	2.31	1.49	0.90	0.56	1.57	-1.19	-10.26	1.00	
47	6781426.46	367277.27	0.0108	0.1645	0.3615	0.5415	0.6794	6.53	2.60	1.47	0.88	0.56	1.65	-1.33	-12.85	1.11	

48	6781412.05	367313.43	0.0665	0.2950	0.4258	0.5988	0.7368	3.91	1.76	1.23	0.74	0.44	1.24	-0.78	-3.30	0.31	
49	6781417.28	367321.52	0.2555	0.3221	0.4648	0.6698	0.8323	1.97	1.63	1.11	0.58	0.26	1.11	-0.52	-0.02	0.59	
50	6781405.84	367331.52	0.2191	0.2681	0.3779	0.5330	0.6523	2.19	1.90	1.40	0.91	0.62	1.40	-0.49	0.00	0.32	
51	6781607.79	367479.86	0.2348	0.2783	0.3687	0.4892	0.5809	2.09	1.85	1.44	1.03	0.78	1.44	-0.40	0.00	1.99	1.39
52	6781610.28	367463.52	0.2066	0.2531	0.3582	0.5081	0.6247	2.27	1.98	1.48	0.98	0.68	1.48	-0.49	0.01	0.71	1.85
53	6781622.48	367412.09	0.0060	0.0324	0.2531	0.4229	0.5472	7.38	4.95	1.98	1.24	0.87	2.72	-1.91	-18.07	1.88	1.19
54	6781644.60	367371.64	0.0033	0.0136	0.0964	0.4842	0.7004	8.26	6.20	3.38	1.05	0.51	3.54	-2.46	-9.12	0.95	1.19
55	6781665.71	367347.00	0.2117	0.2544	0.3464	0.4722	0.5689	2.24	1.97	1.53	1.08	0.81	1.53	-0.44	0.00	2.11	
56	6781670.47	367341.15	0.2377	0.2860	0.3895	0.5305	0.6378	2.07	1.81	1.36	0.91	0.65	1.36	-0.44	0.00	2.78	0.71
57	6781736.57	367403.03	0.2199	0.2594	0.3335	0.4287	0.5035	2.19	1.95	1.58	1.22	0.99	1.58	-0.36	0.00	3.18	
58	6781729.87	367413.90	0.2427	0.2927	0.4005	0.5486	0.6628	2.04	1.77	1.32	0.87	0.59	1.32	-0.45	0.00	1.31	
59	6781708.16	367438.97	0.0018	0.0055	0.0314	0.4169	0.6910	9.11	7.50	4.99	1.26	0.53	4.59	-2.86	5.28	0.62	
60	6781673.11	367464.52	0.0046	0.0207	0.1578	0.3565	0.5317	7.76	5.59	2.66	1.49	0.91	3.25	-2.06	-15.03	1.49	
61	6781661.55	367491.05	0.2001	0.2490	0.3553	0.5061	0.6236	2.32	2.01	1.49	0.98	0.68	1.49	-0.50	-0.02	1.16	
62	6781661.54	367500.51	0.2021	0.2491	0.3547	0.5055	0.6239	2.31	2.01	1.50	0.98	0.68	1.49	-0.50	0.00	2.51	
63	6781759.11	367588.01	0.1941	0.2305	0.3059	0.4061	0.4826	2.37	2.12	1.71	1.30	1.05	1.71	-0.40	0.00	0.80	
64	6781771.11	367578.37	0.0096	0.0513	0.3333	0.5781	0.7572	6.70	4.28	1.58	0.79	0.40	2.22	-1.83	-15.72	0.82	
65	6781779.08	367553.26	0.0054	0.0274	0.1540	0.3374	0.5547	7.52	5.19	2.70	1.57	0.85	3.15	-1.92	-12.39	1.31	
66	6781829.63	367522.06	0.0486	0.2726	0.3981	0.5593	0.6863	4.36	1.87	1.33	0.84	0.54	1.35	-0.84	-4.32	1.27	
67	6781843.06	367511.15	0.2404	0.2891	0.3943	0.5381	0.6479	2.06	1.79	1.34	0.89	0.63	1.34	-0.44	0.00	1.39	
68	6781917.60	367603.29	0.2262	0.2782	0.3960	0.5657	0.6999	2.14	1.85	1.34	0.82	0.51	1.33	-0.50	0.01	1.32	0.55
69	6781905.87	367613.22	0.1558	0.2043	0.3093	0.4627	0.5835	2.68	2.29	1.69	1.11	0.78	1.70	-0.58	-0.08	0.54	0.32
70	6781881.11	367640.33	0.0050	0.0226	0.1270	0.4611	0.7636	7.64	5.47	2.98	1.12	0.39	3.19	-2.19	-8.89	1.39	2.12
71	6781870.46	367691.28	0.0075	0.0470	0.1422	0.2834	0.5102	7.06	4.41	2.81	1.82	0.97	3.01	-1.57	-8.10	2.37	
72	6781837.99	367651.74	0.1966	0.2614	0.3699	0.5137	0.6268	2.35	1.94	1.43	0.96	0.67	1.44	-0.50	-0.14	1.40	1.78
73	6781849.83	367696.75	0.1928	0.2281	0.3010	0.3972	0.4702	2.37	2.13	1.73	1.33	1.09	1.73	-0.39	0.00	1.02	
74	6781863.84	367893.53	0.2046	0.2570	0.3802	0.5630	0.7076	2.29	1.96	1.40	0.83	0.50	1.39	-0.55	0.00	1.21	
75	6781876.91	367873.24	0.0056	0.0260	0.1757	0.4218	0.6089	7.49	5.26	2.51	1.25	0.72	3.01	-2.03	-13.80	1.53	
76	6781918.52	367845.52	0.1582	0.1938	0.2735	0.3856	0.4720	2.66	2.37	1.87	1.37	1.08	1.87	-0.49	0.00	2.85	
77	6781971.80	367810.15	0.1720	0.2437	0.3611	0.5199	0.6408	2.54	2.04	1.47	0.94	0.64	1.48	-0.56	-0.25	1.57	
78	6781991.90	367759.40	0.2036	0.2739	0.3920	0.5491	0.6748	2.30	1.87	1.35	0.86	0.57	1.36	-0.51	-0.16	1.57	
79	6782014.95	367746.70	0.2553	0.3147	0.4496	0.6448	0.8001	1.97	1.67	1.15	0.63	0.32	1.15	-0.51	0.02	1.37	
80	6782026.96	367732.24	0.2029	0.2493	0.3533	0.5010	0.6161	2.30	2.00	1.50	1.00	0.70	1.50	-0.49	0.00	1.33	
81	6782111.24	367805.97	0.1888	0.2363	0.3390	0.4841	0.5972	2.41	2.08	1.56	1.05	0.74	1.56	-0.51	-0.03	0.98	
82	6782106.09	367815.71	0.1566	0.1942	0.2829	0.4132	0.5150	2.68	2.36	1.82	1.28	0.96	1.82	-0.53	0.01	2.60	
83	6782095.47	367830.35	0.2188	0.2594	0.3438	0.4561	0.5420	2.19	1.95	1.54	1.13	0.88	1.54	-0.40	0.00	1.53	
84	6782063.77	367866.45	0.2385	0.2936	0.4189	0.6010	0.7456	2.07	1.77	1.26	0.73	0.42	1.25	-0.51	0.02	1.18	
85	6782027.80	367923.73	0.2137	0.2581	0.3543	0.4874	0.5912	2.23	1.95	1.50	1.04	0.76	1.50	-0.45	0.01	0.56	
86	6781992.30	367902.21	0.2207	0.2616	0.3465	0.4602	0.5479	2.18	1.93	1.53	1.12	0.87	1.53	-0.40	0.01	1.52	
87	6781987.51	367939.29	0.3164	0.3838	0.5313	0.7394	0.9063	1.66	1.38	0.91	0.44	0.14	0.91	-0.47	0.02	1.13	
88	6781978.64	367949.08	0.2322	0.2852	0.4038	0.5709	0.6983	2.11	1.81	1.31	0.81	0.52	1.31	-0.49	-0.01	1.09	
89	6782182.79	368015.57	0.2596	0.3222	0.4676	0.6861	0.8670	1.95	1.63	1.10	0.54	0.21	1.09	-0.54	0.04	0.91	1.10
90	6782169.69	368025.56	0.3378	0.4224	0.6213	0.9310	1.2048	1.57	1.24	0.69	0.10	-0.27	0.68	-0.56	0.09	0.60	1.37
91	6782188.87	368003.07	0.3213	0.3975	0.5736	0.8409	1.0737	1.64	1.33	0.80	0.25	-0.10	0.79	-0.53	0.07	0.38	2.02
92	6782202.51	367987.28	0.3109	0.3862	0.5583	0.8111	1.0187	1.69	1.37	0.84	0.30	-0.03	0.84	-0.53	0.02	0.81	0.96
93	6782202.15	367971.44	0.2926	0.3621	0.5211	0.7545	0.9449	1.77	1.47	0.94	0.41	0.08	0.94	-0.52	0.03	0.82	
94	6782218.22	367965.99	0.1893	0.2395	0.3613	0.5547	0.7242	2.40	2.06	1.47	0.85	0.47	1.46	-0.60	0.08	1.26	0.86
95	6778537.70	365221.25	0.0168	0.2732	0.4174	0.5981	0.7389	5.89	1.87	1.26	0.74	0.44	1.29	-1.11	-10.44	0.32	0.35
96	6778555.34	365195.37	0.0021	0.0073	0.0323	0.2469	0.4941	8.91	7.11	4.95	2.02	1.02	4.69	-2.47	1.89	0.36	3.48
97	6778583.77	365131.66	0.0027	0.0104	0.0459	0.2245	0.3846	8.56	6.59	4.45	2.16	1.38	4.40	-2.20	-3.42	0.39	1.98
98	6778607.90	365090.29	0.0028	0.0118	0.0585	0.5280	0.9635	8.47	6.40	4.10	0.92	0.05	3.81	-2.65	0.98	0.30	

99	6778623.13	365044.20	0.0039	0.0169	0.1075	0.6723	1.1103	8.00	5.89	3.22	0.57	-0.15	3.23	-2.56	-5.83	0.30	1.75
100	6778648.45	365010.41	0.0046	0.0201	0.1794	0.6926	1.0985	7.77	5.64	2.48	0.53	-0.14	2.88	-2.47	-13.67	0.30	1.10
101	6778756.49	364965.04	0.0029	0.0116	0.0481	0.1653	0.3306	8.45	6.43	4.38	2.60	1.60	4.47	-2.00	-4.95	0.36	
102	6778732.49	364998.06	0.0024	0.0087	0.0337	0.0935	0.2869	8.73	6.85	4.89	3.42	1.80	5.05	-1.91	-3.44	0.32	
103	6778717.41	365056.00	0.0020	0.0066	0.0287	0.0884	0.2685	8.97	7.24	5.12	3.50	1.90	5.29	-2.01	-3.12	0.34	2.25
104	6778699.97	365115.36	0.0025	0.0100	0.0467	0.5799	1.1219	8.64	6.64	4.42	0.79	-0.17	3.95	-2.80	5.75	0.32	5.57
105	6778679.39	365178.67	0.0026	0.0100	0.0538	0.2952	0.4458	8.61	6.64	4.22	1.76	1.17	4.20	-2.35	-4.90	0.37	
106	6778660.20	365237.16	0.0018	0.0056	0.0258	0.0864	0.3763	9.14	7.49	5.27	3.53	1.41	5.43	-2.16	-0.96	0.34	3.42
107	6778642.11	365299.63	0.0019	0.0065	0.0291	0.2546	0.5036	9.02	7.26	5.10	1.97	0.99	4.78	-2.54	3.39	0.55	1.44
108	6778628.05	365320.59	0.0015	0.0045	0.0225	0.0617	0.3670	9.37	7.80	5.47	4.02	1.45	5.76	-2.15	-1.12	0.28	
109	6778627.01	365332.94	0.2305	0.2815	0.3958	0.5566	0.6793	2.12	1.83	1.34	0.85	0.56	1.34	-0.48	0.00	0.90	
110	6778621.77	365338.50	0.0167	0.2377	0.3596	0.5094	0.6266	5.90	2.07	1.48	0.97	0.67	1.51	-1.07	-9.53	1.13	0.44
111	6778709.08	365359.02	0.2247	0.2764	0.3939	0.5656	0.7050	2.15	1.86	1.34	0.82	0.50	1.34	-0.51	0.03	1.31	1.17
112	6778721.66	365343.86	0.0016	0.0048	0.0247	0.0683	0.3673	9.30	7.70	5.34	3.87	1.44	5.64	-2.15	-1.97	0.35	
113	6778752.64	365323.44	0.0017	0.0052	0.0247	0.0626	0.1460	9.19	7.59	5.34	4.00	2.78	5.64	-1.87	-5.79	0.12	2.74
114	6778783.49	365264.79	0.0022	0.0076	0.0356	0.2682	0.7419	8.85	7.04	4.81	1.90	0.43	4.58	-2.56	3.22	0.29	0.29
115	6778826.26	365197.81	0.0084	0.0764	0.2656	0.4688	0.6495	6.90	3.71	1.91	1.09	0.62	2.24	-1.60	-12.86	0.35	1.28
116	6778852.29	365176.80	0.0023	0.0087	0.0381	0.1962	0.4482	8.76	6.85	4.71	2.35	1.16	4.64	-2.28	-1.34	0.30	
117	6778873.32	365141.02	0.0023	0.0084	0.0352	0.1734	0.3339	8.78	6.90	4.83	2.53	1.58	4.75	-2.18	-2.08	0.38	1.57
118	6778888.34	365108.19	0.0026	0.0109	0.0472	0.2863	0.4855	8.56	6.52	4.40	1.80	1.04	4.24	-2.32	-1.84	0.33	
119	6778903.50	365054.80	0.0029	0.0122	0.0581	0.3253	0.4996	8.43	6.36	4.11	1.62	1.00	4.03	-2.31	-3.99	0.39	4.57
120	6778955.85	364970.40	0.0026	0.0103	0.0400	0.2370	0.3854	8.59	6.60	4.64	2.08	1.38	4.44	-2.22	-1.05	0.02	2.02
121	6779031.10	365051.10	0.0036	0.0156	0.1353	0.3450	0.4930	8.12	6.00	2.89	1.54	1.02	3.47	-2.19	-15.89	0.01	1.41
122	6779030.13	365054.74	0.0021	0.0075	0.0305	0.1528	0.3453	8.88	7.05	5.04	2.71	1.53	4.93	-2.20	-0.58	0.02	
123	6779002.04	365158.22	0.0019	0.0063	0.0264	0.0769	0.2759	9.04	7.31	5.24	3.70	1.86	5.42	-1.99	-2.40	0.35	2.61
124	6778990.56	365241.77	0.0015	0.0041	0.0189	0.0464	0.0855	9.41	7.93	5.72	4.43	3.55	6.03	-1.76	-6.02	0.02	4.01
125	6778967.18	365325.54	0.0018	0.0057	0.0262	0.0819	0.2416	9.11	7.46	5.26	3.61	2.05	5.44	-2.03	-3.37	0.39	4.64
126	6778915.92	365435.35	0.0021	0.0071	0.0357	0.2402	0.4875	8.91	7.14	4.81	2.06	1.04	4.67	-2.46	-0.24	0.44	2.50
127	6778894.57	365486.43	0.0015	0.0042	0.0208	0.0549	0.1070	9.37	7.89	5.59	4.19	3.22	5.89	-1.86	-5.98	0.34	3.10
128	6778876.99	365530.10	0.0015	0.0043	0.0212	0.0569	0.1659	9.36	7.87	5.56	4.14	2.59	5.85	-1.96	-4.45	0.18	
129	6778864.75	365550.89	0.0061	0.0428	0.3595	0.5283	0.6554	7.35	4.55	1.48	0.92	0.61	2.31	-1.93	-21.46	0.34	
130	6778853.60	365559.39	0.2595	0.3111	0.4220	0.5731	0.6880	1.95	1.68	1.24	0.80	0.54	1.24	-0.43	0.00	0.22	0.14
131	6779085.97	365670.26	0.2318	0.2844	0.4032	0.5734	0.7059	2.11	1.81	1.31	0.80	0.50	1.31	-0.50	0.01	1.19	1.18
132	6779102.71	365637.36	0.0017	0.0052	0.0277	0.3312	0.5802	9.23	7.60	5.17	1.59	0.79	4.79	-2.78	4.91	0.25	0.95
133	6779126.36	365617.33	0.0024	0.0095	0.2693	0.6040	0.8314	8.73	6.72	1.89	0.73	0.27	3.11	-2.78	-33.03	0.37	0.90
134	6779145.38	365589.12	0.0042	0.0207	0.4955	0.8837	1.2100	7.90	5.59	1.01	0.18	-0.27	2.26	-2.59	-33.05	0.31	
135	6779165.37	365571.36	0.0194	0.3655	0.5958	0.9220	1.2067	5.69	1.45	0.75	0.12	-0.27	0.77	-1.24	-11.73	0.46	1.16
136	6779184.98	365540.55	0.3056	0.3764	0.5378	0.7744	0.9677	1.71	1.41	0.89	0.37	0.05	0.89	-0.51	0.03	0.26	
137	6779185.30	365516.30	0.0233	0.2588	0.3915	0.5567	0.6868	5.43	1.95	1.35	0.85	0.54	1.38	-1.02	-8.01	0.35	
138	6779200.53	365496.03	0.0219	0.2314	0.3652	0.5390	0.6765	5.51	2.11	1.45	0.89	0.56	1.49	-1.05	-7.90	0.28	0.32
139	6779444.25	365542.49	0.0060	0.0318	0.3368	0.6403	0.8827	7.39	4.97	1.57	0.64	0.18	2.40	-2.18	-21.34	0.31	1.34
140	6779436.39	365568.14	0.0066	0.0325	0.3126	0.5799	0.7908	7.24	4.94	1.68	0.79	0.34	2.47	-2.08	-19.49	0.25	
141	6779417.14	365589.90	0.0067	0.0375	0.3440	0.6274	0.8590	7.21	4.74	1.54	0.67	0.22	2.32	-2.08	-19.96	0.26	0.82
142	6779394.90	365607.41	0.0067	0.0344	0.3250	0.6203	0.8605	7.21	4.86	1.62	0.69	0.22	2.39	-2.10	-19.47	0.28	
143	6779377.40	365625.53	0.0172	0.2494	0.3965	0.5818	0.7246	5.87	2.00	1.33	0.78	0.46	1.37	-1.12	-9.96	0.31	
144	6779363.07	365655.73	0.0634	0.2945	0.4123	0.5634	0.6774	3.98	1.76	1.28	0.83	0.56	1.29	-0.75	-3.41	0.29	
145	6779356.28	365674.65	0.0117	0.2283	0.3785	0.5600	0.7003	6.41	2.13	1.40	0.84	0.51	1.46	-1.22	-12.26	0.28	0.17
146	6779345.60	365715.00	0.0070	0.0511	0.3740	0.5408	0.6669	7.15	4.29	1.42	0.89	0.58	2.20	-1.85	-20.05	0.21	
147	6779319.44	365760.14	0.0037	0.0179	0.3440	0.5851	0.7543	8.09	5.80	1.54	0.77	0.41	2.70	-2.42	-29.58	0.42	2.97
148	6779311.56	365792.19	0.0032	0.0145	0.3031	0.5874	0.7892	8.31	6.11	1.72	0.77	0.34	2.87	-2.54	-29.92	0.36	
149	6779301.25	365813.97	0.2020	0.2488	0.3526	0.4999	0.6151	2.31	2.01	1.50	1.00	0.70	1.50	-0.50	0.00	0.66	

150	6779293.75	365823.90	0.2378	0.2905	0.4087	0.5751	0.7020	2.07	1.78	1.29	0.80	0.51	1.29	-0.48	0.00	1.21	0.36
151	6779469.02	365855.85	0.2186	0.2721	0.3884	0.5519	0.6777	2.19	1.88	1.36	0.86	0.56	1.37	-0.50	-0.02	2.27	
152	6779482.27	365841.94	0.0062	0.0418	0.3409	0.5191	0.6535	7.34	4.58	1.55	0.95	0.61	2.36	-1.93	-20.72	0.28	
153	6779505.47	365825.60	0.0028	0.0126	0.2861	0.5620	0.7568	8.48	6.31	1.81	0.83	0.40	2.98	-2.59	-30.99	0.33	
154	6779524.89	365808.25	0.0046	0.0238	0.2686	0.4713	0.6202	7.76	5.40	1.90	1.09	0.69	2.79	-2.15	-22.28	0.27	
155	6779541.84	365780.14	0.0549	0.2529	0.3667	0.5147	0.6315	4.19	1.98	1.45	0.96	0.66	1.46	-0.79	-3.47	0.29	
156	6779571.64	365758.77	0.0330	0.2853	0.4219	0.5999	0.7388	4.92	1.81	1.25	0.74	0.44	1.26	-0.95	-6.47	0.31	
157	6779590.91	365726.57	0.0237	0.2909	0.5215	0.8447	1.1323	5.40	1.78	0.94	0.24	-0.18	0.99	-1.23	-9.43	0.30	
158	6779595.65	365710.76	0.0086	0.2198	0.4595	0.7071	0.9136	6.86	2.19	1.12	0.50	0.13	1.27	-1.44	-16.36	0.26	
159	6779611.01	365687.07	0.0083	0.0481	0.4396	0.6864	0.8842	6.91	4.38	1.19	0.54	0.18	2.04	-1.98	-20.78	0.32	
160	6779624.67	365670.07	0.0434	0.1854	0.3364	0.5528	0.7246	4.53	2.43	1.57	0.86	0.46	1.62	-1.01	-3.86	0.29	
161	6779786.61	365721.07	0.0113	0.1946	0.3609	0.5405	0.6790	6.46	2.36	1.47	0.89	0.56	1.57	-1.26	-12.28	0.42	1.28
162	6779769.20	365744.35	0.0460	0.2342	0.3737	0.5648	0.7122	4.44	2.09	1.42	0.82	0.49	1.45	-0.92	-4.18	0.31	
163	6779739.54	365785.69	0.0326	0.2701	0.4001	0.5621	0.6883	4.94	1.89	1.32	0.83	0.54	1.35	-0.93	-6.28	0.30	1.65
164	6779714.26	365826.32	0.1870	0.2681	0.3870	0.5423	0.6653	2.42	1.90	1.37	0.88	0.59	1.38	-0.53	-0.27	0.14	
165	6779692.67	365865.95	0.2644	0.3245	0.4615	0.6608	0.8194	1.92	1.62	1.12	0.60	0.29	1.11	-0.50	0.02	0.33	1.01
166	6779670.99	365877.75	0.0173	0.2480	0.4121	0.6165	0.7777	5.85	2.01	1.28	0.70	0.36	1.33	-1.16	-10.13	0.32	
167	6779653.60	365906.09	0.0079	0.0459	0.3240	0.5534	0.7215	6.99	4.45	1.63	0.85	0.47	2.31	-1.88	-17.37	0.80	
168	6779628.13	365964.14	0.0087	0.2328	0.3849	0.5515	0.6805	6.85	2.10	1.38	0.86	0.56	1.45	-1.27	-14.78	0.51	0.38
169	6779604.16	366009.69	0.0016	0.0045	0.0274	0.2947	0.5994	9.31	7.78	5.19	1.76	0.74	4.91	-2.80	3.95	0.68	
170	6779607.00	366022.70	0.2474	0.3031	0.4291	0.6094	0.7496	2.01	1.72	1.22	0.71	0.42	1.22	-0.49	0.01	0.91	0.58
171	6779765.78	366091.76	0.2317	0.2949	0.4262	0.6116	0.7556	2.11	1.76	1.23	0.71	0.40	1.23	-0.52	-0.05	2.42	
172	6779778.69	366079.03	0.0054	0.0299	0.3021	0.5507	0.7405	7.53	5.06	1.73	0.86	0.43	2.55	-2.13	-21.17	0.47	
173	6779803.90	366060.69	0.2600	0.3216	0.4628	0.6699	0.8365	1.94	1.64	1.11	0.58	0.26	1.11	-0.52	0.02	0.43	
174	6779828.76	366023.93	0.1721	0.2602	0.3762	0.5300	0.6530	2.54	1.94	1.41	0.92	0.61	1.42	-0.55	-0.34	0.57	
175	6779857.88	365988.22	0.2049	0.2719	0.3871	0.5414	0.6604	2.29	1.88	1.37	0.89	0.60	1.38	-0.50	-0.14	0.72	
176	6779877.39	365951.05	0.1684	0.2111	0.3117	0.4606	0.5780	2.57	2.24	1.68	1.12	0.79	1.68	-0.55	0.00	0.95	
177	6779902.65	365911.41	0.1691	0.2121	0.3044	0.4360	0.5397	2.56	2.24	1.72	1.20	0.89	1.72	-0.51	-0.02	1.13	
178	6779921.83	365879.16	0.1920	0.2426	0.3510	0.5061	0.6292	2.38	2.04	1.51	0.98	0.67	1.51	-0.52	-0.03	0.65	
179	6779942.08	365851.81	0.0132	0.1849	0.2996	0.4286	0.5279	6.24	2.43	1.74	1.22	0.92	1.80	-1.11	-9.90	0.94	
180	6779957.96	365834.04	0.0168	0.1839	0.2976	0.4354	0.5408	5.90	2.44	1.75	1.20	0.89	1.80	-1.07	-8.33	0.08	
181	6780252.30	366164.27	0.0082	0.0932	0.2717	0.4704	0.6334	6.93	3.42	1.88	1.09	0.66	2.13	-1.53	-12.86	0.31	1.43
182	6780248.23	366169.88	0.0149	0.2208	0.3542	0.5278	0.6650	6.07	2.18	1.50	0.92	0.59	1.53	-1.14	-10.10	0.12	
183	6780242.75	366187.16	0.2442	0.2889	0.3821	0.5062	0.6009	2.03	1.79	1.39	0.98	0.73	1.39	-0.40	0.01	0.28	
184	6780230.73	366201.97	0.0090	0.0672	0.4005	0.7066	0.9659	6.80	3.90	1.32	0.50	0.05	1.91	-1.87	-17.19	0.62	1.04
185	6780215.28	366229.81	0.2255	0.2773	0.3946	0.5646	0.6996	2.15	1.85	1.34	0.82	0.52	1.34	-0.50	0.02	0.74	
186	6780202.19	366264.73	0.2520	0.3089	0.4376	0.6219	0.7658	1.99	1.69	1.19	0.69	0.39	1.19	-0.50	0.01	0.29	2.53
187	6780193.55	366287.84	0.2048	0.2461	0.3353	0.4585	0.5542	2.29	2.02	1.58	1.12	0.85	1.57	-0.44	0.01	1.00	
188	6780190.35	366296.46	0.2248	0.2766	0.3941	0.5643	0.7004	2.15	1.85	1.34	0.83	0.51	1.34	-0.51	0.02	1.19	
189	6780178.91	366310.61	0.2571	0.3174	0.4548	0.6554	0.8159	1.96	1.66	1.14	0.61	0.29	1.13	-0.51	0.02	0.94	1.26
190	6780161.17	366340.07	0.2401	0.2959	0.4218	0.6021	0.7431	2.06	1.76	1.25	0.73	0.43	1.24	-0.50	0.00	0.95	1.11
191	6780380.88	366456.46	0.2191	0.2819	0.4262	0.6473	0.8294	2.19	1.83	1.23	0.63	0.27	1.23	-0.59	0.00	1.36	
192	6780397.92	366433.65	0.2234	0.2768	0.3991	0.5801	0.7287	2.16	1.85	1.33	0.79	0.46	1.32	-0.53	0.03	0.54	
193	6780408.78	366414.67	0.2260	0.2682	0.3553	0.4705	0.5576	2.15	1.90	1.49	1.09	0.84	1.49	-0.40	0.00	1.05	
194	6780417.70	366403.55	0.2474	0.3111	0.4632	0.6933	0.8789	2.02	1.68	1.11	0.53	0.19	1.11	-0.57	0.02	0.93	
195	6780430.72	366380.04	0.2230	0.2728	0.3847	0.5439	0.6674	2.17	1.87	1.38	0.88	0.58	1.38	-0.49	0.01	0.92	
196	6780460.36	366341.26	0.1877	0.2317	0.3306	0.4723	0.5843	2.41	2.11	1.60	1.08	0.78	1.60	-0.51	0.00	0.77	
197	6780464.00	366331.21	0.2252	0.2770	0.3942	0.5639	0.6988	2.15	1.85	1.34	0.83	0.52	1.34	-0.50	0.02	1.11	
198	6780469.49	366318.55	0.2027	0.2795	0.4183	0.6154	0.7733	2.30	1.84	1.26	0.70	0.37	1.27	-0.58	-0.17	0.41	
199	6780477.32	366300.02	0.2254	0.2810	0.4126	0.6077	0.7603	2.15	1.83	1.28	0.72	0.40	1.28	-0.54	0.01	1.36	
200	6780483.60	366290.06	0.1922	0.2426	0.3612	0.5369	0.6747	2.38	2.04	1.47	0.90	0.57	1.47	-0.56	-0.01	2.25	

201	6780697.51	366439.42	0.2294	0.2767	0.3785	0.5182	0.6256	2.12	1.85	1.40	0.95	0.68	1.40	-0.45	0.00	1.79	0.16
202	6780677.61	366459.58	0.2451	0.3051	0.4325	0.6104	0.7472	2.03	1.71	1.21	0.71	0.42	1.21	-0.49	-0.03	0.27	
203	6780671.29	366467.50	0.2654	0.3251	0.4601	0.6541	0.8056	1.91	1.62	1.12	0.61	0.31	1.12	-0.49	0.01	0.44	1.25
204	6780650.99	366491.06	0.2234	0.2893	0.4427	0.6862	0.8984	2.16	1.79	1.18	0.54	0.15	1.17	-0.62	0.05	0.53	
205	6780634.40	366516.85	0.0101	0.1345	0.2681	0.4364	0.5750	6.63	2.89	1.90	1.20	0.80	2.00	-1.31	-10.86	1.73	2.89
206	6780614.54	366539.27	0.0171	0.1742	0.3478	0.5663	0.7332	5.87	2.52	1.52	0.82	0.45	1.62	-1.25	-9.12	0.81	
207	6780594.58	366568.04	0.1818	0.2340	0.3480	0.5122	0.6388	2.46	2.10	1.52	0.97	0.65	1.53	-0.56	-0.06	1.39	0.95
208	6780583.74	366582.64	0.1780	0.2243	0.3332	0.4949	0.6236	2.49	2.16	1.59	1.01	0.68	1.59	-0.56	0.00	1.00	
209	6780583.33	366590.03	0.1564	0.2208	0.3448	0.5268	0.6742	2.68	2.18	1.54	0.92	0.57	1.55	-0.63	-0.20	1.06	
210	6780579.63	366596.96	0.2111	0.2781	0.3984	0.5631	0.6938	2.24	1.85	1.33	0.83	0.53	1.33	-0.51	-0.11	0.87	0.88
211	6780919.92	366909.55	0.1875	0.2298	0.3244	0.4575	0.5605	2.41	2.12	1.62	1.13	0.84	1.62	-0.49	0.00	0.37	0.52
212	6780924.77	366896.51	0.0118	0.1910	0.2965	0.4192	0.5136	6.41	2.39	1.75	1.25	0.96	1.80	-1.11	-10.60	0.23	
213	6780945.44	366880.25	0.1860	0.2462	0.3294	0.4328	0.5103	2.43	2.02	1.60	1.21	0.97	1.61	-0.42	-0.15	0.96	2.21
214	6780956.40	366870.58	0.1669	0.2040	0.2870	0.4038	0.4933	2.58	2.29	1.80	1.31	1.02	1.80	-0.48	0.00	0.96	
215	6780974.14	366851.24	0.0193	0.1737	0.2607	0.3655	0.4455	5.70	2.53	1.94	1.45	1.17	1.97	-0.95	-6.81	1.79	1.27
216	6780998.89	366832.36	0.0140	0.2467	0.3860	0.5451	0.6676	6.15	2.02	1.37	0.88	0.58	1.42	-1.13	-11.20	0.24	
217	6781019.88	366804.92	0.0112	0.2032	0.4066	0.6113	0.7666	6.48	2.30	1.30	0.71	0.38	1.44	-1.32	-13.32	0.76	1.12
218	6781033.29	366782.22	0.0040	0.0196	0.2778	0.5154	0.6883	7.97	5.67	1.85	0.96	0.54	2.83	-2.30	-24.77	0.01	
219	6781040.25	366771.18	0.0080	0.0473	0.3514	0.5698	0.7415	6.97	4.40	1.51	0.81	0.43	2.24	-1.89	-18.28	0.18	
220	6781044.61	366765.94	0.1982	0.2707	0.4065	0.6014	0.7593	2.34	1.89	1.30	0.73	0.40	1.31	-0.58	-0.14	0.23	1.57

APPENDIX B

SEDIMENT CHEMISTRY

B.1. MAJOR AND MINOR ELEMENTS (%)

sample no	y_proj	x_proj	SiO2	Al2O3	Fe2O3	MnO	MgO	CaO	Na2O	K2O	TiO2	P2O5	TOTAL	L.O.I.
31	6781159	367145	73.2	4.86	11.8	0.17	2.35	3.51	0.58	0.84	2.61	0.08	100	1.16
34	6781226	367105	86.5	4.54	2.95	0.07	1.07	2.09	1.3	1.11	0.3	0.04	100	2.31
35	6781247	367080	85.3	5.1	3.31	0.06	1.16	2.07	1.23	1.2	0.32	0.05	99.8	2.69
36	6781279	367051	86	5.06	2.9	0.05	1.02	1.83	1.19	1.19	0.27	0.05	99.6	2.25
40	6781318	367004	79.2	5.13	6.42	0.1	1.96	3.74	0.8	1.03	1.59	0.06	100	1.76
51	6781608	367480	85.6	4.86	3.39	0.05	1.07	2.56	0.92	1.2	0.37	0.04	100	1.79
52	6781610	367464	86.9	4.55	2.78	0.05	1.02	2.17	1.05	1.13	0.3	0.04	100	1.85
53	6781622	367412	81.4	6.51	4.55	0.06	1.27	2.63	1.36	1.45	0.71	0.06	100	3.78
54	6781645	367372	79.6	8.11	4.6	0.07	1.35	2.38	1.82	1.53	0.5	0.08	100	4.83
56	6781670	367341	79.9	4.95	5.71	0.09	2.21	4.49	0.75	0.98	0.88	0.07	100	2.15
68	6781918	367603	86.8	5.29	2.19	0.04	0.75	2.09	1.13	1.5	0.18	0.04	100	1.99
69	6781906	367613	79.9	5.02	6.73	0.1	1.44	2.93	1	1.11	1.72	0.06	100	2.01
70	6781881	367640	78.2	9.21	4.46	0.07	1.24	2.24	2.03	1.91	0.54	0.08	100	4.97
72	6781838	367652	85	4.84	3.43	0.06	1.32	2.67	1.14	1.12	0.33	0.05	100	2.37
89	6782183	368016	89.3	4.39	1.88	0.03	0.54	1.47	1.09	1.2	0.11	0.03	100	1.78
90	6782170	368026	87	5.5	2.22	0.03	0.63	1.65	1.33	1.57	0.12	0.03	100	2.02
91	6782189	368003	87.1	5.33	2.23	0.03	0.66	1.59	1.41	1.46	0.14	0.04	100	2.02
92	6782203	367987	86.4	5.12	2.79	0.04	0.8	1.84	1.4	1.34	0.21	0.04	99.9	2.27
94	6782218	367966	75.8	5.54	8.53	0.13	2.24	4	1.16	1.04	1.48	0.09	100	1.99
95	6778538	365221	88.2	4.66	2.75	0.05	0.74	1.25	0.92	1.17	0.24	0.04	100	1.38
96	6778555	365195	75	11.4	6.41	0.1	1.36	1.52	1.5	1.76	0.87	0.14	100	8.93
97	6778584	365132	81.2	8.81	4.22	0.06	0.81	1.02	1.29	1.73	0.74	0.09	100	5.82
99	6778623	365044	85.6	7.15	2.87	0.05	0.49	0.73	0.98	1.65	0.53	0.06	100	4.16
100	6778648	365010	87.7	5.81	2.53	0.05	0.43	0.64	0.94	1.49	0.41	0.04	100	2.94
103	6778717	365056	74.1	12.6	6.16	0.08	1.09	0.97	1.87	2.04	0.94	0.16	100	11.8
104	6778700	365115	81.3	9.06	4.02	0.05	0.71	0.75	1.38	1.74	0.6	0.09	99.7	5.86
106	6778660	365237	73.3	12.8	6.71	0.08	1.16	1.02	1.76	1.92	0.83	0.17	99.8	10.2
107	6778642	365300	75.2	10.7	6.53	0.08	1.34	1.58	1.69	1.68	1.08	0.14	100	7.7
110	6778622	365338	81.5	5.19	5.61	0.09	1.46	2.86	0.99	1.09	1.17	0.06	100	2.17
111	6778709	365359	83.6	4.76	4.31	0.08	1.61	3.08	0.87	0.97	0.65	0.06	100	1.71
113	6778753	365323	67.5	15.9	8.44	0.12	1.44	1.07	2.01	2.08	1.01	0.21	99.7	12.8
114	6778783	365265	78.9	9.92	4.56	0.07	0.82	0.8	1.56	1.79	0.62	0.1	99.1	6.86
115	6778826	365198	90.8	4.15	1.64	0.03	0.24	0.44	0.7	1.29	0.32	0.03	99.6	1.51
117	6778873	365141	76.6	11.4	5.3	0.1	0.95	0.86	1.93	2.02	0.7	0.13	100	8.01
119	6778903	365055	83.5	8.31	3.23	0.04	0.54	0.64	1.28	1.95	0.47	0.07	100	4.75
120	6778956	364970	80.5	9.76	4.23	0.06	0.68	0.7	1.44	2.02	0.61	0.1	100	6.44
121	6779031	365051	86.3	6.91	2.7	0.04	0.42	0.55	1.03	1.68	0.43	0.06	100	4.12
123	6779002	365158	74.4	12.6	6.18	0.07	1.03	0.77	2.07	1.96	0.86	0.15	100	9.97
124	6778991	365242	64.8	17.3	8.92	0.09	1.57	0.9	2.56	2.18	1.05	0.21	99.6	14.2
125	6778967	365326	68	15.6	7.81	0.13	1.51	1.24	2.5	2.1	0.93	0.18	100	12.9
126	6778916	365435	76	11.3	5.51	0.08	1.23	1.25	1.88	1.9	0.67	0.13	100	8.23
127	6778895	365486	64.7	17.4	9.1	0.12	1.68	1.16	2.45	2.2	1.02	0.21	100	14.1
130	6778854	365559	89.5	4.02	2.22	0.04	0.72	1.37	0.61	1.07	0.16	0.03	99.7	0.93
131	6779086	365670	83	5.17	4.5	0.08	1.87	3.13	0.82	0.99	0.45	0.05	100	1.81
132	6779103	365637	77.5	9.3	5.9	0.09	1.59	1.95	1.34	1.52	0.78	0.1	100	5.25
133	6779126	365617	82.1	7.92	4.22	0.07	1.08	1.3	1.24	1.55	0.48	0.09	100	4.39
135	6779165	365571	89.7	4.32	2.16	0.05	0.56	1.07	0.8	1.25	0.18	0.03	100	1.61
138	6779201	365496	89.8	4.43	1.99	0.05	0.53	0.85	0.82	1.3	0.23	0.03	100	1.58
139	6779444	365542	89.4	4.72	2.58	0.02	0.34	0.58	0.83	1.38	0.23	0.04	100	2.12
141	6779417	365590	90.7	4.32	1.65	0.04	0.32	0.54	0.88	1.32	0.22	0.03	100	1.57
145	6779356	365675	87.3	4.77	3.06	0.05	0.84	1.32	0.89	1.23	0.4	0.04	99.9	1.35
147	6779319	365760	84.8	6.03	3.67	0.08	0.96	1.58	1.18	1.31	0.36	0.06	100	2.79
150	6779294	365824	82.1	4.96	5.26	0.09	1.76	3.32	0.64	1	0.86	0.05	100	1.44
161	6779787	365721	87.8	4.79	2.73	0.04	0.72	1.45	0.76	1.31	0.39	0.04	100	1.93
163	6779740	365786	88.5	4.26	2.72	0.05	0.71	1.09	1	1.2	0.34	0.03	99.9	1.78
165	6779693	365866	85.6	4.63	4.23	0.07	1.28	1.81	0.76	1.14	0.49	0.05	100	1.01
168	6779628	365964	84.7	5.42	3.84	0.08	1.19	2.09	1.01	1.25	0.39	0.05	100	2.06
170	6779607	366023	84	4.84	4.15	0.07	1.63	3.01	0.8	1	0.53	0.06	100	1.5
181	6780252	366164	81.7	5.68	5.45	0.09	1.51	2.11	1.01	1.26	1.21	0.07	100	1.73
184	6780231	366202	82.5	6.03	4.9	0.07	1.2	1.99	1.31	1.34	0.7	0.05	100	3.37
186	6780202	366265	84.4	4.59	4.67	0.1	1.39	2.21	0.85	1.06	0.7	0.05	100	1.38
189	6780179	366311	84.6	4.64	4.42	0.07	1.27	2.44	0.84	1.07	0.63	0.04	100	1.26
190	6780161	366340	81.1	5.48	5.37	0.08	1.83	3.41	0.89	1.13	0.63	0.06	100	1.84
201	6780698	366439	85.9	4.19	3.38	0.06	1.23	3.06	0.7	1.04	0.43	0.05	100	2
203	6780671	366468	88.1	4.64	2.47	0.04	0.86	1.54	0.97	1.18	0.2	0.05	100	1.68
205	6780634	366517	83	5.92	3.7	0.13	1.24	2.77	1.38	1.36	0.48	0.06	100	3.36
207	6780595	366568	82.1	4.88	5.29	0.08	1.64	3.08	1.11	1.01	0.8	0.06	100	2.3
210	6780580	366597	83.8	4.84	4.46	0.07	1.39	2.76	0.86	1.1	0.69	0.05	100	1.73
211	6780920	366910	86.7	4.68	3.21	0.05	1.1	1.9	0.86	1.13	0.39	0.05	100	1.48
213	6780945	366880	86	4.64	3.24	0.05	1.13	2.34	0.97	1.13	0.42	0.05	100	2.07
215	6780974	366851	83	5.39	4.26	0.08	1.27	3.01	0.95	1.24	0.74	0.05	100	2.4
217	6781020	366805	85.9	5.61	3.04	0.05	0.85	1.77	1.22	1.35	0.22	0.04	100	2.24
220	6781045	366766	85.1	4.39	4.07	0.06	1.42	2.3	0.75	1	0.82	0.05	100	1.75

Element Weight (%) | Normalised to Al

=Element Weight (%)/Al weight (%)

Sample no	y_proj	x_proj	Si	Fe	Mn	Mg	Ca	Na	K	Ti	Al	Si	Fe	Mn	Mg	Ca	Na	K	Ti
31	6781159	367145	34.16	8.23	0.13	1.42	2.51	0.43	0.70	1.57	2.57	13.27	3.20	0.05	0.55	0.97	0.17	0.27	0.61
34	6781226	367105	40.37	2.06	0.05	0.65	1.49	0.96	0.92	0.18	2.40	16.80	0.86	0.02	0.27	0.62	0.40	0.38	0.07
35	6781247	367080	39.82	2.32	0.05	0.70	1.48	0.91	1.00	0.19	2.70	14.75	0.86	0.02	0.26	0.55	0.34	0.37	0.07
36	6781279	367051	40.13	2.03	0.04	0.62	1.31	0.88	0.99	0.16	2.68	14.98	0.76	0.01	0.23	0.49	0.33	0.37	0.06
40	6781318	367004	36.94	4.49	0.08	1.18	2.67	0.59	0.85	0.95	2.72	13.60	1.65	0.03	0.44	0.98	0.22	0.31	0.35
51	6781608	367480	39.94	2.37	0.04	0.65	1.83	0.68	1.00	0.22	2.57	15.52	0.92	0.01	0.25	0.71	0.27	0.39	0.09
52	6781610	367464	40.57	1.94	0.03	0.62	1.55	0.78	0.94	0.18	2.41	16.84	0.81	0.01	0.26	0.64	0.32	0.39	0.08
53	6781622	367412	38.00	3.18	0.05	0.77	1.88	1.01	1.20	0.42	3.45	11.02	0.92	0.01	0.22	0.55	0.29	0.35	0.12
54	6781645	367372	37.13	3.22	0.06	0.81	1.70	1.35	1.27	0.30	4.29	8.65	0.75	0.01	0.19	0.40	0.31	0.30	0.07
56	6781670	367341	37.28	3.99	0.07	1.33	3.21	0.56	0.81	0.53	2.62	14.23	1.52	0.03	0.51	1.22	0.21	0.31	0.20
68	6781918	367603	40.51	1.53	0.03	0.45	1.49	0.84	1.24	0.11	2.80	14.46	0.55	0.01	0.16	0.53	0.30	0.44	0.04
69	6781906	367613	37.26	4.71	0.08	0.87	2.09	0.74	0.92	1.03	2.66	14.02	1.77	0.03	0.33	0.79	0.28	0.35	0.39
70	6781881	367640	36.51	3.12	0.05	0.75	1.60	1.51	1.58	0.33	4.88	7.49	0.64	0.01	0.15	0.33	0.31	0.33	0.07
72	6781838	367652	39.68	2.40	0.04	0.80	1.91	0.85	0.93	0.20	2.56	15.48	0.94	0.02	0.31	0.74	0.33	0.36	0.08
89	6782183	368016	41.67	1.31	0.02	0.33	1.05	0.81	1.00	0.07	2.32	17.93	0.57	0.01	0.14	0.45	0.35	0.43	0.03
90	6782170	368026	40.58	1.55	0.02	0.38	1.18	0.99	1.30	0.07	2.91	13.94	0.53	0.01	0.13	0.40	0.34	0.45	0.02
91	6782189	368003	40.64	1.56	0.02	0.40	1.14	1.05	1.21	0.08	2.82	14.40	0.55	0.01	0.14	0.40	0.37	0.43	0.03
92	6782203	367987	40.30	1.95	0.03	0.48	1.31	1.04	1.11	0.13	2.71	14.87	0.72	0.01	0.18	0.48	0.38	0.41	0.05
94	6782218	367966	35.35	5.97	0.10	1.35	2.86	0.86	0.86	0.89	2.93	12.05	2.03	0.03	0.46	0.97	0.29	0.29	0.30
95	6778538	365221	41.17	1.92	0.04	0.45	0.89	0.68	0.97	0.14	2.47	16.69	0.78	0.02	0.18	0.36	0.28	0.39	0.06
96	6778555	365195	35.00	4.48	0.08	0.82	1.09	1.11	1.46	0.52	6.02	5.82	0.74	0.01	0.14	0.18	0.18	0.24	0.09
97	6778584	365132	37.89	2.95	0.05	0.49	0.73	0.96	1.44	0.44	4.66	8.12	0.63	0.01	0.10	0.16	0.21	0.31	0.10
99	6778623	365044	39.93	2.01	0.04	0.30	0.52	0.73	1.37	0.32	3.79	10.55	0.53	0.01	0.08	0.14	0.19	0.36	0.08
100	6778648	365010	40.94	1.77	0.04	0.26	0.46	0.70	1.24	0.24	3.08	13.31	0.58	0.01	0.08	0.15	0.23	0.40	0.08
103	6778717	365056	34.59	4.31	0.06	0.66	0.69	1.39	1.69	0.56	6.65	5.20	0.65	0.01	0.10	0.10	0.21	0.25	0.08
104	6778700	365115	37.94	2.81	0.04	0.43	0.54	1.02	1.44	0.36	4.80	7.91	0.59	0.01	0.09	0.11	0.21	0.30	0.08
106	6778660	365237	34.20	4.69	0.06	0.70	0.73	1.31	1.59	0.50	6.79	5.04	0.69	0.01	0.10	0.11	0.19	0.23	0.07
107	6778642	365300	35.10	4.57	0.06	0.81	1.13	1.25	1.39	0.65	5.65	6.21	0.81	0.01	0.14	0.20	0.22	0.25	0.11
110	6778622	365338	38.03	3.92	0.07	0.88	2.04	0.73	0.90	0.70	2.75	13.84	1.43	0.03	0.32	0.74	0.27	0.33	0.26
111	6778709	365359	39.01	3.01	0.06	0.97	2.20	0.65	0.80	0.39	2.52	15.48	1.20	0.03	0.39	0.87	0.26	0.32	0.15
113	6778753	365323	31.48	5.90	0.09	0.87	0.76	1.49	1.73	0.61	8.40	3.75	0.70	0.01	0.10	0.09	0.18	0.21	0.07
114	6778783	365265	36.81	3.19	0.05	0.49	0.57	1.16	1.49	0.37	5.25	7.01	0.61	0.01	0.09	0.11	0.22	0.28	0.07
115	6778826	365198	42.36	1.15	0.02	0.14	0.31	0.52	1.07	0.19	2.20	19.28	0.52	0.01	0.07	0.14	0.24	0.49	0.09
117	6778873	365141	35.77	3.71	0.08	0.57	0.61	1.43	1.68	0.42	6.06	5.91	0.61	0.01	0.09	0.10	0.24	0.28	0.07
119	6778903	365055	38.98	2.26	0.03	0.33	0.46	0.95	1.62	0.28	4.40	8.86	0.51	0.01	0.07	0.10	0.22	0.37	0.06
120	6778956	364970	37.54	2.96	0.04	0.41	0.50	1.07	1.68	0.36	5.17	7.27	0.57	0.01	0.08	0.10	0.21	0.32	0.07
121	6779031	365051	40.25	1.89	0.03	0.25	0.39	0.76	1.39	0.26	3.66	11.00	0.52	0.01	0.07	0.11	0.21	0.38	0.07
123	6779002	365158	34.72	4.32	0.05	0.62	0.55	1.54	1.63	0.51	6.65	5.22	0.65	0.01	0.09	0.08	0.23	0.24	0.08
124	6778991	365242	30.23	6.24	0.07	0.95	0.64	1.90	1.81	0.63	9.16	3.30	0.68	0.01	0.10	0.07	0.21	0.20	0.07
125	6778967	365326	31.73	5.46	0.10	0.91	0.89	1.85	1.74	0.56	8.26	3.84	0.66	0.01	0.11	0.11	0.22	0.21	0.07
126	6778916	365435	35.48	3.85	0.06	0.74	0.89	1.39	1.58	0.40	5.99	5.92	0.64	0.01	0.12	0.15	0.23	0.26	0.07
127	6778895	365486	30.17	6.36	0.10	1.01	0.83	1.82	1.83	0.61	9.21	3.28	0.69	0.01	0.11	0.09	0.20	0.20	0.07
130	6778854	365559	41.75	1.55	0.03	0.43	0.98	0.45	0.89	0.09	2.13	19.62	0.73	0.01	0.20	0.46	0.21	0.42	0.04
131	6779086	365670	38.74	3.15	0.06	1.13	2.24	0.61	0.82	0.27	2.74	14.15	1.15	0.02	0.41	0.82	0.22	0.30	0.10
132	6779103	365637	36.15	4.13	0.07	0.96	1.39	0.99	1.26	0.47	4.92	7.34	0.84	0.01	0.19	0.28	0.20	0.26	0.09
133	6779126	365617	38.33	2.95	0.05	0.65	0.93	0.92	1.29	0.29	4.19	9.14	0.70	0.01	0.16	0.22	0.22	0.31	0.07
135	6779165	365571	41.84	1.51	0.04	0.34	0.76	0.59	1.04	0.11	2.29	18.29	0.66	0.02	0.15	0.33	0.26	0.45	0.05
138	6779201	365496	41.93	1.39	0.04	0.32	0.61	0.61	1.08	0.14	2.35	17.88	0.59	0.02	0.14	0.26	0.26	0.46	0.06
139	6779444	365542	41.70	1.80	0.02	0.21	0.41	0.62	1.15	0.14	2.50	16.69	0.72	0.01	0.08	0.17	0.25	0.46	0.05
141	6779417	365590	42.32	1.15	0.03	0.19	0.39	0.65	1.10	0.13	2.29	18.50	0.50	0.01	0.08	0.17	0.29	0.48	0.06
145	6779356	365675	40.74	2.14	0.04	0.51	0.94	0.66	1.02	0.24	2.53	16.13	0.85	0.02	0.20	0.37	0.26	0.40	0.10
147	6779319	365760	39.57	2.57	0.06	0.58	1.13	0.88	1.09	0.21	3.19	12.39	0.80	0.02	0.18	0.35	0.27	0.34	0.07
150	6779294	365824	38.29	3.68	0.07	1.06	2.37	0.47	0.83	0.51	2.63	14.58	1.40	0.03	0.40	0.90	0.18	0.32	0.20
161	6779787	365721	40.99	1.91	0.03	0.43	1.04	0.56	1.09	0.23	2.54	16.16	0.75	0.01	0.17	0.41	0.22	0.43	0.09
163	6779740	365786	41.29	1.90	0.04	0.43	0.78	0.74	1.00	0.21	2.26	18.31	0.84	0.02	0.19	0.35	0.33	0.44	0.09
165	6779693	365866	39.93	2.96	0.05	0.77	1.29	0.56	0.95	0.29	2.45	16.29	1.21	0.02	0.31	0.53	0.23	0.39	0.12
168	6779628	365964	39.54	2.69	0.06	0.72	1.49	0.75	1.04	0.23	2.87	13.78	0.94	0.02	0.25	0.52	0.26	0.36	0.08
170	6779607	366023	39.20	2.90	0.06	0.98	2.15	0.59	0.83	0.32	2.56	15.30	1.13	0.02	0.38	0.84	0.23	0.32	0.13
181	6780252	366164	38.10	3.81	0.07	0.91	1.51	0.75	1.05	0.73	3.01	12.67	1.27	0.02	0.30	0.50	0.25	0.35	0.24
184	6780231	366202	38.49	3.43	0.06	0.72	1.42	0.97	1.11	0.42	3.19	12.06	1.07	0.02	0.23	0.45	0.30	0.35	0.13
186	6780202	366265	39.40	3.27	0.07	0.84	1.58	0.63	0.88	0.42	2.43	16.21	1.34	0.03	0.34	0.65	0.26	0.36	0.17
189	6780179	366311	39.46	3.09	0.05	0.77	1.74	0.62	0.89	0.38	2.46	16.06	1.26	0.02	0.31	0.71	0.25	0.36	0.15
190	6780161	366340	37.85	3.76	0.06	1.10	2.44	0.66	0.94	0.37	2.90	13.05	1.29	0.02	0.38	0.84	0.23	0.32	0.13
201	6780698	366439	40.07	2.36	0.04	0.74	2.19	0.52	0.86	0.26	2.22	18.06	1.07	0.02	0.33	0.99	0.23	0.39	0.12
203	6780671	366468	41.10	1.73	0.03	0.52	1.10	0.72	0.98	0.12	2.46	16.73	0.70	0.01	0.21	0.45	0.29	0.40	0.05
205	6780634	366517	38.74	2.59	0.10	0.75	1.98	1.02	1.13	0.29	3.13	12.36	0.83	0.03	0.24	0.63	0.33	0.36	0.09
207	6780595	366568	38.30	3.70	0.06	0.99	2.20	0.82	0.84	0.48	2.58	14.82	1.43	0.02	0.38	0.85	0.32	0.32	0.19
210	6780580	366597	39.08	3.12	0.05	0.84	1.97	0.64	0.91	0.42	2.56	15.25	1.22	0.02	0.33	0.77	0.25	0.36	0.16
211	6780920	366910	40.48	2.25	0.04	0.66	1.36	0.64	0.94	0.23	2.48	16.34	0.91	0.01	0.27	0.55	0.26	0.38	0.09
213	6780945	366880	40.15	2.27	0.04	0.68	1.67	0.72	0.94	0.25	2.46	16.35	0.92	0.02	0.28	0.68	0.29	0.38	0.10
215	6780974	366851	38.75	2.98	0.06	0.77	2.15	0.70	1.03	0.44	2.85	13.58	1.04	0.02	0.27	0.75	0.25	0.36	0.16
217	6781020	366805	40.11	2.13	0.04	0.51	1.26	0.91	1.12	0.13	2.97	13.50	0.72	0.01	0.17	0.43	0.30	0.38	0.04
220	6781045	366766	39.73	2.85	0.05	0.86	1.64	0.56	0.83	0.49	2.32	17.09	1.22	0.02	0.37	0.71	0.24	0.36	0.21

B.2. TRACE ELEMENTS

BULK VALUES (ppm)

sample no	y_proj	x_proj	Nb	Y	Rb	Zr	Sr	U	Th	Zn	Cu	Ni	Cr	V	La	Pb	Ga	Co	Ce	Nd	AS	Cd	Sn	S
31	6781159	367145	27.3	43.3	24.7	1420.7	134.7	4.6	29	46.4	0	14.3	389	298.5	28.3	12	9	26	128	51	10	18	0	108
34	6781226	367105	4.3	11.3	34.1	119.3	130.3	0.7	3.3	11.8	1.1	7.8	39.7	58.2	0.6	10	9	9	26	8	10	0	154	1050
35	6781247	367080	4.4	11.9	38	128.5	127.8	0.8	2.9	15.1	2.8	8.2	45.3	55.3	0	4	10	15	21	9	11	23	140	1107
36	6781279	367051	4	10.3	37.3	112.8	123.6	0.2	2.9	10.9	0	7.6	40.1	48.6	0	11	12	12	18	6	7	10	169	1073
40	6781318	367004	14.8	29.7	29.9	1326.3	168.5	2	19.3	25.3	4.9	13.9	121.5	154.3	37.5	13	10	17	53	25	6	15	0	147
51	6781608	367480	5.1	13.8	37.4	182.8	162.6	1.8	7.4	11.9	0	10.1	56.3	66.2	0.7	7	10	12	31	13	9	5	120	112
52	6781610	367464	3.5	10.3	34.4	134	141.4	3.3	2.1	9.8	0	8.1	40	60.8	0	10	11	14	27	8	9	16	166	733
53	6781622	367412	5.2	11.4	37.5	135.8	133.1	0	2.2	14	2.3	7.8	40.8	43.9	0	0	10	10	28	16	9	22	164	1177
54	6781645	367372	7.2	14.8	55.7	201.7	147.5	2.1	7.8	29.5	12.6	12.2	55.5	73.8	0	9	13	17	42	11	10	10	89	2408
56	6781670	367341	8	19.7	27.9	264.4	180.8	0.5	4.9	26.5	2.5	13.9	121.4	127.6	0	15	9	18	15	4	11	10	12	181
68	6781918	367603	3.4	8.7	46.2	94.1	169.7	2.6	6.8	6.4	0	6	19.5	47.1	0	3	10	11	14	9	12	15	192	345
69	6781906	367613	15.3	36.9	36.1	1548.1	161.8	3.6	32.2	24.5	0	10.5	157.9	150.3	48.7	7	9	18	106	39	10	3	0	761
70	6781881	367640	8.5	19	71.2	264.7	184.5	3.2	9.5	36.4	10.7	14.5	45.9	85.2	8.5	17	12	14	42	15	15	13	91	3379
72	6781838	367652	4	12.8	34	126.5	153.4	0.4	3.6	11.1	0	9	38.5	59.2	0	6	10	15	25	2	8	5	126	1117
89	6782183	368016	1.4	7.6	36.4	72.1	137	1.5	1.9	1.8	1.3	5.2	10.6	17.9	0	15	11	8	6	0	5	13	221	779
90	6782170	368026	3.6	8.2	45.9	68.9	171.2	0.8	2.2	6.7	1.7	8	16.3	33.5	0	13	11	11	13	4	13	18	187	971
91	6782189	368003	2	7.5	43.2	70.8	160.7	0.5	0	8.5	2.6	8.6	30.2	31.8	0	14	10	9	17	2	10	0	194	980
92	6782203	367987	4.4	10.2	41.6	122.1	159	0.6	3.6	8.5	6.9	8.4	23	38.3	0	9	11	9	20	0	8	19	154	807
94	6782218	367966	14.1	29.7	31.1	681.2	180.9	0	15.6	37.4	4.1	18.6	208.2	184.9	3.3	7	9	20	55	16	10	13	0	804
95	6778538	365221	4.7	12.6	36.6	159.2	118.6	0	3.7	6.4	4.6	7.2	25.1	30	0	3	9	13	14	3	11	11	178	231
96	6778555	365195	10.8	26.4	70.4	310.9	116.7	1.7	10.1	51.2	27.4	16.4	74.1	111.1	29.5	25	14	20	80	32	18	12	72	2159
97	6778584	365132	10.4	23.4	64	328.7	104.5	2.5	8.3	33.1	10.8	9.1	41.8	95.9	9.1	17	12	15	57	32	11	23	150	2599
99	6778623	365044	8.3	17.1	56.5	261.3	94.7	2.2	8.8	18.2	4.1	8.2	22.2	48.3	1.8	13	12	11	51	17	11	0	207	1019
100	6778648	365010	5.5	15.8	46.6	235	84.2	2.8	5	9.4	0.7	4.9	24.2	37.4	1.7	13	13	9	32	13	11	25	214	857
103	6778717	365056	13.1	29.8	79.5	307	115.8	2.6	10.2	67.8	36	14.8	87.3	119.5	57.6	12	15	20	87	38	17	8	98	2957
104	6778700	365115	9.7	21.2	65.3	243.3	97.1	2.2	9.8	37.1	19.3	9.7	35.3	82.7	58.9	7	12	14	69	26	14	20	172	2027
106	6778660	365237	11.6	29	79.3	257.1	107.8	2.3	11	57.9	34.9	19	171.9	124.7	26.2	22	12	22	80	35	17	27	76	5588
107	6778642	365300	11.4	29.9	64.5	596.7	114.3	0	11.7	56.8	22.7	15.7	132.4	139.4	53.5	17	14	23	90	41	13	8	39	3529
110	6778622	365338	13.7	29.6	35	1026.2	154.4	4.4	21.4	24.8	2.8	12.4	100.2	116.3	6.3	8	10	15	75	40	9	16	3	962
111	6778709	365359	7.6	14.7	29.8	274	152.5	2.1	6.7	19.9	3.4	13.2	71.1	84.3	17.7	5	9	16	45	20	9	20	76	871
113	6778753	365323	13.3	33.8	90.1	269.5	115.4	3.3	12.8	73.1	37.1	18	69.8	117.1	37.7	16	16	22	105	56	20	12	42	3332
114	6778783	365265	9.8	23.4	68.5	225.5	101.4	0	6.3	40.1	23.8	15.7	342.1	135.5	14.5	17	11	18	85	31	13	11	140	2907
115	6778826	365198	5.2	12.1	38.9	210.9	66.8	1.5	5.6	0.1	0	1.9	1.4	23	0	14	10	5	23	0	8	3	262	363
117	6778873	365141	12	25.5	77.7	228.9	109.9	1.5	12.1	55.9	34.3	13.6	71.8	104.5	32.1	18	15	17	80	38	18	12	123	2930
119	6778903	365055	8	18	66.9	177.6	97.4	2.4	6.6	27.9	19	9	34.1	66.1	3.3	14	12	13	46	22	14	13	195	1409
120	6778956	364970	9.9	21.6	69.6	212.7	101.6	2.4	10.8	40.6	22.6	12.6	169.7	101	43.7	23	12	15	46	16	15	12	157	1840
121	6779031	365051	6.6	14.9	55	173.1	83.2	0	3.5	18.5	5.2	6	26.1	39.5	5.6	16	9	10	54	22	12	11	207	1594
123	6779002	365158	13.5	31.8	79	259.1	99.7	2.4	11.9	63.2	36.9	15.4	53.9	105.2	9.5	13	16	18	90	45	18	1	99	3309
124	6778991	365242	14.1	36.3	95.6	227.9	102	4.2	15.8	79.1	37.4	16.8	78.4	101.3	18.3	21	14	21	75	26	22	14	36	1405
125	6778967	365326	13.1	33	88.4	259.9	122.8	0	9.1	68.6	39.1	20.9	116.8	114.5	31.1	20	14	21	85	34	19	17	60	3554
126	6778916	365435	8.4	23	75.9	240	126.1	4	8.7	50.1	29.6	15.9	189.5	134	31.3	24	14	18	79	34	15	0	100	4665
127	6778895	365486	12.7	34.5	96.5	232.6	114.3	3.1	16.9	78.6	47.1	23.2	80.9	120.8	14.8	12	14	24	86	39	21	10	29	2221
130	6778854	365559	2.1	8.9	32.8	84.6	114.5	1.6	3	6.9	1.7	6.3	23.3	37.8	0	14	11	9	12	2	9	7	219	191

131	6779086	365670	5.5	16.2	29.4	182.5	151	0.5	2.4	24.1	4.8	16.2	72.9	98.3	0	5	9	15	39	16	7	20	74	526
132	6779103	365637	8.8	23.1	59.1	247.9	124.3	2.3	8.7	44.7	22.1	17.2	76.5	140.5	38.4	19	14	20	64	21	15	7	65	4131
133	6779126	365617	6.6	14.9	55.4	154	111.3	2	10.3	34.1	13.7	13.8	57.1	89.4	2.1	10	12	15	56	21	12	10	133	1609
135	6779165	365571	1.8	7.5	35.7	92.8	97.1	0.7	4.7	1.4	0	5.8	19.4	27.7	0	14	10	6	7	0	6	28	218	917
138	6779201	365496	3.7	9.3	40.1	124.4	92.6	0	5.1	5.5	4.7	5.2	20	31.1	0	13	11	3	9	0	9	21	230	2027
139	6779444	365542	4.4	10.4	40.8	127.3	79	0	2.4	3.8	0	4.8	9	32.2	0	0	8	6	28	13	9	21	215	443
141	6779417	365590	3.3	11.1	39.5	133.6	73.5	0	2.9	1.3	0.7	2.6	10	31.4	0	1	9	7	20	10	9	16	267	527
145	6779356	365675	5.6	12.8	37.6	223.4	106.2	2.8	8.1	10.3	4.8	8.6	42.1	62.7	0	10	9	7	22	11	6	14	169	1471
147	6779319	365760	5.8	13.6	44.5	159.8	126.8	1.8	5.6	17.6	5.9	11.3	51.5	71.5	0	10	11	11	27	13	11	5	138	2389
150	6779294	365824	9	18.6	30.2	388.8	160.6	3.1	5.3	25.5	6.5	16.5	112	113.1	0	13	8	16	25	5	7	7	38	170
161	6779787	365721	5.1	12.7	40.3	216	109.9	2.1	4.9	9.1	0	6.8	39.3	54.6	0	17	8	9	14	11	7	24	185	335
163	6779740	365786	4.8	12.5	34.8	167.7	88.8	1.2	4	8.4	1.9	5.8	32.9	48.7	2.7	10	10	8	26	3	5	1	183	840
165	6779693	365866	5.1	13.3	33.9	173.8	106.4	2.4	6.9	16.7	2.6	10.4	70.6	84.6	0	10	10	13	0	0	7	23	104	615
168	6779628	365964	4.1	12.9	40	183.2	137.5	0	5.1	15	4.7	10.6	49	59.4	0	6	9	12	22	11	8	26	126	1583
170	6779607	366023	5.3	14.5	30.5	227	150.5	1.5	5.6	23.4	3.7	12.7	72.6	94	0	5	7	14	41	23	9	14	105	439
181	6780252	366164	13.8	24.1	41.7	659.2	118.4	3.4	14	29.6	6.8	14.3	111.6	117.7	0.6	4	9	12	47	18	8	4	21	1598
184	6780231	366202	8.1	19.2	45.5	530.6	131	3.6	11	23.5	11.5	13	81.5	98.5	0	13	9	17	44	21	10	0	75	5560
186	6780202	366265	6.1	14.1	32.9	316.3	119.6	2.1	6.7	19.7	3.2	12.1	108.7	99.4	0	14	8	11	25	8	8	18	78	3690
189	6780179	366311	6.9	15.1	32.8	284.1	145.6	1.7	8.1	15.6	5.9	11	86.9	106.8	0	6	11	13	28	11	8	0	75	124
190	6780161	366340	7.7	18	32	293.8	169.5	3.1	9	22.9	5.4	16.5	96	117.3	0.9	8	8	15	34	14	9	12	27	92
201	6780698	366439	4.5	11.9	29.8	221.8	147.6	0	0	13.1	0	11.8	49	57.7	0	12	10	11	27	7	9	21	143	133
203	6780671	366468	2	8.7	35.1	109.9	114.8	0	1.7	9.5	4	8.3	25.4	50.7	0	4	10	10	19	2	8	18	201	2422
205	6780634	366517	7.1	16.2	43.4	265.4	169.4	0.7	7.6	17.6	7.6	13.7	38.2	71.2	0	15	11	9	31	9	9	16	122	3154
207	6780595	366568	7.5	17.1	31.2	459.5	158.3	1.2	8.5	22.5	4.6	17.3	103.8	111.9	0	2	8	12	31	13	5	5	35	624
210	6780580	366597	8.2	18.2	34	414.4	154.7	5.8	11.4	16.7	2.5	11.4	78.5	98.7	0	10	10	14	42	18	10	4	72	231
211	6780920	366910	5.1	12.2	36.6	188.8	123.9	0.7	4.2	15.3	2.8	11.9	36.9	55.2	0	16	9	12	25	5	9	10	152	785
213	6780945	366880	4.6	10.9	35.7	223.1	138.6	1.7	5.5	13.2	0.9	10.9	50.4	63	0	5	8	7	27	12	11	21	147	907
215	6780974	366851	8.8	18.6	39.3	430.8	164.6	0	7.2	18.2	3.8	20	61.3	81.4	0	11	9	15	35	18	8	1	66	1594
217	6781020	366805	2.9	11.1	43.3	117.4	138.1	1.2	4.7	12	6.7	10.9	25	45.7	0	11	10	10	25	5	9	9	173	3395
220	6781045	366766	8.8	16.7	30.8	530.7	115.4	2.5	10.2	17.6	0	12.3	81.7	85.3	0	4	8	10	32	23	11	14	95	207

TRACE ELEMENTS NORMALISED TO Al

sample no	y_proj	x_proj	Nb	Y	Rb	Zr	Sr	U	Th	Zn	Cu	Ni	Cr	V	La	Pb	Ga	Co	Ce	Nd	AS	Cd	Sn	S
31	6781159	367145	0.0011	0.0017	0.0010	0.0552	0.0052	0.0002	0.0011	0.0018	0.0000	0.0006	0.0151	0.0116	0.0011	0.0005	0.0003	0.0010	0.0050	0.0020	0.0004	0.0007	0.0000	0.0042
34	6781226	367105	0.0002	0.0005	0.0014	0.0050	0.0054	0.0000	0.0001	0.0005	0.0000	0.0003	0.0017	0.0024	0.0000	0.0004	0.0004	0.0004	0.0011	0.0003	0.0004	0.0000	0.0064	0.0437
35	6781247	367080	0.0002	0.0004	0.0014	0.0048	0.0047	0.0000	0.0001	0.0006	0.0001	0.0003	0.0017	0.0020	0.0000	0.0001	0.0004	0.0006	0.0008	0.0003	0.0004	0.0009	0.0052	0.0410
36	6781279	367051	0.0001	0.0004	0.0014	0.0042	0.0046	0.0000	0.0001	0.0004	0.0000	0.0003	0.0015	0.0018	0.0000	0.0004	0.0004	0.0004	0.0007	0.0002	0.0003	0.0004	0.0063	0.0401
40	6781318	367004	0.0005	0.0011	0.0011	0.0488	0.0062	0.0001	0.0007	0.0009	0.0002	0.0005	0.0045	0.0057	0.0014	0.0005	0.0004	0.0006	0.0020	0.0009	0.0002	0.0006	0.0000	0.0054
51	6781608	367480	0.0002	0.0005	0.0015	0.0071	0.0063	0.0001	0.0003	0.0005	0.0000	0.0004	0.0022	0.0026	0.0000	0.0003	0.0004	0.0005	0.0012	0.0005	0.0003	0.0002	0.0047	0.0044
52	6781610	367464	0.0001	0.0004	0.0014	0.0056	0.0059	0.0001	0.0001	0.0004	0.0000	0.0003	0.0017	0.0025	0.0000	0.0004	0.0005	0.0006	0.0011	0.0003	0.0004	0.0007	0.0069	0.0304
53	6781622	367412	0.0002	0.0003	0.0011	0.0039	0.0039	0.0000	0.0001	0.0004	0.0001	0.0002	0.0012	0.0013	0.0000	0.0000	0.0003	0.0003	0.0008	0.0005	0.0003	0.0006	0.0048	0.0342
54	6781645	367372	0.0002	0.0003	0.0013	0.0047	0.0034	0.0000	0.0002	0.0007	0.0003	0.0003	0.0013	0.0017	0.0000	0.0002	0.0003	0.0004	0.0010	0.0003	0.0002	0.0002	0.0021	0.0561
56	6781670	367341	0.0003	0.0008	0.0011	0.0101	0.0069	0.0000	0.0002	0.0010	0.0001	0.0005	0.0046	0.0049	0.0000	0.0006	0.0003	0.0007	0.0006	0.0002	0.0004	0.0004	0.0005	0.0069
68	6781918	367603	0.0001	0.0003	0.0016	0.0034	0.0061	0.0001	0.0002	0.0002	0.0000	0.0002	0.0007	0.0017	0.0000	0.0001	0.0004	0.0004	0.0005	0.0003	0.0004	0.0005	0.0069	0.0123
69	6781906	367613	0.0006	0.0014	0.0014	0.0583	0.0061	0.0001	0.0012	0.0009	0.0000	0.0004	0.0059	0.0057	0.0018	0.0003	0.0003	0.0007	0.0040	0.0015	0.0004	0.0001	0.0000	0.0286
70	6781881	367640	0.0002	0.0004	0.0015	0.0054	0.0038	0.0001	0.0002	0.0007	0.0002	0.0003	0.0009	0.0017	0.0002	0.0003	0.0002	0.0003	0.0009	0.0003	0.0003	0.0003	0.0019	0.0693
72	6781838	367652	0.0002	0.0005	0.0013	0.0049	0.0060	0.0000	0.0001	0.0004	0.0000	0.0004	0.0015	0.0023	0.0000	0.0002	0.0004	0.0006	0.0010	0.0001	0.0003	0.0002	0.0049	0.0436
89	6782183	368016	0.0001	0.0003	0.0016	0.0031	0.0059	0.0001	0.0001	0.0001	0.0001	0.0002	0.0005	0.0008	0.0000	0.0006	0.0005	0.0003	0.0003	0.0000	0.0002	0.0006	0.0095	0.0335
90	6782170	368026	0.0001	0.0003	0.0016	0.0024	0.0059	0.0000	0.0001	0.0002	0.0001	0.0003	0.0006	0.0012	0.0000	0.0004	0.0004	0.0004	0.0004	0.0001	0.0004	0.0006	0.0064	0.0333
91	6782189	368003	0.0001	0.0003	0.0015	0.0025	0.0057	0.0000	0.0000	0.0003	0.0001	0.0003	0.0011	0.0011	0.0000	0.0005	0.0004	0.0003	0.0006	0.0001	0.0004	0.0000	0.0069	0.0347
92	6782203	367987	0.0002	0.0004	0.0015	0.0045	0.0059	0.0000	0.0001	0.0003	0.0003	0.0003	0.0008	0.0014	0.0000	0.0003	0.0004	0.0003	0.0007	0.0000	0.0003	0.0007	0.0057	0.0298
94	6782218	367966	0.0005	0.0010	0.0011	0.0232	0.0062	0.0000	0.0005	0.0013	0.0001	0.0006	0.0071	0.0063	0.0001	0.0002	0.0003	0.0007	0.0019	0.0005	0.0003	0.0004	0.0000	0.0274
95	6778538	365221	0.0002	0.0005	0.0015	0.0065	0.0048	0.0000	0.0001	0.0003	0.0002	0.0003	0.0010	0.0012	0.0000	0.0001	0.0004	0.0005	0.0006	0.0001	0.0004	0.0004	0.0072	0.0094
96	6778555	365195	0.0002	0.0004	0.0012	0.0052	0.0019	0.0000	0.0002	0.0009	0.0005	0.0003	0.0012	0.0018	0.0005	0.0004	0.0002	0.0003	0.0013	0.0005	0.0003	0.0002	0.0012	0.0359
97	6778584	365132	0.0002	0.0005	0.0014	0.0070	0.0022	0.0001	0.0002	0.0007	0.0002	0.0002	0.0009	0.0021	0.0002	0.0004	0.0003	0.0003	0.0012	0.0007	0.0002	0.0005	0.0032	0.0557
99	6778623	365044	0.0002	0.0005	0.0015	0.0069	0.0025	0.0001	0.0002	0.0005	0.0001	0.0002	0.0006	0.0013	0.0000	0.0003	0.0003	0.0003	0.0013	0.0004	0.0003	0.0000	0.0055	0.0269
100	6778648	365010	0.0002	0.0005	0.0015	0.0076	0.0027	0.0001	0.0002	0.0003	0.0000	0.0002	0.0008	0.0012	0.0001	0.0004	0.0004	0.0003	0.0010	0.0004	0.0004	0.0008	0.0070	0.0279
103	6778717	365056	0.0002	0.0004	0.0012	0.0046	0.0017	0.0000	0.0002	0.0010	0.0005	0.0002	0.0013	0.0018	0.0009	0.0002	0.0002	0.0003	0.0013	0.0006	0.0003	0.0001	0.0015	0.0445
104	6778700	365115	0.0002	0.0004	0.0014	0.0051	0.0020	0.0000	0.0002	0.0008	0.0004	0.0002	0.0007	0.0017	0.0012	0.0001	0.0003	0.0003	0.0014	0.0005	0.0003	0.0004	0.0036	0.0423
106	6778660	365237	0.0002	0.0004	0.0012	0.0038	0.0016	0.0000	0.0002	0.0009	0.0005	0.0003	0.0025	0.0018	0.0004	0.0003	0.0002	0.0003	0.0012	0.0005	0.0003	0.0004	0.0011	0.0823
107	6778642	365300	0.0002	0.0005	0.0011	0.0106	0.0020	0.0000	0.0002	0.0010	0.0004	0.0003	0.0023	0.0025	0.0009	0.0003	0.0002	0.0004	0.0016	0.0007	0.0002	0.0001	0.0007	0.0624
110	6778622	365338	0.0005	0.0011	0.0013	0.0373	0.0056	0.0002	0.0008	0.0009	0.0001	0.0005	0.0036	0.0042	0.0002	0.0003	0.0004	0.0005	0.0027	0.0015	0.0003	0.0006	0.0001	0.0350
111	6778709	365359	0.0003	0.0006	0.0012	0.0109	0.0061	0.0001	0.0003	0.0008	0.0001	0.0005	0.0028	0.0033	0.0007	0.0002	0.0004	0.0006	0.0018	0.0008	0.0004	0.0008	0.0030	0.0346
113	6778753	365323	0.0002	0.0004	0.0011	0.0032	0.0014	0.0000	0.0002	0.0009	0.0004	0.0002	0.0008	0.0014	0.0004	0.0002	0.0002	0.0003	0.0012	0.0007	0.0002	0.0001	0.0005	0.0397
114	6778783	365265	0.0002	0.0004	0.0013	0.0043	0.0019	0.0000	0.0001	0.0008	0.0005	0.0003	0.0065	0.0026	0.0003	0.0003	0.0002	0.0003	0.0016	0.0006	0.0002	0.0002	0.0027	0.0554
115	6778826	365198	0.0002	0.0006	0.0018	0.0096	0.0030	0.0001	0.0003	0.0000	0.0000	0.0001	0.0001	0.0010	0.0000	0.0006	0.0005	0.0002	0.0010	0.0000	0.0004	0.0001	0.0119	0.0165
117	6778873	365141	0.0002	0.0004	0.0013	0.0038	0.0018	0.0000	0.0002	0.0009	0.0006	0.0002	0.0012	0.0017	0.0005	0.0003	0.0002	0.0003	0.0013	0.0006	0.0003	0.0002	0.0020	0.0484
119	6778903	365055	0.0002	0.0004	0.0015	0.0040	0.0022	0.0001	0.0002	0.0006	0.0004	0.0002	0.0008	0.0015	0.0001	0.0003	0.0003	0.0003	0.0010	0.0005	0.0003	0.0003	0.0044	0.0320
120	6778956	364970	0.0002	0.0004	0.0013	0.0041	0.0020	0.0000	0.0002	0.0008	0.0004	0.0002	0.0033	0.0020	0.0008	0.0004	0.0002	0.0003	0.0009	0.0003	0.0003	0.0002	0.0030	0.0356
121	6779031	365051	0.0002	0.0004	0.0015	0.0047	0.0023	0.0000	0.0001	0.0005	0.0001	0.0002	0.0007	0.0011	0.0002	0.0004	0.0002	0.0003	0.0015	0.0006	0.0003	0.0003	0.0057	0.0436
123	6779002	365158	0.0002	0.0005	0.0012	0.0039	0.0015	0.0000	0.0002	0.0010	0.0006	0.0002	0.0008	0.0016	0.0001	0.0002	0.0002	0.0003	0.0014	0.0007	0.0003	0.0000	0.0015	0.0498
124	6778991	365242	0.0002	0.0004	0.0010	0.0025	0.0011	0.0000	0.0002	0.0009	0.0004	0.0002	0.0009	0.0011	0.0002	0.0002	0.0002	0.0002	0.0008	0.0003	0.0002	0.0002	0.0004	0.0153
125	6778967	365326	0.0002	0.0004	0.0011	0.0031	0.0015	0.0000	0.0001	0.0008	0.0005	0.0003	0.0014	0.0014	0.0004	0.0002	0.0002	0.0003	0.0010	0.0004	0.0002	0.0002	0.0007	0.0430
126	6778916	365435	0.0001	0.0004	0.0013	0.0040	0.0021	0.0001	0.0001	0.0008	0.0005	0.0003	0.0032	0.0022	0.0005	0.0004	0.0002	0.0003	0.0013	0.0006	0.0003	0.0000	0.0017	0.0779
127	6778895	365486	0.0001	0.0004	0.0010	0.0025	0.0012	0.0000	0.0002	0.0009	0.0005	0.0003	0.0009	0.0013	0.0002	0.0001	0.0002	0.0003	0.0009	0.0004	0.0002	0.0001	0.0003	0.0241
130	6778854	365559	0.0001	0.0004	0.0015	0.0040	0.0054	0.0001	0.0001	0.0003	0.0001	0.0003	0.0011	0.0018	0.0000	0.0007	0.0005	0.0004	0.0006	0.0001	0.0004	0.0003	0.0103	0.0090
131	6779086	365670	0.0002	0.0006	0.0011	0.0067	0.0055	0.0000	0.0001	0.0009	0.0002	0.0006	0.0027	0.0036	0.0000	0.0002	0.0003	0.0005	0.0014	0.0006	0.0003	0.0007	0.0027	0.0192
132	6779103	365637	0.0002	0.0005	0.0012	0.0050	0.0025	0.0000	0.0002	0.0009	0.0004	0.0003	0.0016	0.0029	0.0008	0.0004	0.0003	0.0004	0.0013	0.0004	0.0003	0.0001	0.0013	0.0839
133	6779126	365617	0.0002	0.0004	0.0013	0.0037	0.0027	0.0000	0.0002	0.0008	0.0003	0.0003	0.0014	0.0021	0.0001	0.0002	0.0003	0.0004	0.0013	0.0005	0.0003	0.0002	0.0032	0.0384

135	6779165	365571	0.0001	0.0003	0.0016	0.0041	0.0042	0.0000	0.0002	0.0001	0.0000	0.0003	0.0008	0.0012	0.0000	0.0006	0.0004	0.0003	0.0003	0.0000	0.0003	0.0012	0.0095	0.0401
138	6779201	365496	0.0002	0.0004	0.0017	0.0053	0.0039	0.0000	0.0002	0.0002	0.0002	0.0002	0.0009	0.0013	0.0000	0.0006	0.0005	0.0001	0.0004	0.0000	0.0004	0.0009	0.0098	0.0864
139	6779444	365542	0.0002	0.0004	0.0016	0.0051	0.0032	0.0000	0.0001	0.0002	0.0000	0.0002	0.0004	0.0013	0.0000	0.0000	0.0003	0.0002	0.0011	0.0005	0.0004	0.0008	0.0086	0.0177
141	6779417	365590	0.0001	0.0005	0.0017	0.0058	0.0032	0.0000	0.0001	0.0001	0.0000	0.0001	0.0004	0.0014	0.0000	0.0000	0.0004	0.0003	0.0009	0.0004	0.0004	0.0007	0.0117	0.0230
145	6779356	365675	0.0002	0.0005	0.0015	0.0088	0.0042	0.0001	0.0003	0.0004	0.0002	0.0003	0.0017	0.0025	0.0000	0.0004	0.0004	0.0003	0.0009	0.0004	0.0002	0.0006	0.0067	0.0583
147	6779319	365760	0.0002	0.0004	0.0014	0.0050	0.0040	0.0001	0.0002	0.0006	0.0002	0.0004	0.0016	0.0022	0.0000	0.0003	0.0003	0.0003	0.0008	0.0004	0.0003	0.0002	0.0043	0.0748
150	6779294	365824	0.0003	0.0007	0.0012	0.0148	0.0061	0.0001	0.0002	0.0010	0.0002	0.0006	0.0043	0.0043	0.0000	0.0005	0.0003	0.0006	0.0010	0.0002	0.0003	0.0003	0.0014	0.0065
161	6779787	365721	0.0002	0.0005	0.0016	0.0085	0.0043	0.0001	0.0002	0.0004	0.0000	0.0003	0.0015	0.0022	0.0000	0.0007	0.0003	0.0004	0.0006	0.0004	0.0003	0.0009	0.0073	0.0132
163	6779740	365786	0.0002	0.0006	0.0015	0.0074	0.0039	0.0001	0.0002	0.0004	0.0001	0.0003	0.0015	0.0022	0.0001	0.0004	0.0004	0.0004	0.0012	0.0001	0.0002	0.0000	0.0081	0.0372
165	6779693	365866	0.0002	0.0005	0.0014	0.0071	0.0043	0.0001	0.0003	0.0007	0.0001	0.0004	0.0029	0.0035	0.0000	0.0004	0.0004	0.0005	0.0000	0.0000	0.0003	0.0009	0.0042	0.0251
168	6779628	365964	0.0001	0.0004	0.0014	0.0064	0.0048	0.0000	0.0002	0.0005	0.0002	0.0004	0.0017	0.0021	0.0000	0.0002	0.0003	0.0004	0.0008	0.0004	0.0003	0.0009	0.0044	0.0552
170	6779607	366023	0.0002	0.0006	0.0012	0.0089	0.0059	0.0001	0.0002	0.0009	0.0001	0.0005	0.0028	0.0037	0.0000	0.0002	0.0003	0.0005	0.0016	0.0009	0.0004	0.0005	0.0041	0.0171
181	6780252	366164	0.0005	0.0008	0.0014	0.0219	0.0039	0.0001	0.0005	0.0010	0.0002	0.0005	0.0037	0.0039	0.0000	0.0001	0.0003	0.0004	0.0016	0.0006	0.0003	0.0001	0.0007	0.0531
184	6780231	366202	0.0003	0.0006	0.0014	0.0166	0.0041	0.0001	0.0003	0.0007	0.0004	0.0004	0.0026	0.0031	0.0000	0.0004	0.0003	0.0005	0.0014	0.0007	0.0003	0.0000	0.0023	0.1742
186	6780202	366265	0.0003	0.0006	0.0014	0.0130	0.0049	0.0001	0.0003	0.0008	0.0001	0.0005	0.0045	0.0041	0.0000	0.0006	0.0003	0.0005	0.0010	0.0003	0.0003	0.0007	0.0032	0.1519
189	6780179	366311	0.0003	0.0006	0.0013	0.0116	0.0059	0.0001	0.0003	0.0006	0.0002	0.0004	0.0035	0.0043	0.0000	0.0002	0.0004	0.0005	0.0011	0.0004	0.0003	0.0000	0.0031	0.0050
190	6780161	366340	0.0003	0.0006	0.0011	0.0101	0.0058	0.0001	0.0003	0.0008	0.0002	0.0006	0.0033	0.0040	0.0000	0.0003	0.0003	0.0005	0.0012	0.0005	0.0003	0.0004	0.0009	0.0032
201	6780698	366439	0.0002	0.0005	0.0013	0.0100	0.0067	0.0000	0.0000	0.0006	0.0000	0.0005	0.0022	0.0026	0.0000	0.0005	0.0005	0.0005	0.0012	0.0003	0.0004	0.0009	0.0064	0.0060
203	6780671	366468	0.0001	0.0004	0.0014	0.0045	0.0047	0.0000	0.0001	0.0004	0.0002	0.0003	0.0010	0.0021	0.0000	0.0002	0.0004	0.0004	0.0008	0.0001	0.0003	0.0007	0.0082	0.0986
205	6780634	366517	0.0002	0.0005	0.0014	0.0085	0.0054	0.0000	0.0002	0.0006	0.0002	0.0004	0.0012	0.0023	0.0000	0.0005	0.0004	0.0003	0.0010	0.0003	0.0003	0.0005	0.0039	0.1006
207	6780595	366568	0.0003	0.0007	0.0012	0.0178	0.0061	0.0000	0.0003	0.0009	0.0002	0.0007	0.0040	0.0043	0.0000	0.0001	0.0003	0.0005	0.0012	0.0005	0.0002	0.0002	0.0014	0.0242
210	6780580	366597	0.0003	0.0007	0.0013	0.0162	0.0060	0.0002	0.0004	0.0007	0.0001	0.0004	0.0031	0.0039	0.0000	0.0004	0.0004	0.0005	0.0016	0.0007	0.0004	0.0002	0.0028	0.0090
211	6780920	366910	0.0002	0.0005	0.0015	0.0076	0.0050	0.0000	0.0002	0.0006	0.0001	0.0005	0.0015	0.0022	0.0000	0.0006	0.0004	0.0005	0.0010	0.0002	0.0004	0.0004	0.0061	0.0317
213	6780945	366880	0.0002	0.0004	0.0015	0.0091	0.0056	0.0001	0.0002	0.0005	0.0000	0.0004	0.0021	0.0026	0.0000	0.0002	0.0003	0.0003	0.0011	0.0005	0.0004	0.0009	0.0060	0.0369
215	6780974	366851	0.0003	0.0007	0.0014	0.0151	0.0058	0.0000	0.0003	0.0006	0.0001	0.0007	0.0021	0.0029	0.0000	0.0004	0.0003	0.0005	0.0012	0.0006	0.0003	0.0000	0.0023	0.0559
217	6781020	366805	0.0001	0.0004	0.0015	0.0040	0.0046	0.0000	0.0002	0.0004	0.0002	0.0004	0.0008	0.0015	0.0000	0.0004	0.0003	0.0003	0.0008	0.0002	0.0003	0.0003	0.0058	0.1143
220	6781045	366766	0.0004	0.0007	0.0013	0.0228	0.0050	0.0001	0.0004	0.0008	0.0000	0.0005	0.0035	0.0037	0.0000	0.0002	0.0003	0.0004	0.0014	0.0010	0.0005	0.0006	0.0041	0.0089

Leuci (1998) uMgeni Estuary per-anthropogenic values

	Al2O3	Al (ppm)	Zn	Cu	Ni	Cr	V	As	Sn	Pb	Co
Bulk values	13.87	73404.71	109.00	34.50	41.50	116.00	186.00	18.00	10.50	33.40	41.00
Normalised to Al	138653.33		0.0015	0.0005	0.0006	0.0016	0.0025	0.0002	0.0001	0.0005	0.0006

Amatikulu Estuary Enrichment values based on uMgeni Estuary mean pre-anthropogenic values

sample no	y_proj	x_proj	Zn	Cu	Ni	Cr	V	As	Sn	Pb	Co
31	6781159.22	367145.448	1.2	0.0	1.0	9.6	4.6	1.6	0.0	1.0	1.8
34	6781226.09	367105.345	0.3	0.1	0.6	1.0	1.0	1.7	44.8	0.9	0.7
35	6781246.56	367080.46	0.4	0.2	0.5	1.1	0.8	1.7	36.2	0.3	1.0
36	6781279.04	367051.321	0.3	0.0	0.5	0.9	0.7	1.1	44.1	0.9	0.8
40	6781317.53	367004.172	0.6	0.4	0.9	2.8	2.2	0.9	0.0	1.1	1.1
51	6781607.79	367479.863	0.3	0.0	0.7	1.4	1.0	1.4	32.6	0.6	0.8
52	6781610.28	367463.515	0.3	0.0	0.6	1.1	1.0	1.5	48.2	0.9	1.0
53	6781622.48	367412.093	0.3	0.1	0.4	0.7	0.5	1.1	33.3	0.0	0.5
54	6781644.6	367371.643	0.5	0.6	0.5	0.8	0.7	0.9	14.5	0.5	0.7
56	6781670.47	367341.153	0.7	0.2	0.9	2.9	1.9	1.7	3.2	1.3	1.2
68	6781917.6	367603.288	0.2	0.0	0.4	0.4	0.7	1.7	47.9	0.2	0.7
69	6781905.87	367613.224	0.6	0.0	0.7	3.8	2.2	1.5	0.0	0.6	1.2
70	6781881.11	367640.33	0.5	0.5	0.5	0.6	0.7	1.3	13.0	0.8	0.5
72	6781837.99	367651.737	0.3	0.0	0.6	1.0	0.9	1.3	34.4	0.5	1.0
89	6782182.79	368015.57	0.1	0.1	0.4	0.3	0.3	0.9	66.5	1.4	0.6
90	6782169.69	368025.562	0.2	0.1	0.5	0.4	0.5	1.8	44.9	1.0	0.7
91	6782188.87	368003.074	0.2	0.2	0.5	0.7	0.4	1.4	48.1	1.1	0.6
92	6782202.51	367987.282	0.2	0.5	0.5	0.5	0.6	1.2	39.7	0.7	0.6
94	6782218.22	367965.992	0.9	0.3	1.1	4.5	2.5	1.4	0.0	0.5	1.2
95	6778537.7	365221.253	0.2	0.4	0.5	0.6	0.5	1.8	50.4	0.3	0.9
96	6778555.34	365195.374	0.6	1.0	0.5	0.8	0.7	1.2	8.4	0.9	0.6
97	6778583.77	365131.657	0.5	0.5	0.3	0.6	0.8	1.0	22.5	0.8	0.6
99	6778623.13	365044.203	0.3	0.2	0.4	0.4	0.5	1.2	38.2	0.8	0.5
100	6778648.45	365010.41	0.2	0.0	0.3	0.5	0.5	1.5	48.6	0.9	0.5
103	6778717.41	365055.997	0.7	1.2	0.4	0.8	0.7	1.0	10.3	0.4	0.5
104	6778699.97	365115.361	0.5	0.9	0.4	0.5	0.7	1.2	25.1	0.3	0.5
106	6778660.2	365237.162	0.6	1.1	0.5	1.6	0.7	1.0	7.8	0.7	0.6
107	6778642.11	365299.633	0.7	0.9	0.5	1.5	1.0	0.9	4.8	0.7	0.7
110	6778621.77	365338.497	0.6	0.2	0.8	2.3	1.7	1.3	0.8	0.6	1.0
111	6778709.08	365359.023	0.5	0.3	0.9	1.8	1.3	1.5	21.1	0.4	1.1
113	6778752.64	365323.441	0.6	0.9	0.4	0.5	0.6	1.0	3.5	0.4	0.5
114	6778783.49	365264.794	0.5	1.0	0.5	4.1	1.0	1.0	18.6	0.7	0.6
115	6778826.26	365197.806	0.0	0.0	0.2	0.0	0.4	1.5	83.4	1.4	0.4
117	6778873.32	365141.023	0.6	1.2	0.4	0.8	0.7	1.2	14.2	0.7	0.5
119	6778903.5	365054.801	0.4	0.9	0.4	0.5	0.6	1.3	31.0	0.7	0.5
120	6778955.85	364970.405	0.5	0.9	0.4	2.1	0.8	1.2	21.2	1.0	0.5
121	6779031.1	365051.103	0.3	0.3	0.3	0.5	0.4	1.3	39.6	1.0	0.5
123	6779002.04	365158.221	0.6	1.2	0.4	0.5	0.6	1.1	10.4	0.4	0.5
124	6778990.56	365241.769	0.6	0.9	0.3	0.5	0.4	1.0	2.7	0.5	0.4
125	6778967.18	365325.537	0.6	1.0	0.4	0.9	0.5	0.9	5.1	0.5	0.5
126	6778915.92	365435.345	0.6	1.1	0.5	2.0	0.9	1.0	11.7	0.9	0.5
127	6778894.57	365486.427	0.6	1.1	0.4	0.6	0.5	0.9	2.2	0.3	0.5
130	6778853.6	365559.387	0.2	0.2	0.5	0.7	0.7	1.7	71.9	1.4	0.8
131	6779085.97	365670.257	0.6	0.4	1.0	1.7	1.4	1.0	18.9	0.4	1.0
132	6779102.71	365637.356	0.6	1.0	0.6	1.0	1.1	1.2	9.2	0.8	0.7
133	6779126.36	365617.329	0.5	0.7	0.6	0.9	0.8	1.2	22.2	0.5	0.6
135	6779165.37	365571.36	0.0	0.0	0.4	0.5	0.5	1.1	66.6	1.3	0.5
138	6779200.53	365496.034	0.2	0.4	0.4	0.5	0.5	1.6	68.6	1.2	0.2
139	6779444.25	365542.487	0.1	0.0	0.3	0.2	0.5	1.5	60.2	0.0	0.4
141	6779417.14	365589.902	0.0	0.1	0.2	0.3	0.5	1.6	81.6	0.1	0.5
145	6779356.28	365674.65	0.3	0.4	0.6	1.1	1.0	1.0	46.8	0.9	0.5
147	6779319.44	365760.136	0.4	0.4	0.6	1.0	0.9	1.4	30.2	0.7	0.6
150	6779293.75	365823.897	0.7	0.5	1.1	2.7	1.7	1.1	10.1	1.1	1.1
161	6779786.61	365721.068	0.2	0.0	0.5	1.0	0.8	1.1	51.0	1.5	0.6
163	6779739.54	365785.693	0.3	0.2	0.5	0.9	0.9	0.9	56.7	1.0	0.6
165	6779692.67	365865.948	0.5	0.2	0.8	1.8	1.4	1.2	29.7	0.9	0.9
168	6779628.13	365964.136	0.4	0.3	0.7	1.1	0.8	1.1	30.7	0.5	0.7
170	6779607	366022.697	0.6	0.3	0.9	1.8	1.4	1.4	28.6	0.4	1.0
181	6780252.3	366164.274	0.7	0.5	0.8	2.3	1.5	1.1	4.9	0.3	0.7
184	6780230.73	366201.974	0.5	0.8	0.7	1.6	1.2	1.3	16.4	0.9	1.0
186	6780202.19	366264.728	0.5	0.3	0.9	2.8	1.6	1.3	22.4	1.3	0.8
189	6780178.91	366310.605	0.4	0.5	0.8	2.2	1.7	1.3	21.3	0.5	0.9
190	6780161.17	366340.068	0.5	0.4	1.0	2.1	1.6	1.3	6.5	0.6	0.9
201	6780697.51	366439.423	0.4	0.0	0.9	1.4	1.0	1.7	45.1	1.2	0.9
203	6780671.29	366467.501	0.3	0.3	0.6	0.7	0.8	1.3	57.2	0.4	0.7
205	6780634.4	366516.85	0.4	0.5	0.8	0.8	0.9	1.2	27.2	1.1	0.5
207	6780594.58	366568.045	0.6	0.4	1.2	2.5	1.7	0.8	9.5	0.2	0.8
210	6780579.63	366596.963	0.4	0.2	0.8	1.9	1.5	1.6	19.6	0.9	1.0
211	6780919.92	366909.546	0.4	0.2	0.8	0.9	0.9	1.5	42.9	1.4	0.9
213	6780945.44	366880.245	0.4	0.1	0.8	1.3	1.0	1.8	41.8	0.4	0.5
215	6780974.14	366851.241	0.4	0.3	1.2	1.4	1.1	1.1	16.2	0.8	0.9
217	6781019.88	366804.921	0.3	0.5	0.6	0.5	0.6	1.2	40.7	0.8	0.6
220	6781044.61	366765.935	0.5	0.0	0.9	2.2	1.4	1.9	28.6	0.4	0.8

B.3. MAJOR AND MINOR ELEMENT PLOTS

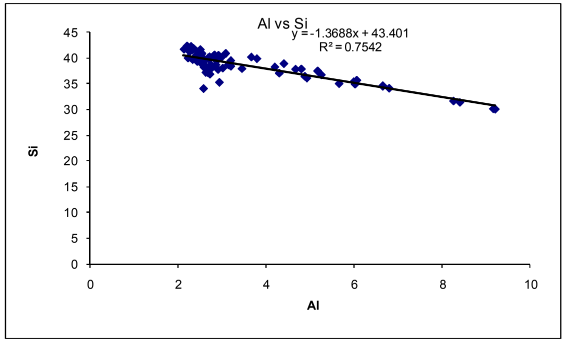

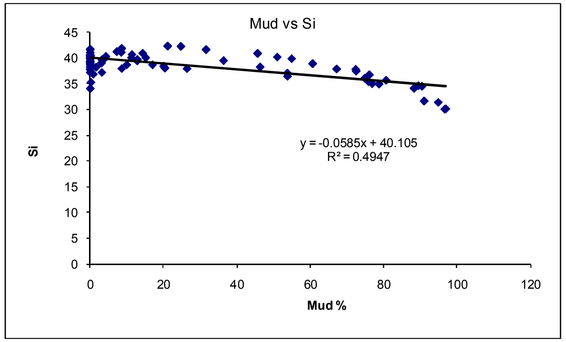

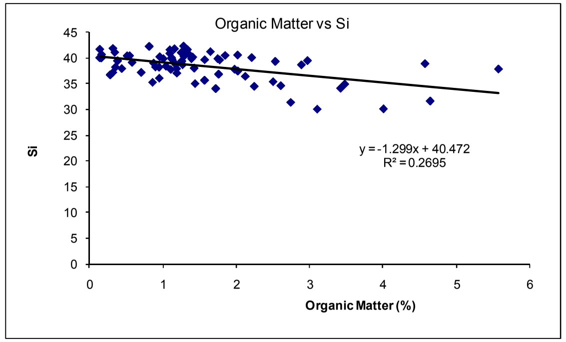

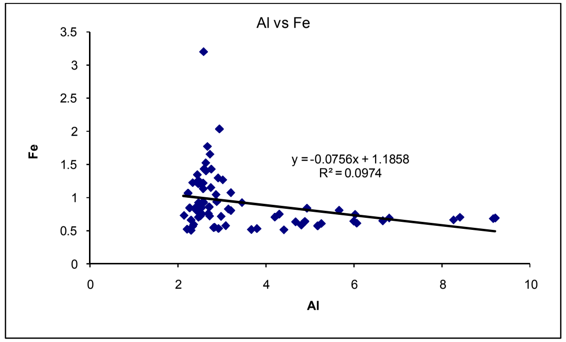

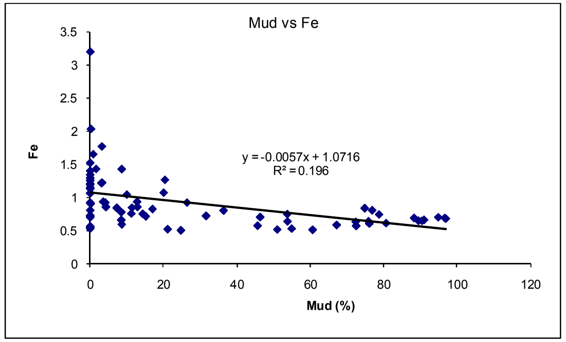

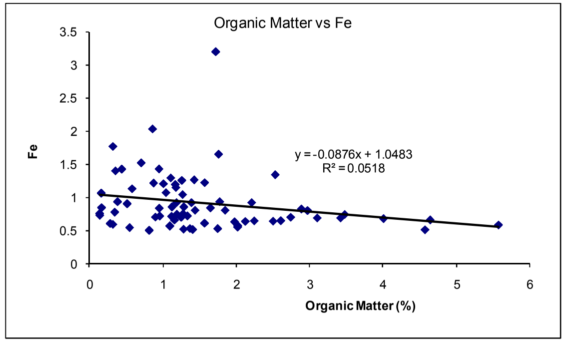

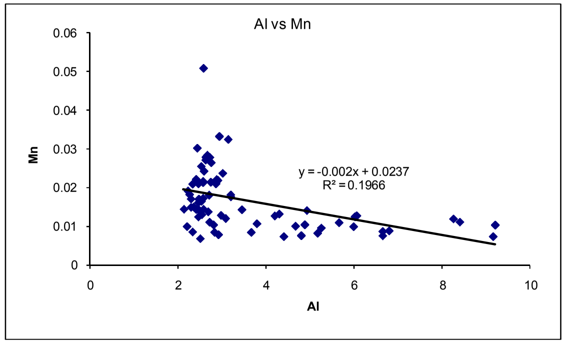

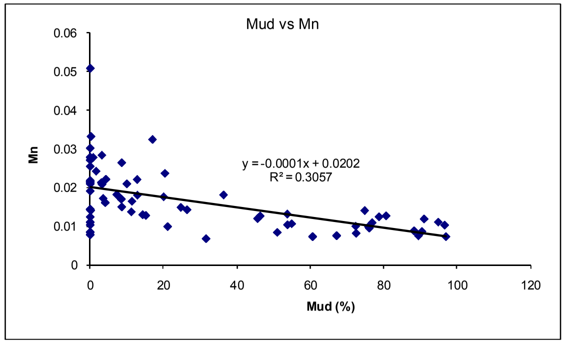

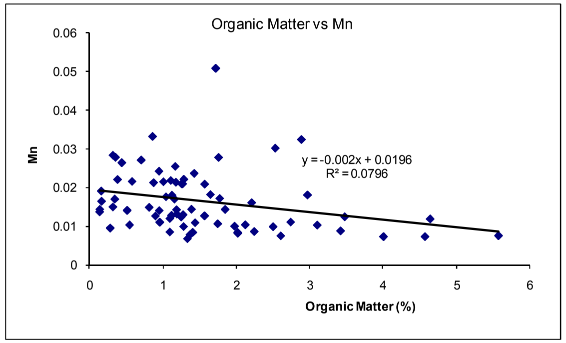

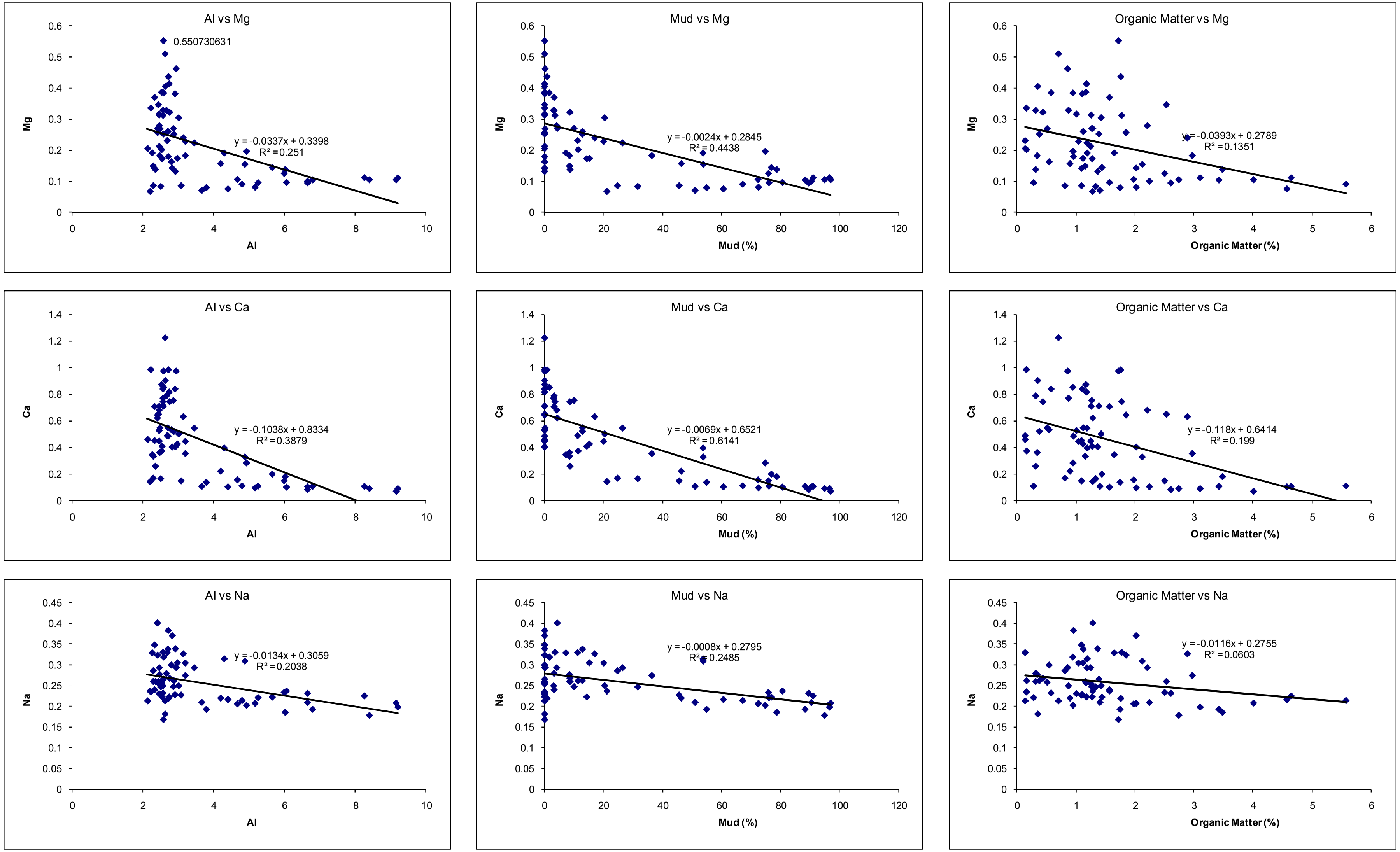
Al vs Mg
0.550730631
y = -0.0337x + 0.3398
R² = 0.251
Mg
Al
Mud vs Mg
y = -0.0024x + 0.2845
R² = 0.4438
Mg
Mud (%)
Organic Matter vs Mg
y = -0.0393x + 0.2789
R² = 0.1351
Mg
Organic Matter (%)
Al vs Ca
y = -0.1038x + 0.8334
R² = 0.3879
Ca
Al
Mud vs Ca
y = -0.0069x + 0.6521
R² = 0.6141
Ca
Mud (%)
Organic Matter vs Ca
y = -0.118x + 0.6414
R² = 0.199
Ca
Organic Matter (%)
Al vs Na
y = -0.0134x + 0.3059
R² = 0.2038
Na
Al
Mud vs Na
y = -0.0008x + 0.2795
R² = 0.2485
Na
Mud (%)
Organic Matter vs Na
y = -0.0116x + 0.2755
R² = 0.0603
Na
Organic Matter (%)

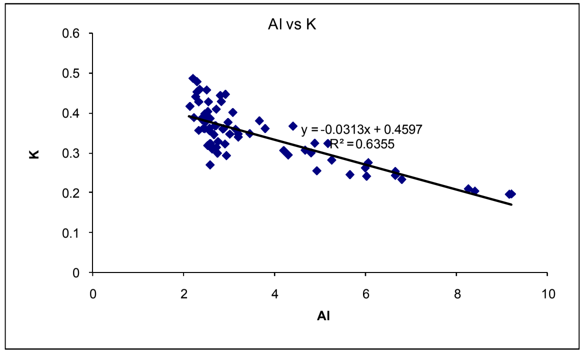
Al vs K
y = -0.0313x + 0.4597
R² = 0.6355
K
Al

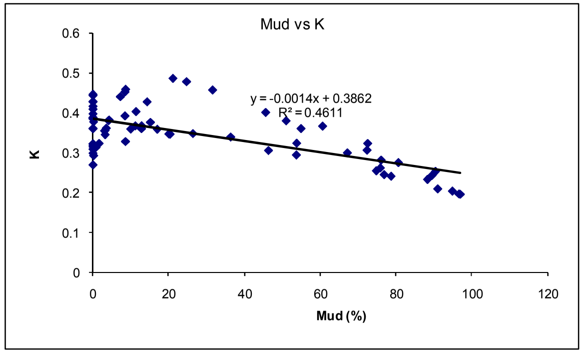
Mud vs K
y = -0.0014x + 0.3862
R² = 0.4611
K
Mud (%)

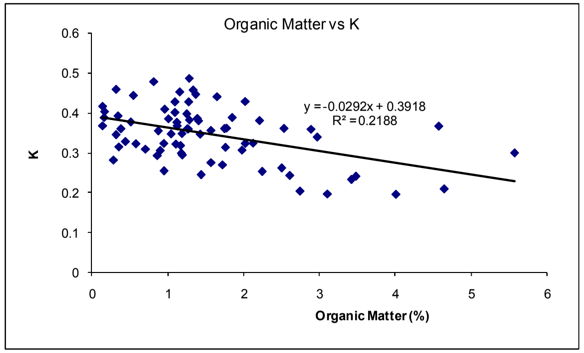
Organic Matter vs K
y = -0.0292x + 0.3918
R² = 0.2188
K
Organic Matter (%)

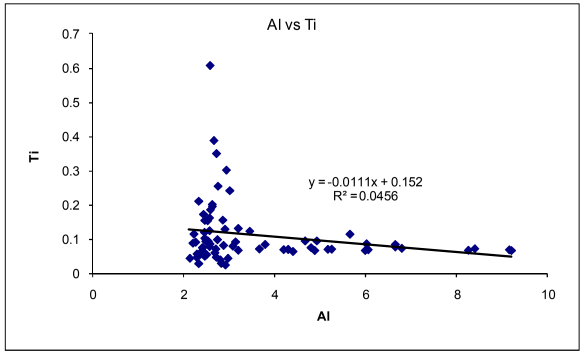
Al vs Ti
y = -0.0111x + 0.152
R² = 0.0456
Ti
Al

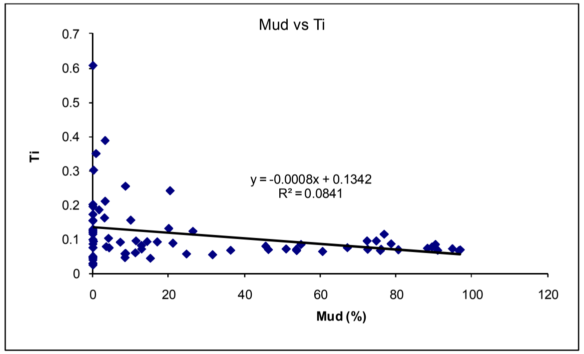
Mud vs Ti
y = -0.0008x + 0.1342
R² = 0.0841
Ti
Mud (%)

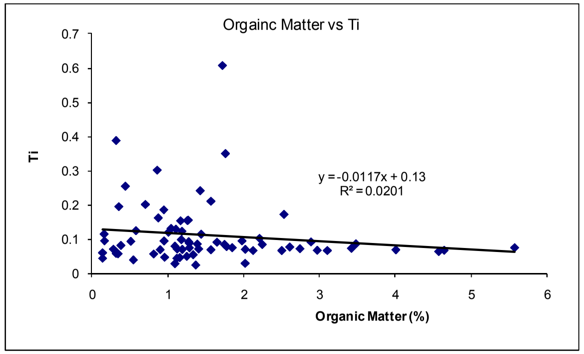
Orgainc Matter vs Ti
y = -0.0117x + 0.13
R² = 0.0201
Ti
Organic Matter (%)

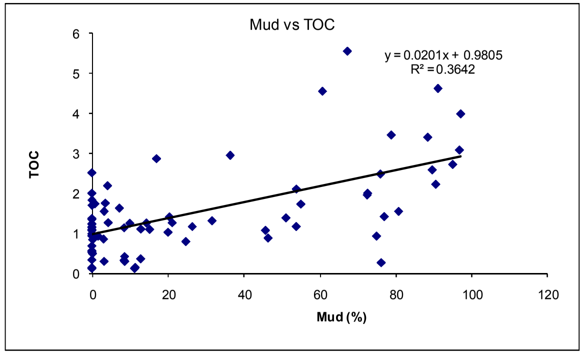
Mud vs TOC
y = 0.0201x + 0.9805
R² = 0.3642
TOC
Mud (%)

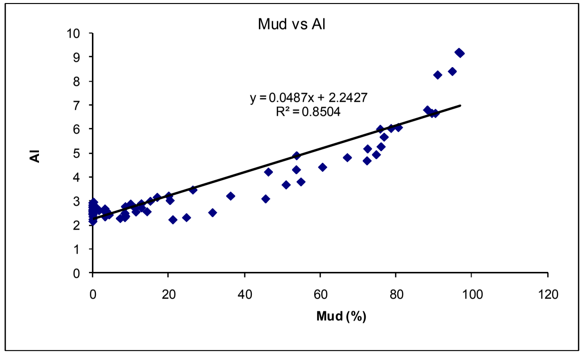
Mud vs Al
y = 0.0487x + 2.2427
R² = 0.8504
Al
Mud (%)

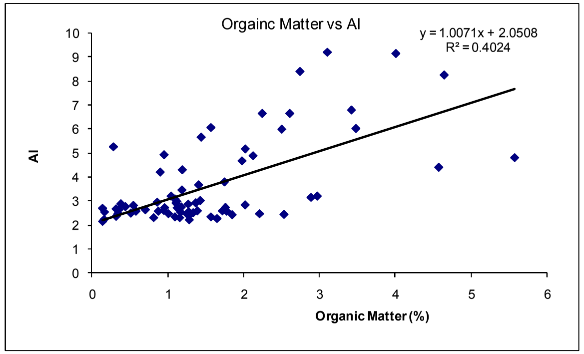
Orgainc Matter vs Al
y = 1.0071x + 2.0508
R² = 0.4024
Al
Organic Matter (%)

B.4. TRACE ELEMENT PLOTS

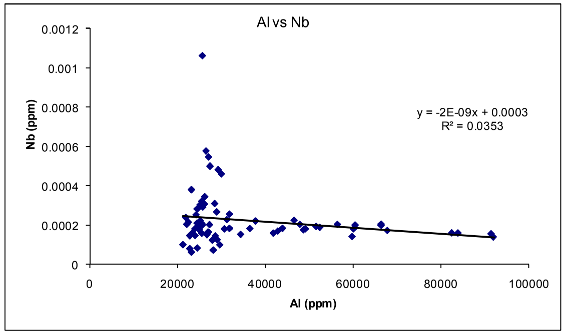

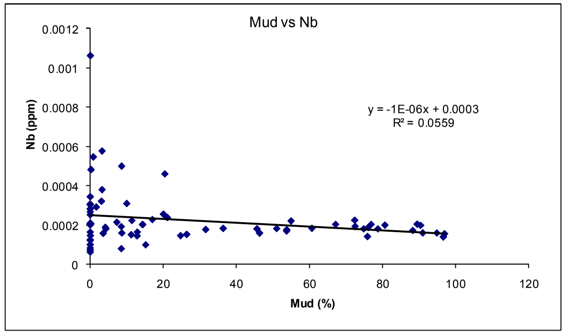

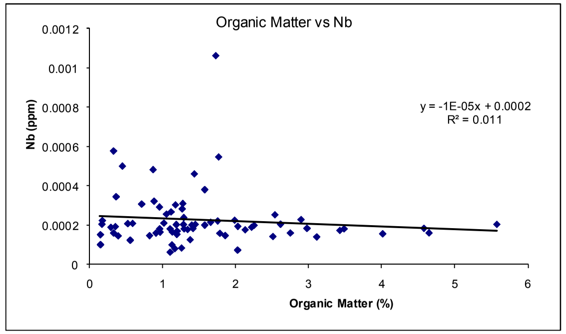

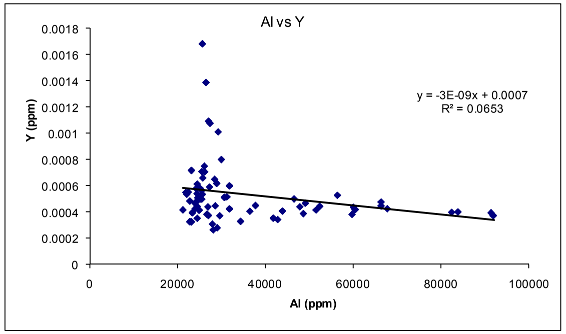

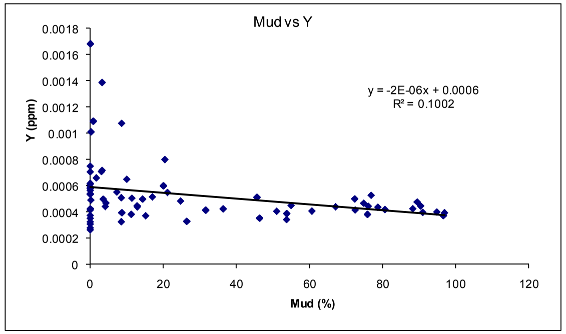

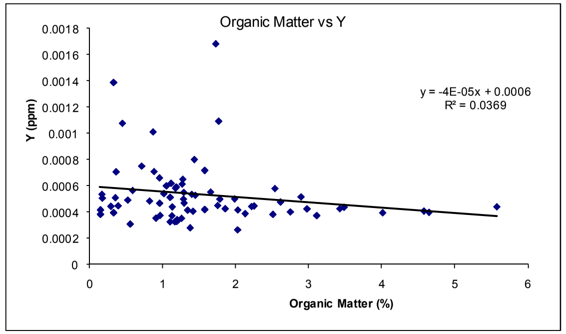

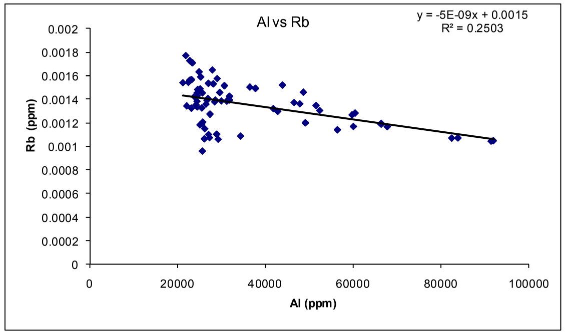

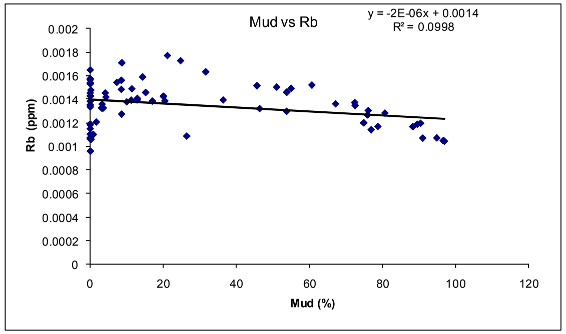

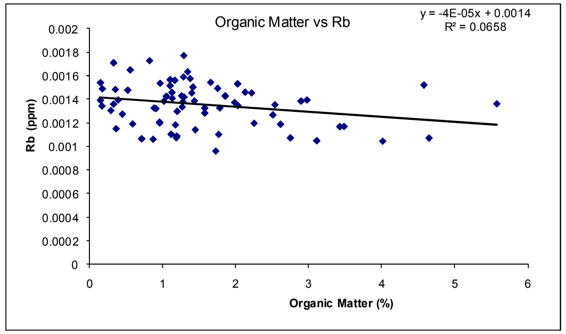

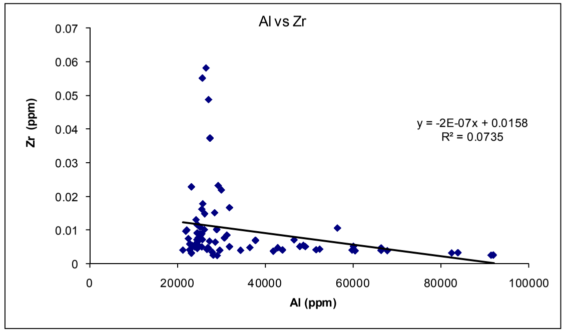
Al vs Zr
Zr (ppm)
Al (ppm)
y = -2E-07x + 0.0158
R² = 0.0735

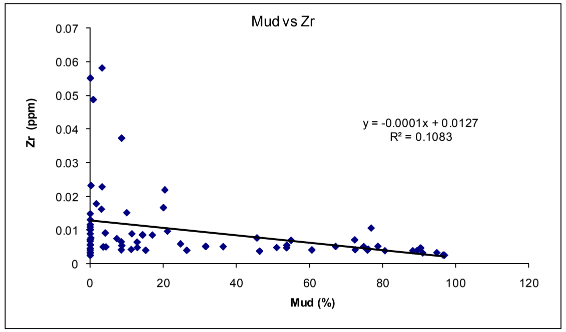
Mud vs Zr
Zr (ppm)
Mud (%)
y = -0.0001x + 0.0127
R² = 0.1083

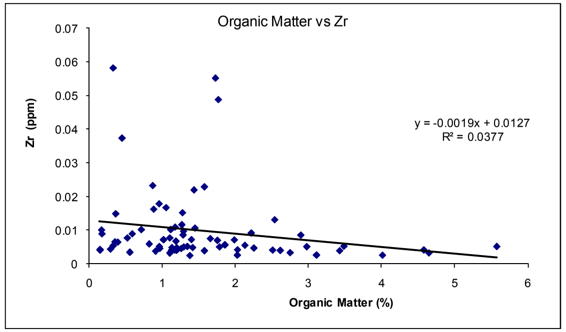
Organic Matter vs Zr
Zr (ppm)
Organic Matter (%)
y = -0.0019x + 0.0127
R² = 0.0377

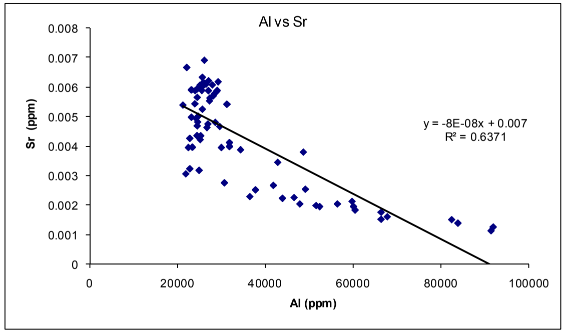
Al vs Sr
Sr (ppm)
Al (ppm)
y = -8E-08x + 0.007
R² = 0.6371

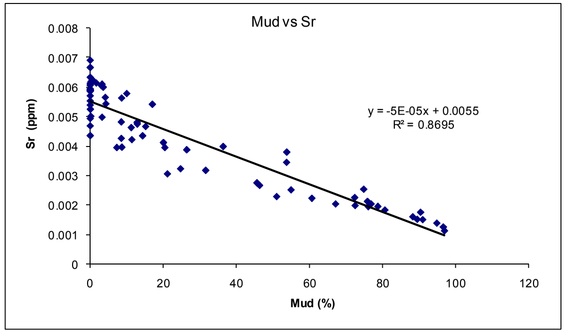
Mud vs Sr
Sr (ppm)
Mud (%)
y = -5E-05x + 0.0055
R² = 0.8695

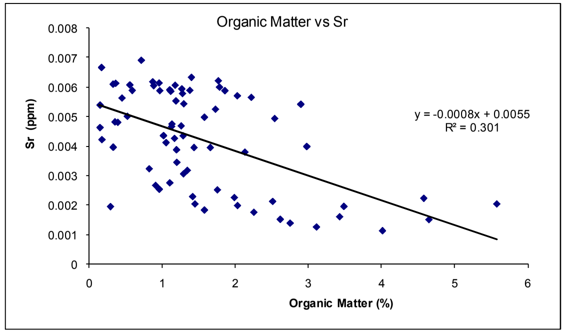
Organic Matter vs Sr
Sr (ppm)
Organic Matter (%)
y = -0.0008x + 0.0055
R² = 0.301

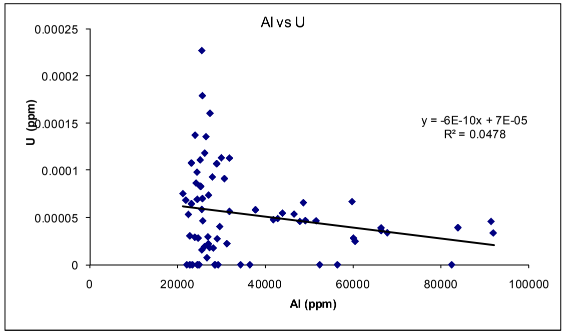
Al vs U
U (ppm)
Al (ppm)
y = -6E-10x + 7E-05
R² = 0.0478

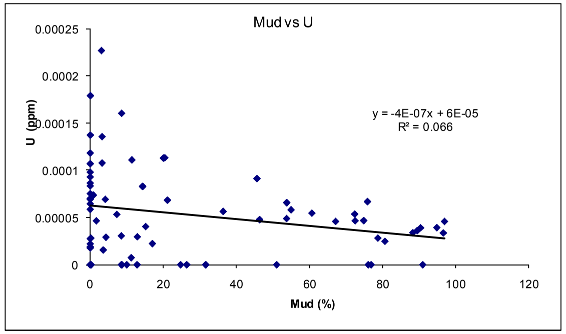
Mud vs U
U (ppm)
Mud (%)
y = -4E-07x + 6E-05
R² = 0.066

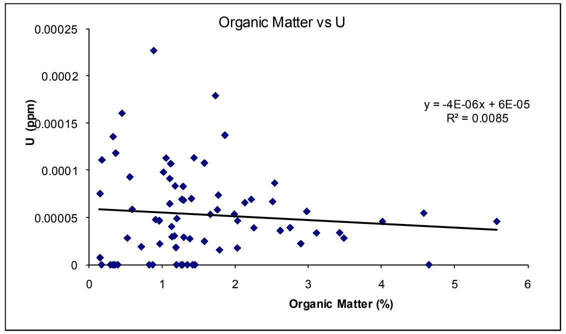
Organic Matter vs U
U (ppm)
Organic Matter (%)
y = -4E-06x + 6E-05
R² = 0.0085

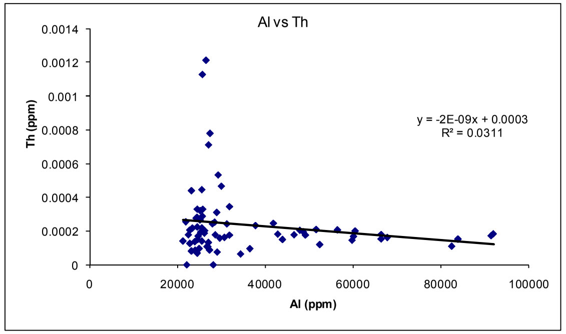
Al vs Th
y = -2E-09x + 0.0003
R² = 0.0311
Th (ppm)
Al (ppm)

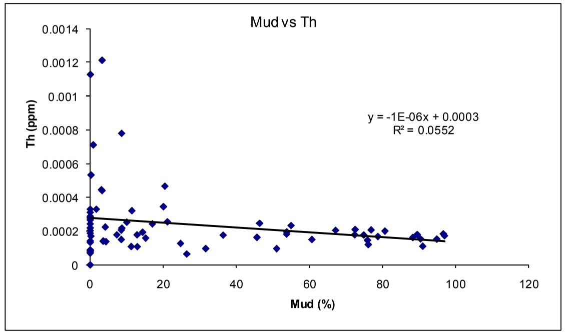
Mud vs Th
y = -1E-06x + 0.0003
R² = 0.0552
Th (ppm)
Mud (%)

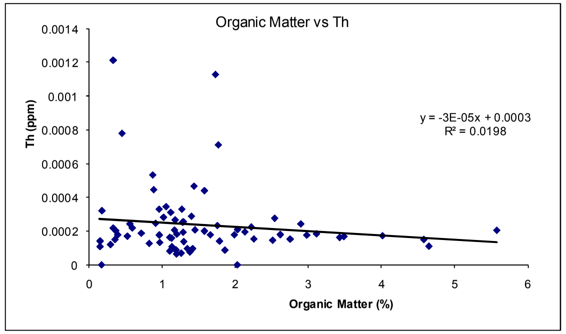
Organic Matter vs Th
y = -3E-05x + 0.0003
R² = 0.0198
Th (ppm)
Organic Matter (%)

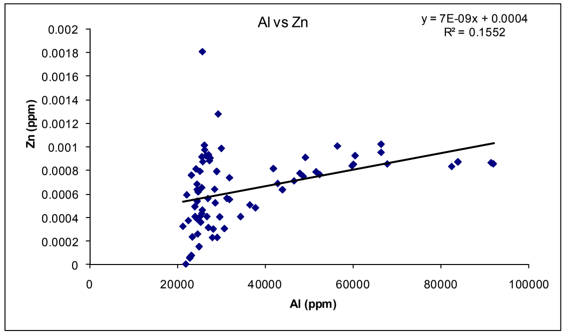
Al vs Zn
y = 7E-09x + 0.0004
R² = 0.1552
Zn (ppm)
Al (ppm)

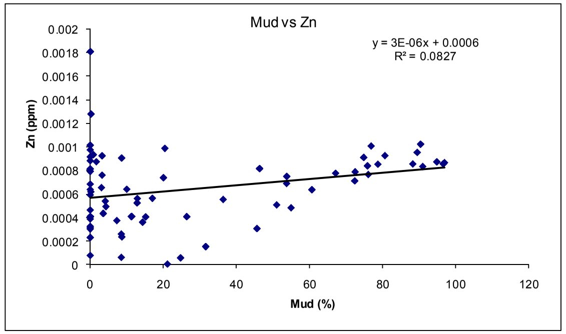
Mud vs Zn
y = 3E-06x + 0.0006
R² = 0.0827
Zn (ppm)
Mud (%)

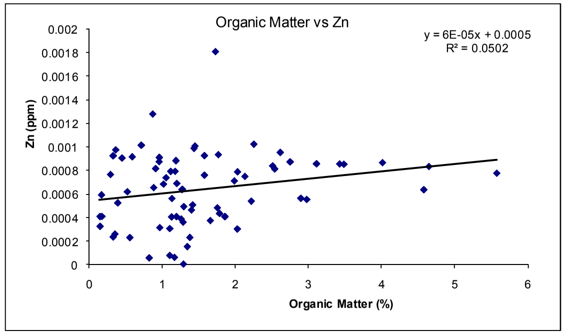
Organic Matter vs Zn
y = 6E-05x + 0.0005
R² = 0.0502
Zn (ppm)
Organic Matter (%)

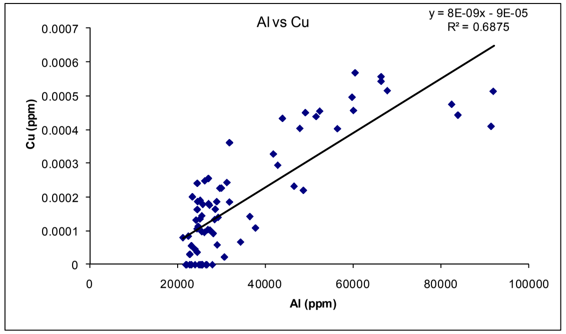
Al vs Cu
y = 8E-09x - 9E-05
R² = 0.6875
Cu (ppm)
Al (ppm)

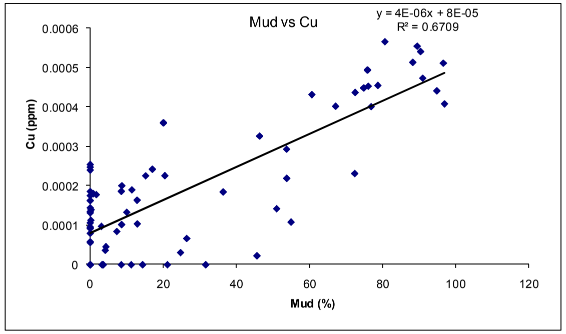
Mud vs Cu
y = 4E-06x + 8E-05
R² = 0.6709
Cu (ppm)
Mud (%)

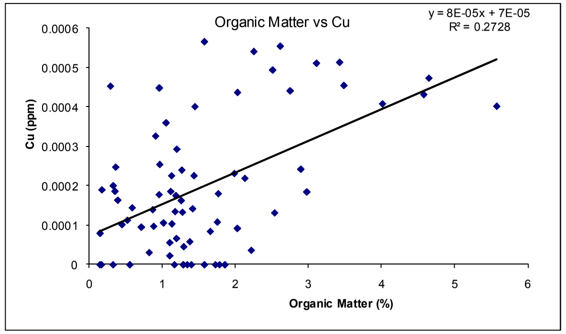
Organic Matter vs Cu
y = 8E-05x + 7E-05
R² = 0.2728
Cu (ppm)
Organic Matter (%)

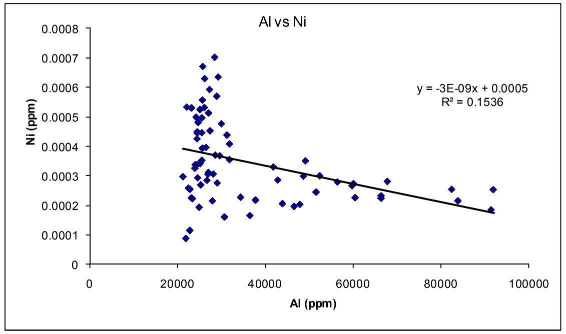
Al vs Ni
y = -3E-09x + 0.0005
R² = 0.1536
Ni (ppm)
Al (ppm)

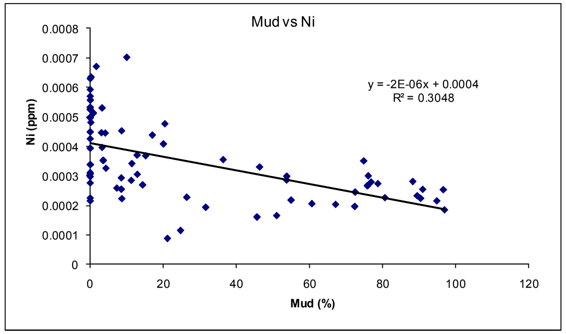
Mud vs Ni
y = -2E-06x + 0.0004
R² = 0.3048
Ni (ppm)
Mud (%)

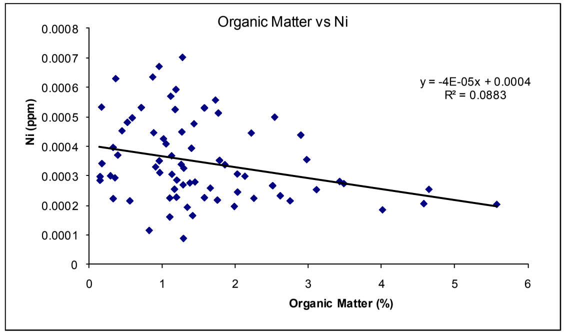
Organic Matter vs Ni
y = -4E-05x + 0.0004
R² = 0.0883
Ni (ppm)
Organic Matter (%)

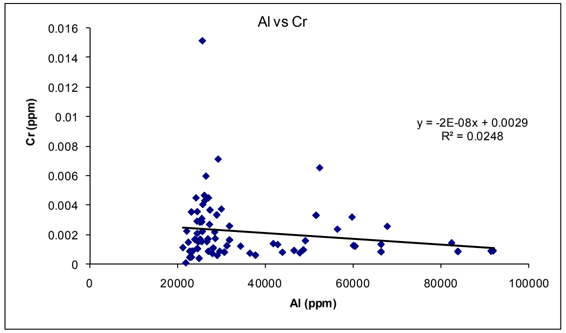
Al vs Cr
y = -2E-08x + 0.0029
R² = 0.0248
Cr (ppm)
Al (ppm)

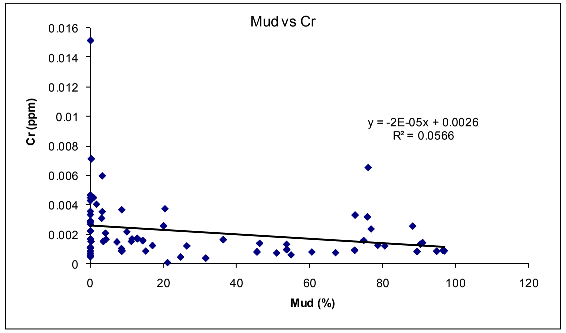
Mud vs Cr
y = -2E-05x + 0.0026
R² = 0.0566
Cr (ppm)
Mud (%)

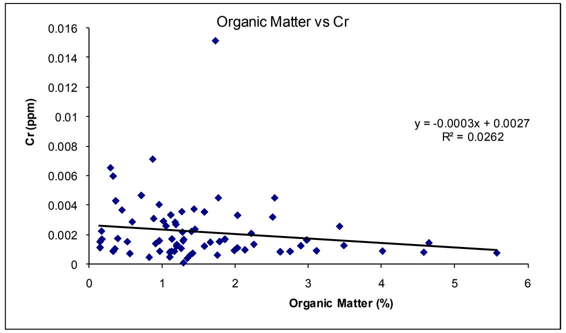
Organic Matter vs Cr
y = -0.0003x + 0.0027
R² = 0.0262
Cr (ppm)
Organic Matter (%)

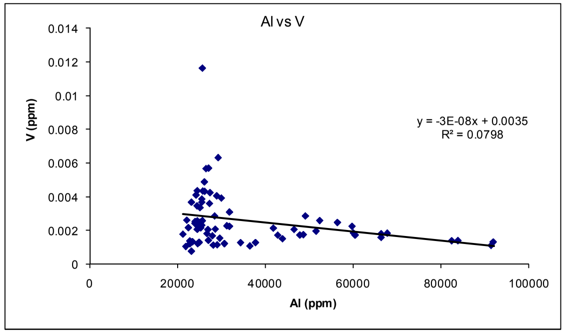
Al vs V
y = -3E-08x + 0.0035
R² = 0.0798
V (ppm)
Al (ppm)

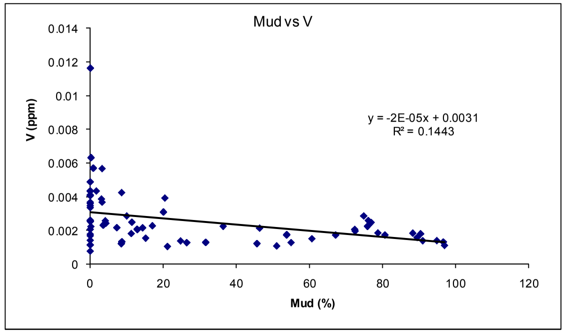
Mud vs V
y = -2E-05x + 0.0031
R² = 0.1443
V (ppm)
Mud (%)

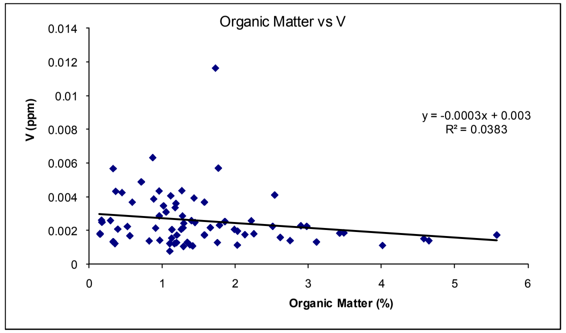
Organic Matter vs V
y = -0.0003x + 0.003
R² = 0.0383
V (ppm)
Organic Matter (%)

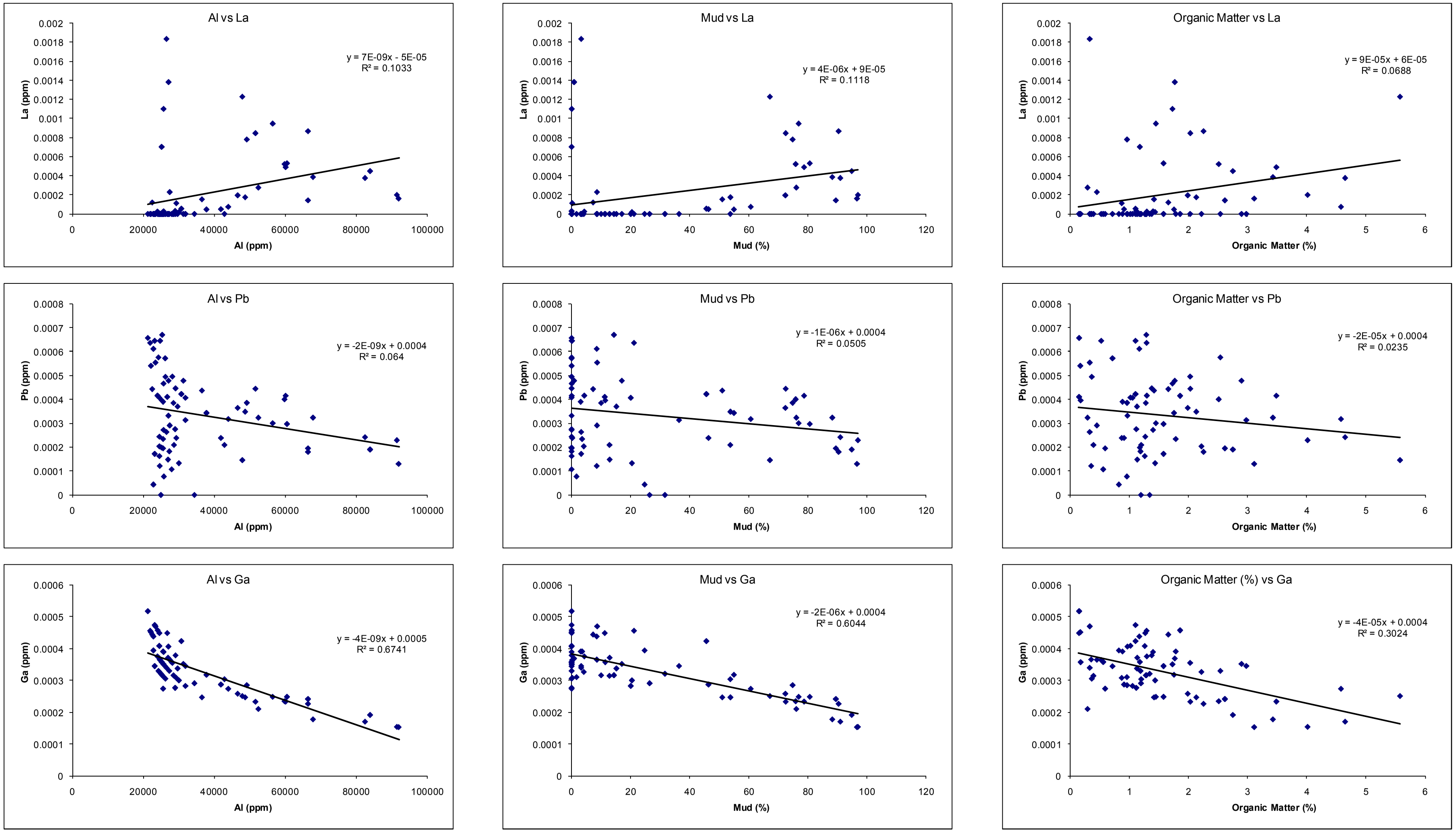

Al vs La
y = 7E-09x - 5E-05
R² = 0.1033
La (ppm)
Al (ppm)
Mud vs La
y = 4E-06x + 9E-05
R² = 0.1118
La (ppm)
Mud (%)
Organic Matter vs La
y = 9E-05x + 6E-05
R² = 0.0688
La (ppm)
Organic Matter (%)
Al vs Pb
y = -2E-09x + 0.0004
R² = 0.064
Pb (ppm)
Al (ppm)
Mud vs Pb
y = -1E-06x + 0.0004
R² = 0.0505
Pb (ppm)
Mud (%)
Organic Matter vs Pb
y = -2E-05x + 0.0004
R² = 0.0235
Pb (ppm)
Organic Matter (%)
Al vs Ga
y = -4E-09x + 0.0005
R² = 0.6741
Ga (ppm)
Al (ppm)
Mud vs Ga
y = -2E-06x + 0.0004
R² = 0.6044
Ga (ppm)
Mud (%)
Organic Matter (%) vs Ga
y = -4E-05x + 0.0004
R² = 0.3024
Ga (ppm)
Organic Matter (%)

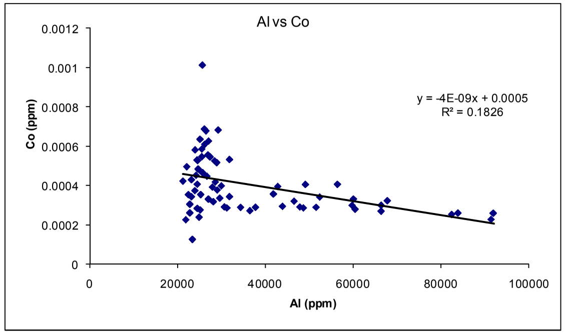
Al vs Co
y = -4E-09x + 0.0005
R² = 0.1826
Co (ppm)
Al (ppm)

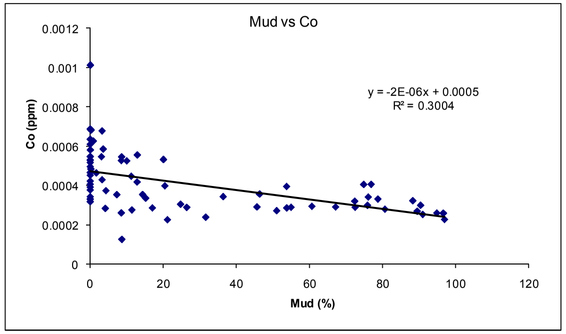
Mud vs Co
y = -2E-06x + 0.0005
R² = 0.3004
Co (ppm)
Mud (%)

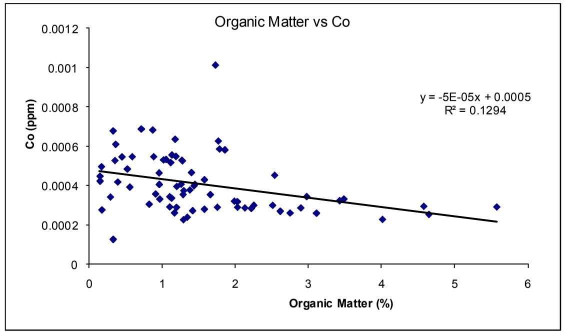
Organic Matter vs Co
y = -5E-05x + 0.0005
R² = 0.1294
Co (ppm)
Organic Matter (%)

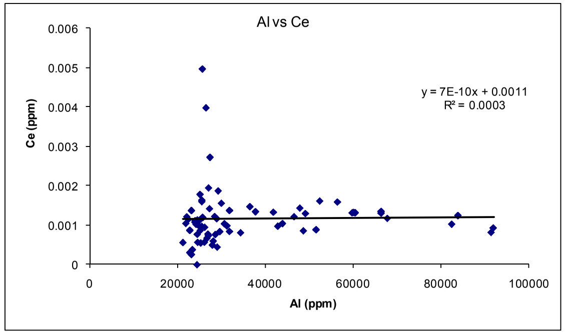
Al vs Ce
y = 7E-10x + 0.0011
R² = 0.0003
Ce (ppm)
Al (ppm)

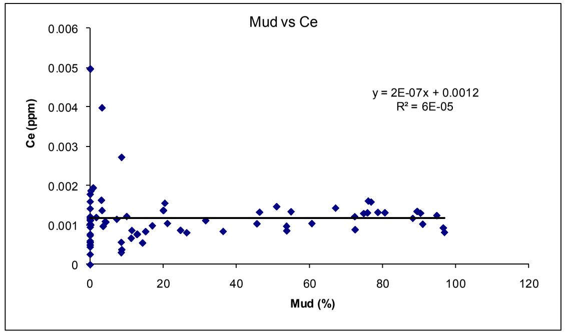
Mud vs Ce
y = 2E-07x + 0.0012
R² = 6E-05
Ce (ppm)
Mud (%)

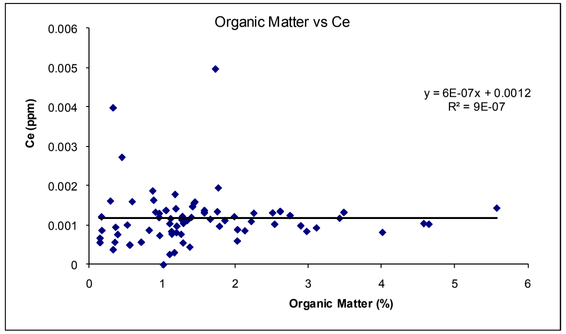
Organic Matter vs Ce
y = 6E-07x + 0.0012
R² = 9E-07
Ce (ppm)
Organic Matter (%)

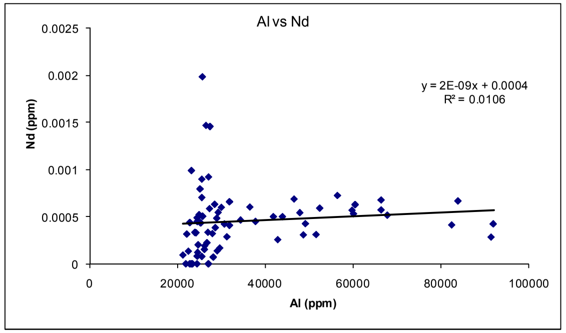
Al vs Nd
y = 2E-09x + 0.0004
R² = 0.0106
Nd (ppm)
Al (ppm)

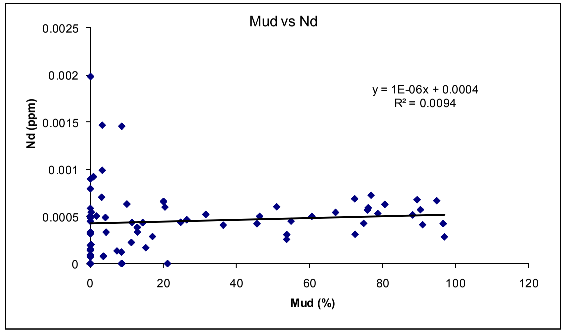
Mud vs Nd
y = 1E-06x + 0.0004
R² = 0.0094
Nd (ppm)
Mud (%)

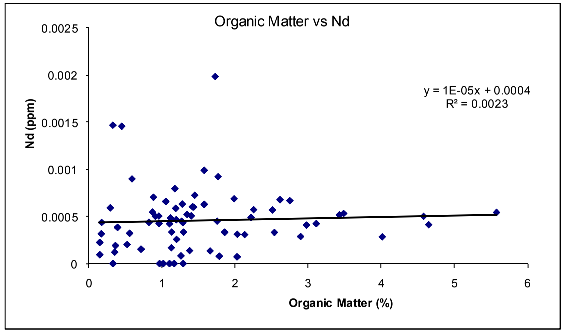
Organic Matter vs Nd
y = 1E-05x + 0.0004
R² = 0.0023
Nd (ppm)
Organic Matter (%)

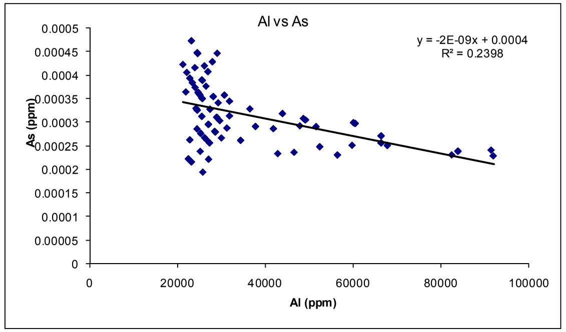
Al vs As
y = -2E-09x + 0.0004
R² = 0.2398
As (ppm)
Al (ppm)

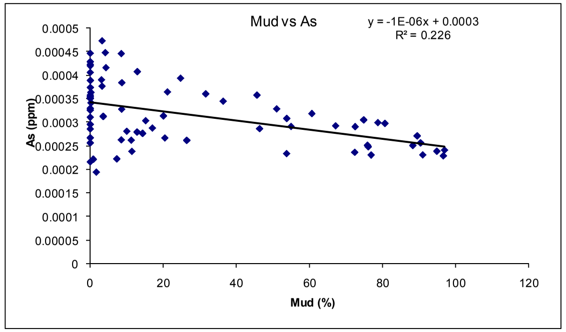
Mud vs As
y = -1E-06x + 0.0003
R² = 0.226
As (ppm)
Mud (%)

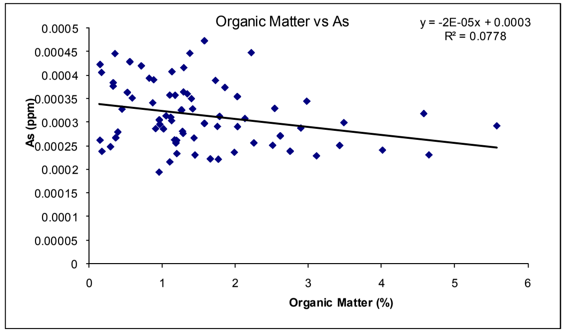
Organic Matter vs As
y = -2E-05x + 0.0003
R² = 0.0778
As (ppm)
Organic Matter (%)

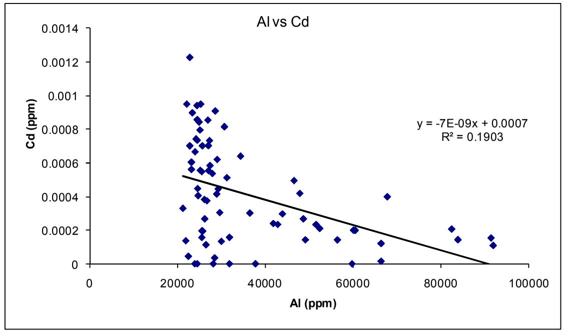
Al vs Cd
y = -7E-09x + 0.0007
R² = 0.1903
Cd (ppm)
Al (ppm)

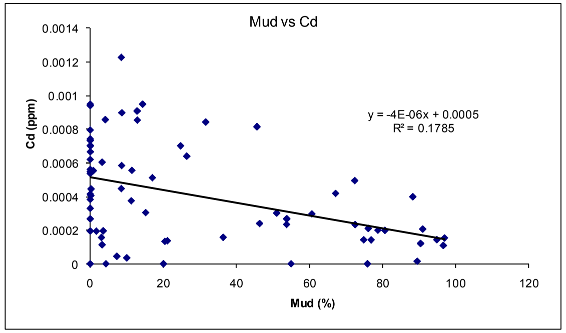
Mud vs Cd
y = -4E-06x + 0.0005
R² = 0.1785
Cd (ppm)
Mud (%)

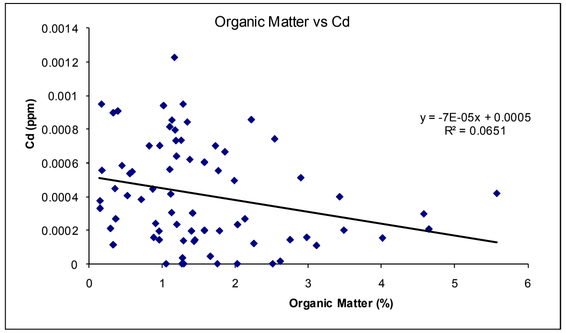
Organic Matter vs Cd
y = -7E-05x + 0.0005
R² = 0.0651
Cd (ppm)
Organic Matter (%)

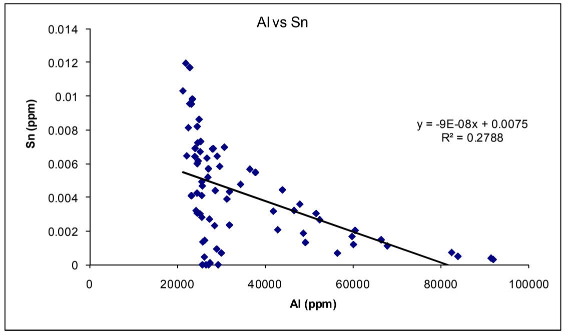
Al vs Sn
y = -9E-08x + 0.0075
R² = 0.2788
Sn (ppm)
Al (ppm)

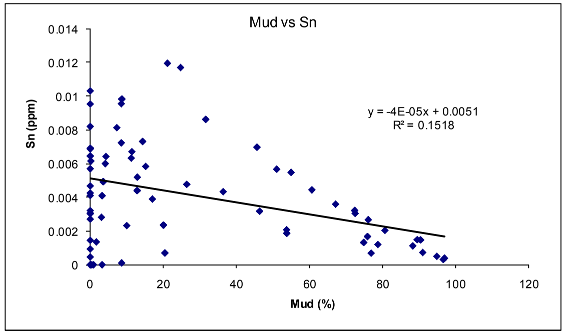
Mud vs Sn
y = -4E-05x + 0.0051
R² = 0.1518
Sn (ppm)
Mud (%)

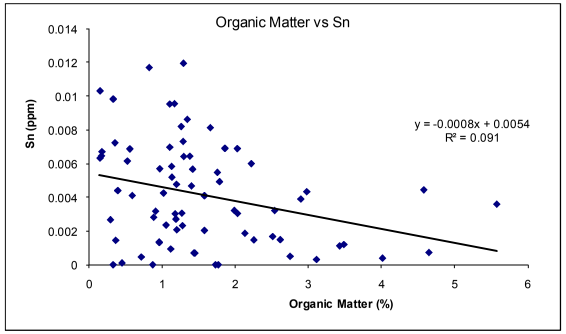
Organic Matter vs Sn
y = -0.0008x + 0.0054
R² = 0.091
Sn (ppm)
Organic Matter (%)

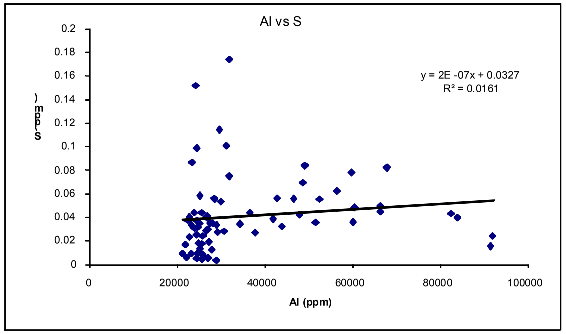
Al vs S
y = 2E -07x + 0.0327
R² = 0.0161
Al (ppm)
0
20000
40000
60000
80000
100000
0.2
0.18
0.16
0.14
0.12
0.1
0.08
0.06
0.04
0.02

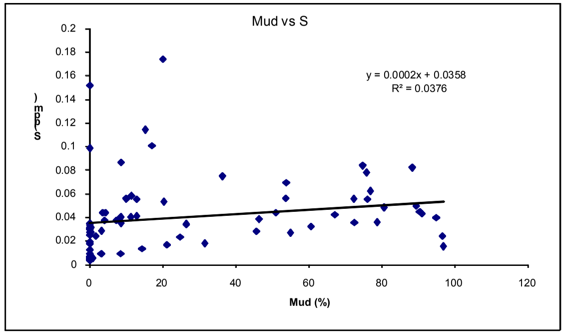
Mud vs S
y = 0.0002x + 0.0358
R² = 0.0376
Mud (%)
0
20
40
60
80
100
120

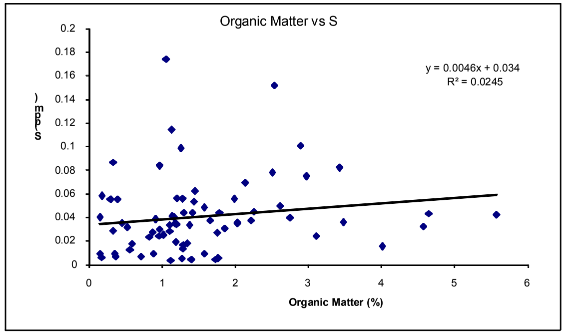
Organic Matter vs S
y = 0.0046x + 0.034
R² = 0.0245
Organic Matter (%)
0
1
2
3
4
5
6